INFORMATION TO USERS

While the most advanced technology has been used to photograph and reproduce this manuscript, the quality of the reproduction is heavily dependent upon the quality of the material submitted. For example:

- Manuscript pages may have indistinct print. In such cases, the best available copy has been filmed.

- Manuscripts may not always be complete. In such cases, a note will indicate that it is not possible to obtain missing pages.

- Copyrighted material may have been removed from the manuscript. In such cases, a note will indicate the deletion.

Oversize materials (e.g., maps, drawings, and charts) are photographed by sectioning the original, beginning at the upper left-hand corner and continuing from left to right in equal sections with small overlaps. Each oversize page is also filmed as one exposure and is available, for an additional charge, as a standard 35mm slide or as a 17"x 23" black and white photographic print.

Most photographs reproduce acceptably on positive microfilm or microfiche but lack the clarity on xerographic copies made from the microfilm. For an additional charge, 35mm slides of 6"x 9" black and white photographic prints are available for any photographs or illustrations that cannot be reproduced satisfactorily by xerography.

Ko, Chung-Ming

COSMIC-RAY MODIFIED STELLAR WINDS

The University of Arizona PH.D. 1986

PLEASE NOTE:

In all cases this material has been filmed in the best possible way from the available copy. Problems encountered with this document have been identified here with a check mark __✓__.

1. Glossy photographs or pages _____
2. Colored illustrations, paper or print _____
3. Photographs with dark background _____
4. Illustrations are poor copy _____
5. Pages with black marks, not original copy _____
6. Print shows through as there is text on both sides of page _____
7. Indistinct, broken or small print on several pages __✓__
8. Print exceeds margin requirements _____
9. Tightly bound copy with print lost in spine _____
10. Computer printout pages with indistinct print _____
11. Page(s) _____ lacking when material received, and not available from school or author.
12. Page(s) _____ seem to be missing in numbering only as text follows.
13. Two pages numbered _____. Text follows.
14. Curling and wrinkled pages _____
15. Dissertation contains pages with print at a slant, filmed as received __✓__
16. Other _____

_____

_____

COSMIC-RAY MODIFIED STELLAR WINDS

by

Chung-Ming Ko

A Dissertation Submitted to the Faculty of the

DEPARTMENT OF PHYSICS

In Partial Fulfillment of the Requirements
For the Degree of

Doctor of Philosophy

In the Graduate College

THE UNIVERSITY OF ARIZONA

1 9 8 6

THE UNIVERSITY OF ARIZONA
GRADUATE COLLEGE

As members of the Final Examination Committee, we certify that we have read the dissertation prepared by Chung-Ming Ko

entitled Cosmic-Ray Modified Stellar Winds

and recommend that it be accepted as fulfilling the dissertation requirement for the Degree of Doctor of Philosophy.

Theodore Bowen	November 19, 1986
Chang-yuan Fan	11/19/86
J. R. Jokipii	19 November 1986
John W. Olsen	1986 November 19
Adam Burrows	11/19/86
Ke Ching Hsieh	19 Nov. 1986

Final approval and acceptance of this dissertation is contingent upon the candidate's submission of the final copy of the dissertation to the Graduate College.

I hereby certify that I have read this dissertation prepared under my direction and recommend that it be accepted as fulfilling the dissertation requirement.

Chang-yuan Fan	11/19/86
Dissertation Director	Date

STATEMENT BY AUTHOR

This dissertation has been submitted in partial fulfillment of requirements for an advanced degree at The University of Arizona and is deposited in the University Library to be made available to borrowers under rules of the Library.

Brief quotations from this dissertation are allowable without special permission, provided that accurate acknowledgment of source is made. Requests for permission for extented quotation from or reproduction of this manuscript in whole or in part may be granted by the head of the major department or the Dean of the Graduate College when in his or her judgement the proposed use of the material is in the interests of scholarship. In all other instances, however, permission must be obtained from the author.

SIGNED: 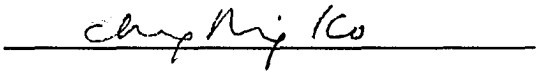

to m o m

ACKNOWLEDGEMENTS

I should like to take this opportunity to express my indebtedness to a number of persons. To Professor J. R. Jokipii I owe my introduction to the subject and guidance on research. I appreciate the many invaluable recommendations and kind encouragements made by Professor C. Y. Fan during my graduate studies. I also thank Professors T. Bowen, A. Burrows and K. C. Hsieh for their reviews and suggestions on the manuscript.

I should render my high esteem to Doctor G. M. Webb. The continuously stimulating discussions with him, in particular at the university café, on the mathematics and physics of cosmic-ray and stellar wind theories were indispensable for the thesis. Thanks are also due to Doctor S. Araki for his advices on the numerical methods used.

This work is supported in part by the National Aeronautics and Space Administration under grant NSG-7101.

Above all my deep gratitude must go to my mother for her irreplaceable care, patience, support and encouragement.

TABLE OF CONTENTS

TABLE OF CONTENTS—Continued

LIST OF ILLUSTRATIONS

LIST OF ILLUSTRATIONS—Continued

LIST OF ILLUSTRATIONS—Continued

Page

Figure

ABSTRACT

A two fluid hydrodynamical model describing the modification of a stellar wind flow due to its interaction with galactic cosmic-rays is investigated. The two fluids consist of the thermal stellar wind gas and the galactic cosmic-rays. A polytropic one fluid model is used to describe the stellar wind gas, and the cosmic-rays modify the wind via their pressure gradient. The cosmic-rays are considered to be a hot low density gas of negligible mass flux, but with a significant pressure and energy flux compared to the thermal gas. The equations used are essentially those employed in two fluid hydrodynamical models of cosmic-ray shock acceleration by the first order Fermi mechanism, but suitably modified to apply in a spherical geometry and including the effects of gravity on the flow. The stellar wind consists of a transonic flow with a termination shock, and subsonic flow outside the shock. The model shows the deceleration of the wind upstream of the shock by the positive galactic cosmic-ray pressure gradient. The dissertation first discusses one fluid polytropic stellar winds and how to insert shocks in the flow. The hydrodynamical equations governing cosmic-ray modified winds are then introduced followed by a discussion of the physics of the interaction between the thermal stellar wind and the cosmic-rays. A description of the singularities of the equations is also presented. The system of equations is first solved by a finite difference method in the test particle approximation in which the

cosmic-rays do not modify the flow, with appropriate boundary conditions applied at infinity, at the wind termination shock, and at the star. A perturbation scheme to determine the modification of the wind by the cosmic-rays is then developed. This scheme applies when the modification of the wind by the cosmic-rays is sufficiently small. Finally a numerical iteration algorithm which uses the test particle solution to start the iteration is employed to exactly solve the equations. This latter method has the advantage that it can be applied when there is a considerable modification of the wind by the cosmic-rays.

CHAPTER 1

INTRODUCTION

Cosmic-rays are high energy charged particles permeating the Galaxy and continually bombarding the Earth at a rate of about one particle per square centimeter per second. A stellar wind is the continuous hydrodynamic expansion of the atmosphere of a star. The wind in most cases of astrophysical interest consists of an ionized gas usually of protons and electrons. In some more exotic cases the gas may have a different composition (e.g. for pulsar stellar winds the gas may be an electron positron plasma c.f. Curtis Michel 1982). For the case of a thermally driven wind, the gas pressure falls off sufficiently rapidly with distance from the star that the pressure gradient forces lift the gas out of the gravitational potential well of the star leading to a net outward acceleration of the gas. The present study contains a synthesis of these two strands of astrophysical research, namely the progagation of cosmic-rays in highly conducting moving plasmas, and the hydrodynamics of stellar winds.

In this chapter we first give a brief history of cosmic-ray research (§1.1). This is followed in §1.2 by a description of the development of equations governing the transport of cosmic-rays, culminating in a description of models currently used in cosmic-ray shock acceleration theory (§1.3). A brief review of Solar wind

research, including a discussion of hydrodynamical models of stellar winds is provided in §1.4. Then in §1.5, we give an outline of the dissertation including a description of a self-consistent model of the modification of a stellar wind by its interaction with a hot, low density cosmic-ray gas. The model is a two fluid hydrodynamical model consisting of cosmic-rays and thermal gas where the two fluids are coupled to each other by hydromagnetic waves travelling in the background fluid which scatter the cosmic-rays. This model provides the basis for the present study on cosmic-ray modified stellar winds. Possible extensions of the dissertation are presented in §1.6.

§1.1 Historical Background of Cosmic-Ray Research

Cosmic-ray research dates back to early this century. Experiments on natural radioactivity by C. T. R. Wilson in 1901, measured the conductivity of pure dust free air in a sealed vessel enclosing an electroscope. Since the vessel was free of radioactive substances it was suspected that the leakage of charge in the electroscope was caused by the presence of natural radioactivity in the air and soil. In 1911 to 1912, V. Hess in a series of balloon experiments measured the residual ionization current in ionization chambers at various heights in the atmosphere. Since the ionization, thought to be caused by high energy γ-rays, increased above heights of 1.5 kilometers, Hess came to the conclusion that the source of the penetrating radiation was extraterrestrial. This radiation was later given the name *Cosmic-Rays* by R. A. Millikan in 1926. The prevailing

idea of cosmic-rays as high energy photons was challenged in 1929 by the coincidence counting experiments performed by W. Bothe and W. Kohlhörster. Their results (and later results by B. Rossi and others) supported the idea that the cosmic-rays were corpuscular in nature.

As early as 1904 C. Störmer, from an analysis of charged particle motion in the Earth's magnetic field had established that charged particles of extraterrestrial origin had much easier access to the Earth over the magnetic poles than at the equator. He established that, depending on particle rigidity (= pc/Ze , where p is the particle momentum, c is the speed of light and Ze is the particle charge), the lower rigidity particles were excluded from the lower latitudes. In 1927, J. Clay published the results of a latitude survey of the cosmic-ray intensity obtained on expeditions from Leiden to Java. He found the intensity to be consistently lower near the equator indicating that the cosmic-rays were high energy charged particles. These results were subsequently confirmed by a world wide cosmic-ray survey organized by A. H. Compton in the 1930's. Later in 1948 the latitude effect was studied in detail at high altitude in an aircraft by H. V. Neher.

Early cosmic-ray research in the 1930's and 1940's, provided a testing ground for the development of nuclear and particle physics, with the detection of subatomic particles such as positron, neutron, μ and π mesons in cosmic-rays (see e.g. the books by Ramakrishnan 1962; Hopper 1964).

In the early 1930's, serious attempts were also made to provide

a continuous registration of cosmic ray intensity. The diurnal (or daily) variations were observed as early as 1933 (Hess and Steinmaurer 1933; Compton and Getting 1935). The 27-day recurrence tendency was reported for the first time by Hess and Graziadei (1936). S. E. Forbush (1937) found that sudden decreases in the cosmic-ray intensity (Forbush decreases) were accompanied by magnetic storms.

Forbush (1954) also showed that there was an 11-year cycle variation of cosmic-ray intensity which was in clear anti-correlation with the solar activity as measured by the sunspot number. This phenomenon is shown in figure 1.1, which has been reproduced from Forbush (1954). It shows the ionization currents (or integral cosmic-ray intensity) for four ground-based ionization chambers and their mean current for the years 1938 to 1952. The sunspot number is

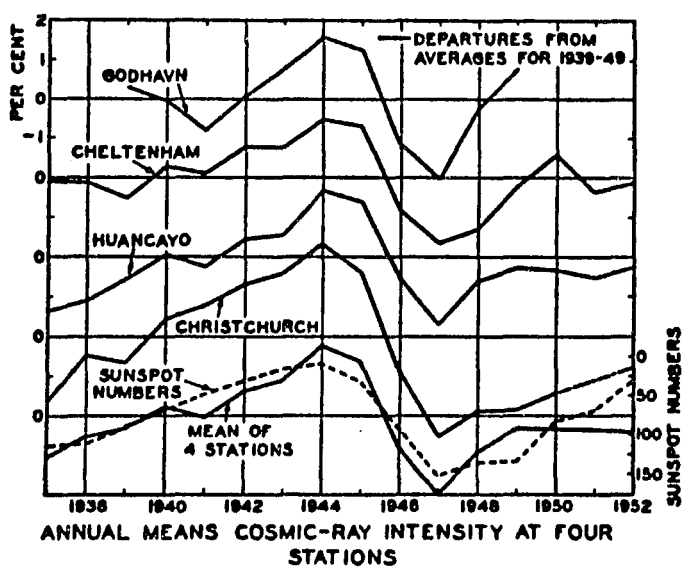

Figure 1.1 Eleven-Year Cycle Variation of Cosimc-Ray Intensity
The anti-correlation between cosmic-ray intensity at four ground-base stations and the eleven-year cycle of solar activity as measured by the sunspot numbers (Forbush 1954).

also plotted with scale reversed.

These time dependent phenomena (or *modulations*) have been studied ever since, with the introduction of the neutron monitor (Simpson, Fonger and Trieman 1953) in the 1950's being the first major attempt to record cosmic-ray intensities at a network of stations on a continuous basis.

Since the advent of balloon and satellite technology the variations in the intensities of specific cosmic-ray nuclei and electrons could be monitored. Neutron monitor observations deep in the atmosphere consist of the registration of secondary atmospheric products of the whole cosmic-ray abundance spectrum. Satellite and balloon observations have the additional advantage that they are not subjected to atmospheric attenuation, and hence extend to much lower energies than observations in the atmosphere. Cosmic-ray proton and α-particle differential intensity spectra, obtained from balloon and satellite experiments have been compiled since 1965 (e.g. Gloeckler and Jokipii 1967; Ormes and Webber 1968; Hsieh 1970; Freier *et al.* 1971; Webber and Lezniak 1973, 1974). Intensity spectra of electrons and positrons have been measured extensively since 1961 (e.g. Earl 1961; Meyer and Vogt 1961; Webber and Chotowski 1967; Beuerman *et al.* 1969; Fanselow *et al.* 1969; Meyer, Schmidt and L'Heureux 1971; Burger and Swanenburg 1971; Fulks, Meyer and L'Heureux 1973; Caldwell *et al.* 1975).

The basis of the theoretical understanding of these phenomena can be traced back to the pioneering work of Fermi (1949), Cocconi (1951) and Terletskii and Logunov (1951) on the diffusion of cosmic-rays

in a stochastic magnetic field. The first observational evidence that diffusion was in fact a good approximation to cosmic-ray motion was given by Meyer, Parker and Simpson (1956), who showed that the intensity time profile, during a Solar flare event of particles with rigidities of 2-4 GeV could be accounted for quantitatively by the solution of a diffusion equation. These ad hoc applications to the propagation of cosmic-rays in interplanetary space have been put on a firm theoretical and observational basis since the confirmation of the existence of a continuous Solar wind by Biermann (1951) from his observations of comet tails and developed on a proper basis by Parker (1958a) with his hydrodynamical model of the expansion of the Solar corona into interplanetary space.

Parker predicted, and it was subsequently confirmed on Mariner II (Neugebauer and Snyder 1962; Synder, Neugebauer and Rao 1963), that there would be a continuous radial flow of ionized gas (mostly protons and electrons) from the Sun into interplanetary space. The radial speed is about 400 km s^{-1} and there are about 5 protons cm^{-3} and 5 electrons cm^{-3} at the orbit of the Earth. This expanding plasma carries with it magnetic fields from the Sun's surface (Parker 1958a). Due to the Sun's rotation the steady state interplanetary magnetic field has the form of an Archimedes spiral on the surface of a cone. In addition to the steady state field there are irregular magnetic fields; all are convected radially with the Solar wind. The irregularities or kinks in the average magnetic field convected with the Solar wind (Parker 1958a) provide a magnetic configuration for the scattering and

consequent diffusion of the cosmic-rays.

Since 1958, there has been an extensive research effort on the effect of the Solar wind on galactic cosmic-rays, and on the propagation of the Solar cosmic-rays. Extensive reviews of this work have been given by e.g. Axford (1970a, b), McKracken and Rao (1970), Jokipii (1971), Wibberenz (1971), Gleeson (1972), Birmingham and Jones (1975), Moraal (1976), Fisk (1979), Gleeson and Webb (1980) and Quenby (1984). More recently cosmic-ray propagation theory, originally used to describe cosmic-ray transport in the Solar wind has been applied and developed to describe *diffusive shock acceleration* of cosmic-rays (see reviews by e.g. Toptygin 1980; Axford 1981; Drury 1983; Forman and Webb 1985 and Blandford and Eichler 1986). For a general discussion on cosmic-rays the reader is referred to the books by Rossi (1964), Ginzburg and Syrovatskii (1964), Pomerantz (1971), Wilson (1976) and Toptygin (1985).

§1.2 Development of the Cosmic-Ray Transport Equations

In order to explain the modulation of the galactic cosmic-rays, Parker (1958b) suggested that cosmic-rays were convected out from the inner Solar system by the magnetic fields carried by the Solar wind as they diffused through the wind due to scattering with the magnetic irregularities. He wrote down a transport equation, neglecting energy changes of particles due to scattering in the random magnetic fields as (c.f. Parker 1958b, 1963):

$$\frac{\partial U_p}{\partial t} + \nabla\cdot(\vec{u}\, U_p - \underline{\underline{\kappa}}\cdot\nabla U_p) = 0 \quad , \qquad (1.1)$$

where $U_p(t,\vec{r},p)$ is the differential number density of cosmic-rays with respect to momentum p at position $\vec{r}$ and time t; $\vec{u}$ is the wind velocity and $\underline{\underline{\kappa}}$ is the diffusion tensor (originally assumed to be isotropic by Parker in 1958). Parker used the steady state spherically symmetric solutions of equation (1.1) to qualitatively account for the 11-year Solar cycle modulation of galactic cosmic-rays, initially discovered by Forbush (1954). This *diffusion-convection* theory was then widely used to interprete the observed cosmic-ray particle spectra and has had some success at high and intermediate energies (e.g. Fan, Gloeckler and Simpson 1965; Silberberg 1966; Gloeckler and Jokipii 1966, 1967; Badhwar *et al.* 1967; O'Gallagher and Simpson 1967; Lockwood and Webber 1967; Ormes and Webber 1968; Ramaty and Lingfelter 1969; Wang 1970).

Later, Parker (1965a, 1966) showed that the particle energy changes of cosmic-rays due to scattering in the magnetic irregularities carried by the wind were not negligible. Parker showed that second order Fermi acceleration could be neglected, and he argued that the cosmic-rays lose energy because of adiabatic deceleration as they scatter between the expanding magnetic field irregularities. The rate of change of momentum of particles due to adiabatic deceleration (Parker 1965a; Dorman 1965) is

$$\langle \dot{p}' \rangle = -\frac{1}{3} p' \nabla\cdot\vec{u} \quad , \tag{1.2}$$

where p' is the particle momentum in the Solar wind frame, and the transport equation is then (Parker 1965a; Jokipii and Parker 1970):

$$\frac{\partial U_{p'}}{\partial t} + \nabla\cdot(\vec{u}\, U_{p'} - \underline{\underline{\kappa}}\cdot\nabla U_{p'}) - \frac{1}{3}\nabla\cdot\vec{u}\,\frac{\partial}{\partial p'}(p' U_{p'}) = 0 \quad , \tag{1.3}$$

where $U_{p'}(t,\vec{r},p')$ is the differential number density with respect to momentum p' in the Solar wind frame, and spatial co-ordinates $\vec{r}$ are defined in a fixed frame. Since the wind speed $u = |\vec{u}| \ll v$ where v is the particle speed, the number density $U_{p'}(t,\vec{r},p')$ is related to the particle number density $U_p(t,\vec{r},p)$ in a fixed frame (e.g. the Solar system frame) by

$$U_p(t,\vec{r},p) = U_{p'}(t,\vec{r},p)\ [1 + O(\delta)] \quad , \tag{1.4}$$

where

$$\delta = p\,\frac{u^2}{v^2}\left|\frac{\partial}{\partial p}[\log(U_p)]\right| \ll 1 \quad . \tag{1.5}$$

Using the transformation (1.4) we obtain the transport equation in the fixed frame as:

$$\frac{\partial U_p}{\partial t} + \nabla\cdot(\vec{u}\,U_p - \underline{\kappa}\cdot\nabla U_p) - \frac{1}{3}\,\nabla\cdot\vec{u}\,\frac{\partial}{\partial p}(p\,U_p) = 0 \quad . \tag{1.6}$$

Webb and Gleeson (1979) have shown that a momentum change rate algebraically identical to the adiabatic deceleration rate (1.2) can be derived by taking into account the fact that locally the wind frame is a non-inertial reference frame. The momentum change rate (1.2) in this development arises from the transformation of momenta between the Solar wind frame and the fixed frame:

$$\vec{p}' = \vec{p} - m\,\vec{u} + O\left(p\frac{u^2}{v^2}\right) \quad . \tag{1.7}$$

where m is the relativistic mass of the cosmic-ray particle. From this equation we note that the momentum $\vec{p}'$ changes from point to point in the wind flow simply because of the spatial variation of the wind velocity $\vec{u}$. Presumably the difference between this interpretation and the

adiabatic deceleration interpretation of Parker (1965a), is that Parker's treatment considers the particle trajectory over an extended volume, taking into account the individual particle energy changes from both betatron deceleration and multiple scattering (c.f. Laster, Lencheck and Singer; 1962; Quenby 1965 and Webb and Gleeson 1979), whereas the interpretation of Webb and Gleeson (1979) is purely a co-ordinate frame effect.

The transport equation (1.6) can also be derived from Boltzmann equation or Liouville's equation. Gleeson and Axford (1967) derived the spherically symmetric transport equation from the Boltzmann equation. In their model the cosmic-rays undergo isotropic, hard sphere scattering with scattering centres embedded in the Solar wind. Dolginov and Toptygin (1966, 1967, 1968) derived the transport equation from the Boltzmann equation (hard sphere model) and also from Liouville's equation for small angle scattering. Gleeson and Axford, and Dolginov and Toptygin also derived an expression for the differential current density or streaming $\vec{S}_p$ per unit momentum interval given by

$$\vec{S}_p = C \vec{u} U_p - \underline{\underline{\kappa}} \cdot \nabla U_p \quad , \tag{1.8}$$

where

$$C = 1 - \frac{1}{3} U_p^{-1} \frac{\partial}{\partial p}(p U_p) \quad , \tag{1.9}$$

is the Compton-Getting factor (Compton and Getting 1935; Gleeson and Axford 1968; Forman 1970). A slightly more general version of the transport equation (1.6) incorporating second order Fermi acceleration and emphasizing the difference between the wave and fluid frames has been derived by Skilling (1975) and Luhmann (1976). Equations (1.6) and

(1.8) can also be written in terms of the mean phase space distribution function $f(t,\vec{r},p)$ (where $U_p = 4\pi p^2 f$) as:

$$\frac{\partial f}{\partial t} + \vec{u}\cdot\nabla f - \nabla\cdot(\underline{\kappa}\cdot\nabla f) - \frac{1}{3}\nabla\cdot\vec{u}\; p\,\frac{\partial f}{\partial p} = 0 \quad , \tag{1.10}$$

$$\vec{S}_p = -4\pi p^2 \left(\frac{1}{3} p \frac{\partial f}{\partial p}\vec{u} + \underline{\kappa}\cdot\nabla f\right) \quad . \tag{1.11}$$

The diffusion tensor $\underline{\kappa}$ in the transport equation (1.6) or (1.10) is in general derived from the theory of the propagation of charged particles in stochastic magnetic fields by a quasilinear approach in which the particle orbit in the first approximation is a helix about the average magnetic field (assumed to be spatially uniform) (see e.g. Jokipii 1971, 1972; Forman, Jokipii and Owens 1974). The tensor basically includes the effects of diffusion both parallel and perpendicular to the average magnetic field, and the curvature and gradient drifts (described by the anti-symmetric components of the tensor) of the particles in the background field. Diffusion parallel to the field is determined by resonant scattering of the particles with small scale magnetic irregularities, whereas diffusion perpendicular to the field is determined by the combined effects of resonant scattering and random walk of the field lines (Jokipii and Parker 1969, 1970).

Equation (1.10) has been used extensively in the theory of cosmic-rays modulation by the Solar wind. Advanced numerical codes to solve equation (1.10) have been developed for example by Jokipii and Kopriva (1979), Kóta and Jokipii (1983), Potgieter and Moraal (1985), Jokipii (1986), and Jokipii and Merényi (1986). These codes includes drift, convection and diffusion of the cosmic-rays in the interplanetry space, and in some cases the diffusive shock acceleration of the

cosmic-rays by the Solar wind termination shock is also considered.

§1.3 Diffusive Shock Acceleration Theory

The transport equation (1.6) or (1.10) has also been used to describe the acceleration of energetic charged particles in shock waves following the publications of Krymskii (1977), Axford, Leer and Skadron (1977), Bell (1978a, b) and Blandford and Ostriker (1978). At a microscopic level, diffusive acceleration of energetic particles at a shock wave results from repeated scattering of the particles back and forth across the shock, with the particles gaining energy in head on collisions with waves or magnetic irregularities in the upstream medium, and losing energy in overtaking collisions with the scatterers in the downstream region. A net momentum change per scattering cycle:

$$\langle \delta p \rangle = \frac{4}{3} p \frac{(V_1 - V_2)}{v} , \qquad (1.12)$$

where V_1 and V_2 are the upstream and downstream wave frame velocity components normal to the shock respectively, and an escape probability into the downstream medium per scattering cycle of $4V_2/v$, results in the formation of a power law distribution function of shock accelerated particles from an initially monoenergetic distribution (Bell 1978a, b; Drury 1983). The downstream distribution of the shock accelerated particles in the case of plane, parallel shocks without losses in which the particles do not modify the flow is of the form $f \propto p^{-\alpha}$ with $\alpha = 3V_1/(V_1 - V_2)$. If the phase speed of the waves relative to the fluid $|\vec{V}_w|$ is much less than the fluid speed $|\vec{u}|$, then $\vec{V} = \vec{u} + \vec{V}_w \approx \vec{u}$. In

this case the spectral index $\alpha \approx 3u_1/(u_1-u_2) = 3q/(q-1)$ depends only on the shock compression ratio $q = u_1/u_2$. These results can be derived by using the microscopic probabilistic arguments given by Bell (1978a, b), or by solving the transport equation (1.10) with a step function flow velocity profile characteristic of the flow in a plane shock and with appropriate boundary conditions. For oblique shocks, the particles also gain energy by drifting in the electric field at the shock (see e.g. Chen 1975; Decker 1979; Terasawa 1979; Pesses 1979, 1981). In this case the particles are still accelerated to a power law, $f \propto p^{-\alpha}$ with $\alpha = 3V_1/(V_1-V_2)$, except that now part of the particle energy changes result from drifting in the electric field at the shock, and part arises from scattering in the upstream and downstream media (c.f. Jokipii 1982).

In some models of diffusive shock acceleration, proper account is taken of the waves generated by the streaming particles using the resonant scattering formulae of plasma kinetic theory (e.g. Bell 1978a, b; Achterberg 1981; McKenzie and Völk 1982; Lee 1982, 1983). Lee (1982, 1983) has applied this theory to account for both the wave and energetic particle spectra observed at the Earth's bow shock and at travelling interplanetary shocks.

In the above simple test particle theory, there is no apparent limit to the amount of energy the particles can extract from the flow. For strong shocks ($u_1/u_2 = 4$), one finds that the steady state cosmic-ray pressure in test particle theory diverges. Clearly the strong energization of particles must affect the flow in such a way as

to limit the energy gain to some reasonable level. In the process the background flow at the shock is modified and the efficiency of the shock acceleration is limited, leading to modified forms of the energetic particle momentum spectra. The nonlinear or hydrodynamic theories of cosmic-ray shock acceleration address these effects.

In the simplest hydrodynamical models (see e.g. Axford, Leer and Skadron 1977; Drury and Völk 1981; Axford, Leer and McKenzie 1982), the phase speed of the waves is assumed to be much smaller than the background fluid flow speed so that to a first approximation the waves can be considered to be magnetic scattering centres embedded in the background flow. The equations governing this simple system are the three hydrodynamical conservation equations (mass, momentum and energy) of the system:

$$\frac{\partial \rho_g}{\partial t} + \nabla.(\rho_g \vec{u}) = 0 \quad , \tag{1.13}$$

$$\frac{\partial}{\partial t}(\rho_g \vec{u}) + \nabla\cdot(\rho_g u^2 + P_g + P_c) = 0 \quad , \tag{1.14}$$

$$\frac{\partial}{\partial t}(\frac{1}{2} \rho_g u^2 + E_g + E_c) + \nabla\cdot[(\frac{1}{2} \rho_g u^2 + E_g + P_g) \vec{u} + F_c] = 0 \quad , \tag{1.15}$$

where ρ_g, P_g, E_g, $\vec{u}$ are the density, pressure, internal energy density and velocity of the thermal gas respectively, and P_c, E_c, F_c are the pressure, energy density and energy flux of the cosmic-rays respectively. The cosmic-rays are considered to be a hot, low density gas with significant pressure P_c, but of negligible density and mass flux. The energy densities E_g and E_c of the two components are related respectively to P_g and P_c through polytropic or adiabatic indices γ_g and γ_c as:

$$E_g = \frac{1}{(\gamma_g - 1)} P_g \quad \text{and} \quad E_c = \frac{1}{(\gamma_c - 1)} P_c \quad . \tag{1.16}$$

For cosmic-rays the adiabatic index lies in the range $4/3 < \gamma_c < 5/3$, with $\gamma_c = 4/3$ for a relativistic gas and $\gamma_c = 5/3$ for a non-relativistic gas.

The cosmic-ray energy equation

$$\frac{\partial E_c}{\partial t} + \nabla \cdot \vec{F}_c = \vec{u} \cdot \nabla P_c \quad , \tag{1.17}$$

where

$$\vec{F}_c = (E_c + P_c)\, \vec{u} - \underline{\underline{\kappa}} \cdot \nabla E_c \quad , \tag{1.18}$$

describes the energy transfer between the cosmic-rays and the thermal gas via the scattering centres. From equation (1.17), the energy transfer rate per unit volume from the scatterers to the cosmic-rays is simply $\vec{u} \cdot \nabla P_c$ (c.f. Jokipii and Parker 1967). Derivations of the cosmic-ray energy equation (1.17) and the energy flux (1.18) showing their relation to the cosmic-ray transport equation (1.6) and streaming (1.8) are given in appendix B.

Equations (1.13) – (1.18) can be combined to show that the entropy of the gas is conserved following the flow:

$$\left(\frac{\partial}{\partial t} + \vec{u} \cdot \nabla\right) \left[P_g / \rho_g^{\gamma_g}\right] = 0 \quad , \tag{1.19}$$

except possibly at gas shocks where the entropy jumps discontinuously. The overall momentum equation (1.14) may be cast in the form:

$$\rho_g \left(\frac{\partial}{\partial t} + \vec{u} \cdot \nabla\right) \vec{u} = - \nabla P_g - \nabla P_c \quad , \tag{1.20}$$

showing that the gas flow may be modified by an adverse cosmic-ray pressure gradient, as occurs for instance upstream of a strongly modified cosmic-ray shock. It should be emphasized that the above

hydrodynamical equations (1.13) – (1.18) apply for general hydrodynamical flows (not necessarily involving shocks), in which the cosmic-rays are coupled to the background flow via scattering with scatterers travelling in the background fluid.

An example of the use of these equations in determining the structure of steady state plane parallel cosmic-ray shocks is shown in figure 1.2. The figure is taken from Drury and Völk (1981). The cosmic-rays are advected into the shock from far upstream ($x \to -\infty$). A sub-shock in the thermal gas occurs at $x = 0$. Upstream of the subshock ($x < 0$), the cosmic-ray pressure increases with increasing x due to first order Fermi acceleration of energetic particles at the shock. The accelerated particles are eventually convected through the sub-shock into the downstream region ($x > 0$), leading to a uniform

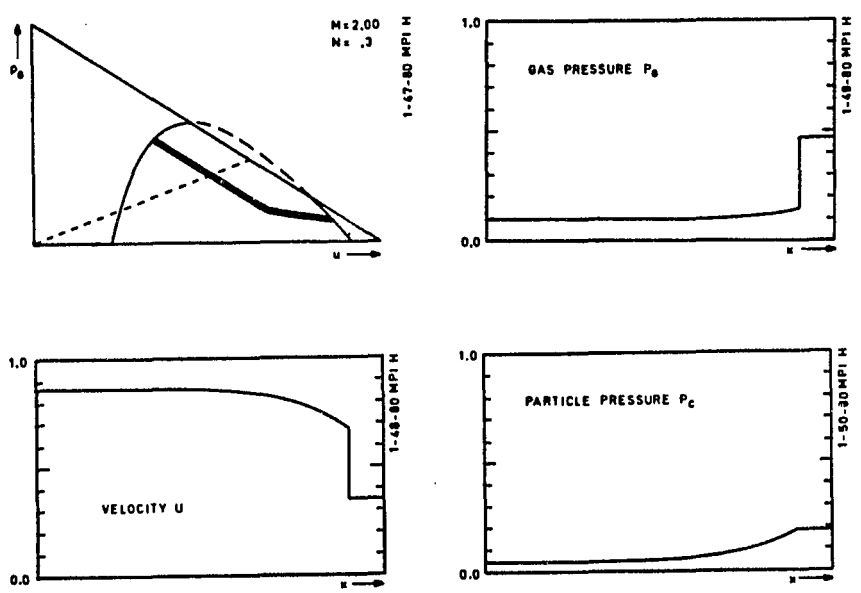

Figure 1.2 Cosmic-Ray Shock Structure
The shock structure for adiabatic exponents 5/3 for the gas and 4/3 for the cosmic rays, shock Mach number $M = 2.0$, and fractional contribution of the cosmic rays to the upstream pressure $N = 0.3$. The flow variables have been normalized to unit total momentum and mass fluxes. As the fluid passes through the shock, its state follows the heavy line in (u,P_G)-diagram (Drury and Völk 1981).

cosmic-ray pressure in the downstream region in the steady state limit. The cosmic-ray pressure gradient points into the upstream medium ($\frac{\partial P_c}{\partial x} \geq 0$) resulting in a deceleration of the fluid just upstream of the sub-shock, in accordance with the Euler equation (1.20). Low and high Mach number shocks in this model can be totally smoothed out by the diffusing cosmic-rays, whereas intermediate Mach number shocks tend to have a gas sub-shock (like that in figure 1.2) embedded in the flow.

The original work on hydrodynamical models of cosmic-ray shocks was carried by Axford, Leer and Skadron (1977), Drury and Völk (1981), and Axford, Leer and McKenzie (1982). Extensions of this work, including the effects of Alfvén waves on the flow (McKenzie and Völk 1982; Völk, Drury and McKenzie 1984), a variable γ_c throughout the flow (Achterberg, Blandford and Periwal 1984), an investigation of how the spectrum may be modified for momentum dependent κ (Eichler 1979, 1981; Heavens 1983), and the effects of oblique magnetic fields (Webb 1983; Kennel, Edmiston and Hada 1985; Webb, Drury and Völk 1986) may be found in the reviews of Drury (1983), Forman and Webb (1985) and Blandford and Eichler (1986).

These equations, modified to apply in a spherical geometry, and including the effects of gravity (§1.5) are the basic equations governing cosmic-ray modified stellar winds.

§1.4 A Brief Review of Solar Wind Research

It was suggested early this century by Birkeland (1908, 1913),

from his 1902 – 1903 Norwegian Aurora Polaris Expedition, that aurora and geomagnetic storms were the results of ionized corpuscular flow from the Sun. More than four decades later, Biermann (1951, 1953) from his observations of comet tails concluded that there was a continuous outflow of particles from the Sun.

It was suggested later by Parker (1958a), that these phenomena could be explained in terms of the continuous hydrodynamical expansion of the Solar corona into interplanetary space. This continuous outflow of ionized gas came to be known as the *Solar wind*, a name originally coined by Parker. Parker argued that the solar wind consisted of a transonic flow with the wind speed being subsonic near the Sun and supersonic beyond a few Solar radii. Parker's theory predicted that the flow speed was supersonic at the orbit of the Earth, and of the order of a few hundred kilometers per second. At about the same time Chamberlain (1961) suggested that the expansion of the corona should be subsonic, which he called the *Solar breeze*. This controversy between Parker's and Chamberlain's theories was later settled by Mariner II data (Neugebauer and Snyder 1962; Snyder, Neugebauer and Rao 1963) which indicated the flow near the Earth was supersonic.

At the Earth the mean flow speed in the quiet Solar wind is typically 400 – 500 km s^{-1}, and the wind has a mean number density of 5 - 10 protons cm^{-3} and 5 - 10 electrons cm^{-3}. The expanding plasma carries with it the *frozen in* magnetic fields from the surface of the Sun. Due to the Sun's rotation, the mean interplanetary magnetic field has the form of an Archimedes spiral on the surface of a cone (c.f.

Parker 1958a).

Subsequent research on the Solar wind has concentrated largely on the driving mechanisms and the energy budget of the wind (see e.g. the reviews by Hollweg 1978; Pneuman 1985; Axford 1985), and on the interaction of the Solar wind with interstellar medium (see e.g. Axford 1972; Wallis 1973). On general disscusions, history and developments of Solar wind research, the reader is referred to Parker (1963), Dessler (1967), Holzer and Axford (1970), Hundhausen (1972), Hollweg (1978), Leer, Holzer and Flå (1982) and Axford (1985). This extensive research literature considers the modification of the wind by such effects as heat conduction, viscosity, Alfvén wave pressure and magnetic forces, momentum and energy addition in the subsonic and supersonic regions of the flow, and charge exchange between the interstellar neutrals and the Solar wind.

In the present work we use the simple one fluid spherically symmetric stellar wind model originally introduced by Parker (1958a), appropriately modified to take into account the modification of the wind by the galactic cosmic-rays. Many of the features of Parker's model can be understood in terms of an analogy between the Solar wind equations and the gas flow through a deLaval nozzle (see e.g. Clauser 1960; Dessler 1967).

A deLaval nozzle is essentially a pipe of varying cross-section, consisting of a converging section and a diverging section joined by a narrow neck as illustrated in figure 1.3. This device is used for example in jet engines to produce a supersonic flow from an initially

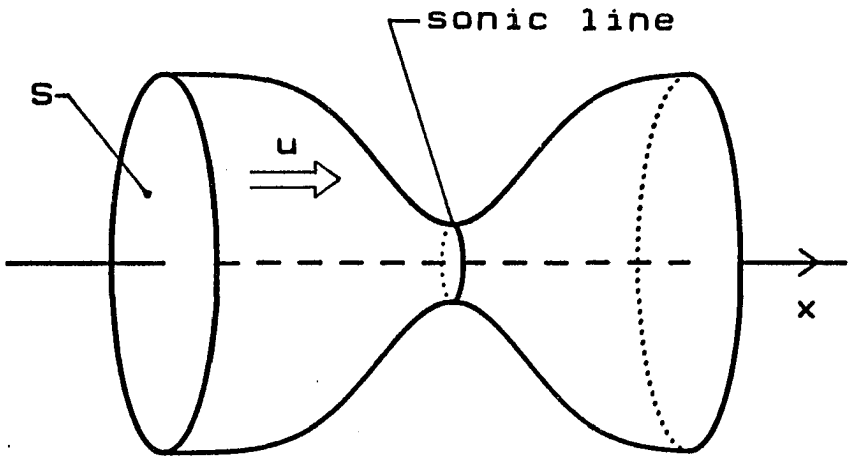

Figure 1.3 The deLaval Nozzle

subsonic flow. The mass and momentum equations for steady state inviscid flow through the nozzle are:

$$\rho\, u\, S = j \quad , \tag{1.21}$$

$$\rho\, u \frac{du}{dx} = - \frac{dP}{dx} \quad , \tag{1.22}$$

where S is the cross-section along the nozzle, and ρ, P, u and j are the density, pressure, flow speed (along the nozzle) and mass flux (which is a constant) of the gas respectively. Differentiating equation (1.21) logarithmically, and combining the result with equation (1.22) we obtain:

$$\frac{dS}{S} = \left[\frac{u^2}{c_s^2} - 1\right] \frac{du}{u} \quad , \tag{1.23}$$

where

$$c_s = \left[\frac{dP}{d\rho}\right]^{1/2} \quad , \tag{1.24}$$

is the sound speed of the gas. Equation (1.23) shows that if the flow

in the converging section of the nozzle is initially subsonic ($u < c_s$) then S decreases and u increases with increasing x. Thus subsonic flow in the converging section of the nozzle is accelerated. The maximum possible flow speed that can be obtained in the converging section in this case is the sound speed, which is achieved in the neck of the nozzle where the cross-section is constant and $\frac{dS}{dx} = 0$. By the same token, supersonic flow is accelerated in the diverging section. This argument shows that initially subsonic flow in the converging section can be accelerated up to the sound speed at the neck and may then be subsequently accelerated to supersonic speeds in the diverging section (possibly by heating this section). On the other hand if the flow speed is subsonic at the neck, the flow in the diverging section will consist of a decelerated subsonic flow (it is then called a *Venturi tube*). It should perhaps be noted, from the point of view of equation (1.23), that if the flow is sonic in the neck of the nozzle, then the flow downstream in the diverging section can be either supersonic or subsonic.

We now show that the flow in Parker's Solar wind model resembles the gas flow through a deLaval nozzle in which the gravitational force on the gas acts in such a way as to constrict the flow as does the converging section of a deLaval nozzle so as to permit the development of sonic flow (e.g. Clauser 1960; Parker 1963; Dessler 1967). For Parker's steady-state, inviscid, stellar wind model, the mass and momentum equations are:

$$\rho \, u \, S_w = j \quad , \tag{1.25}$$

$$\rho\, u \frac{du}{dr} = - \frac{dP}{dr} - \rho \frac{GM_o}{r^2} \quad , \tag{1.26}$$

where S_w is the flow tube cross-section of the wind, and ρ, P, u and j are the density, pressure, radial flow speed and mass flux (which is a constant) of the gas respectively, and r is the radial distance from the star. For spherical expansion the flow tube cross-section $S_w \alpha r^2$, and for non-spherical expansion we take $S_w \alpha r^{\nu}$ ($\nu \neq 2$). The last term in the momentum equation (1.26) is the gravitational force acting on the gas, with G the universal gravitational constant and M_o is the mass of the star. Logarithmically differentating the mass continuity equation (1.25) and using equation (1.26) we obtain:

$$\left[1 - \frac{1}{\nu} \frac{GM_o}{rc_s^2}\right] \frac{dS_w}{S_w} = \left[\frac{u^2}{c_s^2} - 1\right] \frac{du}{u} \quad , \tag{1.27}$$

where we have taken the flow tube cross-section $S_w \alpha r^{\nu}$, and c_s is the gas sound speed given by equation (1.24). A comparison of equations (1.23) and (1.27) shows the close analogy between the wind equation (1.27) and the deLaval nozzle equation (1.23), with the effective change in the nozzle area in the Solar wind case being:

$$dS = \left[1 - \frac{1}{\nu} \frac{GM_o}{rc_s^2}\right] dS_w \quad . \tag{1.28}$$

With $S_w \alpha r^{\nu}$, equation (1.27) can be written as:

$$\left[\nu - \frac{GM_o}{rc_s^2}\right] \frac{dr}{r} = \left[\frac{u^2}{c_s^2} - 1\right] \frac{du}{u} \quad , \tag{1.29}$$

which has a critical point or *sonic point* at $r = r_c$ and $u = c_s$, where

$$r_c = \frac{GM_o}{\nu c_s^2} \quad . \tag{1.30}$$

Equation (1.29) shows that an initially subsonic flow in $r < r_c$ accelerates as r increases (c.f. converging section of a deLaval mozzle), and can achieve a maximum possible velocity equal to the sound speed at the critical point ($r = r_c$). It also shows that supersonic flow in $r > r_c$ is accelerated with increasing r similar to the acceleration of supersonic flow in the diverging section of the deLaval nozzle.

Dessler (1967) has pointed out that if the sonic point r_c lies below the stellar surface (as can occur for example in very hot stars where c_s is sufficiently large; in the case of the Sun this occurs for coronal temperatures $T > 4*10^6$ K), then the only possible solution of the wind equation (1.29) is the stellar breeze solution of Chamberlain (1961). On the other hand, if the coronal gas is too cold, there is not a large enough pressure gradient to lift the gas out of the gravitational potential well of the star, and the only possible solution is then a static atmosphere.

At large distances from the star, (say $r > 1$ A.U. for the case of the Solar wind) the thermal energy of the wind has been converted principally to the bulk flow kinetic energy, and the wind achieves its maximal flow speed. At still larger distances, the wind may undergo a shock transition as the flow begins to feel the external pressure of thermal gas, magnetic fields and cosmic-rays of interstellar origin (c.f. Axford, Dessler and Gottlieb 1963).

A typical example of the flow velocity profile of a one fluid polytropic stellar wind (the type originally considered by Parker 1958a) is displayed in figure 1.4. This wind profile consists of a smooth subsonic-supersonic transition at the sonic point, a shock transition at the termination shock of the wind, and a region of decelerated subsonic flow outside the shock in which the velocity tends to zero at large radii. The flow velocity profile in figure 1.4 assumes the gas has a polytropic equation of state $P \alpha \rho^{\gamma_1}$ inside and $P \alpha \rho^{\gamma_2}$ outside the shock, and $\gamma_1 = 1.3$ and $\gamma_2 = 5/3$. Inside the shock the transonic solution has been chosen as the appropriate solution of the wind equations, and outside the shock the density and pressure of the gas tend to their constant interstellar values $\rho_\infty = 6*10^{-27}$ g cm^{-3} and $P_\infty = 1$ eV cm^{-3} respectively, and the mass loss rate $\dot{M} = 6*10^{11}$ g s^{-1}

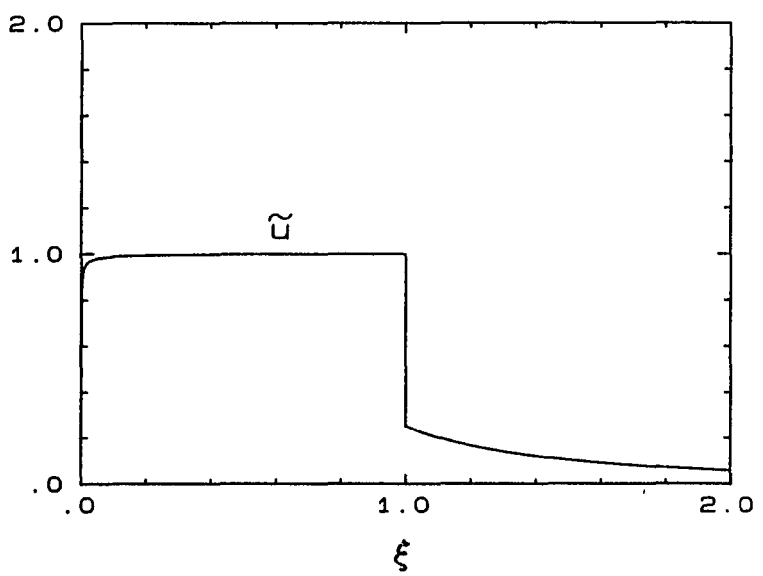

Figure 1.4 One Fluid Polytropic Stellar Wind with $\gamma_1 = 1.3$ and $\gamma_2 = 5/3$

The plotting quantities are $\xi = r/R$ and $\tilde{u} = u/u_o$, where $R = r_{sh} = 65.2$ A.U. and $u_o = u_{1sh} = 364$ km s^{-1}.

throughout the flow. The location of the shock is determined by the Rankine-Hugoniot relations at the shock. The detailed determination of the flow velocity profile of one fluid polytropic stellar wind with termination shock forms the subject matter of chapter 2.

§1.5 Outline of the Dissertation

In this section we present the equations governing cosmic-ray modified stellar winds, and provide an outline of the dissertation. Possible extensions of this work are discussed in §1.6.

By modifying the hydrodynamical equations (1.13) – (1.20) (which were used extensively in hydrodynamical models of cosmic-ray shock acceleration theory) to account for the effects of gravity and spherical symmetry, we obtain the equations governing cosmic-ray modified stellar winds. The steady state, spherically symmetric version of these equations are:

$$\frac{1}{r^2}\frac{d}{dr}(r^2 \rho_g u) = 0 \quad , \tag{1.31}$$

$$\rho_g u \frac{du}{dr} = -\frac{dP_g}{dr} - \frac{dP_c}{dr} - \rho_g \frac{GM_o}{r^2} \quad , \tag{1.32}$$

$$\frac{1}{r^2}\frac{d}{dr}\left[r^2 \rho_g u \left(\frac{1}{2}u^2 + \frac{\gamma_g}{(\gamma_g-1)}\frac{P_g}{\rho_g} - \frac{GM_o}{r}\right) + r^2 F_c\right] = 0 \quad , \tag{1.33}$$

$$\frac{1}{r^2}\frac{d}{dr}(r^2 F_c) = u\frac{dP_c}{dr} \quad , \tag{1.34}$$

$$F_c = \frac{\gamma_c}{(\gamma_c-1)} P_c u - \frac{1}{(\gamma_c-1)} \kappa \frac{dP_c}{dr} \quad . \tag{1.35}$$

The equations represent respectively: the mass continuity equation (1.31) (the cosmic-ray mass flux is assumed negligible); the Euler form

of the total momentum equation (1.32); the total energy equation (1.33) and the cosmic-ray energy equation (1.34) where the cosmic-ray energy flux is given by equation (1.35). As in hydrodynamical models of cosmic-ray shock-acceleration, equations (1.31) – (1.35) may be combined to deduce:

$$\frac{d}{dr}\left[P_g/\rho_g^{\gamma_g}\right] = 0 \quad , \tag{1.36}$$

so that the gas entropy is constant (except at gas shocks) and

$$P_g = A_g \rho_g^{\gamma_g} \quad , \tag{1.37}$$

where A_g is a constant dependent only on the gas entropy.

In the limit $\kappa \to \infty$ (i.e., the cosmic-ray mean free path $\Lambda \to \infty$), these equations reduce to the equations governing one fluid polytropic stellar winds discussed briefly in §1.4, and treated in greater detail in chapter 2. In this limit there is no interaction between the cosmic-rays and the thermal gas, so that the stellar wind is not affected by the cosmic-rays. On the other hand for κ identically zero, the equations (1.31) – (1.37) can be shown to reduce to the equations governing two fluid polytropic stellar winds, in which the cosmic-rays have a polytropic (or adiabatic) equation of state: $P_c \propto \rho_g^{\gamma_c}$ (see chapter 3 for greater detail). For intermediate, finite κ the diffusive effects of the cosmic-rays come into play.

Solutions of the full system of equations (1.31) – (1.35) (see chapter 6), show that inside the termination shock the cosmic-ray pressure P_c is a monotonic increasing function of radius r. Since

$\frac{dP_c}{dr} > 0$, the momentum equation (1.32) shows that the incoming galactic cosmic-rays serve to brake the outflowing wind by their pressure gradient. This effect is illustrated in figure 1.5, where we show the flow velocity u, the cosmic-ray pressure P_c and square of radius times energy flux r^2F_c as functions of radius r. The stellar model used in figure 1.5 has a mass loss rate $\dot{M} = 6*10^{11}$ g s^{-1} , interstellar gas pressure $P_{g\infty} = 1$ eV cm^{-3} , interstellar gas density $\rho_{g\infty} = 6*10^{-27}$ g cm^{-3} , polytropic index of the gas inside and outside the termination shock $\gamma_{g1} = 1.3$ and $\gamma_{g2} = 5/3$ respectively. Also in figure 1.5 the adiabatic index of the cosmic-rays $\gamma_c = 4/3$, the cosmic-ray diffusion coefficients inside and outside the shock $\kappa_1 = \kappa_2 = 4*10^{22}$ cm^2 s^{-1} , and the ratio of the galactic cosmic-ray

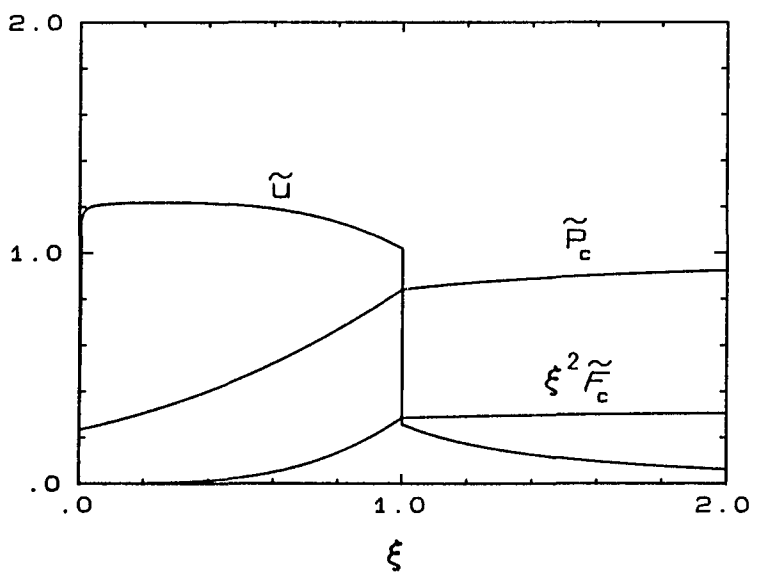

Figure 1.5 Cosmic-Ray Modified Stellar Wind with $\kappa_1 = \kappa_2 = 4*10^{22}$ cm^2 s^{-1}

The plotting quantities are $\xi = r/R$, $\tilde{u} = u/u_o$, $\tilde{P}_c = P_c/P_{co}$ and $\xi^2\tilde{F}_c = \xi^2F_c/F_{co}$, where $R = r_{sh} = 63.0$ A.U. , $u_o = u_{1sh} = 364$ km s^{-1} , $P_{co} = P_{g\infty} = 1$ eV cm^{-3} and $F_{co} = u_oP_{co} = 5.82*10^{-5}$ erg cm^{-2} s^{-1} . The normalized cosmic-ray diffusion coefficients are $\tilde{\kappa}_1 = \kappa_1/\kappa_o = 1.16$ and $\tilde{\kappa}_2 = \kappa_2/\kappa_o = 1.16$, where $\kappa_o = Ru_o = 3.44*10^{22}$ cm^2 s^{-1} .

energy flux to the interstellar gas energy flux $F_{c\infty}/F_{g\infty} = 1/2$. The results in figure 1.5 are taken from chapter 6, where we obtain fairly accurate numerical solutions of the set of the coupled nonlinear equations (1.31) – (1.35). The wind upstream of the shock is seen to be noticeably decelerated by the positive galactic cosmic-ray pressure gradient. This fluid velocity profile should be compared with the velocity profile of the one fluid polytropic stellar wind solution displayed in figure 1.4, where the wind velocity upstream of the shock is essentially constant. The radius of the termination shock is in general modified by the presence of the galactic cosmic-rays.

The detailed nature of the system of equations (1.31) – (1.37) forms the subject matter of the dissertation. In chapter 2, we discuss the nature of one fluid polytropic winds, and how to insert gas shocks in the flow.

In chapter 3, we discuss the properties of the equations governing cosmic-ray modified stellar winds, and provide an analysis of the singular or critical points of the equations. The equations possess a line or surface (depending on the variables used) of critical points on which the acceleration of the fluid is zero and the fluid speed matches the local gas sound speed. The critical points may have saddle or focus behaviour depending on the values of the parameters.

In chapter 4, we obtain numerical solutions of the cosmic-ray energy equation (1.34) in the test particle limit in which the cosmic-rays are assumed not to affect the background flow. Thus we provide a numerical scheme to solve equation (1.34) with the background

flow velocity profile being that of a one fluid polytropic stellar wind with termination shock (like that in figure 1.4), and with appropriate boundary conditions imposed on the cosmic-rays at the origin and at infinity. At the shock, the cosmic-ray pressure and energy flux are continuous, which are the usual boundary conditions applied in cosmic-ray shock acceleration problems.

In chapter 5, a perturbation approach is used to study the influence of the cosmic-rays on the stellar wind and termination shock for the cases where the cosmic-ray effects on the wind are small. The perturbation parameter used in this study is

$$\epsilon \equiv \frac{P_{c\infty}}{P_{g\infty}} \ll 1 \quad , \tag{1.38}$$

where $P_{c\infty}$ and $P_{g\infty}$ are the galactic cosmic-ray and gas pressures respectively. The perturbation approach exploits the numerical techniques (to solve for the test particle cosmic-ray pressure) developed in chapter 4, and takes into account the cosmic-ray modifications of: the critical point of the wind; the thermal gas entropy constants both upstream and downstream of the shock; the location of the shock and the fluid velocity profile.

In chapter 6, a numerical algorithm is devised to solve the equations (1.31) – (1.35) governing cosmic-ray modified winds. The method is an iterative one in which the cosmic-ray energy equation (1.34) is first solved (using the numerical scheme developed in chapter 4) for a given background flow velocity profile (the initial flow profile is chosen to be that of a one fluid polytropic stellar wind with

termination shock). The critical point requirements for a transonic flow inside the shock, and the total energy flux integral of equation (1.33) are then used to obtain a first approximation to the modified wind velocity profile. This completes the first iteration loop, and the new modified wind profile is then used to start the next iteration.

Finally it is worth noting that the system of equations (1.31) – (1.37) include at a hydrodynamical level the physical effects of the modulation of galactic cosmic-rays and their exclusion from the inner Solar cavity; the re-acceleration of the cosmic-rays at the stellar wind termination shock by the first order Fermi mechanism; and the energy changes of the cosmic-rays both upstream and downstream of the shock.

§1.6 Possible Extensions of the Dissertation

In this section we indicate briefly possible extensions of the cosmic-ray modified wind model developed in the present work. One fairly obvious extension of the model would be to determine how the modification of the wind by the cosmic-rays affects the momentum spectrum of the cosmic-rays. Given the modified wind velocity profile, it is fairly straightforward to solve the cosmic-ray transport equation (1.6) to determine by numerical means the differential energy spectrum $U_p(t,\vec{r},p)$ of the cosmic-rays. However, this spectrum is then not necessarily self-consistent with the hydrodynamic solution, since the spectrum in the hydrodynamical equations is governed by γ_c (if $f(t,\vec{r},p) \propto p^{-\alpha}$ then $\gamma_c = \alpha/3$ provided $4 < \alpha < 5$), which we have

taken as a constant in our calculations. Since γ_c may vary with position in the flow, the self-consistent solution for the spectrum and the hydrodynamical equations is clearly a very complex numerical problem, which is presumably quite difficult to solve.

A simple hydrodynamical problem is clearly to include further effects known to be important in the determination of the stellar wind flow. One such example is to incorporate into the model the effects of charge exchange of the interstellar neutrals with the stellar wind. The net effect of charge exchange is to slow down the wind upstream of the shock since there is a momentum transfer between the neutrals and the stellar wind plasma. Along the same lines more complex stellar wind models could be used for the background flow than those used here.

Another direction for further studies is to relax the assumption of spherical symmetry, and to include the effects of anisotropic diffusion of the cosmic-rays in the Parker spiral magnetic field.

It is known (e.g. Cowsik and Lee 1982), that cosmic-rays undergo strong acceleration in accretion flows, both due to adiabatic compressive acceleration in the flow and also by first order Fermi acceleration at the accretion shock. These flows are expected to be strongly modified by the cosmic-rays since very energetic particle spectra are produced. Cowsik and Lee were mainly interested in accretion flows around black holes and neutron stars. Clearly cosmic-ray acceleration in other galactic accretion flows are also of interest. For example Völk (1984) advocated the use of coupled hydrodynamical equations for the thermal gas and cosmic-rays, including

the effects of radiative losses, heat conduction, and effects associated with the Alfvén waves scattering the cosmic-rays, to describe subsonic accretion onto giant molecular clouds. The cosmic-rays accelerated in the flow are expected ultimately to determine the γ-ray flux associated with the clouds. Völk also conjectured that the larger clouds would accrete matter, whereas the smaller clouds may be heated sufficiently to evaporate, thus affecting the overall mass balance of the interstellar medium.

Ipavich (1975) used versions of the hydrodynamical cosmic-ray equations including Alfvénic effects, in the strong scattering limit with $\kappa = 0$, to study the role of cosmic-rays in driving galactic winds. Völk, Breitschwerdt and McKenzie (1986) are also using versions of these equations (with $\kappa \neq 0$) to investigate the importance of cosmic-rays in the formation of galactic winds.

Finally we note that time dependent versions of the hydrodynamical equations have been used by Dorfi and Drury (1985) to study the modification of supernova remnant dynamics by the cosmic-rays.

CHAPTER 2

ONE FLUID POLYTROPIC STELLAR WINDS

In this chapter we briefly review one fluid polytropic stellar winds as developed originally by Parker (1958a). One of our main concerns is to establish a basic wind flow (or accretion flow) with shocks if necessary. In later chapters we shall discuss the modifications of this basic profile by the galactic cosmic rays.

We consider a simple one fluid polytropic wind. In order to mimic heat conduction in the flow the polytropic index, γ, is chosen to lie between 1 and 5/3. The value of $\gamma = 1$ corresponds to an isothermal wind in which heat conduction is maximized. In a more realistic model, one should include, in a physically consistent way, the effects of heat conduction, viscosity, Alfvén wave pressure forces and charge exchange between the wind and interstellar neutrals (see e.g. the reviews by Holzer and Axford 1970; Axford 1972; Hollweg 1978).

§2.1 Basic Equations and Properties of Solutions

For spherically symmetric steady state models, the basic equations governing the flow are the mass, momentum and energy equations:

$$\frac{1}{r^2}\frac{d}{dr}(r^2 \rho u) = 0 \quad , \tag{2.1}$$

$$\rho\, u \frac{du}{dr} = - \frac{dP}{dr} - \rho \frac{GM_o}{r^2} \quad , \tag{2.2}$$

$$\frac{1}{r^2} \frac{d}{dr}\left[r^2\, \rho\, u \left[\frac{1}{2} u^2 + \frac{\gamma}{(\gamma-1)} \frac{P}{\rho} - \frac{GM_o}{r}\right]\right] = 0 \quad , \tag{2.3}$$

where P, ρ, u denote respectively the gas (thermal plasma) pressure, density and radial velocity; γ is the polytropic index of the gas, G is the universal gravitational constant ($= 6.67*10^{-8}$ dyn cm^2 g^{-2}), M_o is the stellar mass and r is radial distance from the star.

From equations (2.1) – (2.3), we can deduce a polytropic equation of state for the gas:

$$P = A \rho^{\gamma} \quad , \tag{2.4}$$

where A is a constant which depends on the entropy of the gas only. Note that only three of the equations (2.1) – (2.4) are independent. Thus, for example the energy equation (2.3) can alternatively be deduced from equations (2.1), (2.2) and (2.4). There are two integrals for the system of equations (2.1) – (2.3), namely, the mass flux, j, and the energy constant, E:

$$j = \rho\, u\, r^2 \quad , \tag{2.5}$$

$$E = \frac{1}{2} u^2 + \frac{\gamma}{(\gamma-1)} \frac{P}{\rho} - \frac{GM_o}{r} \quad . \tag{2.6}$$

It is useful at this point to introduce the dimensionless variables (Chamberlain 1961; Summers 1982):

$$\lambda = \frac{GM_o}{r}\left(\frac{m_g}{kT_o}\right) \quad \text{and} \quad \psi = u^2 \left(\frac{m_g}{kT_o}\right) \quad . \tag{2.7}$$

where k is the Boltzmann constant, m_g is the mean mass per gas particle and T_o is some reference temperature. Note that the quantity $\sqrt{kT_o/m_g}$ is essentially the root mean square (or thermal) speed of the gas

particles at temperature T_o. Using the dimensionless variables ψ and λ, equations (2.1) – (2.4) become:

$$\rho = \rho_o \psi^{-1/2} \lambda^2 \quad , \tag{2.8}$$

$$P = \frac{1}{\gamma} \rho_o \left(\frac{m_g}{kT_o}\right)^{-1} \beta^{(\gamma+1)/2} \psi^{-\gamma/2} \lambda^{2\gamma} \quad , \tag{2.9}$$

$$\frac{1}{2}\left[1 - \beta^{(\gamma+1)/2} \psi^{-(\gamma+1)/2} \lambda^{2(\gamma-1)}\right] \frac{d\psi}{d\lambda} = 1 - 2\beta^{(\gamma+1)/2} \psi^{-(\gamma-1)/2} \lambda^{(2\gamma-3)} \quad , \tag{2.10}$$

$$\bar{E} = \frac{1}{2}\psi - \lambda + \frac{1}{(\gamma-1)} \beta^{(\gamma+1)/2} \psi^{-(\gamma-1)/2} \lambda^{2(\gamma-1)} \quad . \tag{2.11}$$

where

$$\rho_o = j (GM_o)^{-2} \left(\frac{m_g}{kT_o}\right)^{-3/2} \quad , \tag{2.12}$$

$$\beta = \left[\gamma A \rho_o^{(\gamma-1)} \left(\frac{m_g}{kT_o}\right)\right]^{2/(\gamma+1)} \tag{2.13}$$

$$\bar{E} = E \left(\frac{m_g}{kT_o}\right) \quad . \tag{2.14}$$

The general solution of the stellar wind equation in ψ and λ is given by the energy integral (2.11). Given γ and β, we obtain a one parameter family of solution curves by varying the normalised energy flux $\bar{E}$. Equation (2.11) implicitly yields ψ as a function of λ for fixed γ, β and $\bar{E}$. However, the solutions are more conveniently analyzed from equation (2.10) which is a first order nonlinear ordinary differential equation (O.D.E.) in ψ and λ.

Equation (2.9) can be written as:

$$\frac{d\psi}{d\lambda} = \frac{P}{Q} \quad , \tag{2.15}$$

where

$$P = 1 - 2\beta^{(\gamma+1)/2} \psi^{-(\gamma-1)/2} \lambda^{(2\gamma-3)} \quad , \tag{2.16}$$

$$Q = \frac{1}{2}\left[1 - \beta^{(\gamma+1)/2}\ \psi^{-(\gamma+1)/2}\ \lambda^{2(\gamma-1)}\right] \quad . \tag{2.17}$$

Critical points in the flow occur where either (a) $\mathbf{P} = \mathbf{Q} = 0$ or (b) P and Q both become infinite. The critical point ***C***, where $\mathbf{P} = \mathbf{Q} = 0$, occurs when

$$\lambda = \lambda_c = (2\beta)^{(\gamma+1)/(5-3\gamma)} \quad , \tag{2.18}$$

$$\psi = \psi_c = \frac{1}{2}\lambda_c \quad , \tag{2.19}$$

which is known as the *sonic point*. Another critical point in the flow occurs at the origin ***O***, where $\psi = \lambda = 0$, and **P** and **Q** both tend to infinity. The flow speed matches the gas sound speed along a curve (called *sonic line*) in the (λ,ψ) plane obtained by setting $\mathbf{Q} = 0$ in equation (2.17):

$$\psi_{sonic} = \left[\beta^{(\gamma+1)/2}\ \lambda_{sonic}^{2(\gamma-1)}\right]^{2/(\gamma+1)} \quad . \tag{2.20}$$

On the sonic line $u^2 = \gamma P/\rho$.

The nature of the critical points can be determined by linearizing equation (2.15) about these points (see appendix A). When the polytropic index, γ, lies in the range of physical interest (i.e., $1 < \gamma < 5/3$), ***O*** is a node and ***C*** is a saddle point. Figure 2.1 shows some of the possible solution topologies for (a) $1 < \gamma < 3/2$ and (b) $3/2 < \gamma < 5/3$.

Physical solutions are obtained by selecting solution curves in figure 2.1 satisfying some appropriate initial or boundary conditions and inserting a shock if necessary. As an example, the Solar wind is represented by the transonic solution ***ACD*** in figure 2.1(a) (c.f. Parker 1958a, 1965b). The flow is initially subsonic near $\lambda \approx \infty$ ($r \approx 0$) at

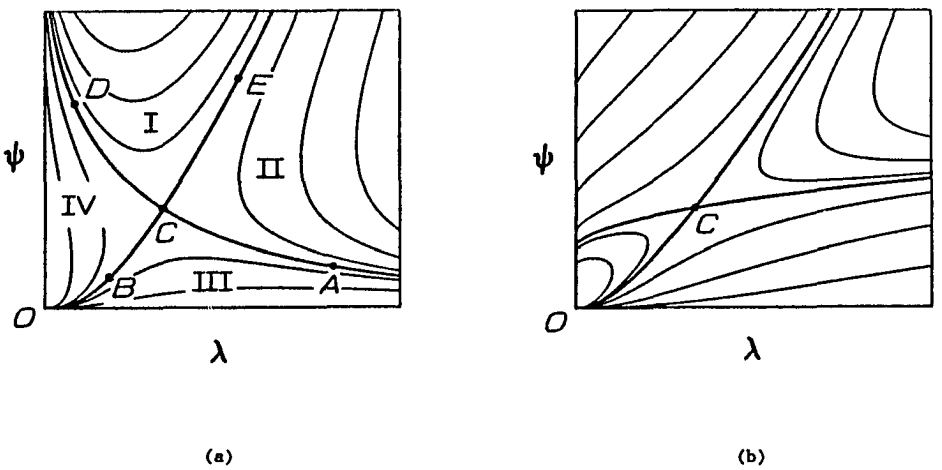

Figure 2.1 Solution Curves of One Fluid Polytropic Stellar Wind Equation
Only two cases with saddle points are shown: (a) $1 < \gamma < 3/2$ and (b) $3/2 < \gamma < 5/3$. *O* is the origin and *C* is the sonic point.

A, passes through the sonic point *C*, and consists of a supersonic flow at $\lambda < \lambda_c$ (i.e. $r > r_c$) on the segment *CD*. In order to match the confining pressure and density of the interstellar medium, it is necessary to insert a gas shock somewhere in the supersonic flow region *CD* ($\lambda < \lambda_c$) (c.f. Holzer and Axford 1970).

Observations of the Solar wind at Earth (e.g. Axford 1985) are:

$$\begin{aligned} \text{mass loss rate, } \dot{M}, &= 10^{12} \text{ g s}^{-1} , \\ \text{energy flux, } F_E, &= 0.16 \text{ erg cm}^{-2} \text{ s}^{-1} , \\ \text{wind speed, } u_E, &= 400 \text{ km s}^{-1} , \\ \text{temperature, } T_E, &= 10^5 \text{ K} ; \end{aligned} \tag{2.21}$$

and those at the coronal base (e.g. Pneuman 1985) are:

$$\begin{aligned} \text{wind speed, } u_b, &= 10 \text{ km s}^{-1} , \\ \text{temperature, } T_b, &= 1.5*10^6 \text{ K} . \end{aligned} \tag{2.22}$$

Since the sound speed of a polytropic gas is $\sqrt{\gamma kT/m_g}$, the sound speed at Earth and at the coronal base are of order 30 km s^{-1} and 120 km s^{-1}

respectively. The observational results (2.21) and (2.22) thus imply that the Solar wind has a subsonic-supersonic transition between the coronal base and Earth. This transition is smooth and cannot involve a gas shock, because a subsonic-supersonic shock is in general unstable (see Landau and Lifshitz 1959). As a result the sonic point lies between Earth and the coronal base. The assertion that ***ACD*** in figure 2.1(a) represents the Solar wind is thus justified.

On the transonic solution,

$$\bar{E} = \bar{E}_c \equiv \frac{(5-3\gamma)}{4(\gamma-1)} \lambda_c = \frac{r_E^2 F_E}{j} \left(\frac{m_g}{kT_o}\right) , \tag{2.23}$$

so that the sonic point occurs at the radius

$$r = r_c \equiv \frac{(5-3\gamma)}{4(\gamma-1)} \frac{GM_o}{r_E^2} \frac{j}{F_E} , \tag{2.24}$$

and the flow speed at the sonic point is

$$u = u_c \equiv \left(\frac{1}{2} \frac{GM_o}{r_c}\right)^{1/2} . \tag{2.25}$$

Investigation of the solution topologies for one fluid polytropic winds indicates that γ must be chosen to lie in the range $1 < \gamma < 3/2$, in order to correspond to the Solar wind. Solutions with $3/2 < \gamma < 5/3$ (c.f. figure 2.1(b)) violate the observed velocity at the coronal base. It is also noted (equation (2.24)) that solutions with $\gamma - 1 \ll 1$ have sonic points beyond Earth (i.e., $r_c > r_E$) A suggested range of γ consistent with observation is $1.1 < \gamma < 1.4$. For instance if $\gamma = 1.3$, we have $r_c = 0.018$ A.U. $= 3.9 r_{sun}$ and $u_c = 157$ km s^{-1} .

Subsonic solutions starting at $\lambda \approx \infty$ (i.e., $r \approx 0$) in the subsonic flow region **III** in figure 2.1(a) correspond to stellar breezes

(Chamberlain 1961). Subsonic flows in region **III** with negative radial velocities correspond to subsonic accretion flows (Bondi 1952; Mestel 1954). It is also possible to obtain accretion flows with shocks. For example, the transonic solution ***BCE*** in figure 2.1(a), starting near $\lambda \approx 0$ (i.e., $r \approx \infty$) represents an initially subsonic accretion flow, which becomes supersonic at $\lambda > \lambda_c$ (i.e., $r < r_c$). In order to match boundary conditions near the stellar surface, it is necessary in many cases to insert a shock in the flow in the region ***CE*** ($\lambda > \lambda_c$). The regions **II** and **IV** in figure 2.1(a) are significant in shock transitions. The downstream flows are usually represented by solution curves in these regions.

§2.2 Stellar Wind Solutions with Shocks

There are two classes of asymptotic behaviour of the stellar wind solutions as $\lambda \to 0$ (i.e., $r \to \infty$). They can be deduced from the energy integral (2.11) with positive finite $\bar{E}$. In one class of solutions:

$$\psi \sim 2\bar{E} \quad \text{as} \quad \lambda \to 0 \ , \tag{2.26}$$

and in the other class of solutions:

$$\psi \sim B\lambda^4 \quad \text{as} \quad \lambda \to 0 \ , \tag{2.27}$$

where

$$B = \left(\frac{\rho_o}{\rho_\infty}\right)^2 = \left[(\gamma-1)\,\bar{E}\,\beta^{-(\gamma+1)/2}\right]^{-2/(\gamma-1)} \ . \tag{2.28}$$

The solution family (2.26) gives a finite fluid velocity at infinity, but the density $\rho = j/(ur^2)$ and pressure $P = A\rho^\gamma$ both tend to zero

as r tends to infinity. On the other hand the solution family (2.27) gives $u \alpha r^{-2}$, but ρ and P tend to finite constant values ρ_∞ and P_∞ respectively as r tends to infinity. Thus for constant finite interstellar gas density and pressure the solution family (2.27) is appropriate at large radius (i.e., small λ). To match the transonic solution ***ACD*** in figure 2.1(a), it is necessary to insert a gas shock (the termination shock) in the flow somewhere in the supersonic region ($\lambda < \lambda_c$). This is illustrated in figure 2.2. However, it should be noted that the solution segment inside the shock ($\lambda > \lambda_{sh}$, i.e., $r < r_{sh}$) and the one outside the shock ($\lambda < \lambda_{sh}$, i.e., $r > r_{sh}$) have different sonic points, ***C***, and normalised entropy constants, β.

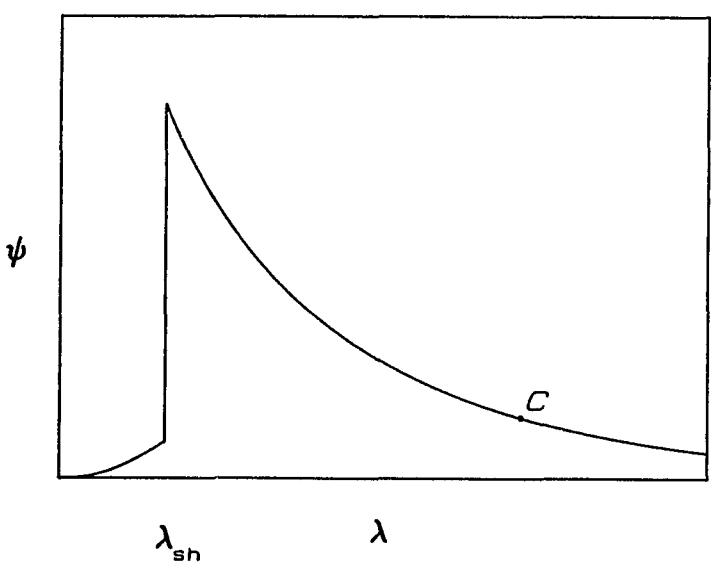

Figure 2.2 Sketch of a one Fluid Polytropic Stellar Wind Velocity Profile

A rough estimate of the location of the termination shock in the case of the Solar wind is obtained by equating the ram pressure of the wind upstream to the net external interstellar pressure (Axford 1985).

The wind velocity between Earth and the upstream side of the shock ($r_{sh} > r_E$) does not vary substantially because in this region the gas is cold and gravitational potential is small (e.g. at Earth, the enthalpy and gravitational potential of the wind are one to two orders of magnitude smaller than the bulk kinetic energy). The wind velocity just upstream of the shock, u_{1sh}, is essentially the same as that at Earth. The thermal pressure downstream is large compared with the ram pressure, so the thermal pressure just downstream of the shock is essentially the same as that of the interstellar medium. Momentum balance at the shock gives

$$P_\infty \approx \rho_{1sh} u_{1sh}^2 \tag{2.29}$$

and mass flux conservation yields

$$r_{sh}^2 \approx \frac{j u_{1sh}}{P_\infty} \approx \frac{\dot{M}}{4\pi} \frac{u_E}{P_\infty} \quad . \tag{2.30}$$

Using canonical values (e.g. Axford 1985) of the mass loss rate $\dot{M} = 10^{12}$ g s^{-1} , wind velocity at Earth $u_E = 400$ km s^{-1} and the interstellar confining pressure (the sum of magnetic, cosmic ray and interstellar gas pressure) $P_\infty = 1$ eV cm^{-3} , equation (2.30) gives $r_{sh} = 94$ A.U. .

A more exact determination of the location of the termination shock of a stellar wind must take into account the wind profile both upstream and downstream of the shock, and the full Rankine-Hugoniot conditions (conservation of mass, momentum and energy flux across the shock). We now show how this may be carried out for the case of a one fluid polytropic wind model. The polytropic index γ_1 and normalized

entropy constant β_1 upstream of the shock are in general different from those (γ_2 and β_2) downstream of the shock.

On either side of the shock, specification of P, ρ, u at a fixed point in the flow uniquely determines the solution of the system of first order coupled O.D.E.s (2.1) – (2.3) for P, ρ, u. This involves 6 constants (which can be considered as initial conditions). In addition to determine the full pressure, density and velocity profiles, the radius of the shock needs to be determined, so that overall there are 7 constants involved. The specification of $\dot{M}$ (or j), P_∞ and ρ_∞, and mass, momentum and energy flux conservation across the shock provide 6 conditions on the flow. The seventh condition to close the system of equations is obtained by choosing the transonic solution inside the shock which is equivalent to specifying $u = u_c$ at $r = r_c$.

We now proceed to determine the radius of the shock. Let subscript 1 and 2 correspond to upstream and downstream quantities respectively from now on. The conservation equations at the shock are:

$$\rho_{1sh}\, u_{1sh}\, r_{sh}^2 = \rho_{2sh}\, u_{2sh}\, r_{sh}^2 = j_1 = j_2 = j \quad , \tag{2.31}$$

$$\rho_{1sh}\, u_{1sh}^2 + P_{1sh} = \rho_{2sh}\, u_{2sh}^2 + P_{2sh} \quad , \tag{2.32}$$

$$j_1\left\{\frac{1}{2}\, u_{1sh}^2 + \frac{\gamma_1}{(\gamma_1-1)}\,\frac{P_{1sh}}{\rho_{1sh}} - \frac{GM_o}{r_{sh}}\right\} = j_2\left\{\frac{1}{2}\, u_{2sh}^2 + \frac{\gamma_2}{(\gamma_2-1)}\,\frac{P_{2sh}}{\rho_{2sh}} - \frac{GM_o}{r_{sh}}\right\} \quad . \tag{2.33}$$

After changing to dimensionless form these equations become:

$$\psi_{1sh}^{1/2} + \frac{1}{\gamma_1}\,\beta_1^{(\gamma_1+1)/2}\,\psi_{1sh}^{-\gamma_1/2}\,\lambda_{sh}^{2(\gamma_1-1)} = \psi_{2sh}^{1/2} + \frac{1}{\gamma_2}\,\beta_2^{(\gamma_2+1)/2}\,\psi_{2sh}^{-\gamma_2/2}\,\lambda_{sh}^{2(\gamma_2-1)} \quad , \tag{2.34}$$

$$\bar{E}_1 = \frac{1}{2}\psi_{1sh} - \lambda_{sh} + \frac{1}{(\gamma_1-1)}\beta_1^{(\gamma_1+1)/2}\psi_{1sh}^{-(\gamma_1-1)/2}\lambda_{sh}^{2(\gamma_1-1)} , \quad (2.35)$$

$$\bar{E}_2 = \frac{1}{2}\psi_{2sh} - \lambda_{sh} + \frac{1}{(\gamma_2-1)}\beta_2^{(\gamma_2+1)/2}\psi_{2sh}^{-(\gamma_2-1)/2}\lambda_{sh}^{2(\gamma_2-1)} , \quad (2.36)$$

$$\bar{E}_1 = \bar{E}_2 = \bar{E} . \quad (2.37)$$

Since the flow is adiabatic (except at the shock) and P_∞, ρ_∞ and j are given, it follows that β_2 can be written in terms of P_∞ and ρ_∞ (by equations (2.4 and (2.13)) as:

$$\beta_2 = \left[\gamma_2 \frac{P_\infty}{\rho_\infty}\left(\frac{\rho_o}{\rho_\infty}\right)^{(\gamma_2-1)}\left(\frac{m_g}{kT_o}\right)\right]^{2/(\gamma_2+1)} . \quad (2.38)$$

Since $\psi \to 0$ as $\lambda \to 0$ (i.e., $u \to 0$ as $r \to \infty$), the normalized energy flux $\bar{E}_2$ is just the normalised enthalpy at infinity:

$$\bar{E}_2 = \frac{\gamma_2}{(\gamma_2-1)}\frac{P_\infty}{\rho_\infty}\left(\frac{m_g}{kT_o}\right) . \quad (2.39)$$

As we choose the transonic solution inside the shock, equations (2.23) and (2.37) give:

$$\beta_1 = \frac{1}{2}\left[\frac{4(\gamma_1-1)}{(5-3\gamma_1)}\frac{\gamma_2}{(\gamma_2-1)}\frac{P_\infty}{\rho_\infty}\left(\frac{m_g}{kT_o}\right)\right]^{(5-3\gamma_1)/(\gamma_1+1)} . \quad (2.40)$$

The upstream and downstream Mach numbers at the shock are given by:

$$M_1^2 = \beta_1^{-(\gamma_1+1)/2}\psi_{1sh}^{(\gamma_1+1)/2}\lambda_{sh}^{-2(\gamma_1-1)} , \quad (2.41)$$

$$M_2^2 = \beta_2^{-(\gamma_2+1)/2}\psi_{2sh}^{(\gamma_2+1)/2}\lambda_{sh}^{-2(\gamma_2-1)} , \quad (2.42)$$

and the shock compression ratio, q, is:

$$q = \left(\frac{\psi_{1sh}}{\psi_{2sh}}\right)^{1/2} . \quad (2.43)$$

Equations (2.34) – (2.43) contain the essential physics needed to

determine the location of the shock and the nature of the flow on both sides of the shock. However, in order to solve these equations for λ_{sh} (i.e., r_{sh}), it is useful to consider the cases $\gamma_1 = \gamma_2$ and $\gamma_1 \neq \gamma_2$ separately. We consider two cases: (a) $1 < \gamma_1 = \gamma_2 = \gamma < 3/2$ and (b) $1 < \gamma_1 < 3/2$ and $\gamma_1 < \gamma_2 < 5/3$.

§2.2.1 Case $1 < \gamma_1 = \gamma_2 = \gamma < 3/2$

To determine λ_{sh}, we first use equations (2.34) – (2.37) and (2.41) – (2.43) to obtain a relation between M_1^2, M_2^2 and q (c.f. Landau and Lifshitz 1959):

$$\frac{M_2^2}{M_1^2} = \frac{\left[\frac{(\gamma+1)}{(\gamma-1)} - q\right]}{q\left[\frac{(\gamma+1)}{(\gamma-1)}q - 1\right]} \quad . \tag{2.44}$$

Equations (2.41) – (2.44) yield an algebraic equation for q:

$$\left(\frac{\beta_1}{\beta_2}\right)^{(\gamma+1)/2} = \frac{q^{\gamma}\left[\frac{(\gamma+1)}{(\gamma-1)} - q\right]}{\left[\frac{(\gamma+1)}{(\gamma-1)}q - 1\right]} \quad . \tag{2.45}$$

Substituting equations (2.43) and (2.45) into equation (2.34) gives

$$\psi_{2sh} = \beta_2 \left[\frac{2}{(\gamma+1)q - (\gamma-1)}\right]^{2/(\gamma+1)} \lambda_{sh}^{4(\gamma-1)/(\gamma+1)} \quad , \tag{2.46}$$

and the energy equation (2.36) then gives

$$\lambda_{sh} - \frac{(\gamma+1)}{2(\gamma-1)}\, q\, \beta_2 \left[\frac{2}{(\gamma+1)q - (\gamma-1)}\right]^{2/(\gamma+1)} \lambda_{sh}^{4(\gamma-1)/(\gamma+1)} + \bar{E}_2 = 0 \quad . \tag{2.47}$$

After determining the compression ratio from equation (2.45), the location of the shock can then be obtained by solving equation (2.47) for λ_{sh}.

The normalized entropy constants β_1 and β_2 and the normalized

energy fluxes $\bar{E}_1$ and $\bar{E}_2$ involve the arbitrary reference temperature T_o. The choice of T_o also determines the scaling for the dimensionless flow variables ψ and λ, but does not affect the resultant physical solution for P, ρ and u. A convenient scaling is obtained by choosing T_o such that

$$\left(\frac{m_g}{kT_o}\right) = \frac{(5-3\gamma)}{4(\gamma-1)} \frac{\rho_\infty}{P_\infty} \quad . \tag{2.48}$$

With this choice of T_o, we have

$$\beta_1 = \frac{1}{2} \quad , \tag{2.49}$$

$$\beta_2 = \left[\frac{(5-3\gamma)}{4} \left(\frac{\rho_o}{\rho_\infty}\right)^{(\gamma-1)}\right]^{2/(\gamma+1)} \quad , \tag{2.50}$$

$$\bar{E}_1 = \bar{E}_2 = \frac{(5-3\gamma)}{4(\gamma-1)} \quad . \tag{2.51}$$

In analyzing equation (2.45), we notice that $(\beta_2/\beta_1)^{(\gamma+1)/2}$ is a monotonic increasing function of q for $\gamma > 1$ and that $(\beta_2/\beta_1)^{(\gamma+1)/2} = 1$ when $q = 1$. This implies that $\beta_2/\beta_1 > 1$ for shocks with compression ratios greater than 1. In other words the entropy increases across a compressive shock (see e.g. Landau and Lifshitz 1959). To ensure that the entropy increases across the shock and that the shock is compressive it is necessary that $\beta_2/\beta_1 > 1$. This restriction from equation (2.38) and (2.40) then implies:

$$j\,(GM_o)^{-2}\, P_\infty^{3/2}\, \rho_\infty^{-5/2} > 2^{(9-7\gamma)/(\gamma-1)/2}\, \gamma^{-3/2}\, (5-3\gamma)^{-(5-3\gamma)/(\gamma-1)/2} \quad . \tag{2.52}$$

Equation (2.47) in general has two roots for λ_{sh}, say, λ_{sh1} and λ_{sh2}. Further analysis shows that $\lambda_{sh1} < \lambda_{c1} < \lambda_{c2} < \lambda_{sh2}$, i.e., the upstream and downstream sonic points lie between the two roots of equation (2.47). Also from energy considerations, the downstream

solution lies in region II or IV (with respect to downstream sonic point) in figure 2.1(a). The flows corresponding to these two λ_{sh}'s are sketched in figure 2.3. Given $\bar{E}_2$ and β_2, figure 2.3(a) illustrates a stellar wind while figure 2.3(b) illustrates an accretion flow.

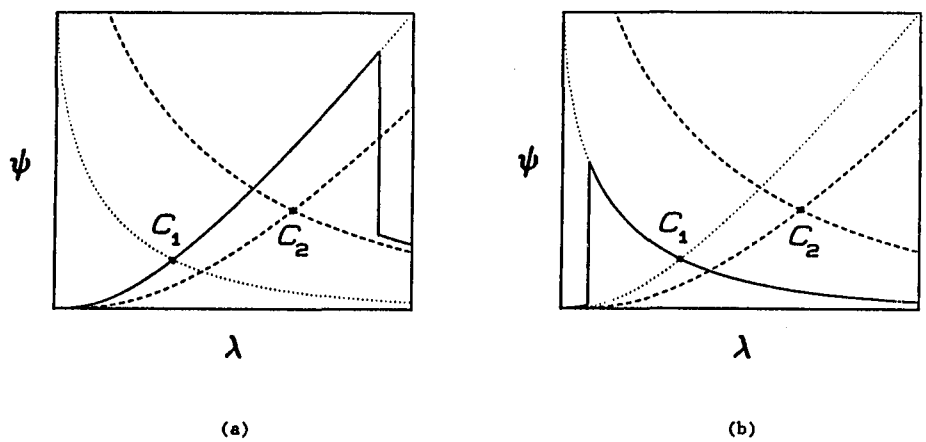

Figure 2.3 Possible Locations of the Shock with One γ
There are two possible values of λ_{sh}: (a) corresponds to a stellar wind flow and (b) corresponds to an accretion flow.

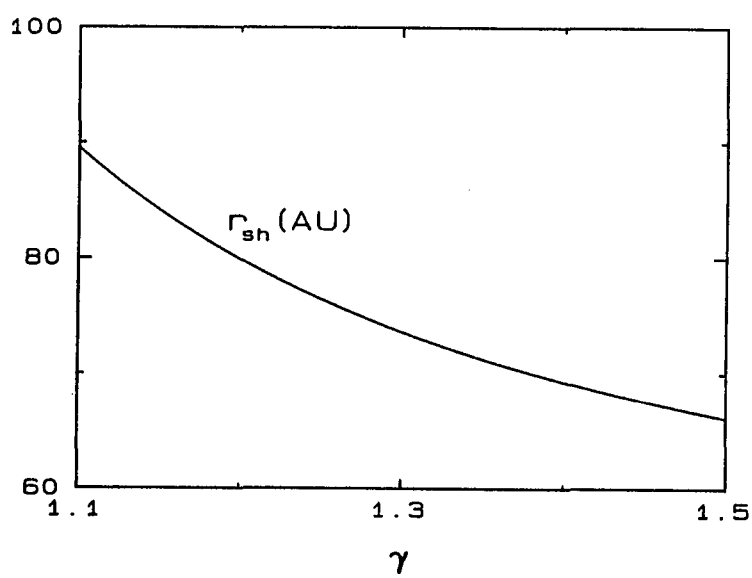

Figure 2.4 Radius of the Stellar Wind Termination Shock with One γ

As an example of the application of equations (2.45) and (2.47) in determining the location of a stellar wind termination shock, consider the case (the Solar wind) where $\dot{M} = 10^{12}$ g s^{-1}, $P_\infty = 1$ eV cm^{-3} and $\rho_\infty = 2*10^{-26}$ g cm^{-3}. The radius of the shock is shown in figure 2.4 as a function of the polytropic index.

§2.2.2 Case $1 < \gamma_1 \leq 3/2$ and $\gamma_1 \leq \gamma_2 \leq 5/3$

In this case equations (2.34) – (2.37) and (2.41) – (2.43) give

$$\frac{M_2^2}{M_1^2} = \frac{\gamma_1}{\gamma_2} \frac{\left[\frac{(\gamma_2+1)}{(\gamma_2-1)} - q\right]}{q\left[\frac{(\gamma_1+1)}{(\gamma_1-1)}q - 1\right]} , \tag{2.53}$$

$$\psi_{2sh} = \alpha \lambda_{sh}^4 , \tag{2.54}$$

where

$$\alpha = \left[\frac{M_2^2}{M_1^2} \frac{\beta_2^{(\gamma_2+1)/2}}{\beta_1^{(\gamma_1+1)/2}} q^{(\gamma_1+1)}\right]^{2/(\gamma_2-\gamma_1)} . \tag{2.55}$$

Equations (2.34) and (2.53) – (2.55) then give

$$\lambda_{sh}^4 = 2 \frac{\gamma_1}{\gamma_2} \frac{\left[q - \frac{\gamma_2(\gamma_1-1)}{\gamma_1(\gamma_2-1)}\right]}{(\gamma_1+1)(q-1)\left[q - \frac{(\gamma_1-1)}{(\gamma_1+1)}\right]} \alpha^{-(\gamma_2+1)/2} \beta_2^{(\gamma_2+1)/2} . \tag{2.56}$$

Substituting (2.54) and (2.56) into (2.36) we obtain

$$\bar{E}_2 = \frac{q\left[q - \frac{\gamma_1(\gamma_2+1)}{\gamma_2(\gamma_1+1)}\right]}{(\gamma_2-1)(q-1)\left[q - \frac{(\gamma_1-1)}{(\gamma_1+1)}\right]} \alpha^{-(\gamma_2-1)/2} \beta_2^{(\gamma_2+1)/2} - \lambda_{sh} \tag{2.57}$$

and this can be written as an equation in q only:

$$\bar{E}_2 = \alpha_1 \, q^{-\gamma_2(\gamma_1-1)/(\gamma_2-\gamma_1)} \left[q - \frac{(\gamma_1-1)}{(\gamma_1+1)}\right]^{(\gamma_1-1)/(\gamma_2-\gamma_1)}$$
$$\cdot \left[q - \frac{\gamma_1(\gamma_2+1)}{\gamma_2(\gamma_1+1)}\right] (q-1)^{-1} \left[\frac{(\gamma_2+1)}{(\gamma_2-1)} - q\right]^{-(\gamma_2-1)/(\gamma_2-\gamma_1)}$$
$$- \alpha_2 \, q^{-\gamma_1(\gamma_2+1)/(\gamma_2-\gamma_1)/4} \left[q - \frac{(\gamma_1-1)}{(\gamma_1+1)}\right]^{(\gamma_1+1)/(\gamma_2-\gamma_1)/4}$$
$$\cdot \left[q - \frac{\gamma_2(\gamma_1-1)}{\gamma_1(\gamma_2-1)}\right]^{1/4} (q-1)^{-1/4} \left[\frac{(\gamma_2+1)}{(\gamma_2-1)} - q\right]^{-(\gamma_2+1)/(\gamma_2-\gamma_1)/4} , \quad (2.58)$$

where

$$\alpha_1 = \frac{\left[\beta_1^{(\gamma_1+1)/2}\right]^{(\gamma_2-1)/(\gamma_2-\gamma_1)}}{\left[\beta_2^{(\gamma_2+1)/2}\right]^{(\gamma_1-1)/(\gamma_2-\gamma_1)}} \frac{1}{(\gamma_2-1)}$$
$$\cdot \left[\frac{\gamma_2(\gamma_1+1)}{\gamma_1(\gamma_1-1)}\right]^{(\gamma_2-1)/(\gamma_2-\gamma_1)} , \quad (2.59)$$

$$\alpha_2 = \frac{\left[\beta_1^{(\gamma_1+1)/2}\right]^{(\gamma_2+1)/(\gamma_2-\gamma_1)/4}}{\left[\beta_2^{(\gamma_2+1)/2}\right]^{(\gamma_1+1)/(\gamma_2-\gamma_1)/4}} \left[\frac{2}{\gamma_1+1}\right]^{1/4}$$
$$\cdot \left[\frac{\gamma_2}{\gamma_1}\right]^{(\gamma_1+1)/(\gamma_2-\gamma_1)/4} \left[\frac{(\gamma_1+1)}{(\gamma_1-1)}\right]^{(\gamma_2+1)/(\gamma_2-\gamma_1)/4} . \quad (2.60)$$

To determine the location of the shock, we first solve equation (2.58) for q, and then determine λ_{sh} from equation (2.56).

The physically relevant solutions of equation (2.58) for q lie in the range $1 < q < \frac{(\gamma_2+1)}{(\gamma_2-1)}$ for $\gamma_2 > \gamma_1$ (and in the range $\frac{\gamma_2(\gamma_1-1)}{\gamma_1(\gamma_2-1)} < q < \frac{(\gamma_2+1)}{(\gamma_2-1)}$ for $\gamma_2 < \gamma_1$). Within the range of the Solar wind parameters (e.g. $\dot{M} = 10^{12}$ g s^{-1} , $P_\infty = 1$ eV cm^{-3} ,

$\rho_\infty = 2*10^{-26}$ g cm^{-3} and $M_o = 2*10^{33}$ g) equation (2.58) in general has three roots for q, say, q_u, q_w and q_a. Substituting these roots in equations (2.41), (2.42) and (2.56) shows that q_u corresponds to an unstable shock, q_w to a stellar wind shock and q_a to an accretion shock. The flow configurations corresponding to these compression ratios are shown in figure 2.5.

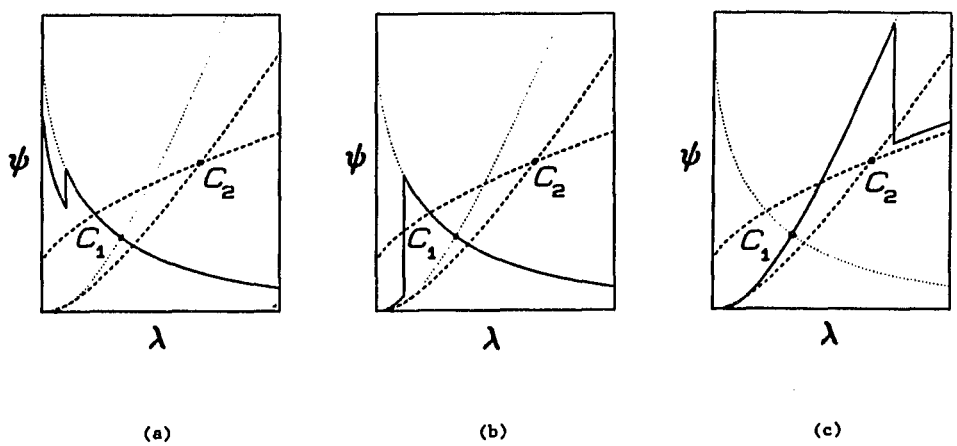

Figure 2.5 Possible Locations of the Shock with Two γ's
There are three possible values of λ_{sh}: (a) corresponds to an unstable shock, (b) corresponds to a stellar wind flow and (c) corresponds to an accretion flow.

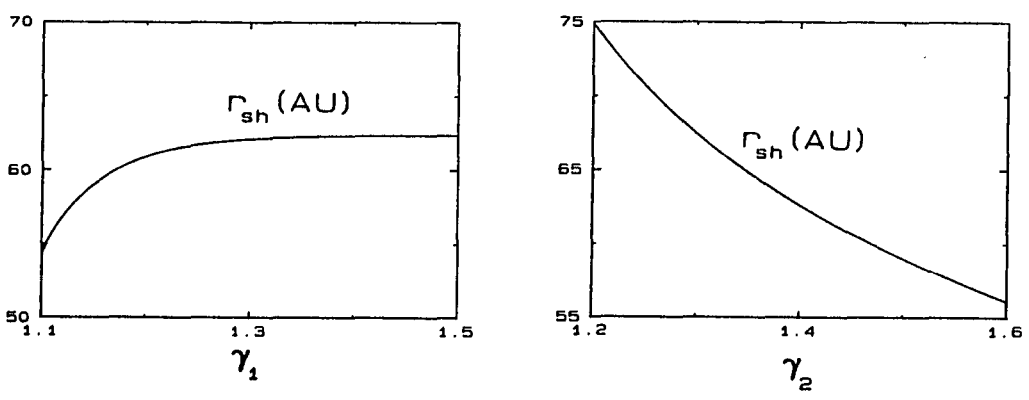

Figure 2.6 Radius of the Stellar Wind Termination Shock with Two γ's
In (a) $\gamma_2 = 5/3$ and in (b) $\gamma_1 = 1.1$.

As an example of the application of equations (2.56) and (2.58) in determining the location of a stellar wind termination shock, consider the case where $\dot{M} = 10^{12}$ g s^{-1}, $P_\infty = 1$ eV cm^{-3}, $\rho_\infty = 2*10^{-26}$ g cm^{-3}. The radius of the shock is shown in figure 2.6 as a function of (a) γ_1 with $\gamma_2 = 5/3$ and (b) γ_2 with $\gamma_1 = 1.1$.

Once the radius of the shock is determined, the stellar wind velocity profile, both inside and outside the shock, is obtained from the energy integral (2.11). Typical flow velocity profiles are shown in figures 2.7 and 2.8, where $\dot{M} = 10^{12}$ g s^{-1}, $P_\infty = 1$ eV cm^{-3} and $\rho_\infty = 2*10^{-26}$ g cm^{-3}. In figure 2.7 $\gamma_1 = \gamma_2 = 1.2$, while in figure 2.8 $\gamma_1 = 1.2$ and $\gamma_2 = 5/3$.

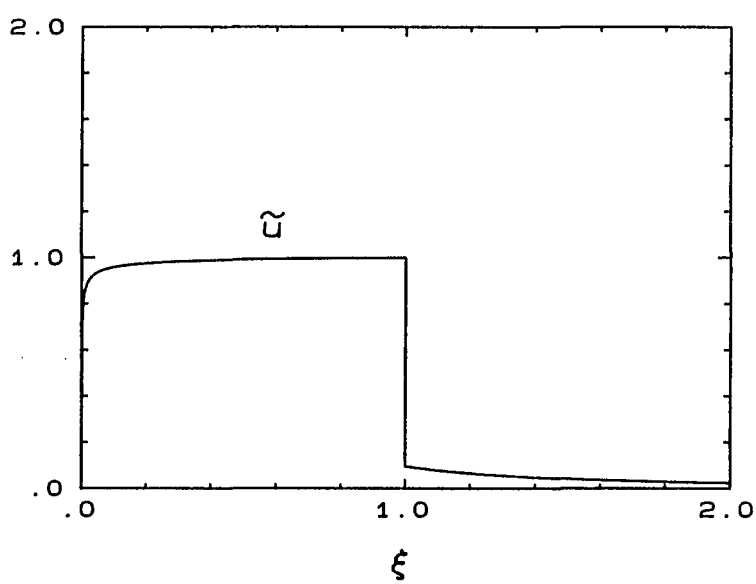

Figure 2.7 One Fluid Polytropic Stellar Wind Velocity Profile with One γ

The plotting quantities are $\xi = r/R$ and $\tilde{u} = u/u_o$, where $R = r_{sh} = 79.9$ A.U. and $u_o = u_{1sh} = 302$ km s^{-1}. The polytropic indices of the gas inside and outside of the shock are $\gamma_1 = \gamma_2 = 1.2$.

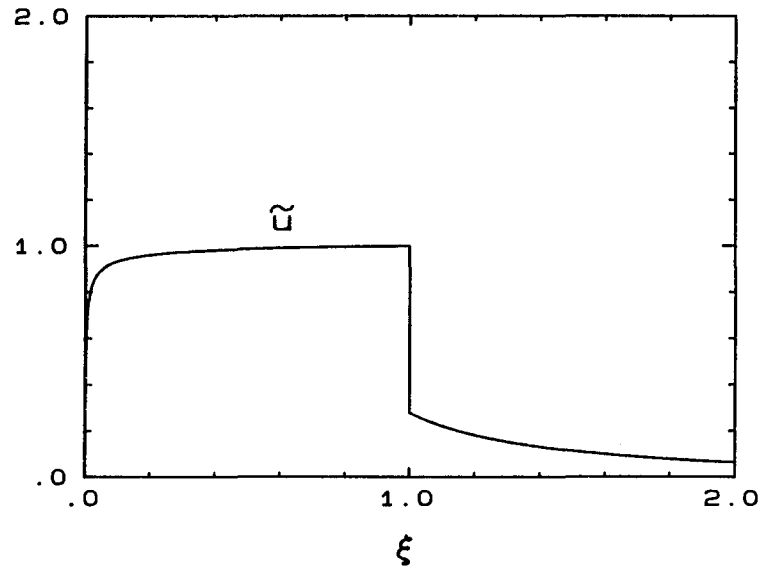

Figure 2.8 One Fluid Polytropic Stellar Wind Velocity Profile with Two γ's
The plotting quantities are $\xi = r/R$ and $\tilde{u} = u/u_o$, where $R = r_{sh} = 60.9$ A.U. and $u_o = u_{1sh} = 192$ km s^{-1}. The polytropic indices of the gas are $\gamma_1 = 1.2$ and $\gamma_2 = 5/3$.

CHAPTER 3

THE EQUATIONS GOVERNING COSMIC-RAY MODIFIED STELLAR WINDS

In Chapter 2, we established the properties of one fluid polytropic stellar wind flows with shocks. In this chapter we address the problem of the modification of a stellar wind flow arising from the interaction between the cosmic-rays and the stellar wind. Various aspects of this problem were first investigated (by means of hydrodynamical models) by Axford and Newman (1965), Jokipii and Parker (1967), and Sousk and Lenchek (1969). Further work on this problem has been carried out by Babayan and Dorman (1984) and Lee and Axford (1986). In addition Axford (1972) and Suess and Dessler (1985) have suggested that the cosmic-rays, by their pressure, may modify the location of the Solar wind termination shock.

We first discuss the physics of the interaction between the cosmic-rays and thermal plasma or gas (§3.1); we then analyze the mathematical properties and singularities of the equations (§3.2) and show (§3.3) that the equations can be reduced to a single nonlinear ordinary differential equation for the normalized fluid velocity variable ψ (equation (2.7) or (3.14)) as a function of the normalized spatial variable λ (equation (2.7) or (3.14)).

§3.1 The Equations and Their Physical Significance

The equations of transport for cosmic-rays propagating in a highly conducting moving plasma, such as the Solar wind, were first established by Parker (1965a), Dolginov and Toptygin (1966, 1967, 1968) and Gleeson and Axford (1967) (see also Jokipii and Parker 1967, 1970; Skilling 1971, 1975; Webb and Gleeson 1979). The cosmic-rays are coupled to the background plasma flow via scattering with magnetohydrodynamic and plasma waves or turbulence (such as Alfvén waves) travelling through the plasma. The main physical mechanism by which the cosmic-rays are scattered is thought to be gyro-resonant interaction with waves of wavelength comparable to the particle gyro-radius (see e.g. Jokipii 1966, 1967). The net effect is that the cosmic-rays tend to be convected along with the background plasma (fluid) flow as they diffuse through the magnetic irregularities carried by the fluid. In the mean wave frame, the cosmic-rays can change their energy due to interaction with random electric fields. This process is known as second order Fermi acceleration (see e.g. Hall and Sturrock 1967; Melrose 1980). Second order Fermi acceleration also results from particle scattering between Alfvén waves travelling in opposite directions in the fluid frame (see Skilling 1975). In the Solar wind, the energy changes of particles from this mechanism can usually be neglected, and the scattering of the cosmic-rays in the wave frame to a first approximation is magnetostatic, so that the cosmic-rays conserve their energy, but change their momentum during scattering. Viewed from a stationary inertial reference frame, magnetostatic scattering can

result in a net cosmic-ray energy change, with the cosmic-rays gaining energy in head-on collisions with the scatterers and losing energy in overtaking collisions.

At a hydrodynamical level, the cosmic-rays may modify the background flow (thermal plasma or gas) via their pressure gradient, ∇P_c, with the net energy transfer rate (per unit volume) from the fluid (via the waves) to the cosmic-rays being given by $\vec{V}\cdot\nabla P_c$, where $\vec{V}$ is the velocity of the scattering wave field ($\vec{V} = \vec{u} + \vec{V}_w$, where $\vec{u}$ is the velocity of the fluid and $\vec{V}_w$ is the phase velocity of the waves relative to the plasma). This hydrodynamical description of the interaction between the cosmic-rays, waves and thermal fluid has been used extensively in self-consistent hydrodynamical models of cosmic-ray shock acceleration (e.g. Axford, Leer and Skadron 1977; Drury and Völk 1981; Eichler 1981; Axford, Leer and McKenzie 1982; McKenzie and Völk 1982; Webb 1983; Völk, Drury and McKenzie 1984; Achterburg, Blandford and Periwal 1984; Webb, Drury and Völk 1986).

The above hydrodynamical model is adapted in the present chapter to describe the self-consistent interaction of cosmic-rays with stellar wind flows. As in the simpler hydrodynamical models of cosmic-ray shock acceleration (e.g. Drury and Völk 1981; Axford, Leer and McKenzie 1982), we assume that the waves may essentially be regarded as magnetostatic scattering centres embedded in the flow ($|\vec{V}_w| \ll |\vec{u}|$) and that the only effect of the waves is to determine the hydrodynamical cosmic-ray diffusion coefficient, κ. Thus for example, the modification of the fluid flow due to the wave pressure force is neglected.

For steady state spherically symmetric winds, the interaction between the wind and cosmic-rays is governed by the total mass, momentum and energy equations for the system:

$$\frac{1}{r^2}\frac{d}{dr}(r^2 \rho_g u) = 0 \quad , \tag{3.1}$$

$$\rho_g u \frac{du}{dr} = -\frac{dP_g}{dr} - \frac{dP_c}{dr} - \rho_g \frac{GM_o}{r^2} \quad , \tag{3.2}$$

$$\frac{1}{r^2}\frac{d}{dr}\left[r^2 \rho_g u \left(\frac{1}{2}u^2 + \frac{\gamma_g}{(\gamma_g-1)}\frac{P_g}{\rho_g} - \frac{GM_o}{r}\right) + r^2 F_c\right] = 0 \quad , \tag{3.3}$$

supplemented by the cosmic-ray energy equation

$$\frac{1}{r^2}\frac{d}{dr}(r^2 F_c) = u\frac{dP_c}{dr} \quad , \tag{3.4}$$

describing the energy transfer between the wind and cosmic-rays, where

$$F_c = \frac{\gamma_c}{(\gamma_c-1)} P_c u - \frac{1}{(\gamma_c-1)} \kappa \frac{dP_c}{dr} \quad , \tag{3.5}$$

is the cosmic-ray energy flux. In equations (3.1) – (3.5), P_g, ρ_g, u and γ_g denote the thermal gas (or plasma) pressure, density, radial flow velocity and polytropic index; γ_c is the cosmic-ray polytropic (or adiabatic) index. The cosmic-ray energy density, E_c, and pressure, P_c, and γ_c are related by the polytropic relation (see appendix B)

$$E_c = \frac{1}{(\gamma_c-1)} P_c \quad . \tag{3.6}$$

In the model the cosmic-rays are considered to be a hot, low density gas with a pressure comparable to that of the thermal gas (the background flow), but with negligible density and mass flux. Equation (3.2) shows that a wind flow will be decelerated by a positive cosmic-ray pressure gradient ($\frac{dP_c}{dr} > 0$), as occurs, for example, in the Solar wind. Note also in equation (3.4) that the net energy transfer

rate (per unit volume) from the wind to the cosmic-rays is $u \frac{dP_c}{dr}$ (c.f. Jokipii and Parker 1967). A derivation of the cosmic-ray energy equation (3.4) is given in appendix B.

By combining the cosmic-ray energy equation (3.4) with the total energy equation (3.3), we obtain the energy equation for the thermal gas in the form:

$$\frac{1}{r^2}\frac{d}{dr}\left[r^2 \rho_g u \left(\frac{1}{2}u^2 + \frac{\gamma_g}{(\gamma_g-1)}\frac{P_g}{\rho_g} - \frac{GM_o}{r}\right)\right] = -u\frac{dP_c}{dr} \quad , \qquad (3.7)$$

showing explicitly that the rate at which gas loses energy to the cosmic-rays (per unit volume) is $u \frac{dP_c}{dr}$. Eliminating the cosmic-ray pressure gradient term in equation (3.7), by means of the momentum equation (3.2) and using the mass continuity equation (3.1) we find

$$\frac{d}{dr}\left[P_g/\rho_g^{\gamma_g}\right] = 0 \quad , \qquad (3.8)$$

which shows that the gas entropy is conserved following the flow and

$$P_g = A_g \rho_g^{\gamma_g} \quad , \qquad (3.9)$$

(except at gas shocks where $P_g/\rho_g^{\gamma_g}$ jumps discontinuously), where A_g is a constant dependent only on the gas entropy. Equation (3.8) is the energy equation for the gas in the frame moving with the fluid (the co-moving frame). This equation shows that there is no energy transfer between the cosmic-rays and thermal plasma in the fluid frame. This result is to be expected since the cosmic-rays are assumed to scatter off magnetostatic irregularities embedded in the flow. However, there is a momentum transfer between the cosmic-rays and thermal plasma in this frame, and this momentum transfer results in the energy exchange

term $u \frac{dP_c}{dr}$ in the fixed frame cosmic-ray energy equation (3.4).

The cosmic-ray energy equation (3.4) can be re-written as:

$$\frac{1}{r^2} \frac{d}{dr}\left[r^2 \kappa \frac{dP_c}{dr}\right] - u \frac{dP_c}{dr} - \gamma_c \frac{1}{r^2} \frac{d}{dr}(r^2 u) P_c = 0 \quad , \qquad (3.10)$$

or alternatively, using the mass continuity equation (3.1), we obtain the cosmic-ray energy equation in the thermodynamical form:

$$u \rho_g^{\gamma_c} \frac{d}{dr}\left[P_c/\rho_g^{\gamma_c}\right] - \frac{1}{r^2} \frac{d}{dr}\left[r^2 \kappa \frac{dP_c}{dr}\right] = 0 \quad . \qquad (3.11)$$

Note that ρ_g is the density of the thermal gas, and not the cosmic-ray mass density (which is assumed to be negligible).

The nature of the cosmic-ray interaction with the thermal plasma becomes relatively transparent in the limits $\kappa \to \infty$ and $\kappa \to 0$. In the limit $\kappa \to \infty$, the diffusive term $\frac{1}{r^2} \frac{d}{dr}\left[r^2 \kappa \frac{dP_c}{dr}\right]$ in equation (3.10) can remain finite only if $\frac{dP_c}{dr} \to 0$, and the diffusive term is then essentially balanced by the term $\gamma_c \frac{1}{r^2} \frac{d}{dr}(r^2 u) P_c$. In this limit there is no interaction between the cosmic-rays and thermal plasma (the scattering mean free path for the cosmic-rays $\Lambda \to \infty$), and since $\frac{dP_c}{dr} \to 0$, equations (3.1) – (3.3) reduce to the one fluid polytropic stellar wind equations (2.1) – (2.3).

For κ identically equal to zero, equation (3.11) implies that the cosmic-rays are compressed adiabatically following the flow. With $\kappa \equiv 0$, equations (3.1) – (3.11) reduce to the equations governing two fluid polytropic stellar winds, which have been investigated by Summers (1982). The work of Summers concerned the nature of electron-proton,

two fluid stellar winds in which the electrons and protons are polytropic gases. However, the cosmic-ray stellar wind equations with $\kappa \equiv 0$ may exhibit a radically different behaviour than the same equations with κ small, (but not zero), especially in the regions of the flow where $\frac{dP_c}{dr}$ becomes large (e.g. as in a boundary layer). Thus for example if $\kappa \to 0$ and $\frac{dP_c}{dr} \to \infty$ in equation (3.11), in such a way that $\frac{1}{r^2}\frac{d}{dr}\left[r^2 \kappa \frac{dP_c}{dr}\right]$ is finite, then clearly the cosmic-rays cease to behave adiabatically. This phenomenon is related to the occurrence of boundary layers in singular perturbation theory for differential equations, in which the behaviour of the equations may be markedly different in regions where the higher order derivatives are large (see e.g. Bender and Orszag 1978; Kevorkian and Cole 1981). Overall then, in the limit $\kappa \to 0$, the cosmic-rays are essentially compressed adiabatically in regions of the flow where $\frac{1}{r^2}\frac{d}{dr}\left[r^2 \kappa \frac{dP_c}{dr}\right]$ is sufficiently small.

The limit $\kappa \to 0$ ($\Lambda \to 0$), corresponds to a strong interaction between the cosmic-rays and thermal plasma, whereas the limit $\kappa \to \infty$ ($\Lambda \to \infty$) corresponds to a weak interaction between the two components.

From equations (3.1) and (3.3) we obtain the conserved mass flux, j, and total energy constant, E:

$$j \equiv \rho_g u r^2 \quad , \tag{3.12}$$

$$E \equiv \frac{1}{2}u^2 + \frac{\gamma_g}{(\gamma_g - 1)}\frac{P_g}{\rho_g} - \frac{GM_o}{r} + \frac{\gamma_c}{(\gamma_c - 1)}\frac{P_c}{\rho_g} - \frac{1}{(\gamma_c - 1)}\frac{r^2 \kappa}{j}\frac{dP_c}{dr} \quad . \tag{3.13}$$

Since the total energy of the system is conserved (c.f. equation (3.13)), a change in the energy of one component of the system results in compensating energy changes of the other components.

§3.2 Properties and Singularities of the Equations

To analyze the mathematical properties of the equations we introduce the dimensionless variables:

$$\lambda \equiv \frac{GM_o}{r}\left(\frac{m_g}{kT_o}\right) \quad , \quad \psi \equiv u^2\left(\frac{m_g}{kT_o}\right) \quad , \quad \bar{P}_c \equiv \frac{P_c}{\rho_o}\left(\frac{m_g}{kT_o}\right) \quad . \tag{3.14}$$

The dimensionless variables λ and ψ, and constants m_g, k and T_o are defined in equation (2.7) et seq, and ρ_o is defined by equation (2.12) or (3.15). In terms of these variables, the mass flux (3.12) and the adiabatic gas law (3.9) yield the gas density ρ_g and pressure P_g in the form:

$$\rho_g = \rho_o \psi^{-1/2} \lambda^2 \quad , \tag{3.15}$$

$$P_g = \frac{1}{\gamma_g}\rho_o\left(\frac{m_g}{kT_o}\right)^{-1} \beta^{(\gamma_g+1)/2} \psi^{-\gamma_g/2} \lambda^{2\gamma_g} \quad , \tag{3.16}$$

where

$$\rho_o \equiv j\,(GM_o)^{-2}\left(\frac{m_g}{kT_o}\right)^{-3/2} \quad , \tag{3.17}$$

$$\beta \equiv \left[\gamma_g A_g \rho_o^{(\gamma_g-1)}\left(\frac{m_g}{kT_o}\right)\right]^{2/(\gamma_g+1)} \quad . \tag{3.18}$$

Similarly the momentum equation (3.2), the energy integral (3.13) and the cosmic-ray energy equation (3.4) become:

$$\frac{1}{2}\left[1 - \beta^{(\gamma_g+1)/2} \psi^{-(\gamma_g+1)/2} \lambda^{2(\gamma_g-1)}\right]\frac{d\psi}{d\lambda}$$

$$= 1 - 2\beta^{(\gamma_g+1)/2} \psi^{-(\gamma_g-1)/2} \lambda^{(2\gamma_g-3)} - \psi^{1/2}\lambda^{-2}\frac{d\bar{P}_c}{d\lambda} \quad , \tag{3.19}$$

$$\bar{E} = \frac{1}{2}\psi - \lambda + \frac{1}{(\gamma_g-1)}\beta^{(\gamma_g+1)/2}\psi^{-(\gamma_g-1)/2}\lambda^{2(\gamma_g-1)}$$

$$+ \frac{\gamma_c}{(\gamma_c-1)}\psi^{1/2}\lambda^{-2}\bar{P}_c + \frac{1}{(\gamma_c-1)}\bar{\kappa}\frac{d\bar{P}_c}{d\lambda} \quad , \tag{3.20}$$

$$\frac{d}{d\lambda}\left[\bar{\kappa}\frac{d\bar{P}_c}{d\lambda}\right] + \psi^{1/2}\lambda^{-2}\frac{d\bar{P}_c}{d\lambda} - \gamma_c\psi^{1/2}\lambda^{-2}\left[\frac{2}{\lambda} - \frac{1}{2\psi}\frac{d\psi}{d\lambda}\right]\bar{P}_c = 0 \quad , \tag{3.21}$$

where

$$\bar{E} = E\left(\frac{m_g}{kT_o}\right) \quad , \tag{3.22}$$

$$\bar{\kappa} = \kappa (GM_o)^{-1}\left(\frac{m_g}{kT_o}\right)^{-\frac{1}{2}} \quad . \tag{3.23}$$

Only two of the equations (3.19) – (3.21) are independent. In order to analyze the singularities (and mathematical properties) of equations (3.19) – (3.21) it is useful to re-write the equations in an autonomous form. Equations (3.19) and (3.20) can be written as an autonomous system, in which λ, ψ and $\bar{P}_c$ depend on a dummy time variable, s (we call this the *Third Order Autonomous System*). Alternatively, equation (3.19) and (3.21) can be written as a *Fourth Order Autonomous System* in which λ, ψ, $\bar{P}_c$ and $\bar{D}_c$ ($\bar{D}_c = \frac{1}{(\gamma_c-1)}\bar{\kappa}\frac{d\bar{P}_c}{d\lambda}$) are regarded as functions of a dummy time variable, s. One of the advantages of the 4^{th} order autonomous system is that the energy integral (3.20) may be used to check the accuracy of the numerical scheme to integrate the system of equations.

We now show that the 3^{rd} order autonomous system has a line of singularities in $(\lambda,\psi,\bar{P}_c)$ space, whereas the 4^{th} order autonomous system has a two dimensional hypersurface of singularities in $(\lambda,\psi,\bar{P}_c,\bar{D}_c)$

space. This behaviour is in contrast to the one fluid polytropic stellar wind model of chapter 2, where the equations have two singular points only, namely, the sonic point at $(\lambda,\psi) = (\lambda_c,\psi_c)$ (equations (2.18) and (2.19)), and the origin $(\lambda,\psi) = (0,0)$.

§3.2.1 The Third Order Autonomous System

By introducing a dummy time variable, s, equations (3.19) and (3.20) can be written in the autonomous form:

$$\frac{d}{ds}\begin{bmatrix}\lambda\\ \psi\\ \bar{P}_c\end{bmatrix} = \begin{bmatrix}Q\\ P\\ QR\end{bmatrix} , \tag{3.24}$$

where

$$P \equiv 1 - 2\beta^{(\gamma_g+1)/2}\psi^{-(\gamma_g-1)/2}\lambda^{(2\gamma_g-3)} - \psi^{1/2}\lambda^{-2}R , \tag{3.25}$$

$$Q \equiv \frac{1}{2}\left[1 - \beta^{(\gamma_g+1)/2}\psi^{-(\gamma_g+1)/2}\lambda^{2(\gamma_g-1)}\right] , \tag{3.26}$$

$$R \equiv (\gamma_c-1)\frac{1}{\kappa}\left[\bar{E} - \frac{1}{2}\psi + \lambda - \frac{1}{(\gamma_g-1)}\beta^{(\gamma_g+1)/2}\cdot\psi^{-(\gamma_g-1)/2}\lambda^{2(\gamma_g-1)} - \frac{\gamma_c}{(\gamma_c-1)}\psi^{1/2}\lambda^{-2}\bar{P}_c\right] . \tag{3.27}$$

Critical points of the system (3.24) occur when $(P,Q,QR)^T$ is a zero vector, i.e., when $P = Q = 0$. The third component of the vector $(P,Q,QR)^T$ is then automatically zero, and in general $R \neq 0$ at a critical point. Using expressions (3.25) – (3.27) for **P**, **Q** and **R** we find that the critical points lie on a line (we called it the *Critical Line*) in $(\lambda,\psi,\bar{P}_c)$ space, which can be expressed in a parametric form in terms of a parameter, τ, as:

$$\lambda = \lambda_c \equiv \tau , \tag{3.28}$$

$$\psi = \psi_c = \beta\, \tau^{4(\gamma_g-1)/(\gamma_g+1)} , \tag{3.29}$$

$$\bar{P}_c = \bar{P}_{cc} = \frac{(\gamma_c-1)}{\gamma_c}\left[\frac{2}{(\gamma_c-1)}\,\bar{\kappa}\,\tau^3 - \frac{1}{(\gamma_c-1)}\,\bar{\kappa}\,\beta^{-1}\,\tau^{8/(\gamma_g+1)} + \bar{E}\,\beta^{-1/2}\,\tau^{4/(\gamma_g+1)} - \frac{1}{2}\,\frac{(\gamma_g+1)}{(\gamma_g-1)}\,\beta^{1/2}\,\tau^{4\gamma_g/(\gamma_g+1)} + \beta^{-1/2}\,\tau^{(\gamma_g+5)/(\gamma_g+1)}\right] . \tag{3.30}$$

In physical terms, the critical line is the locus of points in $(\lambda,\psi,\bar{P}_c)$ space along which the fluid speed matches the thermal gas sound speed (i.e., $u^2 = \gamma_g P_g/\rho_g$) and the acceleration of the fluid is zero (i.e., $u\,\frac{du}{dr} = 0$).

A typical critical line is shown in figure 3.1 for the case $\gamma_g = 1.2$, $\gamma_c = 4/3$, $\beta = 1/2$, $\bar{\kappa} = 10$ and $\bar{E} = 1$. The projection of the critical line on the (λ,ψ) plane (figure 3.1(a)) is simply the gas sonic line where $u^2 = \gamma_g P_g/\rho_g$.

The qualitative behaviour of the solution curves of the system (3.24) near the critical line (3.28) – (3.30) can be studied by linearizing the system of equations around this line. The linearized system of equations can be represented in matrix form:

$$\frac{d}{ds}\begin{bmatrix} \lambda-\lambda_c \\ \psi-\psi_c \\ \bar{P}_c-\bar{P}_{cc} \end{bmatrix} = \underline{\underline{A}}_3 \begin{bmatrix} \lambda-\lambda_c \\ \psi-\psi_c \\ \bar{P}_c-\bar{P}_{cc} \end{bmatrix} , \tag{3.31}$$

where

$$\underline{\underline{A}}_3 = \begin{bmatrix} Q_\lambda & Q_\psi & Q_{\bar{P}_c} \\ P_\lambda & P_\psi & P_{\bar{P}_c} \\ (QR)_\lambda & (QR)_\psi & (QR)_{\bar{P}_c} \end{bmatrix}_c , \tag{3.32}$$

the subscript c denotes the entries of the matrix are evaluated on the

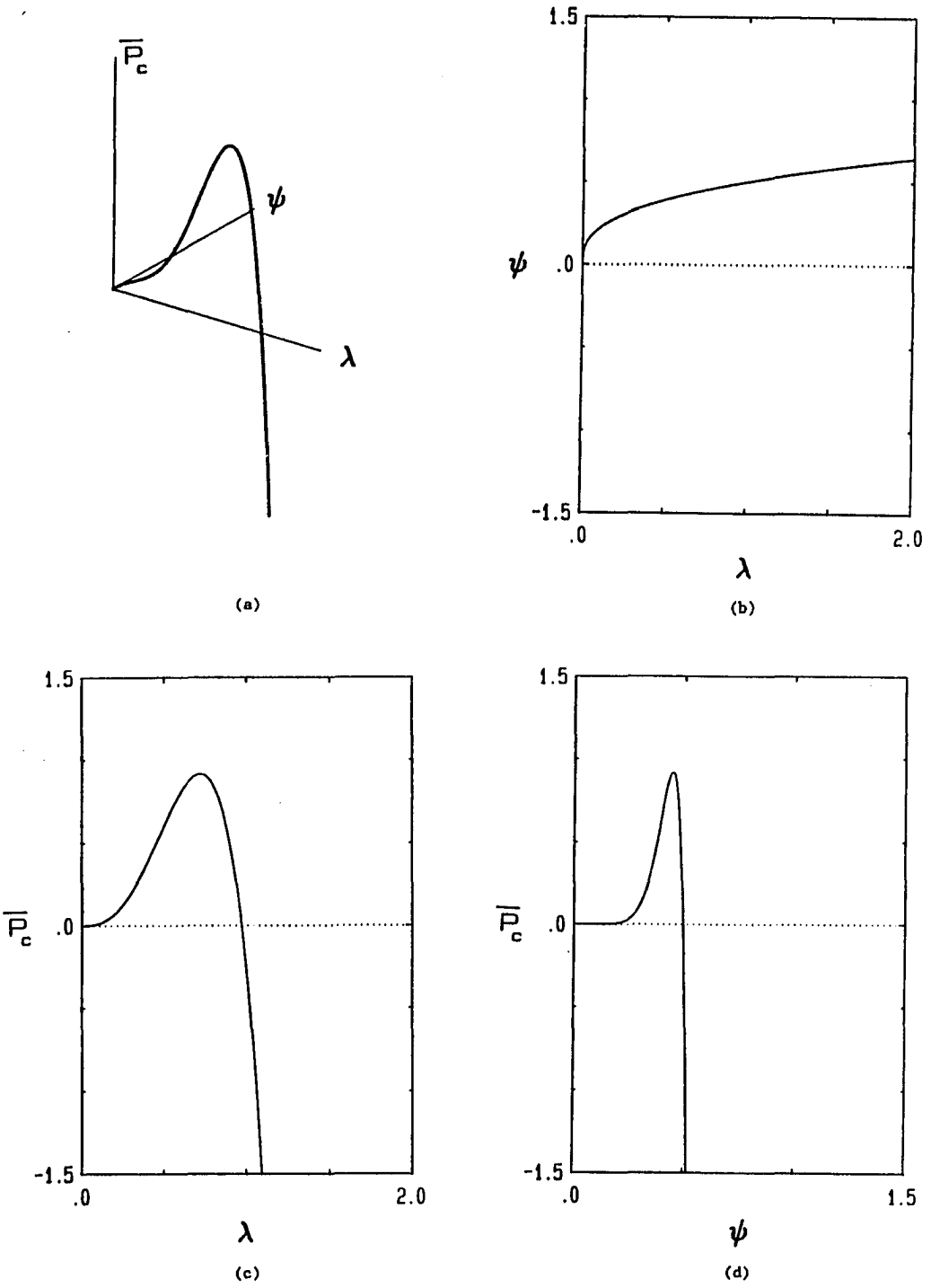

Figure 3.1 Critical Line of the 3rd Order Autonomous System

The critical line is plotted (a) in the 3-D $(\lambda,\psi,\bar{P}_c)$ space and (b) – (d) on the 2-D projections on the (λ,ψ), $(\lambda,\bar{P}_c)$ and $(\psi,\bar{P}_c)$ planes respectively.

critical line, and the notation $Q_\lambda \equiv \frac{\partial Q}{\partial \lambda}$, etc., has been adopted. For simplicity, we assume that the cosmic-ray diffusion coefficient, κ (or $\bar{\kappa}$) is constant. The partial derivatives in the matrix $\underline{\underline{A}}_3$ are then given by:

$$Q_\lambda\big|_c = -(\gamma_g-1)\,\tau^{-1} \quad , \tag{3.33}$$

$$Q_\psi\big|_c = \frac{1}{4}(\gamma_g+1)\,\beta^{-1}\,\tau^{-4(\gamma_g-1)/(\gamma_g+1)} \quad , \tag{3.34}$$

$$Q_{\bar{P}_c}\big|_c = 0 \quad , \tag{3.35}$$

$$\begin{aligned} P_\lambda\big|_c = {} & -2\,(2\gamma_g+1)\,\beta\,\tau^{-2(3-\gamma_g)/(\gamma_g+1)} + 4\,\tau^{-1} \\ & - 2\,(\gamma_c-1)\,\frac{\bar{E}}{\kappa}\,\beta^{1/2}\,\tau^{-(\gamma_g+5)/(\gamma_g+1)} \\ & + \frac{(3\gamma_g-1)}{(\gamma_g-1)}\,(\gamma_c-1)\,\frac{1}{\kappa}\,\beta^{3/2}\,\tau^{-3(3-\gamma_g)/(\gamma_g+1)} \\ & - 3\,(\gamma_c-1)\,\frac{1}{\kappa}\,\beta^{1/2}\,\tau^{-4/(\gamma_g+1)} \quad , \end{aligned} \tag{3.36}$$

$$\begin{aligned} P_\psi\big|_c = {} & (\gamma_g+1)\,\tau^{-1} - \beta^{-1}\,\tau^{-4(\gamma_g-1)/(\gamma_g+1)} \\ & + \frac{1}{2}(\gamma_c-1)\,\frac{\bar{E}}{\kappa}\,\beta^{-1/2}\,\tau^{-4\gamma_g/(\gamma_g+1)} \\ & - \frac{1}{4}\,\frac{(\gamma_g+1)}{(\gamma_g-1)}\,(\gamma_c-1)\,\frac{1}{\kappa}\,\beta^{1/2}\,\tau^{-4/(\gamma_g+1)} \\ & + \frac{1}{2}(\gamma_c-1)\,\frac{1}{\kappa}\,\beta^{-1/2}\,\tau^{-(3\gamma_g-1)/(\gamma_g+1)} \quad , \end{aligned} \tag{3.37}$$

$$P_{\bar{P}_c}\big|_c = \gamma_c\,\frac{1}{\kappa}\,\beta\,\tau^{-8/(\gamma_g+1)} \quad , \tag{3.38}$$

$$(QR)_\lambda\big|_c = (Q_\lambda R)\big|_c \quad , \tag{3.39}$$

$$(QR)_\psi\big|_c = (Q_\psi R)\big|_c \quad , \tag{3.40}$$

$$(QR)_{\bar{P}_c}\big|_c = (Q_{\bar{P}_c} R)\big|_c \quad , \tag{3.41}$$

where the symbol $|_c$ denotes evaluation of the derivatives on the

critical line.

The character of the solution curves in the neighbourhood of a given point on the critical line depends on the eigenvalues of the matrix $\underline{\underline{A}}_3$ (3.32) evaluated at that point. The eigenvectors corresponding to these eigenvalues define a set of preferred (asymptotic) directions for the solution curves as they approach the critical point. The eigenvector $\vec{X}_\mu$ and the corresponding eigenvalue μ satisfy

$$\underline{\underline{A}}_3 \vec{X}_\mu = \mu \vec{X}_\mu \quad . \tag{3.42}$$

For a non-trivial solution for $\vec{X}_\mu$ we require that μ satisfy the eigenvalue (or characteristic) equation,

$$\det(\underline{\underline{A}}_3 - \mu \underline{\underline{I}}) = 0 \quad , \tag{3.43}$$

where $\underline{\underline{I}}$ is the identity matrix. Using the matrix $\underline{\underline{A}}_3$ in equation (3.32), the characteristic equation (3.43) can be reduced to

$$\mu \left[\mu^2 - (Q_\lambda + P_\psi + Q_{\overline{P}_c} R)\big|_c \mu \right.$$
$$\left. + (Q_\lambda P_\psi - Q_\psi P_\lambda + Q_{\overline{P}_c} P_\psi R - P_{\overline{P}_c} Q_\psi R)\big|_c\right] = 0 \quad . \tag{3.44}$$

Using the partial derivatives (3.33) – (3.41) in equation (3.44), we obtain

$$\mu_o = 0 \quad , \tag{3.45}$$

$$\mu_\pm = \frac{1}{2}\left[b \pm (b^2 - 4c)^{1/2}\right] \tag{3.46}$$

for the eigenvalues, where

$$b = 2\tau^{-1} - \beta^{-1}\tau^{-4(\gamma_g-1)/(\gamma_g+1)}$$
$$+ \frac{1}{2}(\gamma_c - 1)\frac{\overline{E}}{\kappa}\beta^{-1/2}\tau^{-4\gamma_g/(\gamma_g+1)}$$

$$- \frac{1}{4} \frac{(\gamma_g+1)}{(\gamma_g-1)} (\gamma_c-1) \frac{1}{\bar{\kappa}} \beta^{1/2} \tau^{-4/(\gamma_g+1)}$$

$$+ \frac{1}{2} (\gamma_c-1) \frac{1}{\bar{\kappa}} \beta^{-1/2} \tau^{-(3\gamma_g-1)/(\gamma_g+1)} , \qquad (3.47)$$

$$c = \frac{3}{2} (\gamma_g+1) \tau^{-2} - 2 \beta^{-1} \tau^{-(5\gamma_g-3)/(\gamma_g+1)}$$

$$+ (\gamma_c-1) \frac{\bar{E}}{\bar{\kappa}} \beta^{-1/2} \tau^{-(5\gamma_g+1)/(\gamma_g+1)}$$

$$+ \frac{1}{2} \left[\gamma_c (\gamma_g+1) - \gamma_g \frac{(\gamma_g+1)}{(\gamma_g-1)} (\gamma_c-1)\right] \frac{1}{\bar{\kappa}} \beta^{1/2} \tau^{-(\gamma_g+5)/(\gamma_g+1)}$$

$$+ \frac{1}{4} \left[(\gamma_g+5) (\gamma_c-1) - \gamma_c (\gamma_g+1)\right] \frac{1}{\bar{\kappa}} \beta^{-1/2} \tau^{-4\gamma_g/(\gamma_g+1)} , \qquad (3.48)$$

and the parameter τ specifies the location along the critical line.

It is instructive to consider the nature of the critical line (3.28) – (3.30) in the limit as $\bar{\kappa} \to \infty$ (i.e., $\kappa \to \infty$) in which there is a weak interaction between the cosmic-rays and the background plasma. In this limit, it is necessary that τ be restricted to the neighbourhood of

$$\tau = (2\beta)^{(\gamma_g+1)/(5-3\gamma_g)} , \qquad (3.49)$$

in order that the cosmic-ray pressure on the critical line (see equation (3.30)) remain finite. Substituting the value (3.49) for τ into equations (3.28) and (3.29), we find that the physically relevant part of the critical line, shrinks to the critical point (λ_c, ψ_c) where

$$\lambda_c = (2\beta)^{(\gamma_g+1)/(5-3\gamma_g)} , \qquad (3.50)$$

$$\psi_c = \frac{1}{2} \lambda_c . \qquad (3.51)$$

This is the critical point of the one fluid polytropic stellar wind discussed in chapter 2 (equations (2.18) and (2.19)). This is expected, since as $\kappa \to \infty$, there is no interaction between the thermal plasma and

the cosmic-rays, so that the cosmic-rays cease to influence the background flow. In this limit, the eigenvalues (3.46) approach the eigenvalues (A.8) characteristic of one fluid polytropic stellar winds, and the critical point is a saddle point for $1 < \gamma_g < 5/3$.

In general, different parts of the critical line (3.28) – (3.30) correspond to different kinds of critical points. As mentioned previously, the behaviour of the solution curves near the critical line depends on the eigenvalues and the directions of the eigenvectors of the matrix $\underline{\underline{A}}_3$ in (3.32). Since the eigenvalues μ_o and $\mu_\pm$ are in general distinct (see equations (3.45) – (3.48)), the matrix $\underline{\underline{A}}_3$ can be diagonalized almost everywhere (except perhaps at some points where $b^2 = 4\,c$ or $c = 0$) along the critical line. So in general $\underline{\underline{A}}_3$ has three independent eigenvectors $\vec{X}_{\mu_o}$ and $\vec{X}_{\mu_\pm}$. The eigenvector $\vec{X}_{\mu_o}$ corresponding to the eigenvalue $\mu = \mu_o = 0$ is in fact tangent to the critical line (see appendix C).

The values of μ_+ and μ_-, at a particular critical point, depend on the values of b and c in equations (3.47) and (3.48) at the point. The critical point is:

(a) a node if $c > 0$ and $b^2 - 4\,c > 0$, so that μ_+ and μ_- are real and of the same sign;

(b) a focus if $b^2 - 4\,c < 0$, so that μ_+ and μ_- are complex conjugates; or

(c) a saddle point if $c < 0$ and $b^2 - 4\,c > 0$, so that μ_+ and μ_- are real and of the opposite sign.

Figure 3.2 shows b, c and $b^2 - 4\,c$ as functions of the

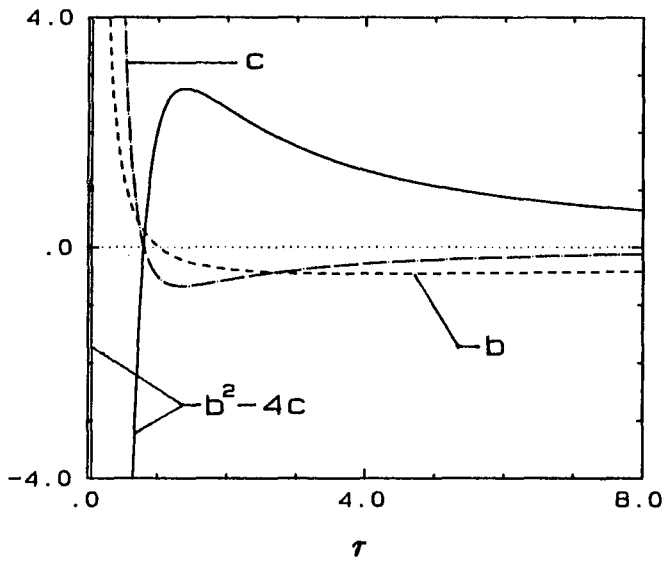

Figure 3.2 The Graphs of b, c and b^2 - 4c as Functions of τ

parameter τ, which determines the location of a particular critical point on the critical line, for the case $\gamma_g = 1.3$, $\gamma_c = 4/3$, $\beta = 1/2$, $\bar{\kappa} = 1$ and $\bar{E} = 1$. The functions b and c are seen to be positive at small τ, changing to negative at larger τ, and tend to zero as τ tends to positive infinity. The function (b^2 - 4 c) changes from positive to negative then to positive with increasing τ ($\tau > 0$), and tends to zero as τ tends to positive infinity. If the normalized diffusion coefficient, $\bar{\kappa}$, is sufficiently small, b^2 - 4 c is positive for all τ. The critical point is then either a node or a saddle point. The curves in figure 3.2 show that as we move along the critical line the critical points are nodes at small τ ($\tau > 0$), changing to foci at larger τ, and then to saddle points at still larger τ.

The autonomous system (3.24) can be integrated numerically as an initial value problem by using a Runge-Kutta integration routine. Typical solution curves are shown in figure 3.3 for the case $\gamma_g = 1.2$,

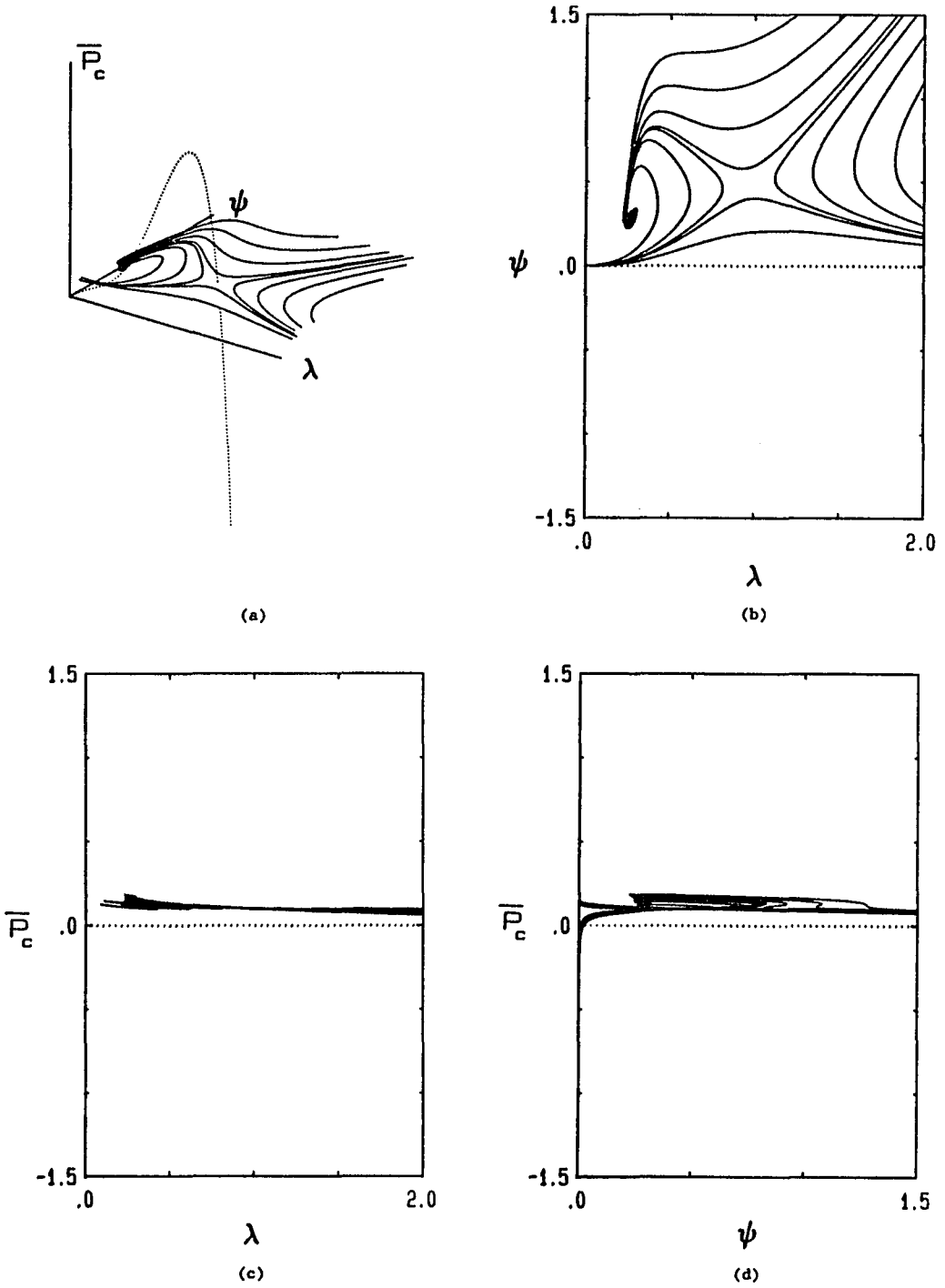

Figure 3.3 Solution Curves of the 3rd Order Autonomous System

Some of the solution curves are plotted (a) in the 3-D $(\lambda,\psi,\overline{P}_c)$ space and (b) – (d) on the 2-D projections on the (λ,ψ), $(\lambda,\overline{P}_c)$ and $(\psi,\overline{P}_c)$ planes respectively. The dotted line in (a) is the critical line of the system.

$\gamma_c = 4/3$, $\beta = 1/2$, $\bar{\kappa} = 10$ and $\bar{E} = 1$. The solution curves were generated by varying the initial values of $(\lambda,\psi,\bar{P}_c)$ at $s = 0$, where s is the dummy time variable in equation (3.24). For large enough $\bar{\kappa}$ (e.g. $\bar{\kappa} > 10$), the solution curves in the (λ,ψ) plane at large enough λ are similar to the one fluid polytropic stellar wind solution curves displayed in figure 2.1(a) (compare figures 2.1(a) and 3.3(a)). However, at smaller λ, the supersonic solution curves in figure 3.3(a) spiral about the critical line (the critical points in this region are foci), and it is impossible for these curves to extend to $\lambda = 0$ (i.e., $r = \infty$). This behaviour is in contrast to the one fluid polytropic stellar wind solutions in figure 2.1(a) where the supersonic solution curves in region **I**, tend to a finite value of ψ as $\lambda \to 0$. The solution curves in both figure 2.1(a) and 3.3(a) both exhibit saddle point behaviour near the sonic point of the one fluid polytropic stellar wind. Further discussion of the 3^{rd} order autonomous system (3.24) is given in appendix C.

§3.2.2 The Fourth Order Autonomous System

Instead of a 3^{rd} order autonomous system we can use a 4^{th} order one to analyze the system of equations (3.19) and (3.21). The procedure and conclusions are basically the same as in the 3^{rd} order system, so we simply state the results. Setting

$$\bar{D}_c \equiv \frac{1}{(\gamma_c - 1)} \bar{\kappa} \frac{d\bar{P}_c}{d\lambda} \quad , \tag{3.52}$$

equations (3.19) and (3.21) can be written as a 4^{th} order autonomous

system:

$$\frac{d}{ds}\begin{pmatrix}\lambda\\ \psi\\ \bar{P}_c\\ \bar{D}_c\end{pmatrix} = \begin{pmatrix} Q\\ P\\ (\gamma_c-1)\,\frac{1}{\bar{\kappa}}\,\bar{D}_c\,Q\\ R\end{pmatrix} , \tag{3.53}$$

where

$$P = 1 - 2\,\beta^{(\gamma_g+1)/2}\,\psi^{-(\gamma_g-1)/2}\,\lambda^{(2\gamma_g-3)} - (\gamma_c-1)\,\frac{1}{\bar{\kappa}}\,\psi^{1/2}\,\lambda^{-2}\,\bar{D}_c , \tag{3.54}$$

$$Q = \frac{1}{2}\left[1 - \beta^{(\gamma_g+1)/2}\,\psi^{-(\gamma_g+1)/2}\,\lambda^{2(\gamma_g-1)}\right] , \tag{3.55}$$

$$R = \psi^{1/2}\,\lambda^{-2}\left[2\,\frac{\gamma_c}{(\gamma_c-1)}\,\lambda^{-1}\,\bar{P}_c\,Q - \frac{1}{\bar{\kappa}}\,\bar{D}_c\,Q - \frac{1}{2}\,\frac{\gamma_c}{(\gamma_c-1)}\,\psi^{-1}\,\bar{P}_c\,P\right] . \tag{3.56}$$

Critical points occur when $P = Q = 0$ (note R is zero if $P = Q = 0$), and they lie on a surface (we called it the *critical surface*). The critical surface, written in terms of two independent parameters τ and σ, is given by:

$$\lambda = \lambda_c = \tau , \tag{3.57}$$

$$\psi = \psi_c = \beta\,\tau^{4(\gamma_g-1)/(\gamma_g+1)} , \tag{3.58}$$

$$\bar{P}_c = \bar{P}_{cc} = \sigma , \tag{3.59}$$

$$\bar{D}_c = \bar{D}_{cc} = \frac{1}{(\gamma_c-1)}\,\bar{\kappa}\left[\beta^{-1/2}\,\tau^{4/(\gamma_g+1)} - 2\,\beta^{1/2}\,\tau^{(3\gamma_g-1)/(\gamma_g+1)}\right] . \tag{3.60}$$

Figure 3.4 shows the (λ,ψ), $(\lambda,\bar{D}_c)$, $(\psi,\bar{D}_c)$ and $(\lambda,\psi,\bar{D}_c)$ projections of the critical surface for the case $\gamma_g = 1.2$, $\gamma_c = 4/3$, $\beta = 1/2$ and $\bar{\kappa} = 10$.

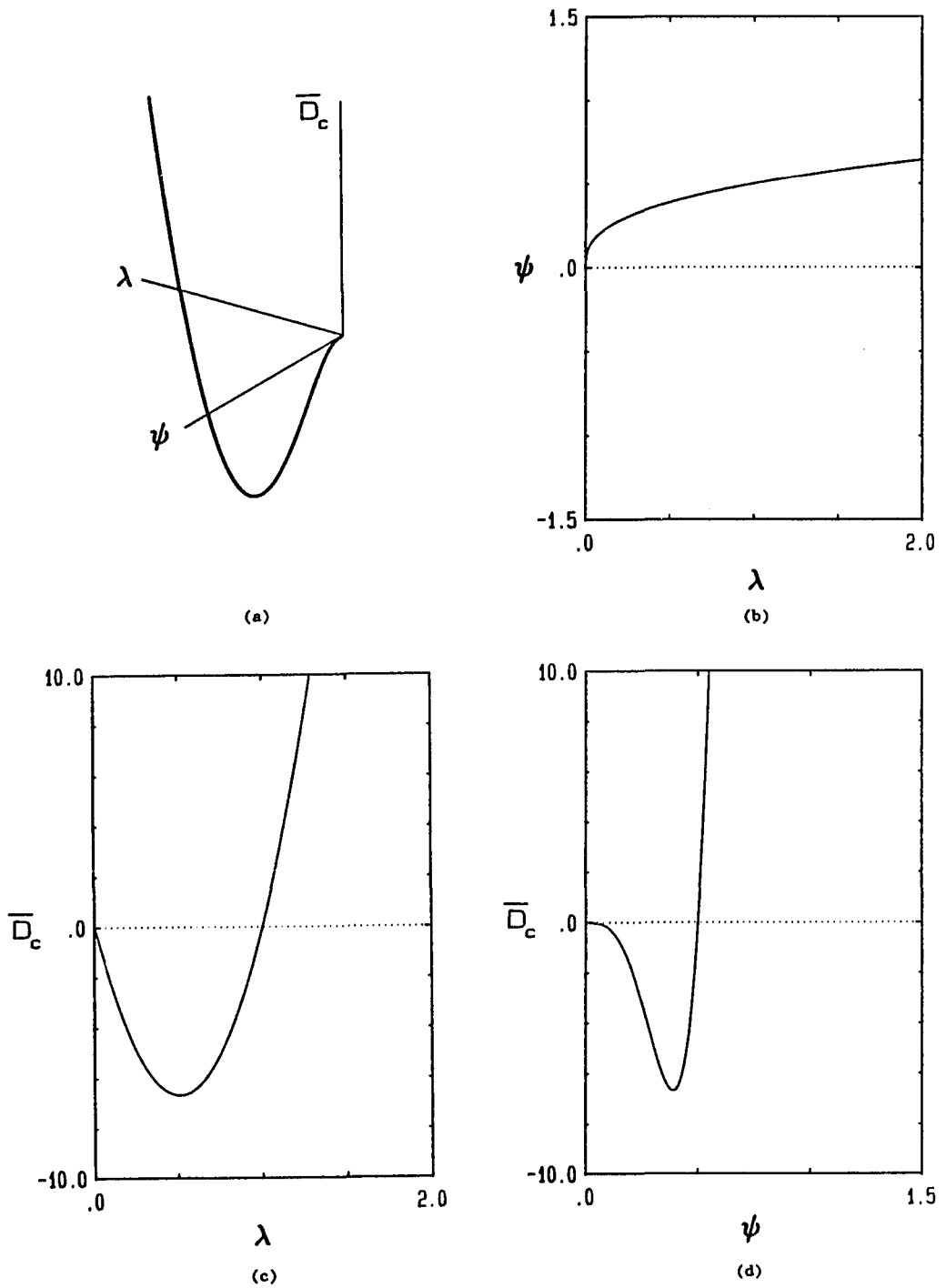

Figure 3.4 Critical Surface of the 4th Order Autonomous System

The critical line is plotted (a) on the 3-D projection on the $(\lambda,\psi,\bar{D}_c)$ space and (b) – (d) on the 2-D projections on the (λ,ψ), $(\lambda,\bar{D}_c)$ and $(\psi,\bar{D}_c)$ planes respectively.

Linearizing the system (3.53) about the critical surface, we obtain:

$$\frac{d}{dt}\begin{bmatrix} \lambda-\lambda_c \\ \psi-\psi_c \\ \bar{P}_c-\bar{P}_{cc} \\ \bar{D}_c-\bar{D}_{cc} \end{bmatrix} = \underline{\underline{A}}_4 \begin{bmatrix} \lambda-\lambda_c \\ \psi-\psi_c \\ \bar{P}_c-\bar{P}_{cc} \\ \bar{D}_c-\bar{D}_{cc} \end{bmatrix} , \tag{3.61}$$

where

$$\underline{\underline{A}}_4 \equiv \begin{bmatrix} Q_\lambda & Q_\psi & Q_{\bar{P}_c} & Q_{\bar{D}_c} \\ P_\lambda & P_\psi & P_{\bar{P}_c} & P_{\bar{D}_c} \\ \left[\frac{(\gamma_c-1)}{\bar{\kappa}}\bar{D}_c Q\right]_\lambda & \left[\frac{(\gamma_c-1)}{\bar{\kappa}}\bar{D}_c Q\right]_\psi & \left[\frac{(\gamma_c-1)}{\bar{\kappa}}\bar{D}_c Q\right]_{\bar{P}_c} & \left[\frac{(\gamma_c-1)}{\bar{\kappa}}\bar{D}_c Q\right]_{\bar{D}_c} \\ R_\lambda & R_\psi & R_{\bar{P}_c} & R_{\bar{D}_c} \end{bmatrix}_c \tag{3.62}$$

and the subscript c denotes the entries of the matrix are evaluated on the critical surface.The various partial derivatives in the matrix (3.62) (for constant $\bar{\kappa}$) are:

$$Q_\lambda\big|_c = -(\gamma_g - 1)\,\tau^{-1} , \tag{3.63}$$

$$Q_\psi\big|_c = \frac{1}{4}(\gamma_g+1)\,\beta^{-1}\,\tau^{-4(\gamma_g-1)/(\gamma_g+1)} , \tag{3.64}$$

$$Q_{\bar{P}_c}\big|_c = 0 , \tag{3.65}$$

$$Q_{\bar{D}_c}\big|_c = 0 , \tag{3.66}$$

$$P_\lambda\big|_c = -2\,(2\gamma_g-1)\,\beta\,\tau^{-2(3-\gamma_g)/(\gamma_g+1)} + 2\,\tau^{-1} , \tag{3.67}$$

$$P_\psi\big|_c = \gamma_g\,\tau^{-1} - \frac{1}{2}\beta^{-1}\,\tau^{-4(\gamma_g-1)/(\gamma_g+1)} , \tag{3.68}$$

$$P_{\bar{P}_c}\big|_c = 0 , \tag{3.69}$$

$$P_{\bar{D}_c}\big|_c = -(\gamma_c-1)\,\frac{1}{\bar{\kappa}}\,\beta^{1/2}\,\tau^{-4/(\gamma_g+1)} , \tag{3.70}$$

$$\left[(\gamma_c-1)\,\frac{1}{\bar{\kappa}}\,\bar{D}_c\,Q\right]_\lambda\Big|_c = (\gamma_c-1)\,\frac{1}{\bar{\kappa}}\,(\bar{D}_c Q_\lambda)\big|_c , \tag{3.71}$$

$$\left[(\gamma_c-1)\,\frac{1}{\kappa}\,\bar{D}_c\,Q\right]_{\psi}\Big|_c = (\gamma_c-1)\,\frac{1}{\kappa}\,(\bar{D}_c Q_{\psi})|_c \quad , \tag{3.72}$$

$$\left[(\gamma_c-1)\,\frac{1}{\kappa}\,\bar{D}_c\,Q\right]_{\bar{P}_c}\Big|_c = (\gamma_c-1)\,\frac{1}{\kappa}\,(\bar{D}_c Q_{\bar{P}_c})|_c \quad , \tag{3.73}$$

$$\left[(\gamma_c-1)\,\frac{1}{\kappa}\,\bar{D}_c\,Q\right]_{\bar{D}_c}\Big|_c = (\gamma_c-1)\,\frac{1}{\kappa}\,(\bar{D}_c Q_{\bar{D}_c})|_c \quad , \tag{3.74}$$

$$\begin{aligned} R_{\lambda}|_c = {} & \frac{(\gamma_g-1)}{(\gamma_c-1)}\left(-2\,\beta\,\tau^{-2(3-\gamma_g)/(\gamma_g+1)} + \tau^{-1}\right) \\ & + \frac{\gamma_c}{(\gamma_c-1)}\left(\beta^{1/2}\,\tau^{-2(\gamma_g+3)/(\gamma_g+1)}\right. \\ & \left. - \beta^{-1/2}\,\tau^{-(5\gamma_g+1)/(\gamma_g+1)}\right)\sigma \quad , \end{aligned} \tag{3.75}$$

$$\begin{aligned} R_{\psi}|_c = {} & \frac{1}{4}\,\frac{(\gamma_g+1)}{(\gamma_c-1)}\left(2\,\tau^{-1} - \beta^{-1}\,\tau^{-4(\gamma_g-1)/(\gamma_g+1)}\right) \\ & + \frac{1}{4}\,\frac{\gamma_c}{(\gamma_c-1)}\left(2\,\beta^{-1/2}\,\tau^{-(5\gamma_g+1)/(\gamma_g+1)}\right. \\ & \left. + \beta^{-3/2}\,\tau^{-4(2\gamma_g-1)/(\gamma_g+1)}\right)\sigma \quad , \end{aligned} \tag{3.76}$$

$$R_{\bar{P}_c}\Big|_c = 0 \quad , \tag{3.77}$$

$$R_{\bar{D}_c}\Big|_c = \frac{1}{2}\,\gamma_c\,\frac{1}{\kappa}\,\tau^{-4}\,\sigma \quad . \tag{3.78}$$

The eigenvalues of the matrix $\underline{\underline{A}}_4$ (3.62) are given by:

$$\mu^2\,(\mu^2 - b'\,\mu + c') = 0 \quad , \tag{3.79}$$

where

$$b' \equiv \tau^{-1} - \frac{1}{2}\,\beta^{-1}\,\tau^{-4(\gamma_g-1)/(\gamma_g+1)} + \frac{1}{2}\,\gamma_c\,\frac{1}{\kappa}\,\tau^{-4}\,\sigma \quad , \tag{3.80}$$

$$\begin{aligned} c' = {} & \frac{1}{2}\,(3\gamma_g-1)\,\tau^{-2} - \beta^{-1}\,\tau^{-(5\gamma_g-3)/(\gamma_g+1)} \\ & + \frac{1}{2}\,(\gamma_g+1)\,\frac{1}{\kappa}\,\beta^{1/2}\,\tau^{-(\gamma_g+5)/(\gamma_g+1)} \\ & - \frac{1}{4}\,(\gamma_g+1)\,\frac{1}{\kappa}\,\beta^{-1/2}\,\tau^{-4\gamma_g/(\gamma_g+1)} + \gamma_c\,\frac{1}{\kappa}\,\tau^{-5}\,\sigma \quad . \end{aligned} \tag{3.81}$$

We can integrate the autonomous system (3.53) numerically and

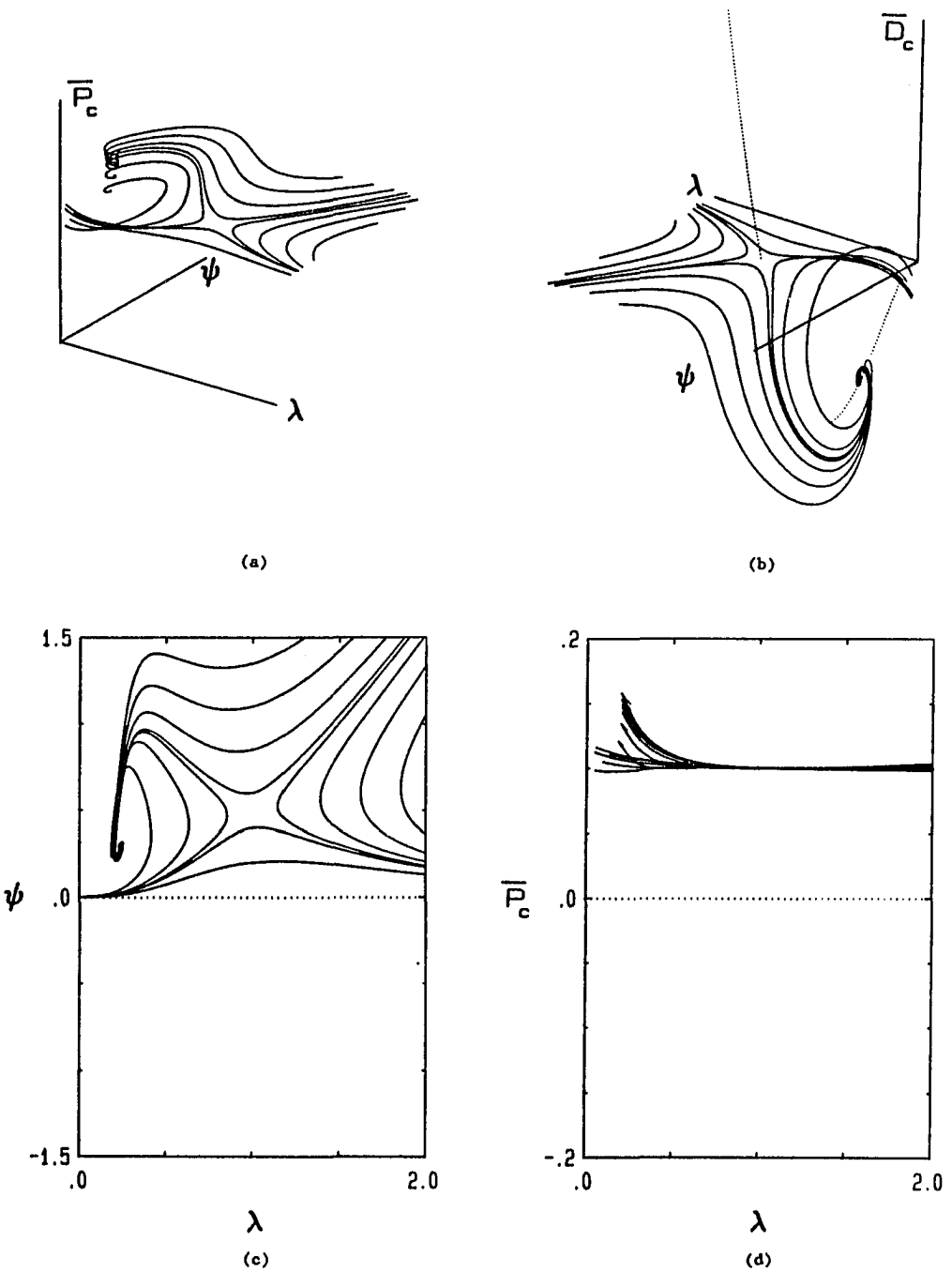

Figure 3.5 Solution Curves of the 4th Order Autonomous System

Some of the solution curves are plotted (a) – (b) on the 3-D projections on the $(\lambda,\psi,\overline{P}_c)$ and $(\lambda,\psi,\overline{D}_c)$ spaces respectively, and (c) – (d) on the 2-D projections on the (λ,ψ) and $(\lambda,\overline{P}_c)$. The dotted line in (b) is the projection of the critical surface of the system on the $(\lambda,\psi,\overline{D}_c)$ space. To be continued···

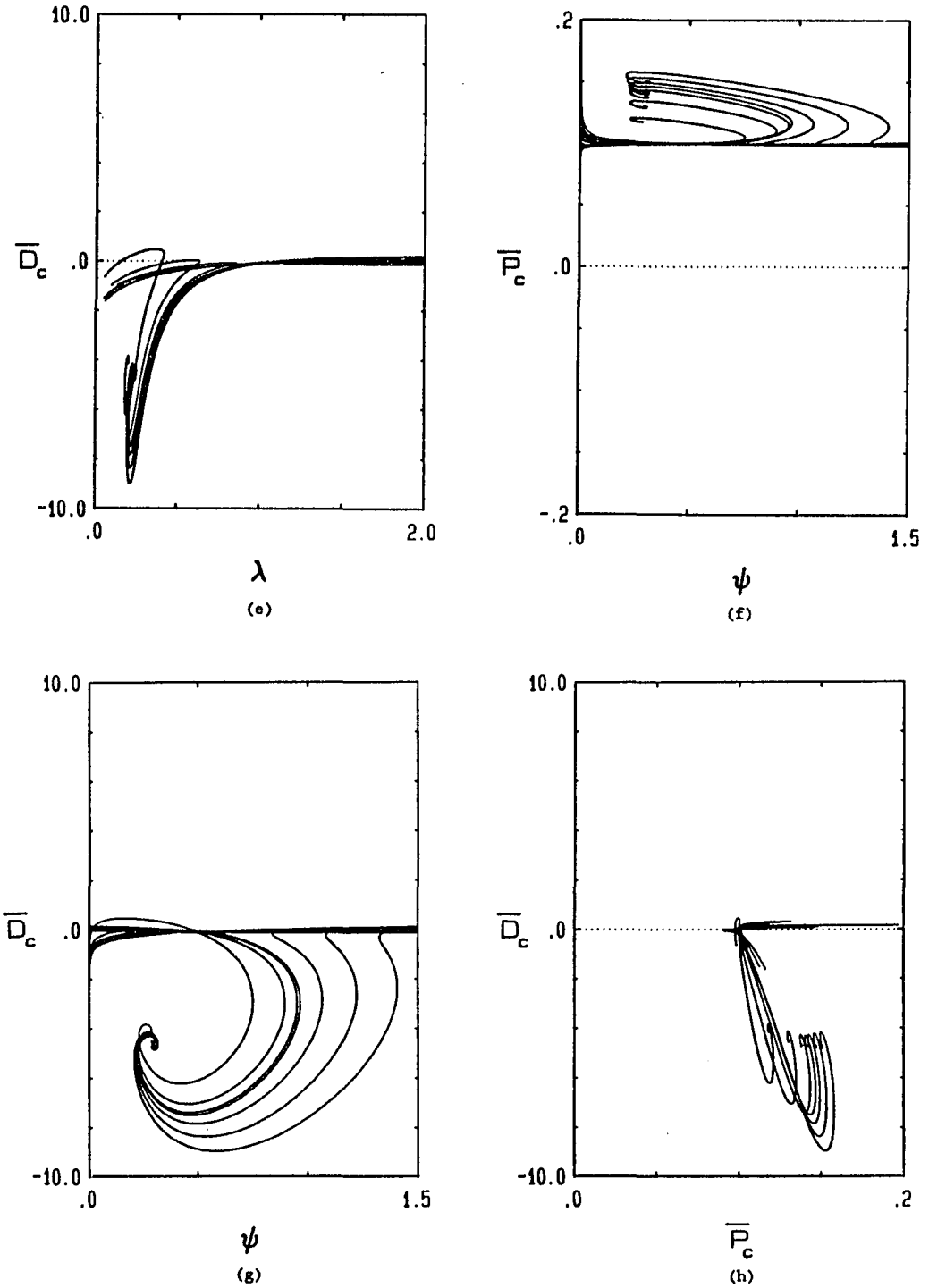

Figure 3.5 Solution Curves of the 4th Order Autonomous System
Cont'd. Some of the solution curves are plotted (e) – (h) on the 2-D projections on the $(\lambda,\overline{D}_c)$, $(\psi,\overline{P}_c)$, $(\psi,\overline{D}_c)$ and $(\overline{P}_c,\overline{D}_c)$ planes respectively.

typical results with $\gamma_g = 1.2$, $\gamma_c = 4/3$, $\beta = 1/2$ and $\bar{\kappa} = 10$ are shown in figure 3.5.

The major difference between the 3^{rd} order system and the 4^{th} order system is that in the 3^{rd} order system we have to specify the normalized total energy flux $\bar{E}$ while in the 4^{th} order system $\bar{E}$ is a free parameter determined by equation (3.20). If we substitute equations (3.20) and (3.59) into equation (3.60), then we obtain the critical line of the 3^{rd} order system (equations (3.28) – (3.30)). We can choose equation (3.30) instead of equation (3.60) to specify $\bar{P}_c$ on the critical surface in the 4^{th} order system, and then consider $\bar{E}$ as one of the parameters (the other one is τ) in the parametric form of the critical surface.

§3.3 Reduction of the Equations to a Second Order Nonlinear Ordinary Differential Equation for ψ with respect to λ

If the normalized energy flux $\bar{E}$ (defined by equation (3.20)) (or energy constant E equation (3.13)) is given, then the thermal plasma cosmic-ray system can be written as a 2^{nd} order nonlinear O.D.E. in ψ with respect to λ.

From equations (3.19) and (3.20), we have

$$\frac{d\bar{P}_c}{d\lambda} = H_1 \quad , \tag{3.82}$$

$$\frac{d\bar{P}_c}{d\lambda} + \gamma_c \frac{1}{\bar{\kappa}} \psi^{1/2} \lambda^{-2} \bar{P}_c = H_2 \quad , \tag{3.83}$$

where

$$H_1 = \psi^{-1/2}\,\lambda^2\left[1 - 2\,\beta^{(\gamma_g+1)/2}\,\psi^{-(\gamma_g-1)/2}\,\lambda^{(2\gamma_g-3)} - \frac{1}{2}\left[1 - \beta^{(\gamma_g+1)/2}\,\psi^{-(\gamma_g+1)/2}\,\lambda^{2(\gamma_g-1)}\right]\frac{d\psi}{d\lambda}\right] , \tag{3.84}$$

$$H_2 = (\gamma_c-1)\,\frac{1}{\bar{\kappa}}\left[\bar{E} - \frac{1}{2}\,\psi + \lambda - \frac{1}{(\gamma_g-1)}\,\beta^{(\gamma_g+1)/2}\,\psi^{-(\gamma_g-1)/2}\,\lambda^{2(\gamma_g-1)}\right] . \tag{3.85}$$

Equation (3.83) can be rearranged to yield:

$$\bar{P}_c = \frac{1}{\gamma_c}\,\bar{\kappa}\,\psi^{-1/2}\,\lambda^2\,(H_2 - H_1) . \tag{3.86}$$

Differentiating this equation by λ and using equation (3.82), we obtain a 2^{nd} order nonlinear O.D.E. in ψ and λ:

$$\frac{d}{d\lambda}\left[\frac{1}{\gamma_c}\,\bar{\kappa}\,\psi^{-1/2}\,\lambda^2\,(H_2 - H_1)\right] = H_1 . \tag{3.87}$$

Substituting H_1 and H_2 from equations (3.84) and (3.85), equation (3.87) can be written as:

$$\begin{aligned}
&\frac{d}{d\lambda}\left[\bar{\kappa}\left[\psi^{-1} - \beta^{(\gamma_g+1)/2}\,\psi^{-(\gamma_g+3)/2}\,\lambda^{2(\gamma_g-1)}\right]\frac{d\psi}{d\lambda}\right] \\
&+ \Big[2\,\bar{\kappa}\,\psi^{-2} + 4\,\bar{\kappa}\,\psi^{-1}\,\lambda^{-1} \\
&\quad - 2\,(\gamma_g+3)\,\bar{\kappa}\,\beta^{(\gamma_g+1)/2}\,\psi^{-(\gamma_g+3)/2}\,\lambda^{(2\gamma_g-3)} \\
&\quad - (\gamma_c-1)\,\bar{E}\,\psi^{-3/2}\,\lambda^{-2} \\
&\quad + \frac{1}{2}\,(\gamma_c+1)\,\psi^{-1/2}\,\lambda^{-2} - (\gamma_c-1)\,\psi^{-3/2}\,\lambda^{-1} \\
&\quad + \frac{(\gamma_c-\gamma_g)}{(\gamma_g-1)}\,\beta^{(\gamma_g+1)/2}\,\psi^{-(\gamma_g+2)/2}\,\lambda^{(2\gamma_g-4)}\Big]\frac{d\psi}{d\lambda} \\
&+ \Big[-8\,\bar{\kappa}\,\psi^{-1}\,\lambda^{-1} \\
&\quad + 4\,(2\gamma_g+1)\,\bar{\kappa}\,\beta^{(\gamma_g+1)/2}\,\psi^{-(\gamma_g+1)/2}\,\lambda^{(2\gamma_g-4)} \\
&\quad - 2\,\frac{d\bar{\kappa}}{d\lambda}\,\psi^{-1} + 4\,\frac{d\bar{\kappa}}{d\lambda}\,\beta^{(\gamma_g+1)/2}\,\psi^{-(\gamma_g+1)/2}\,\lambda^{(2\gamma_g-3)} \\
&\quad + 4\,(\gamma_c-1)\,\bar{E}\,\psi^{-1/2}\,\lambda^{-3}
\end{aligned}$$

$$- 2\,(\gamma_c-1)\,\psi^{1/2}\,\lambda^{-3} + 2\,(2\gamma_c-3)\,\psi^{-1/2}\,\lambda^{-2}$$
$$- 4\,\frac{(\gamma_c-\gamma_g)}{(\gamma_g-1)}\,\beta^{(\gamma_g+1)/2}\,\psi^{-\gamma_g/2}\,\lambda^{(2\gamma_g-5)}\Big]$$
$$= 0 \qquad . \qquad (3.88)$$

Equation (3.88) may be written in a simpler form if we choose the normalized density,

$$\bar{\rho} \equiv \frac{\rho_g}{\rho_o} = \psi^{-1/2}\,\lambda^2 \quad , \qquad (3.89)$$

as the dependent variable, so that equation (3.88) becomes:

$$\frac{d}{d\lambda}\left[\bar{\kappa}\left[\beta^{(\gamma_g+1)/2}\,\bar{\rho}^{\gamma_g} - \bar{\rho}^{-1}\,\lambda^4\right]\frac{d\bar{\rho}}{d\lambda}\right]$$
$$+ \left[-2\,\bar{\kappa}\,\bar{\rho} + (\gamma_c-1)\,\bar{E} - \frac{1}{2}\,(\gamma_c+1)\,\bar{\rho}^{-2}\,\lambda^4 + (\gamma_c-1)\,\lambda\right.$$
$$\left. + \frac{(\gamma_c-\gamma_g)}{(\gamma_g-1)}\,\beta^{(\gamma_g+1)/2}\,\bar{\rho}^{(\gamma_g-1)}\right]\frac{d\bar{\rho}}{d\lambda}$$
$$+ \left[6\,\bar{\kappa}\,\lambda^2 - \frac{d\bar{\kappa}}{d\lambda}\,\bar{\rho}^2 + 2\,\frac{d\bar{\kappa}}{d\lambda}\,\lambda^3 + 2\,\bar{\rho}^{-1}\,\lambda^3 - \bar{\rho}\right]$$
$$= 0 \quad . \qquad (3.90)$$

If $\bar{E}$ is not given, then the thermal plasma cosmic-ray system can only be reduced to a 3^{rd} order nonlinear O.D.E. in ψ with respect to λ. This 3^{rd} order equation is obtained by substituting equation (3.82) into equation (3.21) and then differentiating the resultant equation with respect to λ:

$$H_1 = \frac{d}{d\lambda}\left[\frac{1}{\gamma_c}\,\psi^{-1/2}\,\lambda^2\left[2\,\lambda^{-1} - \frac{1}{2}\,\psi^{-1}\,\frac{d\psi}{d\lambda}\right]^{-1}\right.$$
$$\left.\cdot\left[\frac{d}{d\lambda}(\bar{\kappa}\,H_1) + \psi^{1/2}\,\lambda^2\,H_1\right]\right] \qquad (3.91)$$

Solving equations (3.88) or (3.90) with appropriate boundary conditions is not an easy task. However, these equations might be useful in finding asymptotic solutions as $\lambda \to 0$ or $\lambda \to \infty$, or in

finding approximate solutions as $\bar{\kappa} \to 0$ or as $\bar{\kappa} \to \infty$, etc.. For example, if $\bar{\kappa}$ is constant and independent of λ, and if $\bar{\rho} = \bar{\rho}_\infty$ at $\lambda = 0$ (i.e., $r = \infty$), then the asymptotic behaviour of the normalized density $\bar{\rho}$ as $\lambda \to 0$ (i.e., $r \to \infty$) is given by (see appendix D)

$$\bar{\rho} \sim \bar{\rho}_\infty \left[1 + \beta^{-(\gamma_g+1)/2} \bar{\rho}^{-\gamma_g} \left(\bar{\rho}_\infty - \left.\frac{dP_c}{d\lambda}\right|_{\lambda=0}\right) \lambda + \cdots\right] . \qquad (3.92)$$

It may well be possible to determine the modification of the stellar wind velocity profile by the cosmic-rays by solving equations (3.88) or (3.90) for ψ or $\bar{\rho}$ in terms λ, and subsequently determining the radial variation of the cosmic-ray pressure from equation (3.86). However, we do not use this approach, but instead use a numerical method based on iteration of the equations (3.4) and (3.13) (or equivalently equations (3.20) and (3.21)), using the test particle solution (in which the cosmic-rays are assumed not to affect the flow) to start the iteration (chapter 6). We also use a perturbation method which is applicable when the cosmic-ray pressure is small (chapter 5).

CHAPTER 4

THE TEST PARTICLE PICTURE

Before consisdering the full nonlinear modification of the stellar wind flow by the cosmic-rays, it is instructive first to consider the test particle limit in which the cosmic-ray pressure gradient is sufficiently small, that the cosmic-rays do not significantly modify the wind flow. This limit applies if the cosmic-ray mean free path is sufficiently large, or the cosmic-ray pressure is sufficiently small. The cosmic-rays may then be regarded as test particles propagating in the given background flow (the stellar wind flow), and the cosmic-ray pressure and energy flux variation with radial distance are determined by solving the cosmic-ray energy equation (3.10), with the fluid velocity profile u typically taken to be that of the one fluid polytropic wind discussed in §2.2.

Webb, Forman and Axford (1985) used the test particle picture to study cosmic-ray acceleration at stellar wind termination shocks. Using a reasonably realistic stellar wind flow profile, they obtained analytical solutions for the distribution function, number density, pressure and energy flux of the cosmic-rays. They showed that OB star stellar winds could provide a significant portion of the galactic cosmic-ray energy flux, if effects of losses and magnetic field geometry were not included. Some of their solutions clearly showed the breakdown

of the test particle picture since the emergent cosmic-ray energy flux was a considerable fraction of the mechanical energy of the wind, and the cosmic-ray pressure and energy flux at the shock diverged in some cases. A self consistent treatment, including the effects of the cosmic-rays on the wind, is clearly needed (c.f. Axford, Leer and Skadron 1977; Drury and Völk 1981; Axford, Leer and McKenzie 1982; McKenzie and Völk 1982; Webb 1983). We will come back to a self-consistent treatment in chapter 6.

Since the cosmic-rays do not significanlty modify the wind in the test particle picture, the equations (3.1) - (3.5) are decoupled into two parts: the background flow equations and cosmic-ray energy equation. The background flow equations are exactly the same as those of one fluid polytropic stellar winds, whose properties and solutions were discussed in chapter 2. Using the method in §2.2, we can establish a realistic stellar wind velocity profile with a termination shock. With this profile, the cosmic-ray energy equation (3.4) or (3.10) becomes a linear homogeneous O.D.E. in P_c (the only unkown in the equation). This linear O.D.E. with appropriate boundary conditions can be solved numerically, for instance, by finite difference methods (e.g. Keller 1968). We will use the test particle solution for the iterative process in solving the full nonlinear modification of the wind profile by the cosmic-rays in chapter 6. In this chapter we describe how to solve the cosmic-ray energy equation with a given background velocity profile.

§4.1 Numerical Solution of the Cosmic-Ray Energy Equation

Introducing dimensionless quantities:

$$\xi = \frac{r}{R} \quad , \quad \tilde{\kappa} = \frac{\kappa}{Ru_o} \quad , \quad \tilde{u} = \frac{u}{u_o} \quad , \quad \tilde{P}_c = \frac{P_c}{P_{co}} \quad , \tag{4.1}$$

the cosmic-ray energy equation (3.4) or (3.10) can be written as

$$\frac{1}{\xi^2}\frac{d}{d\xi}\left(\xi^2 \tilde{\kappa} \frac{d\tilde{P}_c}{d\xi}\right) - \tilde{u}\frac{d\tilde{P}_c}{d\xi} - \gamma_c \frac{1}{\xi^2}\frac{d}{d\xi}(\xi^2 \tilde{u})\tilde{P}_c = 0 \quad . \tag{4.2}$$

We later choose the radius of the termination shock as R, the wind velocity just upstream of the shock as u_o, and the galactic cosmic-ray pressure as P_{co} ($P_{co} = P_{c\infty}$). For a diffusion coefficient κ_1 inside the shock (i.e., $0 < r < R$), the parameter $\tilde{\kappa}_1 = \kappa_1/(Ru_o)$ is the inverse of the modulation parameter $\eta_1 = Ru_o/\kappa_1$ used extensively in modulation studies of cosmic-rays (e.g. Fisk 1969; Jokipii 1971; Fisk 1979; Webb, Forman and Axford 1985). For large η_1 (or small $\tilde{\kappa}_1$), the galactic cosmic-rays are effectively excluded from the inner solar cavity (i.e., $0 < r < R$), whereas particles have easier access for smaller η_1. Studies of cosmic-ray acceleration by the first order Fermi mechanism at spherical shocks such as the termination shock to the Solar wind (e.g. Webb, Forman and Axford 1985), and at supernova shocks (e.g. Prishchep and Ptuskin 1981; Ko and Jokipii 1985) show that the shock appears planar to the cosmic-rays if the shock radius R is much greater than the convection diffusion length scales κ_1/u_o and κ_2/u_o ($\kappa = \kappa_2$ just downstream of the shock). Thus the shock appears planar if the diffusion parameters $\tilde{\kappa}_1$ and $\tilde{\kappa}_2$ ($= \kappa_2/(Ru_o)$) are small ($\tilde{\kappa}_1, \tilde{\kappa}_2 \ll 1$). The physical importance of parameters $\tilde{\kappa}_1$ and $\tilde{\kappa}_2$ in determining the coupling between the cosmic-rays and the stellar wind flow becomes

apparent both in the test particle picture (this chapter) and in the full nonlinear problem (chapter 6).

In the test particle picture, $\tilde{u}$ and $\tilde{\kappa}$ are given functions of ξ, so that equation (4.2) is a homogeneous linear 2^{nd} order O.D.E. in $\tilde{P}_c$. There are analytical solutions to equation (4.2) for some particular functional forms of $\tilde{u}$ and $\tilde{\kappa}$ (e.g. $\tilde{u} \propto \xi^{\mu}$ and $\tilde{\kappa} \propto \xi^{\nu}$). If the velocity profile $\tilde{u}$ is a complicated function of ξ (especially when it is given numerically as in the case of the one fluid polytropic stellar wind), then we have to use numerical methods to solve equation (4.2) for $\tilde{P}_c$.

We now discuss the appropriate boundary conditions for equation (4.2) for the case of galactic cosmic-rays interacting with a stellar wind flow and termination shock. As in Webb, Forman and Axford (1985), we specify the galactic cosmic-ray pressure at large distance from the star ($P_c \to P_{c\infty}$ as $r \to \infty$). Since we assume there are no sources or sinks of cosmic-rays at the star, the cosmic-ray energy flux ($4\pi r^2 F_c$) is required to vanish at the origin ($r \to 0$), and the cosmic-ray pressure is expected to be finite. Strictly speaking, we should not extrapolate the stellar wind down to $r = 0$ because of the finite radius of the star r_s. Since the radius of the star is very small compare to the radius of the termination shock ($r_s \sim 10^{-4} r_{sh}$ in case of the Sun), so whether the boundary condition is taken at $r = r_s$ or $r = 0$ should not affect the global behaviour of the solution.

We can in fact show that if the cosmic-ray pressure is finite as $r \to 0$, and for a physically realistic wind flow near $r = 0$, and with

no sources or sinks at $r = 0$, then $4\pi r^2 F_c \to 0$ as $r \to 0$. To see this we first use the one fluid polytropic wind equation (2.11) to determine the wind velocity near $r = 0$. At small radii, the kinetic energy flux of the wind is much less than either the gravitational potential energy or enthalpy flux. For a finite gas energy flux, as $\lambda \to \infty$ (i.e., $r \to 0$) balancing the enthalpy and gravitational potential energy terms in the energy integral (2.11) leads to a fluid velocity profile of the form:

$$\tilde{u} = \tilde{u}_* \, \xi^{(3-2\gamma_{g1})/(\gamma_{g1}-1)} , \qquad \text{as} \quad \xi \to 0 , \tag{4.3}$$

where

$$\tilde{u}_* = j \left[\frac{\gamma_{g1}}{(\gamma_{g1}-1)} A_1 (GM_o)^{-1} \right]^{1/(\gamma_{g1}-1)} u_o^{-1} R^{(3-2\gamma_{g1})/(\gamma_{g1}-1)} . \tag{4.4}$$

In order that $\tilde{u} \to 0$ as $\xi \to 0$, we require $(3-2\gamma_{g1})/(\gamma_{g1}-1) > 0$.

For the case of no sources or sinks at the origin, the net energy flux of cosmic-rays across a sphere of radius r_* can be obtained by integrating the cosmic-ray equation (3.4) over the sphere:

$$4 \pi \xi^2 \tilde{F}_c \big|_{\xi_*} = 4 \pi \int_0^{\xi_*} \tilde{u} \frac{d\tilde{P}_c}{d\xi} \xi^2 \, d\xi , \tag{4.5}$$

where

$$\tilde{F}_c = \frac{\gamma_c}{(\gamma_c-1)} \tilde{P}_c \tilde{u} - \frac{1}{(\gamma_c-1)} \tilde{\kappa} \frac{d\tilde{P}_c}{d\xi} , \tag{4.6}$$

is the normalized cosmic-ray energy flux, and $\xi_* = r_*/R$. Assuming $\tilde{P}_c$ is bounded in $0 < \xi < \xi_*$ ($|\tilde{P}_c| \le |\tilde{P}_c|_{max}$), and integrating the right hand side of equation (4.5) by parts, we obtain (using the triangle inequality)

$$|4\pi\xi^2 \tilde{F}_c|_{\xi_*} \leq 8\pi |\tilde{P}_c|_{max} \tilde{u}_* \xi_*^{1/(\gamma_{g1}-1)} \quad . \qquad (4.7)$$

Thus for $\gamma_{g1} > 1$, $|4\pi\xi^2 \tilde{F}_c|_{\xi_*} \to 0$ as $\xi_* \to 0$; and in order that $\tilde{u} \to 0$ as $\xi \to 0$, we require $(3-2\gamma_{g1})/(\gamma_{g1}-1) > 0$. These conditions together require that we consider one fluid polytropic winds with $1 < \gamma_{g1} < 3/2$.

We can further show (appendix E) that if $\tilde{u} \propto \xi^{\mu}$ and $\tilde{\kappa} \propto \xi^{\nu}$, then $\tilde{P}_c$ is finite and $\frac{d\tilde{P}_c}{d\xi} = 0$ at $\xi = 0$ provided $\mu > \nu$. Thus if $\nu < (3-2\gamma_{g1})/(\gamma_{g1}-1)$ then $\frac{d\tilde{P}_c}{d\xi} = 0$ at $\xi = 0$.

However, the specification of either $\tilde{P}_c$ or $\frac{d\tilde{P}_c}{d\xi}$ at $r = 0$ seems to be immaterial from the point of view of the global solution. Solutions with finite (reasonable size) $\tilde{P}_c$ at the origin are almost the same as those from with $\frac{d\tilde{P}_c}{d\xi} = 0$ at the origin, except in the region very close to the orgin that $\tilde{P}_c$ approaches rapidly to the required value at the origin.

The question now remains of the appropriate boundary conditions to apply to the cosmic-ray pressure and energy flux at the shock. This question has been considered in some detail by Gleeson and Axford (1967), Toptygin (1980), Webb (1983) and Drury (1983). In the absence of sources or sinks at the shock, the appropriate boundary conditions are that the cosmic-ray pressure P_c and energy flux $\vec{F}_c$ should be continuous across the shock. These results are expected from the fact that the cosmic-rays interact with the background flow on the scale

length of the cosmic-ray mean free path which is usually much greater than the shock thickness (for parallel, collisionless shocks, the shock thickness is of the order of c/ω_{pi}, where ω_{pi} is the ion plasma frequency; perpendicular shocks have a much smaller thickness of the order of c/ω_{pe}, where ω_{pe} is the electron plasma frequency, c.f. Kennel 1981). At a shock the mean phase space distribution $f(\vec{r},p,t)$ (averaged over all directions of the particle momentum $\vec{p}$) and the differential flux $\vec{S}_p$ (see appendix B) for the cosmic-rays are continuous at the shock (c.f. Toptygin 1980; Webb 1983; Drury 1983). Since P_c and $\vec{F}_c$ are defined as moments of $f(\vec{r},p,t)$ and $\vec{S}_p$ (c.f. equations (B.6) and (B.7)), the continuity of P_c and $\vec{F}_c$ at the shock then follows automatically. It should be noted however, that the boundary conditions on $f(\vec{r},p,t)$ and $\vec{S}_p$ at the shock have been derived under quite severe physical restrictions, and are not necessarily expected to apply for highly anisotropic cosmic-ray distributions in momentum space.

In summary, the boundary conditions for the cosmic-ray energy equation (4.2), for galactic cosmic-rays in a stellar wind flow with a termination shock are

(a) as $\xi \to \infty$,

$$\tilde{P}_{c2} \to \tilde{P}_{c\infty} \quad ; \tag{4.8}$$

(b) at $\xi = \xi_{sh}$,

$$\tilde{P}_{c1} = \tilde{P}_{c2} \quad , \tag{4.9}$$

$$\frac{\gamma_c}{(\gamma_c-1)} \tilde{P}_{c1} \tilde{u}_1 - \frac{1}{(\gamma_c-1)} \tilde{\kappa}_1 \frac{d\tilde{P}_{c1}}{d\xi}$$

$$= \frac{\gamma_c}{(\gamma_c-1)} \tilde{P}_{c2} \tilde{u}_2 - \frac{1}{(\gamma_c-1)} \tilde{\kappa}_2 \frac{d\tilde{P}_{c2}}{d\xi} \quad ; \tag{4.10}$$

(c) as $\xi \to 0$,

$$4 \pi \xi^2 \left[\frac{\gamma_c}{(\gamma_c-1)} \tilde{P}_{c1} \tilde{u}_1 - \frac{1}{(\gamma_c-1)} \tilde{\kappa}_1 \frac{d\tilde{P}_{c1}}{d\xi} \right] \to 0 \quad ; \tag{4.11}$$

where the subscripts 1 and 2 denote physical values upstream and downstream (i.e., inside and outside) of the shock respectively. For the case of one fluid polytropic wind models, with fluid velocity profile of the form (4.3) near the star, and if the cosmic-ray diffusion coefficient $\tilde{\kappa}_1 \propto \xi^{\nu}$ with $\nu < (3-2\gamma_{g1})/(\gamma_{g1}-1)$, then the boundary condition (4.11) may be replaced by:

$$\frac{d\tilde{P}_{c1}}{d\xi} \to 0 \quad \text{as} \quad \xi \to 0 \tag{4.12}$$

(see appendix E), and we use this for all our calculations.

In self-consistent calculations of the full problem (chapter 6), since the total energy flux (sum of thermal gas and cosmic-ray energy flux) is conserved, it might be more appropriate to specify cosmic-ray energy flux rather than cosmic-ray pressure at infinity. In this case, we replace the boundary condition (4.8) by

$$\tilde{F}_{c2} \to \tilde{F}_{c\infty} \quad . \tag{4.13}$$

Depending on the behaviour of $\tilde{u}_1$ and $\tilde{\kappa}_1$ near the origin ($\xi = 0$), the coefficients of equation (4.2) may diverge as $\xi \to 0$, and this can lead to difficulties in numerical computations. However, it is not necessary to compute these divergent numerical coefficients at $\xi = 0$, if we use the boundary condition (4.12) at $\xi = 0$, since using a crude difference scheme we have $\tilde{P}_c(\xi_1) = \tilde{P}_c(0)$, where ξ_1 is the

first grid point next to $\xi = 0$. On the other hand, if we use a higher order difference scheme, then we have to use both the equation (4.2) and the boundary condition (4.12) at $\xi = 0$ (e.g. Smith 1978). If $\tilde{u}_1 = \tilde{u}_* \xi^{\mu}$ and $\tilde{\kappa}_1 = \tilde{\kappa}_* \xi^{\nu}$ near $\xi = 0$, then equation (4.2), with $\tilde{P}_{c1}$ finite and $\frac{d\tilde{P}_{c1}}{d\xi} = 0$ at $\xi = 0$, can be written as:

$$(\nu + 3)\, \tilde{\kappa}_* \xi^{\nu} \frac{d^2\tilde{P}_{c1}}{d\xi^2} - (\mu + 2)\, \gamma_c\, \tilde{u}_* \xi^{(\mu-1)}\, \tilde{P}_c = 0 \quad . \qquad (4.14)$$

This equation is also true for the time dependent case if we replace the right hand side by an appropriately scaled time derivative of $\tilde{P}_c$. If $\nu \geq 0$ and $\mu \geq 1$ then the coefficients of equation (4.14) are all finite as $\xi \to 0$ (note that if $\nu > 0$ and $\mu > 1$, we only have one condition, namely, equation (4.12) at $\xi = 0$, and equation (4.14) or (4.2) is of no use there). From now on, our numerical solutions are restricted to $\nu \geq 0$ and $\mu = (3-2\gamma_{g1})/(\gamma_{g1}-1) \geq 1$ ($\gamma_{g1} \leq 4/3$), and we concentrate on the case where $\nu = 0$ (i.e., $\tilde{\kappa}_1$ is constant) and $\gamma_{g1} \leq 4/3$.

We employ a finite difference scheme (e.g. Keller 1968) to solve equation (4.2) with boundary conditions (4.8) - (4.12), and the scheme can be summarized as follows. Equation (4.2) is discretized on a uniform grid by a three point scheme inside and outside the shock. At the shock the derivatives in equation (4.10) are discretized by a two point scheme. For constant $\tilde{\kappa}_1$ and $\gamma_{g1} \leq 4/3$, equation (4.2) or (4.14) becomes $3\, \tilde{\kappa}_1 \frac{d^2\tilde{P}_{c1}}{d\xi^2} = 0$ at $\xi = 0$, together with $\frac{d\tilde{P}_{c1}}{d\xi} = 0$, implies $\tilde{P}_c(\Delta\xi) = \tilde{P}_c(0)$ up to 2^{nd} order in $\Delta\xi$, where $\Delta\xi$ is the grid spacing. At

some radius, $\xi = \xi_{max}$, outside the shock we set $\tilde{P}_c(\xi_{max}) = \tilde{P}_{c\infty}$ to approximate the cosmic-ray pressure at infinity. The resultant system of linear equations are (with j denoting the grid point):

(a) $j = 0$ (i.e., $\xi = 0$),

$$- 6\,\tilde{\kappa}_1\,\tilde{P}_c(j) + 6\,\tilde{\kappa}_1\,\tilde{P}_c(j+1) = 0 \quad ; \tag{4.15}$$

(b) $0 < j < j_{sh}$ (i.e., $0 < \xi < \xi_{sh}$),

$$\left[\tilde{\kappa}_1 - \frac{1}{2}\Delta\xi\,(2\,\tilde{\kappa}_1\,\xi^{-1} - \tilde{u}_1)\right]\tilde{P}_c(j-1) - \left[2\,\tilde{\kappa}_1 + (\Delta\xi)^2\,\gamma_c\,\frac{1}{\xi^2}\,\frac{d}{d\xi}(\xi^2\,\tilde{u}_1)\right]\tilde{P}_c(j) + \left[\tilde{\kappa}_1 + \frac{1}{2}\Delta\xi\,(2\,\tilde{\kappa}_1\,\xi^{-1} - \tilde{u}_1)\right]\tilde{P}_c(j+1) = 0 \quad ; \tag{4.16}$$

(c) $j = j_{sh}$ (i.e., $\xi = \xi_{sh}$),

$$\tilde{\kappa}_1\,\tilde{P}_c(j-1) - \left[\tilde{\kappa}_1 + \tilde{\kappa}_2 - \Delta\xi\,\gamma_c\,(\tilde{u}_1 - \tilde{u}_2)\right]\tilde{P}_c(j) + \tilde{\kappa}_2\,\tilde{P}_c(j+1) = 0 \quad ; \tag{4.17}$$

(d) $j_{sh} < j < j_{max}$ (i.e., $\xi_{sh} < \xi < \xi_{max}$),

$$\left[\tilde{\kappa}_2 - \frac{1}{2}\Delta\xi\,(2\,\tilde{\kappa}_2\,\xi^{-1} - \tilde{u}_2)\right]\tilde{P}_c(j-1) - \left[2\,\tilde{\kappa}_2 + (\Delta\xi)^2\,\gamma_c\,\frac{1}{\xi^2}\,\frac{d}{d\xi}(\xi^2\,\tilde{u}_2)\right]\tilde{P}_c(j) + \left[\tilde{\kappa}_2 + \frac{1}{2}\Delta\xi\,(2\,\tilde{\kappa}_2\,\xi^{-1} - \tilde{u}_2)\right]\tilde{P}_c(j+1) = 0 \quad . \tag{4.18}$$

Note that equation (4.14) is simply $\tilde{P}_c(1) = \tilde{P}_c(0)$.

If we choose $\tilde{F}_c(\xi_{max}) = \tilde{F}_{c\infty}$ as boundary condition (equation (4.13)), then the only change is to add one more equation at j_{max}:

(e) $j = j_{max}$ (i.e., $\xi = \xi_{max}$),

$$2\,\tilde{\kappa}_2\,\tilde{P}_c(j-1) + \left[-2\,\tilde{\kappa}_2 - (\Delta\xi)^2\,\gamma_c\,\frac{1}{\xi^2}\,\frac{d}{d\xi}(\xi^2\,\tilde{u}_2) + 2\,\Delta\xi\,\gamma_c\,\frac{\tilde{u}_2}{\tilde{\kappa}_2}\left[\tilde{\kappa}_2 + \frac{1}{2}\Delta\xi\,(2\,\tilde{\kappa}_2\,\xi^{-1} - \tilde{u}_2)\right]\right]\tilde{P}_c(j) = \left[2\,\Delta\xi\,(\gamma_c - 1)\,\frac{1}{\tilde{\kappa}_2}\,\xi^{-2}\left[\tilde{\kappa}_2 + \frac{1}{2}\Delta\xi\,(2\,\tilde{\kappa}_2\,\xi^{-1} - \tilde{u}_2)\right]\right]\tilde{F}_{c\infty} \quad . \tag{4.19}$$

For higher accuracy, we can use a four point or five point scheme for the derivatives in equations (4.2) and (4.10). We have tested the scheme (4.15) - (4.18) by comparing the numerical solution with the analytical solution obtained by Webb, Forman and Axford (1985) (see appendix E), in which the velocity profile:

$$\tilde{u} = \tilde{u}_{1o} [1 - H(\xi-\xi_{sh})] + \tilde{u}_{2o} \xi^{-2} H(\xi-\xi_{sh}) \quad , \qquad (4.20)$$

where $H(\xi)$ is the Heaviside step function, and $\tilde{u}_{1o}$ and $\tilde{u}_{2o}$ are constants; and the diffusion coefficient is of the form:

$$\tilde{\kappa} = \tilde{\kappa}_{1o} \xi [1 - H(\xi-\xi_{sh})] + \tilde{\kappa}_{2o} \xi H(\xi-\xi_{sh}) \quad , \qquad (4.21)$$

where $\tilde{\kappa}_{1o}$ and $\tilde{\kappa}_{2o}$ are constants. The numerical solution agrees very well with the analytical one.

As an example of the scheme, we use the Solar wind as the background flow. For a Solar wind model with $\dot{M} = 6*10^{11}$ g s^{-1}, $P_{g\infty} = 1$ eV cm^{-3}, $\rho_{g\infty} = 6*10^{-27}$ g cm^{-3}, $\gamma_{g1} = 1.3$ and $\gamma_{g2} = 5/3$, the radius of the shock $R = r_{sh} = 65.2$ A.U. and the upstream velocity at the shock $u_o = u_{1sh} = 364$ km s^{-1}. Typical results are shown in figures 4.1 and 4.2. In figure 4.1 $\gamma_c = 4/3$ and $\kappa_1 = \kappa_2 = 10^{23}$ cm^2 s^{-1}, while in figure 4.2 $\gamma_c = 4/3$ and $\kappa_1 = \kappa_2 = 10^{22}$ cm^2 s^{-1}.

It is clear in figures 4.1 and 4.2 that the cosmic-rays are partially excluded from the inner Solar cavity ($0 < r < r_{sh}$) due to the combined action of convection and diffusion. This is the modulation of galactic cosmic-rays (c.f. Parker 1958b, 1965a; Jokipii 1971; Fisk 1979; Quenby 1984). Increasing the modulation parameter $\eta_1 = Ru_o/\kappa_1 = 1/\tilde{\kappa}_1$ (or decreasing $\tilde{\kappa}_1$) leads to a larger modulation

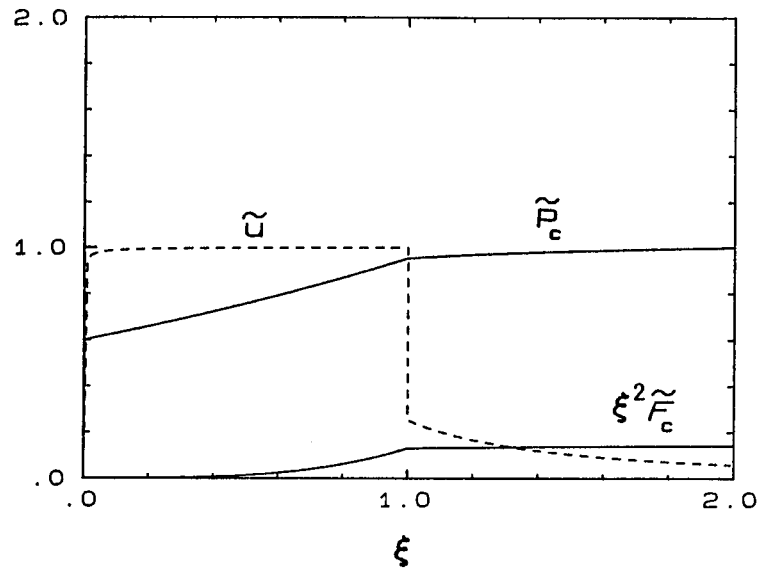

Figure 4.1 Cosmic-Ray Pressure and Energy Flux in the Test Particle Picture with Large κ

The plotting quantities are $\xi = r/R$, $\tilde{u} = u/u_o$, $\tilde{P}_c = P_c/P_{co}$ and $\xi^2\tilde{F}_c = \xi^2 F_c/F_{co}$, where $R = r_{sh} = 65.2$ A.U. , $u_o = u_{1sh} = 364$ km s^{-1} , P_{co} is arbitrary and $F_{co} = u_o P_{co}$. The normalized cosmic-ray diffusion coefficients are $\tilde{\kappa}_1 = \kappa_1/\kappa_o = 2.81$ and $\tilde{\kappa}_2 = \kappa_2/\kappa_o = 2.81$, where $\kappa_o = Ru_o = 3.55*10^{22}$ cm^2 s^{-1} .

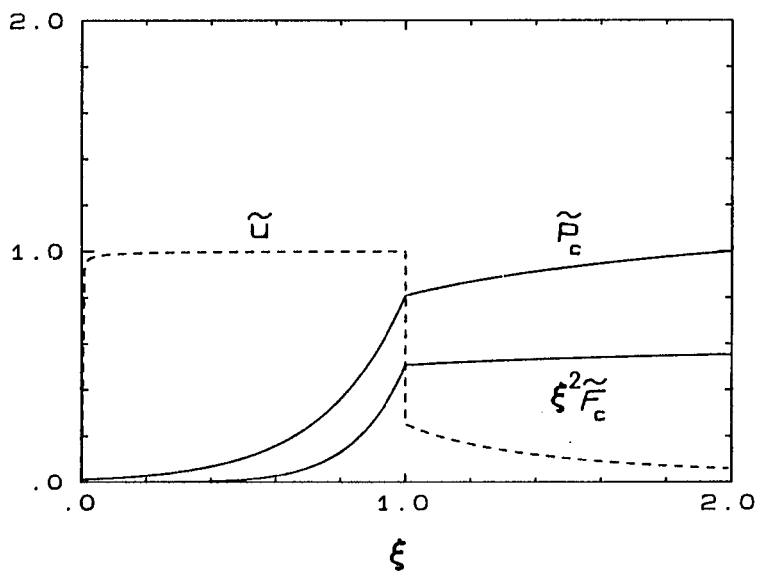

Figure 4.2 Cosmic-Ray Pressure and Energy Flux in the Test Particle Picture with Small κ

The plotting quantities are $\xi = r/R$, $\tilde{u} = u/u_o$, $\tilde{P}_c = P_c/P_{co}$ and $\xi^2\tilde{F}_c = \xi^2 F_c/F_{co}$, where $R = r_{sh} = 65.2$ A.U. , $u_o = u_{1sh} = 364$ km s^{-1} , P_{co} is arbitrary and $F_{co} = u_o P_{co}$. The normalized cosmic-ray diffusion coefficients are $\tilde{\kappa}_1 = \kappa_1/\kappa_o = 0.281$ and $\tilde{\kappa}_2 = \kappa_2/\kappa_o = 0.281$, where $\kappa_o = Ru_o = 3.55*10^{22}$ cm^2 s^{-1} .

effect, and the cosmic-rays are more strongly coupled to the stellar wind flow for larger η_1. Equivalently, the galactic cosmic-rays find it harder to penetrate the inner Solar cavity when the diffusion coefficient is small.

The scheme (4.15) - (4.18) can easily be adapted to solve the time dependent cosmic-ray energy equation:

$$\frac{\partial \tilde{P}_c}{\partial \tau} = \frac{1}{\xi^2}\frac{\partial}{\partial \xi}\left(\xi^2 \tilde{\kappa} \frac{\partial \tilde{P}_c}{\partial \xi}\right) - \tilde{u}\frac{\partial \tilde{P}_c}{\partial \xi} - \gamma_c \frac{1}{\xi^2}\frac{\partial}{\partial \xi}(\xi^2 \tilde{u})\,\tilde{P}_c \quad , \qquad (4.22)$$

where

$$\tau \equiv \frac{t u_o}{R} \quad , \qquad (4.23)$$

is the time in units of the convective time scale R/u_o. We have used a Crank-Nicolson scheme inside and outside the shock and a fully backward implicit scheme right at the shock. Some typical results for the time dependent equation (4.22) are shown in figures 4.3 - 4.5 for a stellar wind model with $\dot{M} = 6*10^{11}$ g s^{-1}, $P_{g\infty} = 1$ eV cm^{-3}, $\rho_{g\infty} = 6*10^{-27}$ g cm^{-3}, $\gamma_{g1} = 1.3$ and $\gamma_{g2} = 5/3$.

In figure 4.3, where $\gamma_c = 4/3$ and $\kappa_1 = \kappa_2\ 10^{22}$ cm^2 s^{-1}, the initial cosmic-ray pressure profile is $\tilde{P}_c = \tilde{P}_{c\infty}$ throughout the whole space. As time increases, the cosmic-rays inside the shock are swept out of the inner region by the stellar wind. It is of interest to note the pressure increase near the shock at early times, which presumably is an indication of shock acceleration of cosmic-rays. The solution at later time is essentially that obtained by solving the steady state equation (4.2).

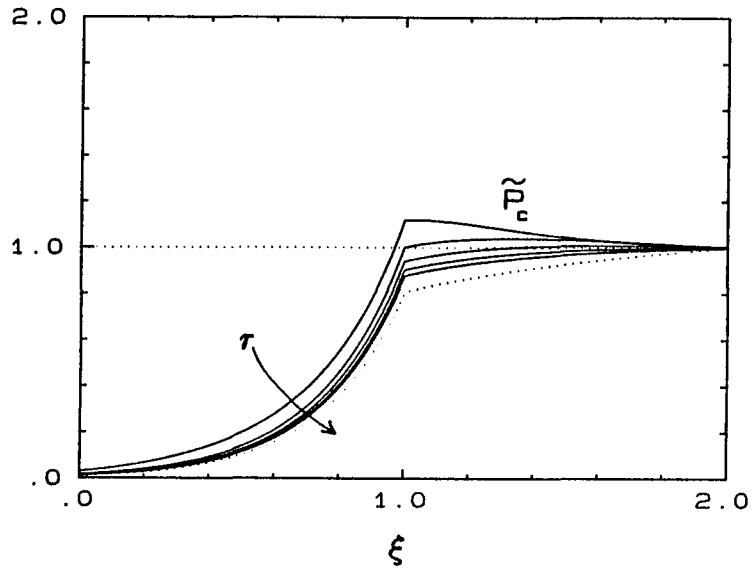

Figure 4.3 Time Evolution of the Cosmic Pressure Profile with $P_c = P_{c\infty}$ Throughout the Whole Space as the Initial Condition

The plotting quantities are $\xi = r/R$, $\tilde{u} = u/u_o$, $\tilde{P}_c = P_c/P_{co}$ and $\tau = t/t_o$, where $R = r_{sh} = 65.2$ A.U. , $u_o = u_{1sh} = 364$ km s^{-1} , P_{co} is arbitrary and $t_o = R/u_o = 0.85$ yr . The normalized cosmic-ray diffusion coefficients are $\tilde{\kappa}_1 = \kappa_1/\kappa_o = 0.281$ and $\tilde{\kappa}_2 = \kappa_2/\kappa_o = 0.281$, where $\kappa_o = Ru_o = 3.55*10^{22}$ cm^2 s^{-1} . The figure shows 5 snapshots of $\tilde{P}_c$ in uniform time interval from $\tau = 0$ to 2. The dotted lines are the initial and steady states of the system.

In figures 4.4 and 4.5 the initial cosmic-ray pressure profile is a gaussian disturbance inside the shock superimposed on the steady state background cosmic-ray pressure profile obtained previously. In figure 4.4 $\gamma_c = 4/3$, $\kappa_1 = 2*10^{21}$ cm^2 s^{-1} and $\kappa_2 = 10^{22}$ cm^2 s^{-1} , while in figure 4.5 $\gamma_c = 4/3$ and $\kappa_1 = \kappa_2 = 10^{22}$ cm^2 s^{-1} . When $\tilde{\kappa} \ll 1$, the diffusion time scale R^2/κ is much larger than the convection time scale R/u_o, and the convection of the gaussian profile is significant as shown in figure 4.4. In figure 4.5 diffusion seems to be more important.

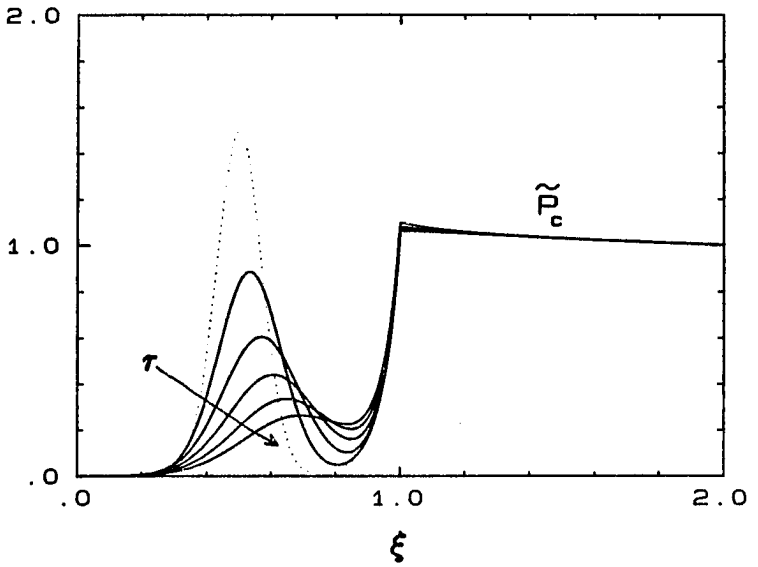

Figure 4.4 Time Evolution of a Gaussian Perturbation Inside the Shock on the Background Cosmic-Ray Pressure Profile in Case of Smaller κ

The plotting quantities are $\xi = r/R$, $\tilde{u} = u/u_o$, $\tilde{P}_c = P_c/P_{co}$ and $\tau = t/t_o$, where $R = r_{sh} = 65.2$ A.U. , $u_o = u_{1sh} = 364$ km s^{-1} , P_{co} is arbitrary and $t_o = R/u_o = 0.85$ yr . The normalized cosmic-ray diffusion coefficients are $\tilde{\kappa}_1 = \kappa_1/\kappa_o = 5.63*10^{-2}$ and $\tilde{\kappa}_2 = \kappa_2/\kappa_o = 0.281$, where $\kappa_o = Ru_o = 3.55*10^{22}$ cm^2 s^{-1} . The figure shows 5 snapshots of $\tilde{P}_c$ in uniform time interval from $\tau = 0$ to 0.2. The dotted lines is the initial state of the system.

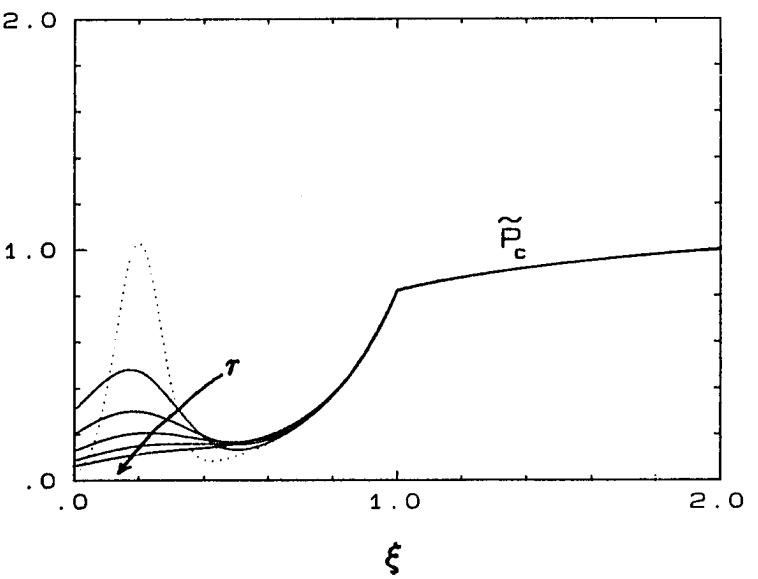

Figure 4.5 Time Evolution of a Gaussian Perturbation Inside the Shock on the Background Cosmic-Ray Pressure Profile in Case of Larger κ

The plotting quantities are $\xi = r/R$, $\tilde{u} = u/u_o$, $\tilde{P}_c = P_c/P_{co}$ and $\tau = t/t_o$, where $R = r_{sh} = 65.2$ A.U. , $u_o = u_{1sh} = 364$ km s^{-1} , P_{co} is arbitrary and $t_o = R/u_o = 0.85$ yr . The normalized cosmic-ray diffusion coefficients are $\tilde{\kappa}_1 = \kappa_1/\kappa_o = 0.281$ and $\tilde{\kappa}_2 = \kappa_2/\kappa_o = 0.281$, where $\kappa_o = Ru_o = 3.55*10^{22}$ cm^2 s^{-1} . The figure shows 5 snapshots of $\tilde{P}_c$ in uniform time interval from $\tau = 0$ to 0.1. The dotted lines is the initial state of the system.

CHAPTER 5

PERTURBATION SOLUTIONS

In chapter 4, we discussed the test particle limit of the cosmic-ray stellar wind system, in which the cosmic-ray pressure gradient was small enough that its effects on the background flow could be neglected. A natural question to ask now is: what are the modifications of the background flow if the backreaction of the cosmic-rays cannot be neglected?

In this chapter we consider the modifications of the wind flow by a finite, but small cosmic-ray pressure (small pressure gradient also). A perturbation approach is used, in which the perturbation parameter,

$$\epsilon \equiv \frac{P_{c\infty}}{P_{g\infty}} , \tag{5.1}$$

is the ratio of the galactic cosmic-ray pressure to the interstellar gas pressure. Since ϵ is assumed to be small, the radial variation of the cosmic-ray pressure in the lowest order of approximation is given by the test particle solution of the cosmic-ray energy equation (3.4) or (4.2). The test particle cosmic-ray pressure solution is then used to determine the modification of the velocity profile of the wind and the location of the termination shock to $O(\epsilon)$. The process can be iterated to presumably obtain a convergent solution for P_g, ρ_g, u and P_c as

functions of radius provided ϵ is sufficiently small. This idea is employed in chapter 6 to find the solution to the full cosmic-ray modified stellar wind problem numerically. It is also possible to obtain higher order perturbation equations, but we restrict our calculations to $O(\epsilon)$ corrections. A similar perturbation approach has been used by Blandford (1980), Drury (1983) and Heavens (1983) to determine the power law momentum spectral index of the phase space distribution function in plane weakly modified cosmic-ray shocks.

For most cases considered it is found that the wind just upstream of the shock is noticeably decelerated by the positive galactic cosmic-ray pressure gradient ($\frac{dP_c}{dr} > 0$), and the stellar wind termination shock occurs at a smaller radius in the cosmic-ray modified wind flow than in the unperturbed wind. However, the simplified model in §5.1 indicates that if there is strong acceleration of the cosmic-rays at the termination shock, so that the cosmic-ray energy flux at the shock exceeds the galactic cosmic-ray energy flux, then the shock occurs at a larger radius than for the unperturbed wind.

We first consider a simplified model (§5.1) where an analytical solution is possible, and then go to the full problem in §5.2. In the simplified model the unperturbed wind velocity upstream of the shock is taken to be constant, and the effects of gravity are nelgected. The full perturbation solution (§5.2) uses the fluid velocity profile of the one fluid polytropic stellar wind (§2.2) for the unperturbed fluid velocity. The perturbation analysis takes into account cosmic-ray modifications of the critical point of the wind, the thermal gas entropy

constants, the location of the shock and the fluid velocity profile.

As in chapter 3, it is convenient to work in terms of normalized variables. The normalized thermal gas and cosmic-ray energy fluxes are

$$\bar{E}_g = \frac{1}{2}\psi - \lambda + \frac{1}{(\gamma_g-1)}\beta^{(\gamma_g+1)/2}\psi^{-(\gamma_g-1)/2}\lambda^{2(\gamma_g-1)} , \quad (5.2)$$

$$\bar{E}_c = \frac{\gamma_c}{(\gamma_c-1)}\psi^{1/2}\lambda^{-2}\bar{P}_c + \frac{1}{(\gamma_c-1)}\bar{\kappa}\frac{d\bar{P}_c}{d\lambda} , \quad (5.3)$$

where λ, ψ, $\bar{P}_c$, β and $\bar{\kappa}$ are defined in §3.2. Since the total energy is conserved,

$$\bar{E} = \bar{E}_g + \bar{E}_c , \quad (5.4)$$

is a constant (c.f. equation (3.20)). In matching momentum fluxes at the shock, it is useful to use the normalized gas momentum flux

$$\bar{G}_g = (P_g + \rho_g u^2)\frac{1}{\rho_o}\left(\frac{m_g}{kT_o}\right) , \quad (5.5)$$

which in terms of λ and ψ may be written as

$$\bar{G}_g = \psi^{1/2}\lambda^2 + \frac{1}{\gamma_g}\beta^{(\gamma_g+1)/2}\psi^{-\gamma_g/2}\lambda^{2\gamma_g} . \quad (5.6)$$

Finally, the cosmic-ray pressure variation with radial distance is governed by the normalized cosmic-ray energy equation (3.21):

$$\frac{d}{d\lambda}\left(\bar{\kappa}\frac{d\bar{P}_c}{d\lambda}\right) + \psi^{1/2}\lambda^{-2}\frac{d\bar{P}_c}{d\lambda} - \gamma_c\psi^{1/2}\lambda^{-2}\left(\frac{2}{\lambda} - \frac{1}{2\psi}\frac{d\psi}{d\lambda}\right)\bar{P}_c = 0 . \quad (5.7)$$

§5.1 Perturbation Solution for the Simplified Model

In this section we consider a simplified model, in which the thermal gas is considered to be cold inside the termination shock, and the effects of gravity are neglected. Upstream of the shock, the unperturbed wind velocity is constant, and the gas enthalpy is

considered negligible compared to the wind kinetic energy flux. Outside the shock, the plasma is hot, and the gas enthalpy dominates the kinetic energy flux, and the unperturbed flow is incompressible with $u \propto 1/r^2$.

The energy and momentum fluxes of the thermal gas in the simplified model are (c.f. equations (5.2) and (5.6)):

$$\bar{E}_{g1} = \frac{1}{2}\psi_1 \quad , \tag{5.8}$$

$$\bar{E}_{g2} = \frac{1}{(\gamma_{g2}-1)}\beta_2^{(\gamma_{g2}+1)/2}\psi_2^{-(\gamma_{g2}-1)/2}\lambda^{2(\gamma_{g2}-1)} \quad , \tag{5.9}$$

$$\bar{G}_{g1} = \psi_1^{1/2}\lambda^2 \quad , \tag{5.10}$$

$$\bar{G}_{g2} = \frac{1}{\gamma_{g2}}\beta_2^{(\gamma_{g2}+1)/2}\psi_2^{-\gamma_{g2}}\lambda^{2\gamma_{g2}} \quad , \tag{5.11}$$

where the subscripts 1 and 2 denote the upstream and downstream quantities respectively.

For the wind the appropriate boundary conditions are $\psi \to 0$, $P_g \to P_{g\infty}$, $\rho \to \rho_{g\infty}$ as $r \to \infty$ (i.e., $\lambda \to 0$), and that ψ is finite as $r \to 0$ (i.e., $\lambda \to \infty$). At the shock the gas mass, momentum and energy fluxes are conserved (c.f. §2.2). For the cosmic-rays, $P_c \to P_{c\infty}$ as $r \to \infty$ (i.e., $\lambda \to 0$), and P_c is finite as $r \to 0$ (i.e., $\lambda \to \infty$). The cosmic-ray pressure and energy flux are continuous at the shock (c.f. §4.1). In terms of normalized variables, these boundary conditions are:

(a) At $\lambda = 0$ (i.e., $r \to \infty$),

$$\bar{E}_{g2} = \bar{E}_{g\infty} = \frac{\gamma_{g2}}{(\gamma_{g2}-1)}\frac{P_{g\infty}}{\rho_{g\infty}}\left(\frac{m_g}{kT_o}\right) \quad , \tag{5.12}$$

$$\bar{P}_{c2} = \bar{P}_{c\infty} \quad , \tag{5.13}$$

and for physical solutions $\bar{\kappa}\frac{d\bar{P}_c}{d\lambda}$ is finite as $\lambda \to 0$.

(b) At the shock $\lambda = \lambda_{sh}$ (i.e., $r = r_{sh}$),

$$\bar{G}_{g1sh} = \bar{G}_{g2sh} \quad , \tag{5.14}$$

$$\bar{P}_{c1sh} = \bar{P}_{c2sh} \quad , \tag{5.15}$$

$$\bar{E}_{g1sh} = \bar{E}_{g2sh} \quad , \tag{5.16}$$

$$\bar{E}_{c1sh} = \bar{E}_{c2sh} \quad . \tag{5.17}$$

(c) As $\lambda \to \infty$ (i.e., $r \to 0$),

$$|\psi_1| < \infty \quad \text{and} \quad |\bar{P}_{c1}| < \infty \quad . \tag{5.18}$$

We now pose the problem in the following way. If the galactic cosmic-ray pressure is zero ($\bar{P}_{c\infty} = 0$) the velocity profile is then the unperturbed (or zeroth order) profile. We want to investigate the effects of a finite, but small, galactic cosmic-ray pressure on this unperturbed velocity profile. Suppose ψ and $\bar{P}_c$ can be expanded in the following perturbation series, with the small parameter $\epsilon \equiv P_{c\infty}/P_{g\infty}$:

$$\psi = \psi^{(0)}\left[1 + \epsilon\, \psi^{(1)} + \epsilon^2\, \psi^{(2)} + \cdots\right] \quad , \tag{5.19}$$

$$\bar{P}_c = \epsilon\, \bar{P}_c^{(1)} + \epsilon^2\, \bar{P}_c^{(2)} + \cdots \quad . \tag{5.20}$$

Similarly the gas and cosmic-ray energy fluxes $\bar{E}_g$ and $\bar{E}_c$ are expanded as:

$$\bar{E}_g = E_g^{(0)} + \epsilon\, \bar{E}_g^{(1)} + \epsilon^2\, \bar{E}_g^{(2)} + \cdots \quad , \tag{5.21}$$

$$\bar{E}_c = \epsilon\, \bar{E}_c^{(1)} + \epsilon^2\, \bar{E}_c^{(2)} + \cdots \quad . \tag{5.22}$$

In view of the boundary conditions at $\lambda = 0$ (i.e., $r \to \infty$), we have

$$\bar{E}_{g2} = \bar{E}_{g\infty}^{(0)} = \frac{\gamma_{g2}}{(\gamma_{g2}-1)} \frac{P_{g\infty}}{\rho_{g\infty}} \left(\frac{m_g}{kT_o}\right) \quad , \tag{5.23}$$

$$\bar{E}_{c2} = \epsilon\, \bar{E}_{c\infty}^{(1)} = \epsilon \left[\frac{\gamma_c}{(\gamma_c-1)} \frac{P_{g\infty}}{\rho_{g\infty}} \left(\frac{m_g}{kT_o}\right) + \frac{1}{(\gamma_c-1)}\, \bar{\kappa}_2 \left.\frac{d\bar{P}_{c2}^{(1)}}{d\lambda}\right|_0\right] \quad . \tag{5.24}$$

The cosmic-ray diffusion coefficient is assumed to depend only on the radius.

Using the perturbation expansions (5.19) – (5.24), and the total

energy flux (5.4), the gas energy fluxes (5.8) and (5.9) and the cosmic-ray energy equation (5.7) we obtain the zeroth order ($O(\epsilon^0)$) flow equations,

$$\frac{1}{2}\,\psi_1^{(0)} = \bar{E}_{g\infty}^{(0)} \quad , \tag{5.25}$$

$$\frac{1}{(\gamma_{g2}-1)}\,\beta_2^{(\gamma_{g2}+1)/2}\left[\psi_2^{(0)}\right]^{-(\gamma_{g2}-1)/2}\lambda^{2(\gamma_{g2}-1)} = \bar{E}_{g\infty}^{(0)} \quad . \tag{5.26}$$

The 1st order ($O(\epsilon^1)$) equations are

$$\hat{L}_c\,\bar{P}_c^{(1)} = 0 \quad , \tag{5.27}$$

$$\frac{1}{2}\,\psi_1^{(0)}\,\psi_1^{(1)} + \frac{\gamma_c}{(\gamma_c-1)}\left[\psi_1^{(0)}\right]^{1/2}\lambda^{-2}\,\bar{P}_{c1}^{(1)} + \frac{1}{(\gamma_c-1)}\,\bar{\kappa}_1\left[\bar{P}_{c1}^{(1)}\right]' = \bar{E}_{c\infty}^{(1)} \quad , \tag{5.28}$$

$$-\frac{1}{2}\,\beta_2^{(\gamma_{g2}+1)/2}\left[\psi_2^{(0)}\right]^{-(\gamma_{g2}-1)/2}\lambda^{2(\gamma_{g2}-1)}\,\psi_2^{(1)} + \frac{\gamma_c}{(\gamma_c-1)}\left[\psi_2^{(0)}\right]^{1/2}\lambda^{-2}\,\bar{P}_{c2}^{(1)} + \frac{1}{(\gamma_c-1)}\,\bar{\kappa}_2\left[\bar{P}_{c2}^{(1)}\right]' = \bar{E}_{c\infty}^{(1)} \quad ; \tag{5.29}$$

and the 2nd order ($O(\epsilon^2)$) equations are

$$\hat{L}_c\,\bar{P}_c^{(2)} = -\left[\psi^{(0)}\right]^{1/2}\lambda^{-2}\left[\frac{1}{2}\,\psi^{(1)}\left[\bar{P}_c^{(1)}\right]' - \gamma_c\left[\left[\lambda^{-1} - \frac{1}{4}\left[\psi^{(0)}\right]^{-1}\left[\psi^{(0)}\right]'\right]\psi^{(1)} - \frac{1}{2}\left[\psi^{(1)}\right]'\right]\bar{P}_c^{(1)}\right] \quad , \tag{5.30}$$

$$\frac{1}{2}\,\psi_1^{(0)}\,\psi_1^{(2)} + \frac{\gamma_c}{(\gamma_c-1)}\left[\psi_1^{(0)}\right]^{1/2}\lambda^{-2}\,\bar{P}_{c1}^{(2)} + \frac{1}{(\gamma_c-1)}\,\bar{\kappa}_1\left[\bar{P}_{c1}^{(2)}\right]' = -\frac{1}{2}\,\frac{\gamma_c}{(\gamma_c-1)}\left[\psi_1^{(0)}\right]^{1/2}\lambda^{-2}\,\psi_1^{(1)}\,\bar{P}_{c1}^{(1)} \quad , \tag{5.31}$$

$$-\frac{1}{2}\,\beta_2^{(\gamma_{g2}+1)/2}\left[\psi_2^{(0)}\right]^{-(\gamma_{g2}-1)/2}\lambda^{2(\gamma_{g2}-1)}\,\psi_2^{(2)} + \frac{\gamma_c}{(\gamma_c-1)}\left[\psi_2^{(0)}\right]^{1/2}\lambda^{-2}\,\bar{P}_{c2}^{(2)} + \frac{1}{(\gamma_c-1)}\,\bar{\kappa}_2\left[\bar{P}_{c2}^{(2)}\right]' = -\frac{1}{2}\,\frac{\gamma_c}{(\gamma_c-1)}\left[\psi_2^{(0)}\right]^{1/2}\lambda^{-2}\,\psi_2^{(1)}\,\bar{P}_{c2}^{(1)}$$

$$- \frac{1}{8} (\gamma_{g2}+1) \beta_2^{(\gamma_{g2}+1)/2} \left[\psi_2^{(0)}\right]^{-(\gamma_{g2}-1)/2} \lambda^{2(\gamma_{g2}-1)} \left[\psi_2^{(1)}\right]^2 \quad ; \qquad (5.32)$$

where

$$\hat{L}_c = \bar{\kappa} \frac{d^2}{d\lambda^2} + \left[\bar{\kappa}' + \left[\psi^{(0)}\right]^{1/2} \lambda^{-2}\right] \frac{d}{d\lambda}$$
$$- \gamma_c \left[\psi^{(0)}\right]^{1/2} \lambda^{-2} \left[2\lambda^{-1} - \frac{1}{2}\left[\psi^{(0)}\right]^{-1} \left[\psi^{(0)}\right]'\right] \quad , \qquad (5.33)$$

and the superscript ' denotes derivative with respect to λ. The strategy of solving these equations at $O(\epsilon)$ is to first solve the test particle cosmic-ray energy equation (5.27) for $\bar{P}_c^{(1)}$, and then solve the perturbed total energy equations (5.28) and (5.29) for $\psi^{(1)}$ in the upstream and downstream regions of the shock. The solutions for $\bar{P}_c^{(1)}$ and $\psi^{(1)}$ must be matched at the shock by using the momentum amd energy balance conditions (5.14) – (5.17).

However, the location of the shock is altered by the perturbing influence of the cosmic-rays, and we assume the perturbed shock radius is given by the expansion

$$\lambda_{sh} = \lambda_{sh}^{(0)} + \epsilon \lambda_{sh}^{(1)} + \epsilon^2 \lambda_{sh}^{(2)} + \cdots \quad . \qquad (5.34)$$

It is found that the 1^{st} order correction $\lambda_{sh}^{(1)}$ is dependent on the gas energy flux difference $\bar{E}_{gsh} - \bar{E}_{g\infty}$ (up to $O(\epsilon)$), or alternatively on $\bar{E}_{c\infty} - \bar{E}_{csh}$ (see equation (5.47)).

We now proceed to obtain solutions of the perturbation equations up to $O(\epsilon)$. Using Taylor series expansions, ψ, $\bar{P}_c$ and $\bar{\kappa}$ at the perturbed shock radius may be expressed as:

$$\psi(\lambda_{sh}) = \psi_{sh}^{(0)} \left[1 + \epsilon \left[\lambda_{sh}^{(1)} \left[\psi_{sh}^{(0)}\right]^{-1} \left[\psi_{sh}^{(0)}\right]' + \psi_{sh}^{(1)}\right] + \cdots\right] \quad , \qquad (5.35)$$

$$\bar{P}_c(\lambda_{sh}) = \epsilon \bar{P}_{csh}^{(1)} + \cdots \quad , \qquad (5.36)$$

$$\bar{\kappa}(\lambda_{sh}) = \bar{\kappa}_{sh} + \epsilon\, \lambda_{sh}^{(1)}\, \bar{\kappa}'_{sh} + \cdots \quad , \tag{5.37}$$

where the subscript sh denotes quatities (except λ) are evaluated at the unperturbed shock radius ($\lambda = \lambda_{sh}^{(0)}$). The expressions (5.35) – (5.37) apply on both sides of the shock, and the Taylor series expansions are justified by the fact that the quantities on the upstream and downstream branches (excluding the shock) are smooth.

Using the perturbation expansions (5.19) – (5.24) and (5.35) – (5.37), the conservation of momentum and energy fluxes of the thermal gas and the cosmic-rays at the shock (equations (5.14) – (5.17)) yields conservation equations at different orders of ϵ. At zeroth order energy and momentum flux conservation of the thermal gas gives:

$$\frac{1}{2}\,\psi_{1sh}^{(0)} = \frac{1}{(\gamma_{g2}-1)}\,\beta_2^{(\gamma_{g2}+1)/2}\left[\psi_{2sh}^{(0)}\right]^{-(\gamma_{g2}-1)/2}\left[\lambda_{sh}^{(0)}\right]^{2(\gamma_{g2}-1)}$$

$$= \bar{E}_{g\infty}^{(0)} \quad , \tag{5.38}$$

$$\left[\psi_{1sh}^{(0)}\right]^{1/2} = \frac{1}{\gamma_{g2}}\,\beta_2^{(\gamma_{g2}+1)/2}\left[\psi_{2sh}^{(0)}\right]^{-\gamma_{g2}/2}\left[\lambda_{sh}^{(0)}\right]^{2(\gamma_{g2}-1)} \quad . \tag{3.39}$$

At 1^{st} order ($O(\epsilon)$) balancing the cosmic-ray pressure and energy flux results in:

$$\bar{P}_{c1sh}^{(1)} = \bar{P}_{c2sh}^{(1)} \quad , \tag{5.40}$$

$$\frac{\gamma_c}{(\gamma_c-1)}\left[\psi_{1sh}^{(0)}\right]^{1/2}\left[\lambda_{sh}^{(0)}\right]^{-2}\bar{P}_{c1sh}^{(1)} + \frac{1}{(\gamma_c-1)}\,\bar{\kappa}_1\left[\bar{P}_{c1sh}^{(1)}\right]'$$

$$= \frac{\gamma_c}{(\gamma_c-1)}\left[\psi_{2sh}^{(0)}\right]^{1/2}\left[\lambda_{sh}^{(0)}\right]^{-2}\bar{P}_{c2sh}^{(1)} + \frac{1}{(\gamma_c-1)}\,\bar{\kappa}_2\left[\bar{P}_{c2sh}^{(1)}\right]'$$

$$\equiv \bar{E}_{csh}^{(1)} \quad . \tag{5.41}$$

Balancing the thermal gas energy and momentum fluxes at the shock at $O(\epsilon)$ gives:

$$\frac{1}{2}\,\psi_{1sh}^{(0)}\left[\left(\psi_{1sh}^{(0)}\right)^{-1}\left(\psi_{1sh}^{(0)}\right)'\lambda_{sh}^{(1)}+\psi_{1sh}^{(1)}\right]$$

$$=\beta_2^{(\gamma_{g2}+1)/2}\left(\psi_{2sh}^{(0)}\right)^{-(\gamma_{g2}-1)/2}\left(\lambda_{sh}^{(0)}\right)^{2(\gamma_{g2}-1)}$$

$$\cdot\left[2\left(\lambda_{sh}^{(0)}\right)^{-1}\lambda_{sh}^{(1)}-\frac{1}{2}\left[\left(\psi_{2sh}^{(0)}\right)^{-1}\left(\psi_{2sh}^{(0)}\right)'\lambda_{sh}^{(1)}+\psi_{2sh}^{(1)}\right]\right]\quad,\tag{5.42}$$

$$\frac{1}{2}\left(\psi_{1sh}^{(0)}\right)^{1/2}\left[\left(\psi_{1sh}^{(0)}\right)^{-1}\left(\psi_{1sh}^{(0)}\right)'\lambda_{sh}^{(1)}+\psi_{1sh}^{(1)}\right]$$

$$=\beta_2^{(\gamma_{g2}+1)/2}\left(\psi_{2sh}^{(0)}\right)^{-\gamma_{g2}/2}\left(\lambda_{sh}^{(0)}\right)^{2(\gamma_{g2}-1)}$$

$$\cdot\left[2\,\frac{(\gamma_{g2}-1)}{\gamma_{g2}}\left(\lambda_{sh}^{(0)}\right)^{-1}\lambda_{sh}^{(1)}\right.$$

$$\left.-\frac{1}{2}\left[\left(\psi_{2sh}^{(0)}\right)^{-1}\left(\psi_{2sh}^{(0)}\right)'\lambda_{sh}^{(1)}+\psi_{2sh}^{(1)}\right]\right]\quad.\tag{5.43}$$

Using the zeroth order energy and momentum flux conservation equations (5.38) and (5.39), we can eliminate the normalized gas entropy constant in equations (5.42) and (5.43) to obtain:

$$\left(\psi_{1sh}^{(0)}\right)^{-1}\left(\psi_{1sh}^{(0)}\right)'\lambda_{sh}^{(1)}+\psi_{1sh}^{(1)}=\left(\psi_{2sh}^{(0)}\right)^{-1}\left(\psi_{2sh}^{(0)}\right)'\lambda_{sh}^{(1)}+\psi_{2sh}^{(1)}\quad,\tag{5.44}$$

$$\psi_{1sh}^{(1)}=\left[4\,\frac{(\gamma_{g2}-1)}{(\gamma_{g2}+1)}\left(\lambda_{sh}^{(0)}\right)^{-1}-\left(\psi_{1sh}^{(0)}\right)^{-1}\left(\psi_{1sh}^{(0)}\right)'\right]\lambda_{sh}^{(1)}\quad.\tag{5.45}$$

Using the expression (5.8) to determine $\bar{E}_{gsh}$, and using overall energy flux conservation (equation (5.4)) we find (up to $O(\epsilon)$):

$$\bar{E}_{gsh}-\bar{E}_{g\infty}^{(0)}=\epsilon\left[\bar{E}_{c\infty}^{(1)}-\bar{E}_{csh}^{(1)}\right]$$

$$=\frac{1}{2}\,\epsilon\,\psi_{1sh}^{(0)}\left[\left(\psi_{1sh}^{(0)}\right)^{-1}\left(\psi_{1sh}^{(0)}\right)'\lambda_{sh}^{(1)}+\psi_{1sh}^{(1)}\right]\quad,\tag{5.46}$$

so that equation (5.45) may be rearranged to yield:

$$\lambda_{sh}^{(1)}=\frac{1}{2}\,\frac{(\gamma_{g2}+1)}{(\gamma_{g2}-1)}\left(\psi_{1sh}^{(0)}\right)^{-1}\lambda_{sh}^{(0)}\left[\bar{E}_{c\infty}^{(1)}-\bar{E}_{csh}^{(1)}\right]\quad.\tag{5.47}$$

The interesting physical result here is that $\lambda_{sh}^{(1)}>0$, and the radius of the shock in the cosmic-ray modified wind, r_{sh}, is smaller than that

of the unperturbed wind, $r_{sh}^{(0)}$, if the cosmic-ray energy flux at infinity exceeds its value at the shock. On the other hand if the cosmic-ray energy flux at the shock exceeds the cosmic-ray energy flux at infinity (presumably due to effective acceleration and containment of the cosmic-rays near the shock), then $r_{sh} > r_{sh}^{(0)}$, and the cosmic-rays force the shock outward. From equations (5.14), (5.16), (5.38) and (5.39), we notice that the compression ratios $q \equiv (\psi_{1sh}/\psi_{2sh})^{1/2}$ and $q^{(0)} \equiv (\psi_{1sh}^{(0)}/\psi_{2sh}^{(0)})^{1/2}$ are equal, and

$$q = q^{(0)} = \frac{2\gamma_{g2}}{(\gamma_{g2}-1)} \quad . \tag{5.48}$$

This is a result of the simplified model. A cold gas upstream and a very hot gas downstream imply an infinitely strong shock, and the compression ratio (5.48) exceeds the compression ratio $(\gamma_{g2}+1)/(\gamma_{g2}-1)$ expected for an infinite Mach number shock (see §2.2 for details). Basically, this is a consequence of neglecting the downstream ram pressure and kinetic energy flux of the gas, and is a major defect of the simplified model. However, this defect is eliminated in the extension of the perturbation method, using the one fluid polytropic stellar wind (with shock) for the background flow (§5.2).

If the diffusion coefficient is proportional to radius and of the form:

$$\bar{\kappa} = \bar{\kappa}_{1o}\, \lambda^{-1}\, [1 - H(\lambda_{sh}-\lambda)] + \bar{\kappa}_{2o}\, \lambda^{-1}\, H(\lambda_{sh}-\lambda) \quad , \tag{5.49}$$

there are simple analytical solutions to equations (5.25) – (5.29) subject to the appropriate boundary conditions. These analytical solutions show the basic features of the more realistic model (see §5.2

and chapter 6). Investigation of equations (5.25) – (5.29) shows that the equations can be solved step by step. We first find the unperturbed flow profile (equation (5.25) and (5.26)), then solve equation (5.27) for the (1^{st} order) cosmic-ray pressure (c.f. Webb, Forman and Axford 1985 and appendix E), then find the 1^{st} order correction to the background flow, and we can go on to 2^{nd} order corrections in a straight forward way.

Below, we give the perturbation solution corresponding to the diffusion coefficient (5.49). The unperturbed velocity profile is

$$\psi_1^{(0)} = 2\,\bar{E}_{g\infty}^{(0)} = \frac{2\gamma_{g2}}{(\gamma_{g2}-1)}\,\frac{P_{g\infty}}{\rho_{g\infty}}\left(\frac{m_g}{kT_o}\right) , \tag{5.50}$$

$$\psi_2^{(0)} = \left(\frac{\rho_o}{\rho_{g\infty}}\right)^2 \lambda^4 , \tag{5.51}$$

$$\lambda_{sh}^{(0)} = \left[\frac{(\gamma_{g2}-1)}{2\gamma_{g2}}\, j^{-2}\, P_{g\infty}\, \rho_{g\infty}\right]^{1/4} (GM_o)\left(\frac{m_g}{kT_o}\right) . \tag{5.52}$$

The 1^{st} order cosmic-ray pressure is (note the shock is at $\lambda_{sh}^{(0)}$):

$$\bar{P}_{c1}^{(1)} = \frac{1}{D}\left(\frac{\lambda}{\lambda_{sh}^{(0)}}\right)^{-\alpha} \frac{P_{g\infty}}{\rho_o}\left(\frac{m_g}{kT_o}\right) , \tag{5.53}$$

$$\bar{P}_{c2}^{(1)} = \frac{1}{D}\left[\left[\gamma_c - q\left(\gamma_c - \frac{\alpha}{\eta_1}\right)\right] \exp\left[\frac{1}{2}\,\eta_2\left[1 - \left(\frac{\lambda}{\lambda_{sh}^{(0)}}\right)^2\right]\right] + q\left(\gamma_c - \frac{\alpha}{\eta_1}\right) - (\gamma_c - 1)\right] \frac{P_{g\infty}}{\rho_o}\left(\frac{m_g}{kT_o}\right) , \tag{5.54}$$

where

$$D \equiv 1 + [\exp(\tfrac{1}{2}\eta_2) - 1]\left[\gamma_c - q\left(\gamma_c - \frac{\alpha}{\eta_1}\right)\right] , \tag{5.55}$$

$$\alpha \equiv \frac{1}{2}\left((\eta_1 - 2) + [(\eta_1 - 2)^2 + 8\,\gamma_c\,\eta_1]^{1/2}\right) , \tag{5.56}$$

$$\eta_1 = \frac{r_{sh}^{(0)} u_{1sh}^{(0)}}{\kappa_1} = \frac{1}{\bar{\kappa}_{1o}} \left[\psi_1^{(0)}\right]^{1/2} , \tag{5.57}$$

$$\eta_2 = \frac{r_{sh}^{(0)} u_{2sh}^{(0)}}{\kappa_2} = \frac{1}{\bar{\kappa}_{2o}} \frac{\rho_o}{\rho_{g\infty}} \left[\lambda_{sh}^{(0)}\right]^2 . \tag{5.58}$$

The 1^{st} order correction to the velocity profile is

$$\psi_1^{(1)} = \frac{1}{D}\left[\frac{(\gamma_{g2}-1)}{\gamma_{g2}}(D-1) + \frac{2\alpha}{(\alpha+2)}\left[1 - \left[\frac{\lambda}{\lambda_{sh}^{(0)}}\right]^{-(\alpha+2)}\right]\right] , \tag{5.59}$$

$$\psi_2^{(1)} = -\frac{2}{\gamma_{g2}}\frac{1}{D}\exp(\tfrac{1}{2}\eta_2)\left[\gamma_c - q\left[\gamma_c - \frac{\alpha}{\eta_1}\right]\right] \cdot \left[1 - \exp\left[-\frac{1}{2}\eta_2\left[\frac{\lambda}{\lambda_{sh}^{(0)}}\right]^2\right]\right] , \tag{5.60}$$

and the corrections at the shock are

$$\lambda_{sh}^{(1)} = \frac{(\gamma_{g2}+1)}{4\gamma_{g2}}\frac{(D-1)}{D}\lambda_{sh}^{(0)} , \tag{5.61}$$

$$\psi_{sh}^{(1)} = \frac{(\gamma_{g2}-1)}{\gamma_{g2}}\frac{(D-1)}{D} , \tag{5.62}$$

$$\psi_{sh}^{(1)} = -\frac{2}{\gamma_{g2}}\frac{(D-1)}{D} . \tag{5.63}$$

From equations (3.14), the radius of the shock and the stellar wind velocity in physical units are

$$r_{sh} = r_{sh}^{(0)}\left[1 - \epsilon\left[\lambda_{sh}^{(0)}\right]^{-1}\lambda_{sh}^{(1)} + \cdots\right] , \tag{5.64}$$

$$u = u^{(0)}\left[1 + \frac{1}{2}\epsilon\,\psi^{(1)} + \cdots\right] , \tag{5.65}$$

where $r_{sh}^{(0)}$ and $u^{(0)}$ are the unperturbed radius of the shock and stellar wind profile respectively.

For the perturbed shock radius, r_{sh}, to be less than the unperturbed shock radius, $r_{sh}^{(0)}$, we require $\lambda_{sh}^{(1)}$ to be positive (see equation (5.64)). From equation (5.61) we find $\lambda_{sh}^{(1)} > 0$ whenever

$$\gamma_c - q\left(\gamma_c - \frac{\alpha}{\eta_1}\right) > 0 \quad , \tag{5.66}$$

and this occurs if

$$\frac{1}{\eta_1} > \frac{1}{2}\frac{(q-1)}{q}\left[(\gamma_c - 1)\, q - \gamma_c\right] \quad , \tag{5.67}$$

or if

$$\frac{1}{\eta_1} < \frac{1}{2} - \gamma_c \frac{(q-1)}{q} \quad . \tag{5.68}$$

Since the condition (5.68) is never satisfied in practice (for $q = 2\gamma_{g2}/(\gamma_{g2}-1)$ from equation (5.48), condition (5.68) is impossible if $\gamma_{g2} > 0$, $\gamma_c > 0$ and $\eta_1 > 0$), then $r_{sh} < r_{sh}^{(0)}$ if condition (5.67) is satisfied.

To obtain some physical insight into the condition (5.66) we note from equation (5.54) that

$$\frac{dP_{c2}}{dr} = \frac{1}{D}\eta_2\left[\gamma_c - q\left(\gamma_c - \frac{\alpha}{\eta_1}\right)\right]\left(\frac{\lambda}{\lambda_{sh}^{(0)}}\right)^2 \cdot \exp\left[\frac{1}{2}\eta_2\left[1 - \left(\frac{\lambda}{\lambda_{sh}^{(0)}}\right)^2\right]\right]\frac{P_{c\infty}}{r} \quad . \tag{5.69}$$

Comparing condition (5.66) and equation (5.69) we see that $r_{sh} < r_{sh}^{(0)}$ whenever the cosmic-ray pressure gradient outside the shock is positive. If on the other hand $\frac{dP_{c2}}{dr} < 0$, the cosmic-ray pressure (and energy flux) at the shock exceeds that at infinity (presumably due to very effective acceleration of cosmic-rays at the shock), so that $r_{sh} > r_{sh}^{(0)}$, and the cosmic-rays push the shock outward. If the shock compression ratio $q < \gamma_c/(\gamma_c-1)$ (e.g. $q < 4$ if $\gamma_c = 4/3$), condition (5.67) always holds. If the shock compression ratio $q < \gamma_c/(\gamma_c-1)$, then condition (5.67) implies that $r_{sh} < r_{sh}^{(0)}$ if the

modulation paramater $\eta_1 = r_{sh}^{(0)} u_{1sh}^{(0)}/\kappa_1$ is small enough (or κ_1 large enough).

Numerical examples illustrating the perturbation scheme are shown in figures 5.1 and 5.2 for a stellar wind model with $\dot{M} = 6*10^{11}$ g s^{-1}, $P_{g\infty} = 1$ eV cm^{-3}, $\rho_{g\infty} = 6*10^{-27}$ g cm^{-3} and $\gamma_{g2} = 5/3$. Figure 5.1, for which $\gamma_c = 4/3$, shows the radial variation of the unperturbed fluid velocity $u^{(0)}/u_{1sh}^{(0)}$ (curve *a*); the radial variation of $P_c/P_{c\infty}$ (curve *d*); and the modified stellar wind profile $u/u_{1sh}^{(0)}$ (curve *b*) for an example in which there is relatively weak coupling between the cosmic-rays and the thermal gas: $\kappa_1/\left[r_{sh}^{(0)} u_{1sh}^{(0)}\right] = 5$ ($\eta_1 = 0.2$) and $\kappa_2/\left[r_{sh}^{(0)} u_{1sh}^{(0)}\right] = 5$ ($\eta_2 = 0.2$). The parameter $\epsilon = 1$ since $P_{c\infty} = P_{g\infty} = 1$ in this example. The fluid

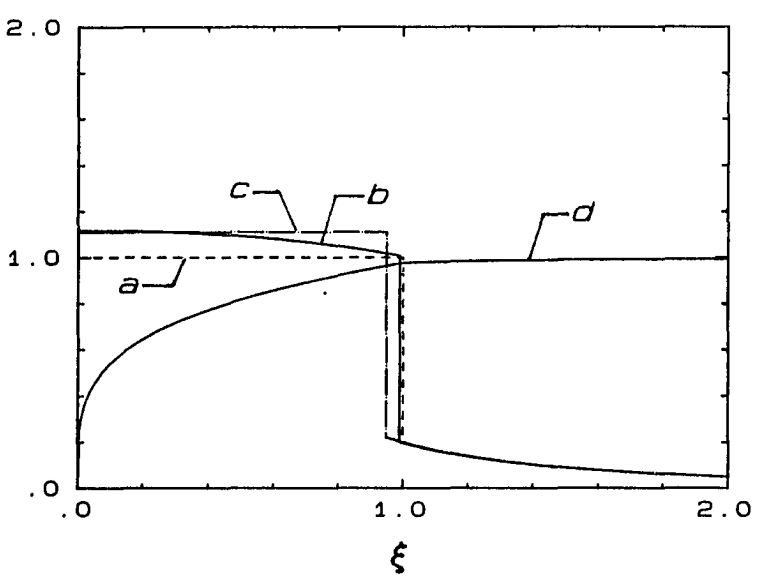

Figure 5.1 Perturbation Solution for the Simplified Model with Large κ

The plotting quantities are $\xi = r/R$, $\tilde{u} = u/u_o$ and $\tilde{P}_c = P_c/P_{co}$, where $R = r_{sh}^{(0)} = 69.6$ A.U., $u_o = u_{1sh}^{(0)} = 365$ km s^{-1}, $P_{co} = \epsilon P_{g\infty}$ and $\epsilon = 1$. The normalized cosmic-ray diffusion coefficients are $\tilde{\kappa}_1 = \kappa_1/\kappa_o = 5$ and $\tilde{\kappa}_2 = \kappa_2/\kappa_o = 5$, where $\kappa_o = Ru_o = 3.81*10^{22}$ cm^2 s^{-1}.

upstream of the shock in the cosmic-ray modified wind is seen to have been significantly decelerated ($\approx 10\%$) by the positive cosmic-ray pressure gradient, (as expected from the gas momentum equation (3.2)), and the shock occurs at a smaller radius than in the unmodified wind ($r_{sh} < r_{sh}^{(0)}$). The curve *c* shows for comparison, the wind velocity profile of an unmodified wind with the same total energy flux and gas density at infinity as the cosmic-ray modified wind. Accordingly, $P_{g\infty}$ is replaced by $P_{g\infty} + \frac{(\gamma_{g2}-1)}{\gamma_{g2}} \frac{\rho_{g\infty} F_{c\infty}}{j^2}$.

In cases of pure one fluid polytropic stellar winds (curves *a* and *c*) the gas is assumed incompressible outside the shock and consequently the gas pressure just outside the shock is $P_{g\infty}$. Balancing this pressure against the upstream ram pressure; and noting the gas density just upstream of the shock is given by $\rho_{1sh} = j/\left[\left[r_{sh}^{(0)}\right]^2 u_{1sh}^{(0)}\right]$, we obtain

$$r_{sh}^{(0)} = \left[j\, u_{1sh}^{(0)}\, P_{g\infty}^{-1}\right]^{1/2} \tag{5.70}$$

(c.f. equation (2.30)), and $u_{1sh}^{(0)}$ is given by equation (5.50). On the other hand for the cosmic-ray modified wind the location of the shock to $O(\epsilon)$ is given by (use equations (5.46), (5.47) and (5.64)):

$$r_{sh} = r_{sh}^{(0)} \left[1 - \frac{1}{2} \frac{(\gamma_{g2}+1)}{(\gamma_{g2}-1)} \left[\bar{E}_{gsh} - \bar{E}_{g\infty}^{(0)}\right] \left[\psi_{1sh}^{(0)}\right]^{-1}\right] \tag{5.71}$$

Thus in the cosmic-ray modified stellar wind, the shock location depends on the value of the normalized gas energy constant at the shock, $\bar{E}_{gsh}$, and r_{sh} decreases as $\bar{E}_{gsh}$ increases.

A further example of the perturbation solution is shown in

figure 5.2, for which $\gamma_c = 4/3$ and the cosmic-ray diffusion coefficients are $\kappa_1 = \kappa_2 = r_{sh}^{(0)} u_{1sh}^{(0)}$ ($\eta_1 = \eta_2 = 1$). The wind just upstream of the shock is more strongly decelerated and r_{sh} is smaller than for the example in figure 5.1 where $\kappa / r_{sh}^{(0)} u_{1sh}^{(0)} = 5$. These two examples show that the wind is more strongly modified, the smaller the value of κ_1 and κ_2, since the cosmic-rays are then more strongly coupled to the wind.

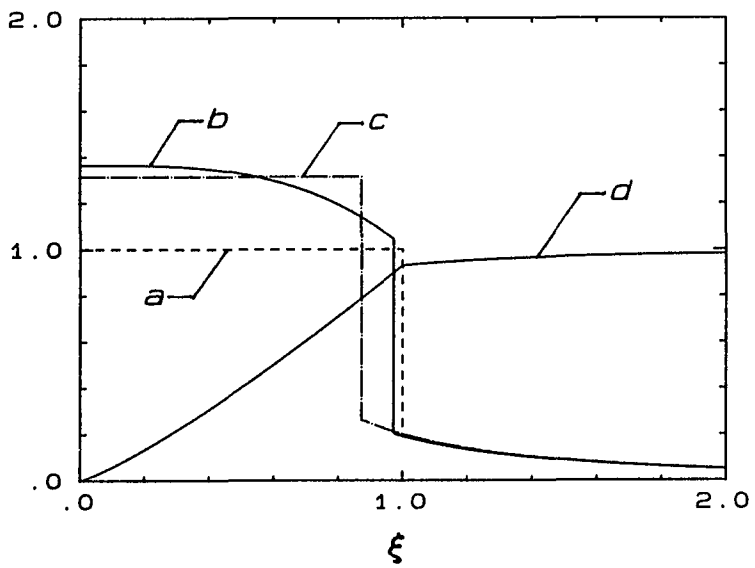

Figure 5.2 Perturbation Solution for the Simplified Model with Small κ

The plotting quantities are $\xi = r/R$, $\bar{u} = u/u_o$ and $\bar{P}_c = P_c/P_{co}$, where $R = r_{sh}^{(0)} = 69.6$ A.U. , $u_o = u_{1sh}^{(0)} = 365$ km s^{-1} , $P_{co} = \epsilon P_{g\infty}$ and $\epsilon = 1$. The normalized cosmic-ray diffusion coefficients are $\tilde{\kappa}_1 = \kappa_1/\kappa_o = 1$ and $\tilde{\kappa}_2 = \kappa_2/\kappa_o = 1$, where $\kappa_o = Ru_o = 3.81 * 10^{22}$ cm^2 s^{-1} .

Since we have not as yet developed a method to solve the full nonlinear system of equations (see chapter 6) it is difficult to gauge how accurate the perturbation scheme is. We expect the scheme to be more accurate, the smaller the value of $\epsilon = P_{c\infty}/P_{g\infty}$, and the larger the cosmic-ray diffusion coefficient, since for large diffusion

coefficients the coupling between the wind and the cosmic-rays is weak.

§5.2 Perturbation Solution for a More Realistic Model

In this section the perturbation analysis is carried out using the one fluid polytropic stellar wind of §2.2 for the unperturbed background flow. The fundamental equations are (5.2) – (5.7). Thus the gas normalized energy fluxes upstream and downstream of the shock are:

$$\bar{E}_{g1} = \frac{1}{2}\psi_1 - \lambda + \frac{1}{(\gamma_{g1}-1)}\beta_1^{(\gamma_{g1}+1)/2}\psi_1^{-(\gamma_{g1}-1)/2}\lambda^{2(\gamma_{g1}-1)} , \quad (5.72)$$

$$\bar{E}_{g2} = \frac{1}{2}\psi_2 - \lambda + \frac{1}{(\gamma_{g2}-1)}\beta_2^{(\gamma_{g2}+1)/2}\psi_2^{-(\gamma_{g2}-1)/2}\lambda^{2(\gamma_{g2}-1)} . \quad (5.73)$$

The boundary conditions are the same as §5.1 (equations (5.12) – (5.18)) except $\bar{P}_c$ is finite as $r \to 0$ (equation (5.18)) is replaced by

$$\frac{dP_c}{dr} = 0 . \quad (5.74)$$

This is more suitable for numerical calculations (see §4.1).

We use the same perturbation scheme as in §5.1, but in addition to equations (5.19) – (5.22) we need to expand the normalized gas entropy constants β_1 and β_2 on both sides of the shock in terms of the perturbation parameter $\epsilon \equiv P_{c\infty}/P_{g\infty}$:

$$\beta_1 = \beta_1^{(0)}(1 + \epsilon\,\beta_1^{(1)} + \cdots) , \quad (5.75)$$

$$\beta_2 = \beta_2^{(0)}(1 + \epsilon\,\beta_2^{(1)} + \cdots) . \quad (5.76)$$

The entropy change across the shock depends on the compression ratio of the shock which in turns depends on the modification of the shock by the cosmic-rays. The downstream entropy constant is determined by the gas pressure and density at infinity. Since $P_{g\infty}$ and $\rho_{g\infty}$ are the same for both the unperturbed wind and for the cosmic-ray modified wind, it

follows that the downstream normalized entropy constant is the same in both cases, and

$$\beta_2 = \beta_2^{(0)} = \left[\gamma_{g2} \frac{P_{g\infty}}{\rho_{g\infty}} \left(\frac{\rho_o}{\rho_{g\infty}}\right)^{(\gamma_{g2}-1)} \left(\frac{m_g}{kT_o}\right)\right]^{2/(\gamma_{g2}+1)} \tag{5.77}$$

(c.f. equation (2.38)). Thus $\beta_2^{(i)} = 0$, for $i \geq 1$.

The zeroth order perturbation of the total energy equation (5.4) gives

$$\frac{1}{2}\psi^{(0)} - \lambda + \frac{1}{(\gamma_g-1)}\left[\beta^{(0)}\right]^{(\gamma_g+1)/2}\left[\psi^{(0)}\right]^{-(\gamma_g-1)/2}\lambda^{2(\gamma_g-1)} = \bar{E}_{g\infty}^{(0)} , \tag{5.78}$$

where $\bar{E}_{g\infty}^{(0)}$ is defined by equation (5.23). At $O(\epsilon)$, the cosmic-ray energy equation (5.7), and the total energy equation (5.4) imply

$$\hat{L}_c \bar{P}_c^{(1)} = 0 , \tag{5.79}$$

$$\frac{1}{2}\psi^{(0)}\psi^{(1)}\left[1 - \left[\beta^{(0)}\right]^{(\gamma_g+1)/2}\left[\psi^{(0)}\right]^{-(\gamma_g+1)/2}\lambda^{2(\gamma_g-1)}\right] + \frac{1}{2}\frac{(\gamma_g+1)}{(\gamma_g-1)}\left[\beta^{(0)}\right]^{(\gamma_g+1)/2}\left[\psi^{(0)}\right]^{-(\gamma_g-1)/2}\lambda^{2(\gamma_g-1)}\beta^{(1)} + \frac{\gamma_c}{(\gamma_c-1)}\left[\psi^{(0)}\right]^{1/2}\lambda^{-2}\bar{P}_c^{(1)} + \frac{1}{(\gamma_c-1)}\bar{\kappa}\left[\bar{P}_c^{(1)}\right]' = \bar{E}_{c\infty}^{(1)} , \tag{5.80}$$

where $\hat{L}_c$ and $\bar{E}_{c\infty}^{(1)}$ are defined by equations (5.33) and (5.24) respectively.

The major difference between perturbation equations (5.78) – (5.80) and perturbation equations (5.25) – (5.29) is that the former set of equations contains the extra unknowns $\beta_1^{(0)}$ and $\beta_2^{(1)}$. As in §2.2, $\beta_1^{(0)}$ and $\beta_2^{(1)}$ can be determined by the requirement that the upstream solution is a transonic solution. The critical point of the

perturbed stellar wind is expected to depend on the cosmic-rays. Thus we assume that the perturbed critical point in the λ–ψ plane can be expanded in a power series in ϵ of the form:

$$\lambda_c = \lambda_c^{(0)} + \epsilon\, \lambda_c^{(1)} + \cdots \quad . \tag{5.81}$$

$$\psi(\lambda_c) = \psi_c^{(0)} \left[1 + \epsilon \left[\lambda_c^{(1)} \left[\psi_c^{(0)} \right]^{-1} \left[\psi_c^{(0)} \right]' + \psi_c^{(1)} \right] + \cdots \right] \quad , \tag{5.82}$$

where the subscript c denotes quantities (except λ) are evaluated at the unperturbed critical point $\lambda_c^{(0)}$. From §3.2, we recall that the cosmic-ray stellar wind system exhibits critical behaviour when the fluid velocity matches the local thermal gas sound speed and the acceleration of the fluid is zero. From equations (3.57) – (3.60), we see that fluid velocity matches the local gas sound speed when

$$\psi_c = \beta_1\, \lambda_c^{4(\gamma_{g1}-1)/(\gamma_{g1}+1)} \quad , \tag{5.83}$$

and the acceleration of the fluid is zero when

$$\frac{d\bar{P}_c}{d\lambda} = \beta_1^{-1/2}\, \lambda_c^{4/(\gamma_{g1}+1)} - 2\, \beta_1^{1/2}\, \lambda_c^{(3\gamma_{g1}-1)/(\gamma_{g1}+1)} \quad . \tag{5.84}$$

Using the perturbation expansions (5.75), (5.81), (5.82) and (5.20) for β_1, λ_c, ψ_c and $\bar{P}_c$, equations (5.83) and (5.84) at zeroth order yield:

$$\psi_c^{(0)} = \beta_1^{(0)} \left[\lambda_c^{(0)} \right]^{4(\gamma_{g1}-1)/(\gamma_{g1}+1)} \quad , \tag{5.85}$$

$$\left[\beta_1^{(0)} \right]^{-1/2} \left[\lambda_c^{(0)} \right]^{4/(\gamma_{g1}+1)} - 2 \left[\beta_1^{(0)} \right]^{1/2} \left[\lambda_c^{(0)} \right]^{(3\gamma_{g1}-1)/(\gamma_{g1}+1)} = 0 \quad . \tag{5.86}$$

Solving equation (5.86) for $\lambda_c^{(0)}$ in terms of $\beta_1^{(0)}$, and substituting the result in equation (5.85) we obtain

$$\lambda_c^{(0)} = \left[2\beta_1^{(0)} \right]^{(\gamma_{g1}+1)/(5-3\gamma_{g1})} \quad , \tag{5.87}$$

$$\psi_c^{(0)} = \frac{1}{2}\, \lambda_c^{(0)} \quad . \tag{5.88}$$

Note that the point $(\lambda_c^{(0)}, \psi_c^{(0)})$ is the critical point of the unperturbed one fluid polytropic stellar wind (c.f. equations (2.18) and (2.19)). At $O(\epsilon)$ equations (5.83) and (5.84) yield:

$$\left[\psi_c^{(0)}\right]^{-1} \left[\psi_c^{(0)}\right]' \lambda_c^{(1)} + \psi_c^{(1)} = \beta_1^{(1)} + 4 \frac{(\gamma_{g1}-1)}{(\gamma_{g1}+1)} \left[\lambda_c^{(0)}\right]^{-1} \lambda_c^{(1)} \quad , \tag{5.89}$$

$$\left[\bar{P}_{cc}^{(1)}\right]' = -\sqrt{2} \left[\lambda_c^{(0)}\right]^{3/2} \left[\beta_1^{(1)} - \frac{(5-3\gamma_{g1})}{(\gamma_{g1}+1)} \left[\lambda_c^{(0)}\right]^{-1} \lambda_c^{(1)}\right] \quad , \tag{5.90}$$

and these equations are the $O(\epsilon)$ critical point requirements.

Since the total energy flux for the cosmic-ray modified stellar wind system is conserved so that

$$\bar{E} = \bar{E}_{g\infty}^{(0)} + \epsilon \bar{E}_{c\infty}^{(1)} = \bar{E}_{gc}^{(0)} + \epsilon \left[\bar{E}_{gc}^{(1)} + \epsilon \bar{E}_{cc}^{(1)}\right] + \cdots \quad , \tag{5.91}$$

where $\bar{E}_{g\infty}^{(0)}$ and $\bar{E}_{c\infty}^{(1)}$ are given by equations (5.23) and (5.24) respectively. At zeroth order, equation (5.91) combined with equations (5.2), (5.87) and (5.88) yields

$$\bar{E}_{g\infty}^{(0)} = \frac{(5-3\gamma_{g1})}{4(\gamma_{g1}-1)} \lambda_c^{(0)} \quad . \tag{5.92}$$

Hence

$$\lambda_c^{(0)} = \frac{4(\gamma_{g1}-1)}{(5-3\gamma_{g1})} \bar{E}_{g\infty}^{(0)} \quad , \tag{5.93}$$

$$\beta_1^{(0)} = \frac{1}{2} \left[\lambda_c^{(0)}\right]^{(5-3\gamma_{g1})/(\gamma_{g1}+1)} \quad , \tag{5.94}$$

so that the unperturbed critical point $\lambda_c^{(0)}$ and the normalized entropy constant $\beta_1^{(0)}$ are given in terms of $\bar{E}_{g\infty}^{(0)}$ and γ_{g1}. At $O(\epsilon)$, the total energy equation (5.91), gives

$$\bar{E}_{c\infty}^{(1)} = \frac{1}{4} \frac{(\gamma_{g1}+1)}{(\gamma_{g1}-1)} \lambda_c^{(0)} \beta_1^{(1)} + \bar{E}_{cc}^{(1)} \quad . \tag{5.95}$$

From equations (5.89), (5.90) and (5.95) we can now solve for $\psi_c^{(1)}$, $\lambda_c^{(1)}$

and $\beta_1^{(1)}$ in terms of the test particle cosmic-ray quantities $\bar{E}_{cc}^{(1)}$ and $\left[\bar{P}_{cc}^{(1)}\right]'$ (which in turn are determined by solving the normalized cosmic-ray energy (5.79) in the unperturbed flow) to obtain:

$$\beta_1^{(1)} = 4 \frac{(\gamma_{g1}-1)}{(\gamma_{g1}+1)} \left[\lambda_c^{(0)}\right]^{-1} \left[\bar{E}_{c\infty}^{(1)} - \bar{E}_{cc}^{(1)}\right] , \tag{5.96}$$

$$\lambda_c^{(1)} = \frac{(\gamma_{g1}+1)}{(5-3\gamma_{g1})} \lambda_c^{(0)} \left[\beta_1^{(1)} + \frac{1}{\sqrt{2}} \left[\lambda_c^{(0)}\right]^{-3/2} \left[\bar{P}_{cc}^{(1)}\right]'\right] , \tag{5.97}$$

$$\psi_c^{(1)} = \beta_1^{(1)} + \left[4 \frac{(\gamma_{g1}-1)}{(\gamma_{g1}+1)} \left[\lambda_c^{(0)}\right]^{-1} - \left[\psi_c^{(0)}\right]^{-1} \left[\psi_c^{(0)}\right]'\right] \lambda_c^{(1)} . \tag{5.98}$$

Since

$$\left[\psi_c^{(0)}\right]' = \frac{2}{(\gamma_{g1}+1)} \left[(\gamma_{g1}-1) - \frac{1}{\sqrt{2}} (5-3\gamma_{g1})^{1/2}\right] , \tag{5.99}$$

for the one fluid polytropic stellar wind (see appendix A), we can write equation (5.98) as

$$\psi_c^{(1)} = \beta_1^{(1)} + \frac{\sqrt{8}}{(\gamma_{g1}+1)} (5-3\gamma_{g1})^{1/2} \left[\lambda_c^{(0)}\right]^{-1} \lambda_c^{(1)} . \tag{5.100}$$

Thus equations (5.96) – (5.100) now completely determine $\beta_1^{(1)}$, $\lambda_c^{(1)}$ and $\psi_c^{(1)}$ in terms of cosmic-ray quantities at the unperturbed critical point.

We now discuss the boundary conditions at the shock and determine the modified quantities at the shock. As discussed in chapter 4, the thermal gas and cosmic-rays are decoupled at the shock. Balancing the momentum and energy fluxes of the thermal gas at the shock, we obtain (c.f. equations (5.2) and (5.6)):

$$\psi_{1sh}^{1/2} + \frac{1}{\gamma_{g1}} \beta_1^{(\gamma_{g1}+1)/2} \psi_{1sh}^{-\gamma_{g1}/2} \lambda_{sh}^{2(\gamma_{g1}-1)}$$
$$= \psi_{2sh}^{1/2} + \frac{1}{\gamma_{g2}} \beta_2^{(\gamma_{g2}+1)/2} \psi_{2sh}^{-\gamma_{g2}/2} \lambda_{sh}^{2(\gamma_{g2}-1)} , \tag{5.101}$$

$$\bar{E}_{gsh} = \frac{1}{2}\psi_{1sh} - \lambda_{sh} + \frac{1}{(\gamma_{g1}-1)}\beta_1^{(\gamma_{g1}+1)/2}\psi_{1sh}^{-(\gamma_{g1}-1)/2}\lambda_{sh}^{2(\gamma_{g1}-1)}, \quad (5.102)$$

$$\bar{E}_{gsh} = \frac{1}{2}\psi_{2sh} - \lambda_{sh} + \frac{1}{(\gamma_{g2}-1)}\beta_2^{(\gamma_{g2}+1)/2}\psi_{2sh}^{-(\gamma_{g2}-1)/2}\lambda_{sh}^{2(\gamma_{g2}-1)}. \quad (5.103)$$

Similarly, balancing the cosmic-ray pressure and energy flux at the shock gives:

$$\bar{P}_{c1sh} = \bar{P}_{c2sh}, \quad (5.104)$$

$$\frac{\gamma_c}{(\gamma_c-1)}\psi_{1sh}^{1/2}\lambda_{sh}^{-2}\bar{P}_{c1sh} + \frac{1}{(\gamma_c-1)}\bar{\kappa}_{1sh}\left.\frac{d\bar{P}_{c1}}{d\lambda}\right|_{sh} = \frac{\gamma_c}{(\gamma_c-1)}\psi_{2sh}^{1/2}\lambda_{sh}^{-2}\bar{P}_{c2sh} + \frac{1}{(\gamma_c-1)}\bar{\kappa}_{2sh}\left.\frac{d\bar{P}_{c2}}{d\lambda}\right|_{sh} \equiv \bar{E}_{csh}. \quad (5.105)$$

Using the expansions (5.34) – (5.37) we obtain at zeroth order:

$$\left[\psi_{1sh}^{(0)}\right]^{1/2} + \frac{1}{\gamma_{g1}}\left[\beta_1^{(0)}\right]^{(\gamma_{g1}+1)/2} \cdot \left[\psi_{1sh}^{(0)}\right]^{-\gamma_{g1}/2}\left[\lambda_{sh}^{(0)}\right]^{2(\gamma_{g1}-1)} = \left[\psi_{2sh}^{(0)}\right]^{1/2} + \frac{1}{\gamma_{g2}}\left[\beta_2^{(0)}\right]^{(\gamma_{g2}+1)/2} \cdot \left[\psi_{2sh}^{(0)}\right]^{-\gamma_{g2}/2}\left[\lambda_{sh}^{(0)}\right]^{2(\gamma_{g2}-1)}, \quad (5.106)$$

$$\bar{E}_{g\infty}^{(0)} = \frac{1}{2}\psi_{1sh}^{(0)} - \lambda_{sh}^{(0)} + \frac{1}{(\gamma_{g1}-1)}\left[\beta_1^{(0)}\right]^{(\gamma_{g1}+1)/2}\left[\psi_{1sh}^{(0)}\right]^{-(\gamma_{g1}-1)/2}\left[\lambda_{sh}^{(0)}\right]^{2(\gamma_{g1}-1)}, \quad (5.107)$$

$$\bar{E}_{g\infty}^{(0)} = \frac{1}{2}\psi_{2sh}^{(0)} - \lambda_{sh}^{(0)} + \frac{1}{(\gamma_{g2}-1)}\left[\beta_2^{(0)}\right]^{(\gamma_{g2}+1)/2}\left[\psi_{2sh}^{(0)}\right]^{-(\gamma_{g2}-1)/2}\left[\lambda_{sh}^{(0)}\right]^{2(\gamma_{g2}-1)}; \quad (5.108)$$

and at 1st order ($O(\epsilon)$):

$$\bar{P}^{(1)}_{c1sh} = \bar{P}^{(1)}_{c2sh} \quad , \tag{5.109}$$

$$\frac{\gamma_c}{(\gamma_c-1)} \left[\psi^{(0)}_{1sh}\right]^{1/2} \left[\lambda^{(0)}_{sh}\right]^{-2} \bar{P}^{(1)}_{c1sh} + \frac{1}{(\gamma_c-1)} \bar{\kappa}_{1sh} \left[\bar{P}^{(1)}_{c1sh}\right]'$$

$$= \frac{\gamma_c}{(\gamma_c-1)} \left[\psi^{(0)}_{2sh}\right]^{1/2} \left[\lambda^{(0)}_{sh}\right]^{-2} \bar{P}^{(1)}_{c2sh} + \frac{1}{(\gamma_c-1)} \bar{\kappa}_{2sh} \left[\bar{P}^{(1)}_{c2sh}\right]'$$

$$= \bar{E}^{(1)}_{csh} \quad . \tag{5.110}$$

$$\frac{1}{2} \psi^{(0)}_{1sh} \psi^{(1)}_{1sh} \left[1 - \left[\beta^{(0)}_1\right]^{(\gamma_{g1}+1)/2} \cdot \left[\psi^{(0)}_{1sh}\right]^{-(\gamma_{g1}+1)/2} \left[\lambda^{(0)}_{sh}\right]^{2(\gamma_{g1}-1)}\right]$$

$$+ \frac{1}{2} \frac{(\gamma_{g1}+1)}{(\gamma_{g1}-1)} \left[\beta^{(0)}_1\right]^{(\gamma_{g1}+1)/2} \cdot \left[\psi^{(0)}_{1sh}\right]^{-(\gamma_{g1}-1)/2} \left[\lambda^{(0)}_{sh}\right]^{2(\gamma_{g1}-1)} \beta^{(1)}_1$$

$$= \bar{E}^{(1)}_{c\infty} - \bar{E}^{(1)}_{csh} \quad , \tag{5.111}$$

$$\frac{1}{2} \psi^{(0)}_{2sh} \psi^{(1)}_{2sh} \left[1 - \left[\beta^{(0)}_2\right]^{(\gamma_{g2}+1)/2} \cdot \left[\psi^{(0)}_{2sh}\right]^{-(\gamma_{g2}+1)/2} \left[\lambda^{(0)}_{sh}\right]^{2(\gamma_{g2}-1)}\right]$$

$$+ \frac{1}{2} \frac{(\gamma_{g2}+1)}{(\gamma_{g2}-1)} \left[\beta^{(0)}_2\right]^{(\gamma_{g2}+1)/2} \cdot \left[\psi^{(0)}_{2sh}\right]^{-(\gamma_{g2}-1)/2} \left[\lambda^{(0)}_{sh}\right]^{2(\gamma_{g2}-1)} \beta^{(1)}_2$$

$$= \bar{E}^{(1)}_{c\infty} - \bar{E}^{(1)}_{csh} \quad , \tag{5.112}$$

$$\left[\left[\psi^{(0)}_{1sh}\right]^{-1/2} \left[1 - \frac{2}{\gamma_{g1}} \left[\beta^{(0)}_1\right]^{(\gamma_{g1}+1)/2} \cdot \left[\psi^{(0)}_{1sh}\right]^{-(\gamma_{g1}-1)/2} \left[\lambda^{(0)}_{sh}\right]^{(2\gamma_{g1}-3)}\right]$$

$$- \left[\psi^{(0)}_{2sh}\right]^{-1/2} \left[1 - \frac{2}{\gamma_{g2}} \left[\beta^{(0)}_2\right]^{(\gamma_{g2}+1)/2} \cdot \left[\psi^{(0)}_{2sh}\right]^{-(\gamma_{g2}-1)/2} \left[\lambda^{(0)}_{sh}\right]^{(2\gamma_{g2}-3)}\right]$$

$$- \left[\bar{E}_{c\infty}^{(1)} - \bar{E}_{csh}^{(1)}\right] \left[\left[\psi_{2sh}^{(0)}\right]^{-1/2} - \left[\psi_{1sh}^{(0)}\right]^{-1/2}\right]$$

$$- \frac{(\gamma_{g2}+1)}{2\gamma_{g2}(\gamma_{g2}-1)} \left[\beta_2^{(0)}\right]^{(\gamma_{g2}+1)/2}$$

$$\cdot \left[\psi_{2sh}^{(0)}\right]^{-\gamma_{g2}/2} \left[\lambda_{sh}^{(0)}\right]^{2(\gamma_{g2}-1)} \beta_2^{(1)}$$

$$+ \frac{(\gamma_{g1}+1)}{2\gamma_{g1}(\gamma_{g1}-1)} \left[\beta_1^{(0)}\right]^{(\gamma_{g1}+1)/2}$$

$$\cdot \left[\psi_{1sh}^{(0)}\right]^{-\gamma_{g1}/2} \left[\lambda_{sh}^{(0)}\right]^{2(\gamma_{g1}-1)} \beta_1^{(1)} \quad . \tag{5.113}$$

In the above equations $\bar{E}_{g\infty}^{(0)}$, $\bar{E}_{c\infty}^{(1)}$ and $\bar{E}_{csh}^{(1)}$ are defined by equations (5.23), (5.24) and (5.110) respectively. The compression ratio of the shock can be expanded as:

$$q = \left[\frac{\psi_{1sh}}{\psi_{2sh}}\right]^{1/2} = q^{(0)} \left[1 + \epsilon\, q^{(1)} + \cdots\right] \quad , \tag{5.114}$$

where

$$q^{(0)} = \left[\frac{\psi_{1sh}^{(0)}}{\psi_{2sh}^{(0)}}\right]^{1/2} \quad , \tag{5.115}$$

$$q^{(1)} = \frac{1}{2} \left[\left[\left[\psi_{1sh}^{(0)}\right]^{-1} \left[\psi_{1sh}^{(0)}\right]' \lambda_{sh}^{(1)} + \psi_{1sh}^{(1)}\right] - \left[\left[\psi_{2sh}^{(0)}\right]^{-1} \left[\psi_{2sh}^{(0)}\right]' \lambda_{sh}^{(1)} + \psi_{2sh}^{(1)}\right]\right] \quad , \tag{5.116}$$

and $\left[\psi^{(0)}\right]'$ is obtained by differentiating (5.78) with respect to λ:

$$\left[\psi^{(0)}\right]' = 2 \left[1 - 2 \left[\beta^{(0)}\right]^{(\gamma_g+1)/2} \left[\psi^{(0)}\right]^{-(\gamma_g-1)/2} \lambda^{(2\gamma_g-3)}\right] \cdot \left[1 - \left[\beta^{(0)}\right]^{(\gamma_g+1)/2} \left[\psi^{(0)}\right]^{-(\gamma_g+1)/2} \lambda^{2(\gamma_g-1)}\right]^{-1} \quad . \tag{5.117}$$

The unperturbed fluid velocity profile is the one fluid polytropic stellar wind discussed in §2.2, with energy integral (5.78), and critical point given by equations (5.87), (5.88), (5.93) and (5.94).

With this velocity profile, we can solve the cosmic-ray energy equation (5.79) with appropriate boundary conditions (see §4.1) to obtain the test particle cosmic-ray pressure. The 1^{st} order correction to the upstream normalized entropy constant $\beta_1^{(1)}$, is then given by equation (5.96). Using this value of $\beta_1^{(1)}$, the modified wind profile is then obtained by solving (5.80) for $\psi^{(1)}$. The 1^{st} order correction to the shock radius is given by equation (5.113), and the fluid velocity in the region between the perturbed and unperturbed shock radii is determined by interpolation.

Numerical examples illustrating the perturbation scheme are shown in figures 5.3 and 5.4 for a stellar wind model with $\dot{M} = 6*10^{11}$ g s^{-1}, $P_{g\infty} = 1$ eV cm^{-3}, $\rho_{g\infty} = 6*10^{-27}$ g cm^{-3}, $\gamma_{g1} = 1.3$ and $\gamma_{g2} = 5/3$. Figure 5.3, for which $\gamma_c = 4/3$ and $\kappa_1 = \kappa_2 = 10^{23}$ cm^2 s^{-1}, shows the unperturbed fluid velocity profile (curve ***a***), the modified fluid velocity profile (curve $\boldsymbol{b_1}$), and the test particle solution for the cosmic-ray pressure (curve $\boldsymbol{d_1}$). As in figures 5.1 and 5.2, curve ***c*** shows for comparison a one fluid polytropic stellar wind solution (without cosmic-rays), with the same total energy flux and interstellar gas density as the cosmic-ray modified stellar wind. As in the simpler models in §5.1 (c.f. figure 5.1 and 5.2), the fluid upstream of the shock is decelerated by the positive cosmic-ray pressure gradient. The shock radius for the cosmic-ray modified wind in this example is less than that the shock radius for the unperturbed wind (c.f. curves ***a*** and $\boldsymbol{b_1}$).

We also attempt to quantify the accuracy of the perturbation

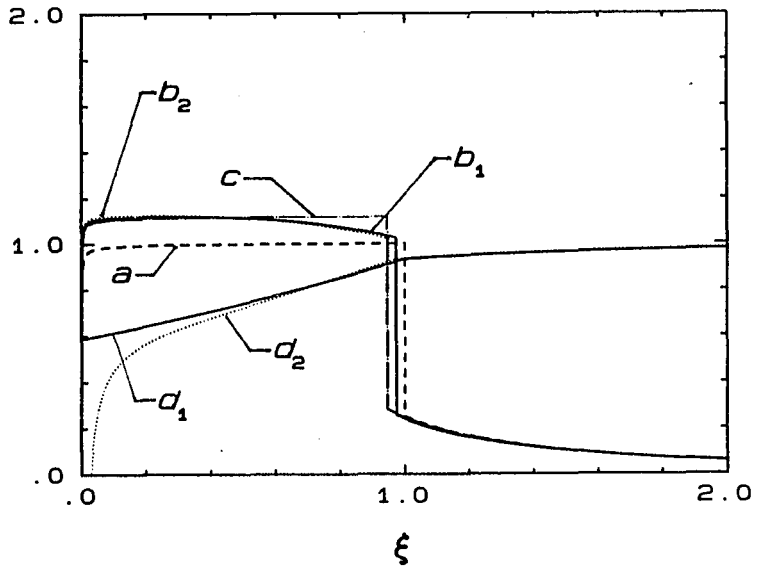

Figure 5.3 Perturbation Solution for a More Realistic Model with Larger κ

The plotting quantities are $\xi = r/R$, $\bar{u} = u/u_o$ and $\bar{P}_c = P_c/P_{co}$, where $R = r_{sh}^{(0)} = 65.2$ A.U. , $u_o = u_{1sh}^{(0)} = 364$ km s^{-1} , $P_{co} = \epsilon P_{g\infty}$ and $\epsilon = 1$. The normalized cosmic-ray diffusion coefficients are $\bar{\kappa}_1 = \kappa_1/\kappa_o = 2.81$ and $\bar{\kappa}_2 = \kappa_2/\kappa_o = 2.81$, where $\kappa_o = Ru_o = 3.55*10^{22}$ cm^2 s^{-1} .

solution. The curve d_1 shows the test particle cosmic-ray pressure, whereas curve d_2 is the corresponding solution for cosmic-ray pressure of the full nonlinear system of O.D.E.s (equations (3.19) and (3.21)) for the cosmic-ray modified stellar wind. The solution of the full nonlinear system is obtained by integrating equations (3.19) and (3.21) by a Runge-Kutta routine with initial conditions (for ψ, $\bar{P}_c$ and $\frac{d\bar{P}_c}{d\lambda}$) chosen to be those from the perturbation solution at the shock. The two solutions for $P_c/P_{c\infty}$ are very similar at $r/r_{sh}^{(0)} > 0.7$, but are significantly different at smaller radii. On the other hand, the perturbation solution for the modified wind profile (curve b_1) closely approximates the Runge-Kutta solution (curve b_2).

Figure 5.4, for which $\gamma_c = 4/3$ and $\kappa_1 = \kappa_2 = 10^{22}$ cm^2 s^{-1}, shows a further example of the perturbation solution, but for a smaller diffusion coefficient than in figure 5.3. The cosmic-ray pressure gradient is larger, and the modified shock is pushed further in (compared to the unperturbed shock) than the example in figure 5.3. The relative accuracy of the perturbation solution as compared to a Runge-Kutta solution of the full nonlinear system is also shown. As in figure 5.3, the cosmic-ray modified stellar wind profile of the perturbation and Runge-Kutta solutions are similar, but there is a discrepancy between the corresponding solutions for $P_c/P_{c\infty}$ (curves d_1 and d_2) at small radii.

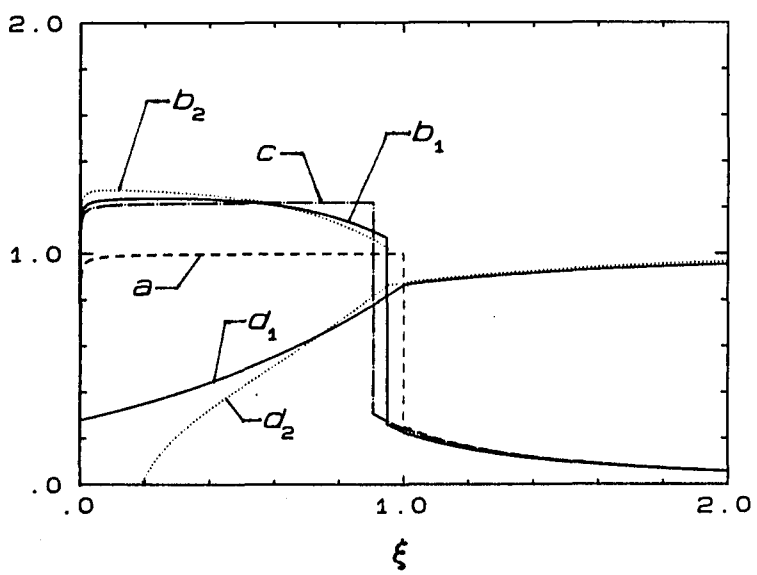

Figure 5.4 Perturbation Solution for a More Realistic Model with Smaller κ

The plotting quantities are $\xi = r/R$, $\bar{u} = u/u_o$ and $\bar{P}_c = P_c/P_{co}$, where $R = r_{sh}^{(0)} = 65.2$ A.U., $u_o = u_{1sh}^{(0)} = 364$ km s^{-1}, $P_{co} = \epsilon P_{g\infty}$ and $\epsilon = 1$. The normalized cosmic-ray diffusion coefficients are $\tilde{\kappa}_1 = \kappa_1/\kappa_o = 1.13$ and $\tilde{\kappa}_2 = \kappa_2/\kappa_o = 1.13$, where $\kappa_o = Ru_o = 3.55*10^{22}$ cm^2 s^{-1}.

CHAPTER 6

NUMERICAL SOLUTION OF THE COSMIC-RAY MODIFIED STELLAR WIND PROBLEM

In previous chapters we studied the properties of the set of equations describing cosmic-ray modified stellar winds (chapter 3). We also discussed some approximate solutions namely: the test particle limit (chapter 4) where the galactic cosmic-ray pressure was small enough that the background stellar wind flow was not significantly modified by the cosmic-rays; and a perturbation solution (chapter 5) in which the galactic cosmic-ray pressure is small but finite, and the background flow is modified by the cosmic-rays. In the present chapter we describe a numerical method to self-consistently solve the cosmic-ray modified stellar wind problem.

The main advantage of the numerical method in this chapter compared to the perturbation scheme of chapter 5 is that the full set of nonlinear equations can be solved to a high degree of accuracy, and the cosmic-rays are no longer regarded as a perturbation. The method is an iteration scheme in which the cosmic-ray energy equation is first solved for a given background flow velocity profile (initially the flow profile is chosen to be that of a one fluid polytropic stellar wind with a termination shock). The critical point requirements are then used to determine an improved estimate of the upstream entropy constant of the gas, and improved estimates of the location of shock and critical point.

The total energy flux integral (with cosmic-ray energy flux given by the test particle picture) is then used to obtain the modified wind profile. This completes the first iteration loop, and the new modified wind profile is then used to start the next iteration.

The equations are solved for two cases. In the first case the diffusion coefficient outside the shock, κ_2, is infinite, so that the cosmic-rays freely escape across the boundary at $r = r_{sh}$ (the shock radius). Since $\kappa_2 = \infty$, the cosmic-rays are unaffected by the shock or the downstream flow, and there is no acceleration at the shock. The model with $\kappa_2 = \infty$, is a conventional modulation model, in which the cosmic-ray intensity, pressure and energy flux are uniform outside the shock. In the second more realistic case the downstream diffusion coefficient is finite, and the cosmic-rays are accelerated at the shock, and interact with both the upstream and downstream flow. Both models show that the cosmic-rays decelerate the wind just upstream of the shock.

The solution method adopted implicitly assumes that the shock is not totally smoothed out by the cosmic-rays as can occur for example in two fluid hydrodynamical models of cosmic-ray shocks (see Drury and Völk 1981; Axford, Leer and McKenzie 1982). Drury and Völk (1981) in their work on cosmic-ray modified shocks, obtained in some instances up to three possible downstream states for a given upstream state (c.f. also Achterberg, Blandford and Periwal 1984, for multiple solutions of the cosmic-ray shock structure problem). The numerical solution of the cosmic-ray modified stellar wind obtained in the present chapter, for

given boundary conditions at $r = 0$ and $r = \infty$, appears to be unique. However, it may well be that there are multiple solutions of the cosmic-ray modified stellar wind problem similar to those obtained by Drury and Völk (1981).

In §6.1 we outline the iteration scheme used to solve the equations. Numerical examples illustrating the iteration scheme are given in §6.2.

§6.1 Equations and Algorithm

From chapter 3 we recall that the equations governing the cosmic-ray modified stellar wind system are (equations (3.1) – (3.5)):

$$\frac{1}{r^2}\frac{d}{dr}(r^2 \rho_g u) = 0 \quad , \tag{6.1}$$

$$\rho_g u \frac{du}{dr} = -\frac{dP_g}{dr} - \frac{dP_c}{dr} - \rho_g \frac{GM_o}{r^2} \quad , \tag{6.2}$$

$$\frac{1}{r^2}\frac{d}{dr}\left[r^2 \rho_g u \left(\frac{1}{2}u^2 + \frac{\gamma_g}{(\gamma_g - 1)}\frac{P_g}{\rho_g} - \frac{GM_o}{r}\right) + r^2 F_c\right] = 0 \quad , \tag{6.3}$$

$$\frac{1}{r^2}\frac{d}{dr}(r^2 F_c) = u\frac{dP_c}{dr} \quad , \tag{6.4}$$

$$F_c = \frac{\gamma_c}{(\gamma_c - 1)} P_c u - \frac{1}{(\gamma_c - 1)} \kappa \frac{dP_c}{dr} \quad . \tag{6.5}$$

Suppose that the stellar wind velocity profile has a shock, then on either side of the shock, specification of P_g, ρ_g, u, P_c and F_c at a fixed point in the flow uniquely determines the solution of the system of first order coupled O.D.E.s (6.1) – (6.5) (c.f. §2.2). Since P_g, ρ_g, u, P_c and F_c need to be obtained on both sides of the shock, this involes 10 constants (which can be considered as initial conditions to equations (6.1) – (6.5)). However, the radius of the shock needs to be

determined, so that overall 11 constants are involved.

To determine the 11 constants it is necessary to impose 11 conditions on the flow. Two ways in which this can be achieved are oulined below:

(a) Specification of P_g, ρ_g, $\dot{M}$ ($= 4\pi\rho_g u r^2$), P_c and F_c at infinity imposes five conditions on the system. Conservation of the gas mass, momentum and energy fluxes, and continuity of the cosmic-ray pressure and energy flux at the shock imposes five more conditions. The remaining condition is to choose the transonic solution inside the shock (c.f. §2.2).

(b) Specification of P_g, ρ_g, $\dot{M}$ and P_c (or F_c) at infinity imposes four conditions. At the origin requiring P_c to be finite (or $\frac{dP_c}{dr} = 0$) is a fifth condition. The remaining conditions are the five conservation requirements at the shock and choosing the transonic solution inside the shock.

The disadvantage of using the set of conditions (a) is that there is no guarantee that the cosmic-ray pressure will be finite at the origin. An incorrect choice of P_c and F_c at infinity, can lead to a solution in which P_c diverges at the origin. However, by using a shooting method with a judicious choice of initial conditions at infinity, it may be possible to obtain the physically realistic solution of equations (6.1) – (6.5) in which P_c is finite at the origin.

We choose to solve the system of equations (6.1) – (6.5) using

the set of boundary conditions (b), in which either P_c is finite or $\frac{dP_c}{dr} = 0$ as $r \to 0$. One drawback in applying set (b) is that if we specify cosmic-ray pressure at infinity, then the total energy flux (or equivalently the cosmic-ray energy flux at infinity) is not known initially, and must be determined after the equations (6.1) – (6.5) have been solved. If the gas energy and cosmic-ray energy fluxes are specified at infinity, then the total energy flux of the system is known at the outset, but the cosmic-ray pressure at infinity must then be determined from the solution.

We now describe an algorithm to solve the set of equations (6.1) – (6.5) subject to boundary conditions (b). Firstly, we reduce equations (6.1) – (6.5) to two coupled equations: the total energy integral (see §3.2) and the cosmic-ray energy equation (see §4.1). The two relevant equations (3.20) and (4.2) can be written as:

$$\bar{E} = \bar{E}_g + \bar{E}_c \quad , \tag{6.6}$$

$$\frac{1}{\xi^2}\frac{d}{d\xi}\left(\xi^2 \tilde{\kappa} \frac{d\tilde{P}_c}{d\xi}\right) - \tilde{u}\frac{d\tilde{P}_c}{d\xi} - \gamma_c \frac{1}{\xi^2}\frac{d}{d\xi}(\xi^2 \tilde{u})\tilde{P}_c = 0 \quad , \tag{6.7}$$

where

$$\bar{E}_g = \frac{1}{2}\psi - \lambda + \frac{1}{(\gamma_g - 1)}\beta^{(\gamma_g+1)/2}\psi^{-(\gamma_g-1)/2}\lambda^{2(\gamma_g-1)} \quad , \tag{6.8}$$

$$\bar{E}_c = \frac{\gamma_c}{(\gamma_c - 1)}\psi^{1/2}\lambda^{-2}\bar{P}_c + \frac{1}{(\gamma_c - 1)}\bar{\kappa}\frac{d\bar{P}_c}{d\lambda} \quad . \tag{6.9}$$

The quantities λ, ψ, $\bar{P}_c$, β, $\bar{E}$ and $\bar{\kappa}$ are defined by equations (3.14), (3.22) and (3.23), and ξ, $\tilde{u}$, $\tilde{P}_c$ and $\tilde{\kappa}$ are defined by equation (4.1). Although different scales are used in equations (6.6) and (6.7), we find that the equations are easier to handle in this way because of the

techniques we have developed in §2.2 and §4.1. Note that $\bar{P}_c$ and $\bar{E}_c$ are related to $\tilde{P}_c$ and $\tilde{F}_c$ by

$$\bar{P}_c = \frac{P_{co}}{\rho_o}\left(\frac{m_g}{kT_o}\right)\tilde{P}_c \quad , \tag{6.10}$$

$$\bar{E}_c = P_{co} R^2 u_o j^{-1}\left(\frac{m_g}{kT_o}\right)\tilde{F}_c \quad , \tag{6.11}$$

where

$$\tilde{F}_c = \frac{\gamma_c}{(\gamma_c-1)}\tilde{P}_c\tilde{u} - \frac{1}{(\gamma_c-1)}\tilde{\kappa}\frac{d\tilde{P}_c}{d\xi} \quad . \tag{6.12}$$

We use an iterative approach to self-consistently solve equations (6.6) and (6.7) with the assumption that the flow contains a shock somewhere in the vicinity of the termination shock of the one fluid polytropic stellar wind solution used in the first iteration. We initially set up the fluid velocity profile of the one fluid polytropic stellar wind including a termination shock as in §2.2. Using this background velocity profile we then solve the cosmic-ray energy equation (6.7) (in test particle picture) for $\tilde{P}_c$ and $\tilde{F}_c$ by the difference scheme developed in §4.1. The critical point requirements for the cosmic-ray modified stellar wind (see §3.2) are then used to determine the modified normalized entropy constant β_1^* for the flow inside the shock. These requirements also lead to an improved estimate of the locations of the critical point and the shock.

In determining the locations of the critical point and the shock, we have to make use of the thermal gas energy flux which depends on the total energy and cosmic-ray energy fluxes (c.f. equation (6.6)). If the cosmic-ray pressure is specified at infinity, then the total

energy flux changes at each iteration. In this case the total energy flux is taken as

$$\bar{E} = \bar{E}_{g\infty} + \bar{E}_{cmax} \quad , \tag{6.13}$$

where

$$\bar{E}_{g\infty} = \frac{\gamma_{g2}}{(\gamma_{g2}-1)} \frac{P_{g\infty}}{\rho_{g\infty}} \left(\frac{m_g}{kT_o}\right) \quad , \tag{6.14}$$

$$\bar{E}_{cmax} = P_{co} R^2 u_o j^{-1} \left(\frac{m_g}{kT_o}\right) \tilde{F}_c(\xi_{max}) \quad , \tag{6.15}$$

and ξ_{max} is the maximum radius used in the difference scheme in solving for the cosmic-ray pressure. If we specfiy the cosmic-ray energy flux at infinity (i.e., we use equation (4.13) as one of the boundary conditions), then the total energy flux is constant during the iteration process. We still use the approximation (6.13), but $\bar{E}$ is now a constant.

We now proceed to find the modified normalized entropy constant β_1^* upstream of the shock (β_2 does not change, c.f. §5.2). We determine expressions for β_1^* and the modified critical point λ_c^* in terms of the cosmic-ray quantities $\bar{P}_{cc}$ and $\bar{E}_{cc}$ evaluated at the approximate critical point obtained in the previous iteration. Since the critical point ($\lambda = \lambda_c$) in general does not coincide with one of the grid points of the difference scheme in solving for $\tilde{P}_c$, it is necessary to evaluate $\bar{P}_{cc}$ and $\bar{E}_{cc}$ by interpolation. From §3.2, we have

$$\psi_c = \beta_1^* \left(\lambda_c^*\right)^{4(\gamma_{g1}-1)/(\gamma_{g1}+1)} \quad , \tag{6.16}$$

$$\left.\frac{d\bar{P}_c}{d\lambda}\right|_c = \left(\beta_1^*\right)^{-1/2} \left(\lambda_c^*\right)^{4/(\gamma_{g1}+1)} - 2 \left(\beta_1^*\right)^{1/2} \left(\lambda_c^*\right)^{(3\gamma_{g1}-1)/(\gamma_{g1}+1)} \quad , \tag{6.17}$$

on the critical surface. Substituting the expressions (6.16) and (6.17) into equations (6.8) and (6.9) we obtain the gas and cosmic-ray energy fluxes $\bar{E}_{gc}$ and $\bar{E}_{cc}$ at the critical point in the form

$$\bar{E}_{gc} = \frac{1}{2}\frac{(\gamma_{g1}+1)}{(\gamma_{g1}-1)}\beta_1^*\left[\lambda_c^*\right]^{4(\gamma_{g1}-1)/(\gamma_{g1}+1)} - \lambda_c^* \quad , \tag{6.18}$$

$$\bar{E}_{cc} = \frac{\gamma_c}{(\gamma_c-1)}\left[\beta_1^*\right]^{1/2}\left[\lambda_c^*\right]^{-4/(\gamma_{g1}+1)}\bar{P}_{cc} + \frac{1}{(\gamma_c-1)}\bar{\kappa}\left(\left[\beta_1^*\right]^{-1/2}\left[\lambda_c^*\right]^{4/(\gamma_{g1}+1)} - 2\left[\beta_1^*\right]^{1/2}\left[\lambda_c^*\right]^{(3\gamma_{g1}-1)/(\gamma_{g1}+1)}\right) . \tag{6.19}$$

From overall energy conservation (equation (6.6)) we also have

$$\bar{E}_{gc} = \bar{E} - \bar{E}_{cc} \quad . \tag{6.20}$$

Solving equation (6.18) for β_1^* gives

$$\beta_1^* = 2\frac{(\gamma_{g1}-1)}{(\gamma_{g1}+1)}\left[\bar{E}_{gc} + \lambda_c^*\right]\left[\lambda_c^*\right]^{-4(\gamma_{g1}-1)/(\gamma_{g1}+1)} \quad , \tag{6.21}$$

and substituting this value of β_1^* in equation (6.19) yields

$$\bar{E}_{cc} = \frac{\gamma_c}{(\gamma_c-1)}\left[2\frac{(\gamma_{g1}-1)}{(\gamma_{g1}+1)}\left[\bar{E}_{gc} + \lambda_c^*\right]\right]^{1/2}\left[\lambda_c^*\right]^{-2}\bar{P}_{cc} + 4\frac{(\gamma_{g1}-1)}{(\gamma_{g1}+1)}\left[2\frac{(\gamma_{g1}-1)}{(\gamma_{g1}+1)}\left[\bar{E}_{gc} + \lambda_c^*\right]\right]^{-1/2}\lambda_c^* \cdot \frac{1}{(\gamma_c-1)}\bar{\kappa}\left[\frac{(5-3\gamma_{g1})}{4(\gamma_{g1}-1)}\lambda_c^* - \bar{E}_{gc}\right] . \tag{6.22}$$

Taking into account the expression (6.20) for $\bar{E}_{gc}$, equation (6.22) can now be solved to obtain the new approximate critical point λ_c^* in terms of $\bar{P}_{cc}$ and $\bar{E}_{cc}$ evaluated at the critical point obtained in the previous iteration. Equation (6.21) then yields β_1^* in terms of $\bar{E}_{cc}$ and λ_c^*. Equation (6.22) can also be written in the form:

$$\lambda_c^* = \frac{(\gamma_{g1}+1)}{(5-3\gamma_{g1})}(\gamma_c-1)\frac{1}{\kappa}\left[2\frac{(\gamma_{g1}-1)}{(\gamma_{g1}+1)}\left(\bar{E}_{gc}+\lambda_c^*\right)\right]^{1/2}\left(\lambda_c^*\right)^{-1}$$
$$\cdot\left[\bar{E}_{cc}-\frac{\gamma_c}{(\gamma_c-1)}\left[2\frac{(\gamma_{g1}-1)}{(\gamma_{g1}+1)}\left(\bar{E}_{gc}+\lambda_c^*\right)\right]^{1/2}\left(\lambda_c^*\right)^{-2}\bar{P}_{cc}\right]$$
$$+\frac{4(\gamma_{g1}-1)}{(5-3\gamma_{g1})}\bar{E}_{gc} \quad . \tag{6.23}$$

Thus λ_c^* can be solved either by iteration from equation (6.23), or by using a bisection method on equation (6.22) or (6.23).

To determine the modified shock radius, we first note that

$$\bar{E}_{gsh} = \bar{E} - \bar{E}_{csh} \tag{6.24}$$

gives the gas energy flux at the shock radius λ_{sh} (or r_{sh}) of the previous iteration. Using this value for the gas energy flux, and the value of β_1^* calculated from equation (6.21), we determine the new shock radius λ_{sh}^* (or r_{sh}^*) as in §2.2. Having determined the new shock radius we re-scale the radial variable from $\xi = r/r_{sh}$ to $\xi^* = r/r_{sh}^*$ (i.e., we choose the spatial scale R as r_{sh}^*). As a consequence of re-scaling the radial variable, it is then necessary to replace $\tilde{\kappa} = \kappa/(r_{sh}u_o)$ by $\tilde{\kappa}^* = \kappa/(r_{sh}^*u_o)$ in further calculations. A similar re-scaling process must be carried out for the thermal gas energy flux profile, since the numerical solution grid is either stretched or contracted by the re-scaling. Practically speaking, we stretch or contract the thermal gas energy flux profile ($\tilde{F}_g$ or $\bar{E}_g$) along the radial axis until r_{sh} coincides with r_{sh}^*, and take this new profile ($\tilde{F}_g^*$ or $\bar{E}_g^*$) as the modified thermal gas energy flux with the new shock radius r_{sh}^*. The modified velocity ($\tilde{u}$ or ψ^*) can then be determined from equation (6.8) as in §2.2. With this new profile, we can determine the modified cosmic-ray

pressure by using the test particle calculation. This completes an iteration loop. The iteration process can be summarized in the following diagrams:

(a) Specification of galactic cosmic-ray pressure,

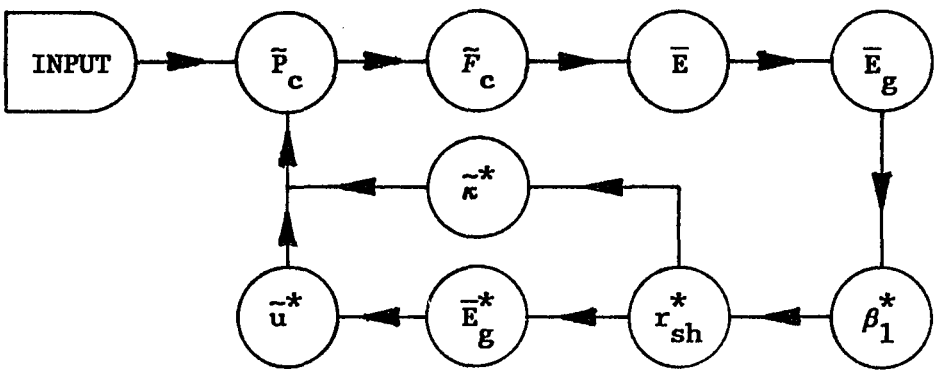

(b) Specification of galactic cosmic-ray energy flux (equivalently, total energy flux),

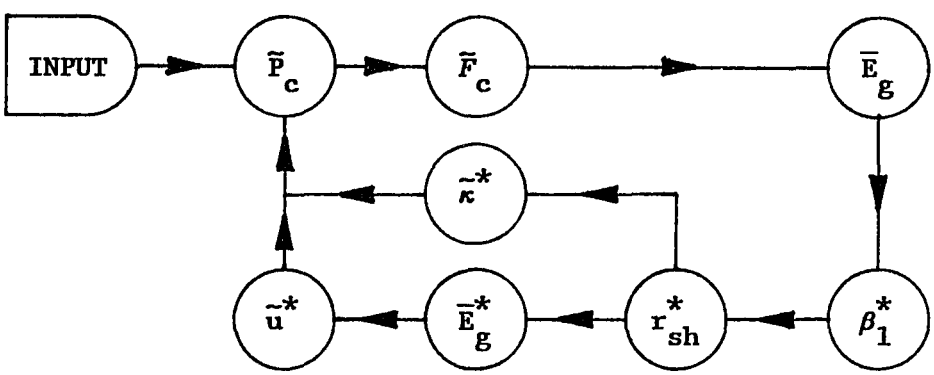

The input to the iteration loop includes the one fluid polytropic stellar wind. Note that $\bar{E}_g = \bar{E}_g^*$ on the grid points.

The major disadvantage of this algorithm is that we cannot specify both galactic cosmic-ray pressure and energy flux. Otherwise, we will over determine the system, because we require a finite

cosmic-ray pressure at the origin.

§6.2 Applications of the Algorithm

In this section we present numerical examples of the algorithm developed in §6.1. We first consider the case where the diffusion coefficient is infinite outside the shock ($\kappa_2 = \infty$), and the cosmic-rays are unaffected by the flow outside the shock. We then go on to consider examples in which κ_2 is finite outside the shock.

§6.2.1 Case $\kappa_2 = \infty$

For $\kappa_2 = \infty$, there is no interaction between the cosmic-rays and the thermal gas outside the shock, and the cosmic-ray pressure and energy flux at the shock are the same as those at infinity. We only need to calculate the cosmic-ray pressure inside the shock. We require the cosmic-ray pressure to be finite at the origin, so we can choose either the cosmic-ray pressure or the energy flux at the shock (equivalently, at infinity) but not both as the remaining boundary condition for the cosmic-ray energy equation (6.7). In the following computation, we take the specification of the energy flux as the boundary condition, so we have a fixed total energy flux before iteration. Even if the thermal gas energy flux at the shock is known from the boundary condition (actually it is equal to the enthalpy flux at infinity), the radius of the shock cannot be determined at the start of the iteration process, because the entropy constant inside the shock changes in each iteration. Figures 6.1 and 6.2 show the radial

variation of $\tilde{P}_c = P_c/P_{co}$, $\xi^2\tilde{F}_c = r^2F_c/(R^2u_oP_{co})$ and $\tilde{u} = u/u_o$, where R is the radius of the shock, u_o is the velocity just upstream of the shock of the initial one fluid polytropic stellar wind without cosmic-rays and P_{co} is the gas pressure at infinity, $P_{g\infty}$. The stellar wind model used in figure 6.1 and 6.2 has $\dot{M} = 6*10^{11}$ g s^{-1} , $P_{g\infty} = 1$ eV cm^{-3} , $\rho_{g\infty} = 6*10^{-27}$ g cm^{-3} , $\gamma_{g1} = 1.3$ and $\gamma_{g2} = 5/3$. In figure 6.1 $\gamma_c = 4/3$, $\kappa_1 = \kappa_2 = 10^{23}$ cm^2 s^{-1} and $F_{c\infty}/F_{g\infty} = 0.3$, while in figure 6.2 $\gamma_c = 4/3$, $\kappa_1 = \kappa_2 = 10^{22}$ cm^2 s^{-1} and $F_{c\infty}/F_{g\infty} = 1$. The features of $\tilde{P}_c$, $\xi^2\tilde{F}_c$ and $\tilde{u}$ are basically the same as in chapter 5. The wind just upstream of the shock is decelerated by the positive cosmic-ray pressure gradient. In the radial range $0.04 < r/R < 0.6$ in figure 6.2, the wind velocity is essentially constant, and the cosmic-ray energy flux is essentially zero. In this region the total energy flux is essentially the kinetic energy flux of the wind. As the shock is approached from the upstream side the kinetic energy of the wind decreases, with part of the energy being converted to cosmic-ray energy, and part being used to incease the enthalpy of the gas. The deceleration of the wind is more prominent if κ_1 is smaller (figure 6.2) when compared with the larger κ_1 case (figure 6.1).

The iterative solution was compared with Runge-Kutta integration of the equations using the values of the iteration solution at the shock as initial values. The two agree very well with each other. Actually, the fractional discrepancy between them is smaller than 10^{-5} (except at region close to the origin) provided that the galactic cosmic_ray pressure is not too large, say $P_{c\infty} < P_{g\infty}$. One defect in the algorithm

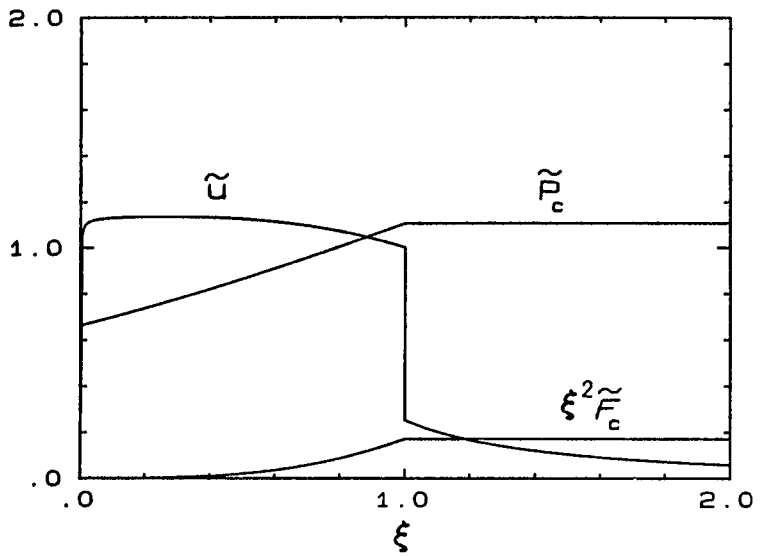

Figure 6.1 Exact Solution for the Case κ_1 is Large and κ_2 is Infinite

The plotting quantities are $\xi = r/R$, $\tilde{u} = u/u_o$, $\tilde{P}_c = P_c/P_{co}$ and $\xi^2\tilde{F}_c = \xi^2 F_c/F_{co}$, where $R = r_{sh} = 65.1$ A.U. , $u_o = 364$ km s^{-1} , $P_{co} = P_{g\infty} = 1$ eV cm^{-3} and $F_{co} = u_o P_{co} = 5.82*10^{-5}$ erg cm^{-2} s^{-1} . The normalized cosmic-ray diffusion coefficients are $\tilde{\kappa}_1 = \kappa_1/\kappa_o = 2.81$ and $\tilde{\kappa}_2 = \kappa_2/\kappa_o = 2.81$, where $\kappa_o = Ru_o = 3.55*10^{22}$ cm^2 s^{-1} .

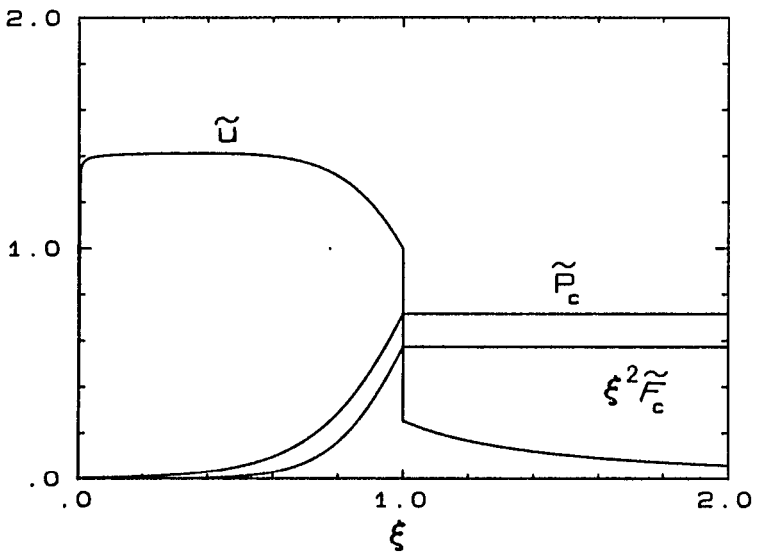

Figure 6.2 Exact Solution for the Case κ_1 is Small and κ_2 is Infinite

The plotting quantities are $\xi = r/R$, $\tilde{u} = u/u_o$, $\tilde{P}_c = P_c/P_{co}$ and $\xi^2\tilde{F}_c = \xi^2 F_c/F_{co}$, where $R = r_{sh} = 65.1$ A.U. , $u_o = 364$ km s^{-1} , $P_{co} = P_{g\infty} = 1$ eV cm^{-3} and $F_{co} = u_o P_{co} = 5.82*10^{-5}$ erg cm^{-2} s^{-1} . The normalized cosmic-ray diffusion coefficients are $\tilde{\kappa}_1 = \kappa_1/\kappa_o = 0.282$ and $\tilde{\kappa}_2 = \kappa_2/\kappa_o = 0.282$, where $\kappa_o = Ru_o = 3.55*10^{22}$ cm^2 s^{-1} .

is that the iteration initially converges very fast to a solution (presumably one of the physical ones, since the solution agrees very well with the Runge-Kutta solution), but then starts to diverge with further iterations. This defect becomes more serious if the cosmic-ray pressure at infinity is large.

§6.2.2 Case κ_2 is finite

We now go on to the general case where κ_2 is finite. We specify the galactic cosmic-ray energy flux in order to have a fixed total energy flux during the iteration. Two typical results are shown in figures 6.3 and 6.4 for a stellar wind model $\dot{M} = 6*10^{11}$ g s^{-1}, $P_{g\infty} = 1$ eV cm^{-3}, $\rho_{g\infty} = 6*10^{-27}$ g cm^{-3}, $\gamma_{g1} = 1.3$ and $\gamma_{g2} = 5/3$. In figure 6.3 $\gamma_c = 4/3$, $\kappa_1 = \kappa_2 = 10^{23}$ cm^2 s^{-1} and $F_{c\infty}/F_{g\infty} = 0.25$, while in figure 6.4 $\gamma_c = 4/3$, $\kappa_1 = \kappa_2 = 10^{22}$ cm^2 s^{-1} and $F_{c\infty}/F_{g\infty} = 1$. They show the same features as in figures 6.1 and 6.2, where the wind is decelerated just upstream of the shock. The deceleration is more pronounced, the smaller the value of κ (c.f. figures 6.3 and 6.4).

The algorithm has the same problem as in previous case where $\kappa_2 = \infty$, namely the iteration converges to a solution for a while and then diverges with further iterations. Even though the algorithm has this defect, the iteration solution agrees very well with the Runge-Kutta solution. The fractional discrepancy is about 10^{-4}.

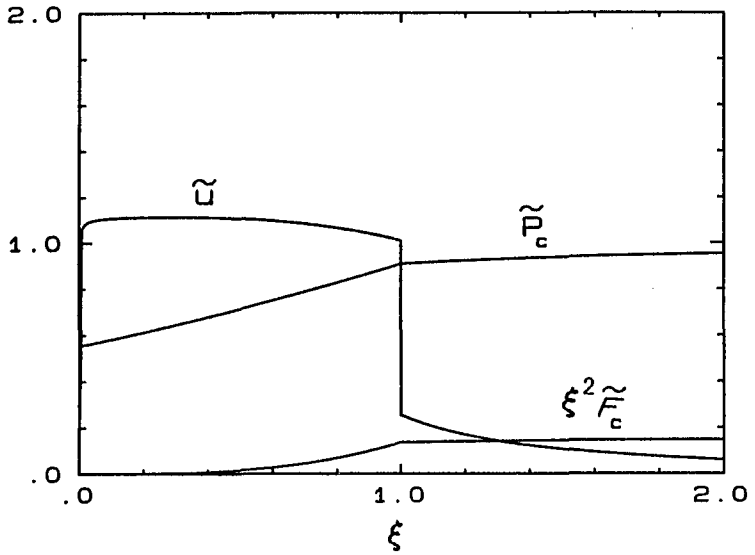

Figure 6.3 Exact Solution for the Case κ_1 and κ_2 are Large

The plotting quantities are $\xi = r/R$, $\tilde{u} = u/u_o$, $\tilde{P}_c = P_c/P_{co}$ and $\xi^2\tilde{F}_c = \xi^2 F_c/F_{co}$, where $R = r_{sh} = 64.0$ A.U. , $u_o = 364$ km s^{-1} , $P_{co} = P_{g\infty} = 1$ eV cm^{-3} and $F_{co} = u_o P_{co} = 5.82*10^{-5}$ erg cm^{-2} s^{-1} . The normalized cosmic-ray diffusion coefficients are $\tilde{\kappa}_1 = \kappa_1/\kappa_o = 2.86$ and $\tilde{\kappa}_2 = \kappa_2/\kappa_o = 2.86$, where $\kappa_o = Ru_o = 3.49*10^{22}$ cm^2 s^{-1} .

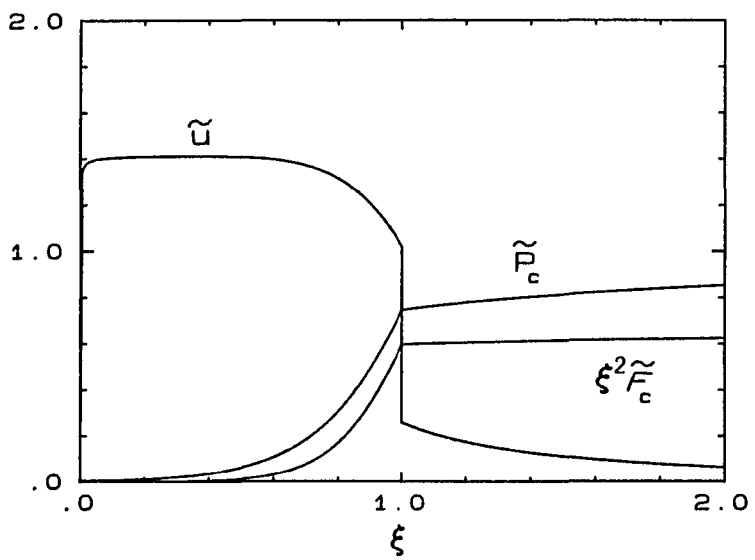

Figure 6.4 Exact Solution for the Case κ_1 and κ_2 are Small

The plotting quantities are $\xi = r/R$, $\tilde{u} = u/u_o$, $\tilde{P}_c = P_c/P_{co}$ and $\xi^2\tilde{F}_c = \xi^2 F_c/F_{co}$, where $R = r_{sh} = 62.5$ A.U. , $u_o = 364$ km s^{-1} , $P_{co} = P_{g\infty} = 1$ eV cm^{-3} and $F_{co} = u_o P_{co} = 5.82*10^{-5}$ erg cm^{-2} s^{-1} . The normalized cosmic-ray diffusion coefficients are $\tilde{\kappa}_1 = \kappa_1/\kappa_o = 0.294$ and $\tilde{\kappa}_2 = \kappa_2/\kappa_o = 0.294$, where $\kappa_o = Ru_o = 3.41*10^{22}$ cm^2 s^{-1} .

§6.3 Conclusion

In this dissertation we developed a self-consistent hydrodynamical model describing the modification of a stellar wind by the galactic cosmic-rays. The model was inspired in part by the work on cosmic-ray modified shock waves initially developed by Axford, Leer and Skadron (1977), Drury and Völk (1981) and Axford, Leer and McKenzie (1982). These models describe at a hydrodynamical level the acceleration of cosmic-rays in plane parallel shocks by the first order Fermi mechanism (c.f. Axford, Leer and Skadron 1977; Krymskii 1977; Bell 1978a, b; Blandford and Ostriker 1978). Hydromagnetic waves (e.g. Alfven waves) or magnetic irregularities travelling in the background gas scatter the cosmic-rays, and are the intermediary via which energy and momentum are transferred between the thermal gas and the cosmic-rays. This coupling can be described by a mean hydrodynamical diffusion coefficient which in general depends on the power in the scattering wave field.

To model the iteraction of the cosmic-rays with a stellar wind flow, it is necessary to modify the above hydrodynamical equations to apply in a spherical geometry, and to include the effects of gravity on the flow. In contrast to cosmic-ray acceleration in plane parallel shocks, where the cosmic-rays continuously gain energy by scattering back and forth across the shock, cosmic-rays propagating in a stellar wind with termination shock tend to lose energy in the diverging flow upstream of the shock due to adiabatic deceleration (e.g. Parker 1965a), which is offset to some extent by Fermi acceleration at the shock. This

added complication of the transport of cosmic-rays in the stellar wind problem is mainly due to the spherical geometry of the flow.

The basic equations governing the cosmic-ray modified stellar wind system are equations (6.1) – (6.5). The main purpose of the present work is to solve these equations self-consistently. In doing so, we made use of the techniques developed in chapters 2 and 4. In chapter 2, we learnt how to set up a stellar wind velocity profile including a termination shock. In chapter 4, we developed a finite difference scheme to solve the cosmic-ray energy equations (6.4) – (6.5) with a given background flow velocity profile. Employing the techniques developed in chapters 2 and 4, an iterative algorithm was devised in this chapter to solve the set of equations (6.1) –(6.5) to a high degree of accuracy. Each of the solution examples in figures 6.1 - 6.4 shows the same characteristics, namely, a sub-shock and deceleration of the flow velocity upstream of the shock. In one dimensional two fluid hydrodynamical models of cosmic-ray shocks (Drury and Völk 1981; Axford, Leer and Mckenxie 1982), smooth transitions from upstream to downstream state are possible. The absence of smooth transitions in our calculation may only be an artifact of the solution method we used. The reason is two fold: firstly, we searched for solutions using the one fluid polytropic stellar wind with has a termination shock to start the iteration; secondly, and more importantly, the iteration algorithm developed in this chapter does not applied for large galactic cosmic-ray pressures or energy fluxes, which can presumably smooth out the termination shock completely. Drury and Völk (1981) also showed that

for one dimensional cosmic-ray shocks, up to three possible downstream states could be obtained for a given upstream state for small upstream cosmic-ray pressures, and Mach numbers of order greater than five. We speculated that the cosmic-ray modified wind also possesses multiple solutions (at least in the small diffusion coefficient or large shock radius cases), but the solution obtained in this chapter, for given boundary conditions at the origin (or the star) and infinity, appears to be unique. This might also be an artifact of the solution method used. The other possible reason for the lack of multiple solutions is that the Mach number of the termination shock is so large that there is only one solution.

The influence of galactic cosmic-ray pressure on the stellar wind can easily be seen in the perturbation approach discussed in chapter 5. The perturbation solutions showed that the flow velocity upstream of the shock was decelerated and the stellar wind termination shock was pushed inward by the positive galactic cosmic-ray pressure gradient.

The mathematical characteristics of the set of equations governing cosmic-ray modified stellar winds (equations (6.1) – (6.5)) were discussed in chapter 3. Analysis showed that the singularities of these equations were considerably more complex than those of the one fluid polytopic stellar winds (c.f. chapter 2). The topology of the solution curves in the vicinity of the singularities is an intriguing mathematical problem and is interesting to pursue.

APPENDIX A

CRITICAL POINTS OF THE ONE FLUID POLYTROPIC STELLAR WIND MOMENTUM EQUATION

In this appendix we determine the nature of the critical points of the one fluid polytropic stellar wind momentum equation (2.10):

$$\frac{1}{2}\left[1 - \beta^{(\gamma+1)/2}\,\psi^{-(\gamma+1)/2}\,\lambda^{2(\gamma-1)}\right]\frac{d\psi}{d\lambda} = 1 - 2\,\beta^{(\gamma+1)/2}\,\psi^{-(\gamma-1)/2}\,\lambda^{(2\gamma-3)} \quad . \tag{A.1}$$

This equation can be written as an autonomous system of O.D.E.s:

$$\frac{d}{ds}\begin{bmatrix}\lambda\\ \psi\end{bmatrix} = \begin{bmatrix}Q\\ P\end{bmatrix} \quad , \tag{A.2}$$

where

$$P \equiv 1 - 2\,\beta^{(\gamma+1)/2}\,\psi^{-(\gamma-1)/2}\,\lambda^{(2\gamma-3)} \quad , \tag{A.3}$$

$$Q \equiv \frac{1}{2}\left[1 - \beta^{(\gamma+1)/2}\,\psi^{-(\gamma+1)/2}\,\lambda^{2(\gamma-1)}\right] \quad . \tag{A.4}$$

One critical point of these equations (the sonic point of equation (A.1)) occurs where $P = Q = 0$. Setting $P = Q = 0$ in equations (A.3) and (A.4) we obtain

$$\psi_c = \frac{1}{2}\lambda_c = \frac{1}{2}(2\beta)^{(\gamma+1)/(5-3\gamma)} \quad . \tag{A.5}$$

After linearizing around $(\lambda,\psi) = (\lambda_c,\psi_c)$, the system of equations (A.2) may be written as:

$$\frac{d}{ds}\begin{bmatrix}\lambda-\lambda_c\\ \psi-\psi_c\end{bmatrix} = \underline{\underline{A}}\begin{bmatrix}\lambda-\lambda_c\\ \psi-\psi_c\end{bmatrix} \quad , \tag{A.6}$$

where

$$\underline{\underline{A}} \equiv \begin{bmatrix}Q_\lambda & Q_\psi\\ P_\lambda & P_\psi\end{bmatrix}_c = \begin{bmatrix}-(\gamma-1) & \frac{1}{2}(\gamma+1)\\ (3-2\gamma) & (\gamma-1)\end{bmatrix}\lambda_c^{-1} \quad . \tag{A.7}$$

The matrix $\underline{A}$ has eigenvalues

$$\mu_{\pm} = \pm\left(\frac{5-3\gamma}{2}\right)^{1/2} \lambda_c^{-1} \quad . \tag{A.8}$$

For $1 < \gamma < 5/3$, the eigenvalues $\mu_{\pm}$ are real and of opposite sign which indicates that the critical point is a saddle point. The eigenvectors corresponding to μ_+ and μ_- are $(1, \frac{2}{(\gamma+1)}[(\gamma-1) + \sqrt{(5-3\gamma)/2}])^T$ and $(1, \frac{2}{(\gamma+1)}[(\gamma-1) - \sqrt{(5-3\gamma)/2}])^T$ respectively. For $\gamma > 5/3$, the eigenvalues are complex conjugates. The critical point is then either a centre or a focus (spiral point) (e.g. see Coddington and Levinson 1955). Note the linear analysis indicates that for $\gamma > 5/3$, the critical point is a centre. However, the full nonlinear system (A.2) at this point may be either a focus or a centre.

The point $(\lambda,\psi) = (0,0)$ is also a critical point since P and Q both become infinite at this point. To see this we note that the solution curves passing through (0,0) behave like $\psi \sim B\,\lambda^4$ as $\lambda \to 0$ see §2.2). So if we write the equation (A.1) as:

$$\frac{d}{ds}\begin{bmatrix}\lambda\\ \psi\end{bmatrix} = \begin{bmatrix}Q'\\ P'\end{bmatrix} = \begin{bmatrix}1/P\\ 1/Q\end{bmatrix} \quad , \tag{A.9}$$

then by equations (A.3), (A.4) and $\psi \sim B\,\lambda^4$ as $\lambda \to 0$ we have, as $(\lambda,\psi) \to (0,0)$,

$$P' \to -2\,\beta^{-(\gamma+1)/2}\,B^{(\gamma+1)/2}\,\lambda^4 \to 0 \quad , \tag{A.10}$$

$$Q' \to -\frac{1}{2}\,\beta^{-(\gamma+1)/2}\,B^{(\gamma-1)/2}\,\lambda \to 0 \quad . \tag{A.11}$$

This verifies that $(\lambda,\psi) = (0,0)$ is indeed a critical point. In fact, this point a node since $\psi \sim B\,\lambda^4$ as $\lambda \to 0$.

APPENDIX B

COSMIC-RAY ENERGY EQUATION AND COSMIC-RAY ENERGY FLUX

In this appendix, we derive the cosmic-ray energy equation (3.4) and the expression (3.5) for the cosmic-ray energy flux, from the cosmic-ray transport equation (e.g. Parker 1965a; Gleeson and Axford 1967; Jokipii and Parker 1970; Skilling 1975)

$$\frac{\partial f}{\partial t} + \vec{u}\cdot\nabla f - \nabla\cdot(\underline{\underline{\kappa}}\cdot\nabla f) - \frac{1}{3}\nabla\cdot\vec{u}\; p\,\frac{\partial f}{\partial p} = Q \quad , \tag{B.1}$$

where $f(\vec{x},p,t)$ is the mean phase space distribution for cosmic-rays (averaged over all directions of the individual particle momentum $\vec{p}$), $\underline{\underline{\kappa}}$ is the diffusion tensor, $\vec{u}$ is the background fluid velocity and Q is the source term. The effects of second order Fermi acceleration have been neglected in transport equation (B.1). Strictly speaking the velocity $\vec{u}$ should be replaced by the velocity of the waves that scatter the cosmic-rays, $\vec{V} = \vec{u} + \vec{V}_w$, where $\vec{V}_w$ is the velocity of the waves relative to the fluid, but since $|\vec{V}_w| \ll |\vec{u}|$ we have $\vec{V} \approx \vec{u}$ to a first approximation. It can also be shown (e.g. Dolginov and Toptygin 1966; Gleeson and Axford 1967) that the net streaming flux of particles with momentum in the range (p,p+dp) is given by

$$\vec{S}_p = -4\pi p^2 \left(\frac{1}{3} p \frac{\partial f}{\partial p}\vec{u} + \underline{\underline{\kappa}}\cdot\nabla f\right) \quad . \tag{B.2}$$

In terms of the differential number density $U_p \equiv 4\pi p^2 f$ and the streaming flux $\vec{S}_p$, the transport equation can also be written in the conservation form

$$\frac{\partial U_p}{\partial t} + \nabla\cdot\vec{S}_p + \frac{\partial}{\partial p}\left(\frac{1}{3}\, p\, \vec{u}\cdot\nabla U_p\right) = 4\pi p^2 Q \quad . \tag{B.3}$$

To obtain the cosmic-ray equation (3.4), multiply the cosmic-ray continuity equation (B.3) by the particle kinetic energy $T = (p^2c^2 + m_o^2c^4)^{1/2} - m_oc^2$ (where m_o is the rest mass of the particle and c is the speed of light) and then integrate over all momenta p we find:

$$\frac{\partial E_c}{\partial t} + \nabla\cdot\vec{F}_c = \vec{u}\cdot\nabla P_c + Q^* \quad , \tag{B.4}$$

where

$$E_c \equiv \int_0^\infty T\, U_p\, dp \quad , \tag{B.5}$$

is the cosmic-ray energy density;

$$\vec{F}_c \equiv \int_0^\infty T\, \vec{S}_p\, dp \quad , \tag{B.6}$$

is the cosmic-ray energy flux;

$$P_c \equiv \frac{1}{3}\int_0^\infty v\, p\, U_p\, dp \quad , \tag{B.7}$$

is the cosmic-ray pressure (v is the individual particle speed); and

$$Q^* \equiv \int_0^\infty 4\pi p^2\, T\, Q\, dp \quad . \tag{B.8}$$

Substituting the expression (B.2) for $\vec{S}_p$ in equation (B.6) and integrating over all momenta, we obtain

$$\vec{F}_c = (E_c + P_c)\,\vec{u} - \langle\underline{\kappa}\rangle\cdot\nabla E_c \quad , \tag{B.9}$$

where

$$\langle\underline{\kappa}\rangle\cdot\nabla E_c \equiv \int_0^\infty \underline{\kappa}\cdot\nabla(T\, U_p)\, dp \quad . \tag{B.10}$$

In obtaining the $\vec{u}\cdot\nabla P_c$ term in equation (B.4) and the expression (B.9) for $\vec{F}_c$, we have used the result

$$\int_0^\infty T \frac{\partial}{\partial p}(p\, U_p)\, dp = -3 P_c \quad , \tag{B.11}$$

which is obtained by integrating by parts and assuming that the distribution function, f, is such that $T p^3 f \to 0$ as $p \to 0$ and $p \to \infty$. Note also that $\frac{dT}{dp} = v$ gives the individual particle speed.

For a fully relativistic cosmic-ray gas, equations (B.5) and (B.7) yield the polytropic relation (or the caloric equation of state):

$$E_c = \frac{1}{(\gamma_c - 1)} P_c \quad , \tag{B.12}$$

where $\gamma_c = 4/3$ is the cosmic-ray adiabatic (or polytropic) index. An equation of state of the form (B.12) also applies for a non-relativistic cosmic-ray gas (in which $\gamma_c = 5/3$), and also for a cosmic-ray gas whose distribution function has a momentum spectrum of the form $f \propto p^{-\alpha}$ with α constant and $4 < \alpha < 5$ (in this case $\gamma_c = \alpha/3$). These examples suggest in general that γ_c lies in the range $4/3 < \gamma_c < 5/3$. For the equation of state (B.12), the cosmic-ray energy flux (B.9) reduces to

$$\vec{F}_c = \frac{\gamma_c}{(\gamma_c - 1)} P_c \vec{u} - \frac{1}{(\gamma_c - 1)} \underline{\kappa} . \nabla P_c \quad . \tag{B.13}$$

APPENDIX C

THIRD ORDER REAL LINEAR AUTONOMOUS SYSTEM OF ORDINARY DIFFERENTIAL EQUATIONS

In this appendix we disscuss the qualitative behaviour of a general third order (or three dimensional) real linear autonomous system of O.D.E.'s. The system can be represented by

$$\frac{d\vec{X}}{dt} = \underline{\underline{A}}\,\vec{X} \quad , \tag{C.1}$$

where $\vec{X} = (x,y,z)^T$ and $\underline{\underline{A}}$ is a general 3*3 matrix. Since every matrix can be brought to one of the real Jordan canonical forms (see e.g. Hirsch and Smale 1974) by similarity transformations, so it is sufficient for us to consider $\underline{\underline{A}}$ in Jordan form only. There are four cases:

I. $$\underline{\underline{A}} = \begin{pmatrix} \mu_1 & 0 & 0 \\ 0 & \mu_2 & 0 \\ 0 & 0 & \mu_3 \end{pmatrix} , \tag{C.2}$$

II. $$\underline{\underline{A}} = \begin{pmatrix} a & -b & 0 \\ b & a & 0 \\ 0 & 0 & \mu_3 \end{pmatrix} , \tag{C.3}$$

III. $$\underline{\underline{A}} = \begin{pmatrix} \mu_1 & 0 & 0 \\ 1 & \mu_1 & 0 \\ 0 & 0 & \mu_3 \end{pmatrix} , \tag{C.4}$$

IV. $$\underline{\underline{A}} = \begin{pmatrix} \mu & 0 & 0 \\ 1 & \mu & 0 \\ 0 & 1 & \mu \end{pmatrix} . \tag{C.5}$$

The solutions of equation (C.1) corresponding to these Jordan canonical forms are:

$$\text{I.} \qquad \begin{bmatrix} x \\ y \\ z \end{bmatrix} = \begin{bmatrix} x_o\, e^{\mu_1 t} \\ y_o\, e^{\mu_2 t} \\ z_o\, e^{\mu_3 t} \end{bmatrix}, \tag{C.6}$$

$$\text{II.} \qquad \begin{bmatrix} x \\ y \\ z \end{bmatrix} = \begin{bmatrix} [x_o \cos(bt) - y_o \sin(bt)]\, e^{at} \\ [x_o \sin(bt) + y_o \cos(bt)]\, e^{at} \\ z_o\, e^{\mu_3 t} \end{bmatrix}, \tag{C.7}$$

$$\text{III.} \qquad \begin{bmatrix} x \\ y \\ z \end{bmatrix} = \begin{bmatrix} x_o\, e^{\mu_1 t} \\ x_o\, t\, e^{\mu_1 t} + y_o\, e^{\mu_1 t} \\ z_o\, e^{\mu_3 t} \end{bmatrix}, \tag{C.8}$$

$$\text{IV.} \qquad \begin{bmatrix} x \\ y \\ z \end{bmatrix} = \begin{bmatrix} x_o\, e^{\mu t} \\ x_o\, t\, e^{\mu t} + y_o\, e^{\mu t} \\ \frac{1}{2} x_o\, t^2\, x_o\, e^{\mu t} + y_o\, t\, e^{\mu t} + z_o\, e^{\mu t} \end{bmatrix}. \tag{C.9}$$

Since the real parameters μ_1, μ_2, μ_3, a, b and μ can be positive, negative or zero and can equal each other, there are 20 distinct configurations for case I, 18 for case II, 13 for case III and 3 for case IV.

As an example, let us consider the case corresponding to §3.2.1. In this case, μ_1, μ_2 and μ_3 are distinct and one of them, say μ_3, is zero, so that case I and II are the relevant ones. From equations (C.6) and (C.7) we notice that each solution curve lies in a plane parallel to x-y plane, because $z = z_o$ at any time. The three different configurations, node, focus and saddle, are sketched in figures C.1 – C.3 with the z-axis as the line of critical points.

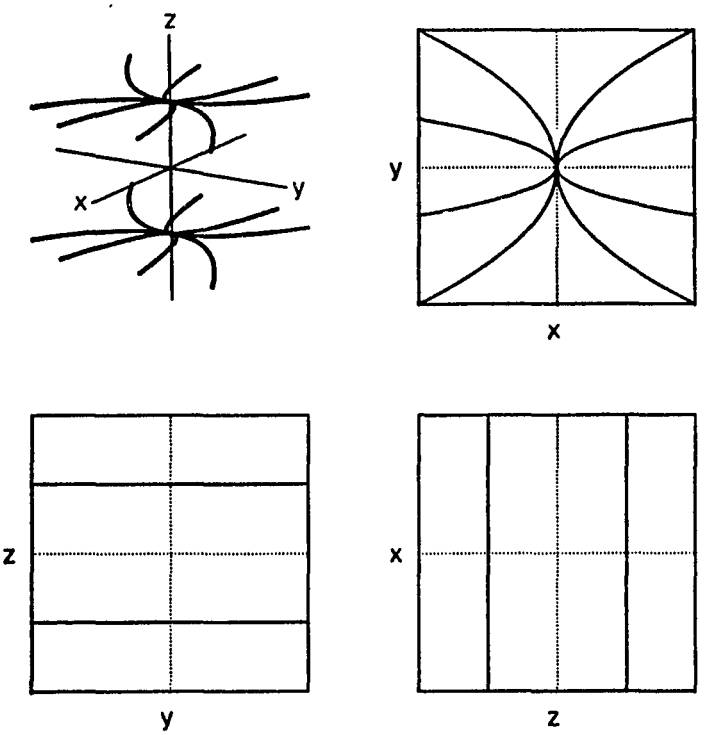

Figure C.1 Sketches of Solution Curves Around the Nodes with $\mu_1 > \mu_2 > \mu_3 = 0$

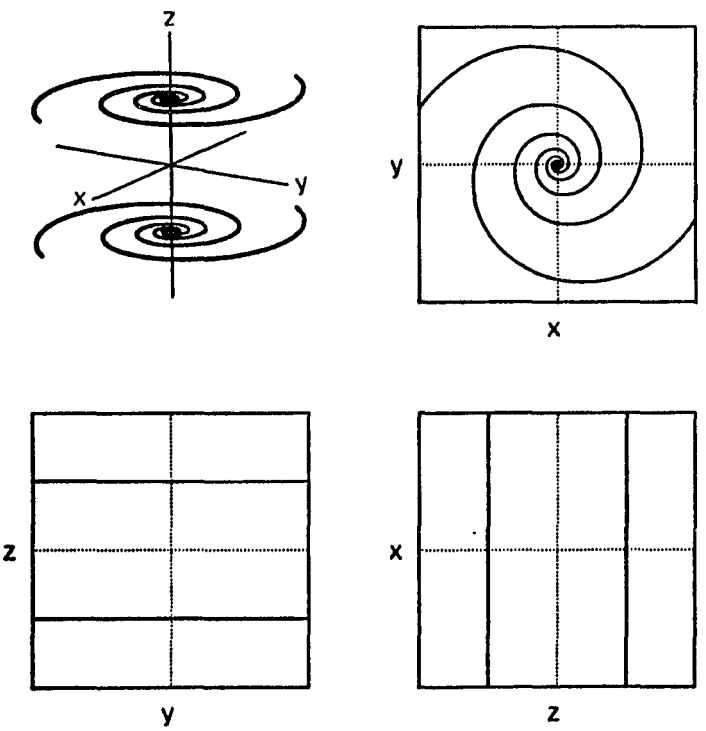

Figure C.2 Sketches of Solution Curves Around the Foci with $a > \mu_3 = 0 > b$

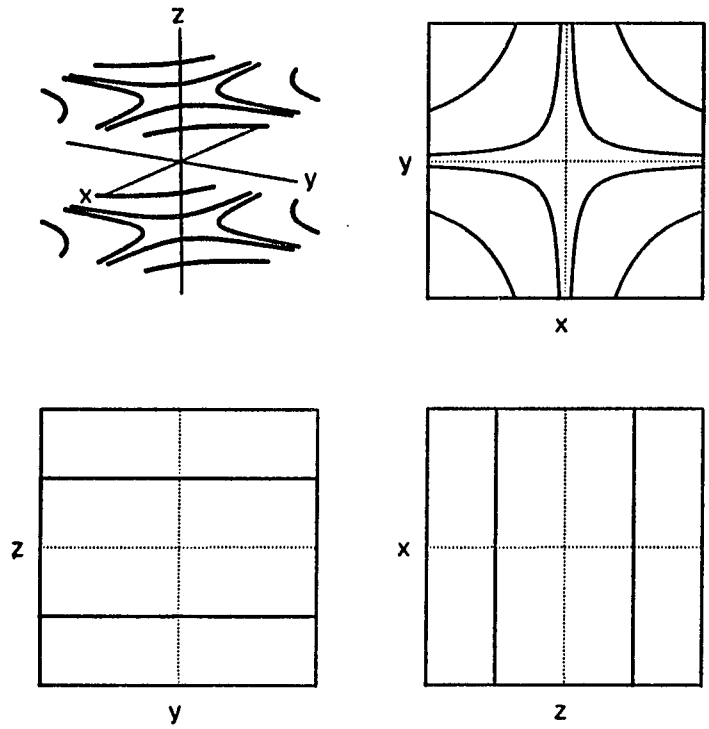

Figure C.3 Sketches of Solution Curves Around the Saddles with $\mu_1 > \mu_3 = 0 > \mu_2$

We now consider the eigenvectors corresponding to the matrices (C.2) – (C.5). Case I has 3 eigenvectors, $(1,0,0,)^T$, $(0,1,0)^T$ and $(0,0,1)^T$; case II has 1 real eigenvector, $(0,0,1)^T$; case III has 2 eigenvectors, $(0,1,0)^T$ and $(0,0,1)^T$; case IV has 1 eigenvector, $(0,0,1)^T$. If the parameters, μ_1, μ_2, μ_3 and μ, are not zero, then the real eigenvectors correspond to some preferred directions for the solution curves of the system under investigation. If some of the eigenvalues are zero, then those eigenvectors corresponding to zero eigenvalues are tangent (or parallel) to the critical line or surface of the system. This can be seen as follows. The matrix $\underline{A}$ in equation (C.1) is singular because some of its eigenvalues are zero. Critical points occur when $\frac{d\vec{X}}{dt} = 0$, i.e, when

$$\underline{\underline{A}}\,\vec{X} = \underline{\underline{A}}\begin{bmatrix} x \\ y \\ z \end{bmatrix} = 0 \quad . \tag{C.10}$$

This is a system of dependent linear equations if the matrix $\underline{\underline{A}}$ is singular. The solution is a line or a surface (or even the whole three dimensional space if $\underline{\underline{A}}$ is a null matrix), and we called this the *Critical Line* or *Surface*. Now if μ^* is one of the real eigenvalues of $\underline{\underline{A}}$, then the components of the eigenvector corresponding to μ^* are given by the following system of linear equations:

$$(\underline{\underline{A}} - \mu^*\underline{\underline{I}})\begin{bmatrix} x \\ y \\ z \end{bmatrix} = 0 \quad . \tag{C.11}$$

If $\mu^* = 0$, then equation (C.10) is exactly the same as equation (C.11), and the direction of the critical line (or surface) is the same as the direction of the eigenvector corresponding to the zero eigenvalue.

This property of zero eigenvalue is true in nonlinear system also. Consider the following system:

$$\frac{d}{dt}\begin{bmatrix} x \\ y \\ z \end{bmatrix} = \begin{bmatrix} P(x,y,z) \\ Q(x,y,z) \\ R(x,y,z) \end{bmatrix} \quad , \tag{C.12}$$

where

$$R(x,y,z) = \alpha(x,y,z)\,P(x,y,z) + \beta(x,y,z)\,Q(x,y,z) \quad , \tag{C.13}$$

so that R depends on P and Q. Assume that the surface $P(x,y.z) = 0$ and $Q(x,y,z) = 0$ intersect, then the system will have a critical line, and along this line (the intersection line of $P = Q = 0$) we have $\frac{d}{dt}(x,y,z)^T = 0$. At a point on this critical line, the tangent vector has to be perpendicular to both normal vectors to the surfaces

$P(x,y,z) = 0$ and $Q(x,y,z) = 0$. Let $\vec{t} = (u,v,w)^T$ be the tangent vector, then we have

$$\vec{t} \cdot \nabla P|_c = 0 \quad , \tag{C.14}$$

$$\vec{t} \cdot \nabla Q|_c = 0 \quad , \tag{C.15}$$

where the subscript c denotes quantities are evaluated at the critical line. The relations (C.14) and (C.15) can be written in the matrix form:

$$\underline{\underline{B}}^* \begin{bmatrix} u \\ v \\ w \end{bmatrix} \equiv \begin{bmatrix} P_x & P_y & P_z \\ Q_x & Q_y & Q_z \end{bmatrix}_c \begin{bmatrix} u \\ v \\ w \end{bmatrix} = 0 \quad , \tag{C.16}$$

and solving this matrix equation for $(u,v,w)^T$ yields the direction of the tangent vector to the critical line.

Linearizing the nonlinear autonomous system (C.12) about its critical line we obtain

$$\frac{d}{dt}\begin{bmatrix} x-x_c \\ y-y_c \\ z-z_c \end{bmatrix} = \underline{\underline{B}} \begin{bmatrix} x-x_c \\ y-y_c \\ z-z_c \end{bmatrix} \quad , \tag{C.17}$$

where

$$\underline{\underline{B}} = \begin{bmatrix} P_x & P_y & P_z \\ Q_x & Q_y & Q_z \\ \alpha P_x + \beta Q_x & \alpha P_y + \beta Q_y & \alpha P_z + \beta Q_z \end{bmatrix} \quad , \tag{C.18}$$

and $(x_c,y_c,z_c)^T$ is a point on the critical line. The matrix $\underline{\underline{B}}$ in equation (C.18) is singular so at least one of its eigenvalues is zero. The eigenvector $(x-x_c,y-y_c,z-z_c)$ corresponding to the zero eigenvalue, satisfies the following equation

$$\underline{\underline{B}} \begin{bmatrix} x-x_c \\ y-y_c \\ z-z_c \end{bmatrix} = 0 \quad . \tag{C.19}$$

By comparing equations (C.16) and (C.18), we notice that they are exactly the same set of linear equations (because the third row of the matrix $\underline{\underline{\mathbf{B}}}$ is a linear combination of the first two rows). As a result the eigenvector corresponding to the zero eigenvalue of the linearized system is tangent (or parallel) to the critical line of the nonlinear system.

APPENDIX D

ASYMPTOTIC SOLUTIONS

In this appendix we give an example of the application of equation (3.90), namely, we want to find the asymptotic behaviour of $\bar{\rho}$ as $\lambda \to 0$. The energy integral (3.13) and the energy equation of the thermal plasma (3.12) can be written in terms of $\bar{\rho}$ and λ, where $\bar{\rho} \equiv \psi^{-1/2}\ \lambda^2$,

$$\bar{E} = \frac{1}{2}\bar{\rho}^{-2}\lambda^4 - \lambda + \frac{1}{(\gamma_g-1)}\beta^{(\gamma_g+1)/2}\bar{\rho}^{(\gamma_g-1)} + \frac{\gamma_c}{(\gamma_c-1)}\bar{\rho}^{-1}\bar{P}_c + \frac{1}{(\gamma_c-1)}\bar{\kappa}\frac{d\bar{P}_c}{d\lambda} \quad , \tag{D.1}$$

$$\left[\beta^{(\gamma_g+1)/2}\bar{\rho}^{(\gamma_g-2)} - \bar{\rho}^{-3}\lambda^4\right]\frac{d\bar{\rho}}{d\lambda} = 1 - 2\bar{\rho}^{-2}\lambda^3 - \bar{\rho}^{-1}\frac{d\bar{P}_c}{d\lambda} \quad . \tag{D.2}$$

Following the same procedure as §3.3, equation (3.90) can be written in the form:

$$\begin{aligned}
&\left[\beta^{(\gamma_g+1)/2}\bar{\rho}^{\gamma_g} - \bar{\rho}^{-3}\lambda^4\right]\frac{d^2\bar{\rho}}{d\lambda^2} \\
&+ \left[\gamma_g\beta^{(\gamma_g+1)/2}\bar{\rho}^{(\gamma_g-1)} + \bar{\rho}^{-2}\lambda^4\right]\left(\frac{d\bar{\rho}}{d\lambda}\right)^2 \\
&+ \left[-2\bar{\rho} - 4\bar{\rho}^{-1}\lambda^3 + (\gamma_c-1)\frac{1}{\bar{\kappa}}\bar{E} - \frac{1}{2}(\gamma_c+1)\frac{1}{\bar{\kappa}}\bar{\rho}^{-2}\lambda^4\right. \\
&\quad + (\gamma_c-1)\frac{1}{\bar{\kappa}}\lambda + \frac{(\gamma_c-\gamma_g)}{(\gamma_g-1)}\frac{1}{\bar{\kappa}}\beta^{(\gamma_g+1)/2}\bar{\rho}^{(\gamma_g-1)} \\
&\quad \left. + \frac{1}{\bar{\kappa}}\frac{d\bar{\kappa}}{d\lambda}\beta^{(\gamma_g+1)/2}\bar{\rho}^{\gamma_g} - \frac{1}{\bar{\kappa}}\frac{d\bar{\kappa}}{d\lambda}\bar{\rho}^{-1}\lambda^4\right]\frac{d\bar{\rho}}{d\lambda}
\end{aligned}$$

$$+ \left[6\,\lambda^2 + \frac{2}{\bar{\kappa}}\,\bar{\rho}^{-1}\,\lambda^3 - \frac{1}{\bar{\kappa}}\,\bar{\rho} - \frac{1}{\bar{\kappa}}\,\frac{d\bar{\kappa}}{d\lambda}\,\bar{\rho}^{-2} + \frac{2}{\bar{\kappa}}\,\frac{d\bar{\kappa}}{d\lambda}\,\lambda^3 \right]$$

$$= 0 \quad . \tag{D.3}$$

For a finite value of $\bar{E}$, and the cosmic-ray energy flux as $r \to \infty$, in equation (D.1), the density $\bar{\rho}$ in general must be finite as $r \to \infty$ ($\rho \to \rho_\infty$ as $r \to \infty$). Thus at large radii, we may write

$$\bar{\rho} = \bar{\rho}_\infty\,(1 + \delta) \quad , \tag{D.4}$$

where

$$\delta(\lambda) \to 0 \quad , \qquad \text{as } \lambda \to 0 \quad . \tag{D.5}$$

We consider two cases: (a) $\bar{\kappa}$ is constant and (b) $\bar{\kappa} = \bar{\kappa}_o\,\lambda^{-\nu}$ with $\nu > 0$.

§D.1 Case $\bar{\kappa}$ is Constant

Substituting equation (D.4) into equation (D.3) and letting $\lambda \to 0$ we obtain (keeping only the largest terms in each coefficient) the equation governing the asymptotic behaviour of $\bar{\rho}$ (or δ):

$$\frac{d^2\delta}{d\lambda^2} + \gamma_g \left(\frac{d\delta}{d\lambda}\right)^2$$

$$+ \left[-2\,\beta^{-(\gamma_g+1)/2}\,\bar{\rho}_\infty^{-(\gamma_g-1)} + (\gamma_c-1)\,\frac{1}{\bar{\kappa}}\,\bar{E}\,\beta^{-(\gamma_g+1)/2}\,\bar{\rho}_\infty^{-\gamma_g} + \frac{(\gamma_c-\gamma_g)}{(\gamma_g-1)}\,\frac{1}{\bar{\kappa}}\,\bar{\rho}_\infty^{-1} \right] \frac{d\delta}{d\lambda}$$

$$- \frac{1}{\bar{\kappa}}\,\beta^{-(\gamma_g+1)/2}\,\bar{\rho}_\infty^{-\gamma_g} = 0 \quad . \tag{D.6}$$

Introducing a new independent variable χ to replace δ (e.g. see Murphy 1960):

$$\frac{d\delta}{d\lambda} = \frac{1}{\gamma_g}\,\frac{1}{\chi}\,\frac{d\chi}{d\lambda} \quad , \tag{D.7}$$

equation (D.6) reduces to the linear equation:

$$\frac{d^2\chi}{d\lambda^2} + b\,\frac{d\chi}{d\lambda} + \gamma_g\, c\,\chi = 0 \quad ; \tag{D.8}$$

where

$$b = -2\,\beta^{-(\gamma_g+1)/2}\,\bar{\rho}_\infty^{-(\gamma_g-1)} + (\gamma_c-1)\,\frac{1}{\bar{\kappa}}\,\bar{E}\,\beta^{-(\gamma_g+1)/2}\,\bar{\rho}_\infty^{-\gamma_g} + \frac{(\gamma_c-\gamma_g)}{(\gamma_g-1)}\,\frac{1}{\bar{\kappa}}\,\bar{\rho}_\infty^{-1} \quad , \tag{D.9}$$

$$c = -\frac{1}{\bar{\kappa}}\,\beta^{-(\gamma_g+1)/2}\,\bar{\rho}_\infty^{-\gamma_g} \quad . \tag{D.10}$$

The general solution of equation (D.8) is

$$\chi = A_1 \exp(\alpha_+\lambda) + A_2 \exp(\alpha_-\lambda) \quad , \tag{D.11}$$

where

$$\alpha_\pm = \frac{1}{2}\left[-b \pm (b^2 - 4\,\gamma_g\, c)^{1/2}\right] \tag{D.12}$$

and A_1, A_2 are constants. Equations (D.7) and (D.11) give the general solution of equation (D.6)

$$\delta = \frac{1}{\gamma_g}\log\left[A_1^* \exp(\alpha_+\lambda) + A_2^* \exp(\alpha_-\lambda)\right] \quad , \tag{D.13}$$

where A_1^* and A_2^* are constants. The appropriate boundary conditions at $\lambda = 0$ (actually they are initial conditions according to equation (D.6)) are equations (D.2) and (D.5). Thus at $\lambda = 0$:

$$\delta = 0 \quad , \tag{D.14}$$

$$\left.\frac{d\delta}{d\lambda}\right|_0 = \Delta = \beta^{-(\gamma_g+1)/2}\,\bar{\rho}_\infty^{-\gamma_g}\left(\bar{\rho}_\infty - \left.\frac{d\bar{P}_c}{d\lambda}\right|_0\right) \quad . \tag{D.15}$$

Substituting equations (D.14) and (D.15) into equation (D.13) gives

$$A_1^* = \frac{(\gamma_g\,\Delta - \alpha_-)}{(\alpha_+ - \alpha_-)} \quad , \quad A_2^* = \frac{(\gamma_g\,\Delta - \alpha_+)}{(\alpha_- - \alpha_+)} \quad . \tag{D.16}$$

Although equation (D.13) is the solution of equation (D.6), it is only an approximation to the solution of equation (D.3) as $\lambda \to 0$. If we

expand equation (D.13) we get the asymptotic solution for equation (D.3) as $\lambda \to 0$. As $\lambda \to 0$,

$$\delta \sim \Delta \lambda - \frac{1}{2\gamma_g} (\gamma_g \Delta - \alpha_-) (\gamma_g \Delta - \alpha_+) \lambda^2 + \cdots \quad . \tag{D.17}$$

Hence the density $\bar{\rho}$ near $\lambda = 0$ is given by

$$\bar{\rho} \sim \bar{\rho}_\infty + \left.\frac{d\bar{\rho}}{d\lambda}\right|_0 \lambda \quad , \tag{D.18}$$

which is just the Taylor series expansion of $\bar{\rho}$ around $\lambda = 0$. The above analysis has the advantage that we don't have to assume $\bar{\rho}$ can be expanded by a Taylor series beforehand.

§D.2 Case $\bar{\kappa} = \bar{\kappa}_o \lambda^{-\nu}$ with $\nu > 0$

With $\bar{\kappa} = \bar{\kappa}_o \lambda^{-\nu}$, $\nu > 0$, then as $\lambda \to 0$ equation (D.3) becomes (keeping only the largest terms in each coefficient):

$$\frac{d^2\delta}{d\lambda^2} + \gamma_g \left(\frac{d\delta}{d\lambda}\right)^2 - \nu \lambda^{-1} \frac{d\delta}{d\lambda} + \nu \Delta' \lambda^{-1} = 0 \quad , \tag{D.19}$$

where

$$\Delta' \equiv \beta^{-(\gamma_g+1)/2} \bar{\rho}_\infty^{-(\gamma_g-1)} \quad . \tag{D.20}$$

Introducting two new variables ω and ζ to replace δ and λ:

$$\delta = \frac{1}{\gamma_g} \log(C\omega) \quad , \quad \zeta = \lambda^{(\nu+1)} \tag{D.21}$$

(C is a constant), the non-linear O.D.E. (D.19) reduces to a linear O.D.E. in ω and ζ,

$$\frac{d^2\omega}{d\zeta^2} + \gamma_g \nu (\nu + 1)^{-2} \Delta' \zeta^{-(2\nu+1)/(\nu+1)} \omega = 0 \quad . \tag{D.22}$$

Equation (D.22) is of the form

$$\frac{d^2y}{dx^2} + a x^k y = 0 \quad . \tag{D.23}$$

This equation can be transformed to Bessel's equation (e.g. see Murphy 1960) by taking the following changes of variables in sequence:

$$y = \sqrt{x}\, y_1 \quad , \quad x_1 = x^{(k+2)/2} \quad , \quad x_2 = \frac{2}{(k+2)} \sqrt{a}\, x_1 \quad . \qquad (D.24)$$

After some manipulations equation (D.23) becomes:

$$x_2^2 \frac{d^2 y_1}{dx_2^2} + x_2 \frac{dy_1}{dx_2} - [(k+2)^{-2} - x_2^2]\, y_1 = 0 \quad , \qquad (D.25)$$

which is Bessel's equation of order $1/(k+2)$ .Thus the general solution to equation (D.22) is:

(a) if ν is not an integer,

$$\omega = C_1 \sqrt{\zeta}\, J_{(\nu+1)}(2\sqrt{\gamma_g \nu \Delta'}\, \zeta^{1/2/(\nu+1)}) + C_2 \sqrt{\zeta}\, J_{-(\nu+1)}(2\sqrt{\gamma_g \nu \Delta'}\, \zeta^{1/2/(\nu+1)}) \quad ; \qquad (D.26)$$

(b) if ν is an integer,

$$\omega = C_1 \sqrt{\zeta}\, J_{(\nu+1)}(2\sqrt{\gamma_g \nu \Delta'}\, \zeta^{1/2/(\nu+1)}) + C_2 \sqrt{\zeta}\, Y_{(\nu+1)}(2\sqrt{\gamma_g \nu \Delta'}\, \zeta^{1/2/(\nu+1)}) \quad , \qquad (D.27)$$

where C_1, C_2 are constants, and $J_p(z)$ and $Y_p(z)$ are Bessel and Neuman function respectively. The power series expansion of $J_p(z)$ and $Y_p(z)$ are (e.g. Whittaker and Watson 1927):

$$J_p(z) = \sum_{k=0}^{\infty} \frac{(-1)^k}{k!\Gamma(p+k+1)} \left(\frac{z}{2}\right)^{(p+2k)} \quad , \qquad (D.28)$$

$$Y_p(z) = -\sum_{k=0}^{p-1} \frac{(p-k-1)!}{k!} \left(\frac{z}{2}\right)^{(-p+2k)} + \sum_{k=0}^{\infty} \frac{(-1)^k}{k!\,(p+k)!} \left(\frac{z}{2}\right)^{(p+2k)} \left[2 \log\left(\frac{z}{2}\right) + 2\gamma - \sum_{m=1}^{p+k} m^{-1} - \sum_{m=1}^{k} m^{-1}\right] \quad , \qquad (D.29)$$

where

$$\gamma = \lim_{m \to \infty} \{1 + \frac{1}{2} + \cdots + \frac{1}{m} - \log(m)\} = 0.5772157 \qquad (D.30)$$

is the Euler's constant. Substituting equations (D.26) - (D.29) into equation (D.21) we obtain

(a) if ν is not an integer,

$$\delta = \frac{1}{\gamma_g} \log\left[C_1 \sum_{k=0}^{\infty} \frac{(-1)^k}{k!\Gamma(\nu+k+2)} (\gamma_g \nu \Delta')^{(\nu+2k+1)/2} \lambda^{(\nu+k+1)} + C_2 \sum_{k=0}^{\infty} \frac{(-1)^k}{k!\Gamma(-\nu+k)} (\gamma_g \nu \Delta')^{(-\nu+2k-1)/2} \lambda^k \right] ; \quad (D.31)$$

(b) if ν is an integer,

$$\delta = \frac{1}{\gamma_g} \log\left[C_1 \sum_{k=0}^{\infty} \frac{(-1)^k}{k!(\nu+k+1)!} (\gamma_g \nu \Delta')^{(\nu+2k+1)/2} \lambda^{(\nu+k+1)} - C_2 \sum_{k=0}^{\nu} \frac{(\nu-k)!}{k!} (\gamma_g \nu \Delta')^{(-\nu+2k-1)/2} \lambda^k + C_2 \sum_{k=0}^{\infty} \frac{(-1)^k}{k!(\nu+k+1)!} (\gamma_g \nu \Delta')^{(\nu+2k+1)/2} \lambda^{(\nu+k+1)} \cdot \left[\log(\gamma_g \nu \Delta' \lambda) + 2\gamma - \sum_{m=1}^{\nu+k+1} m^{-1} - \sum_{m=1}^{k} m^{-1} \right] \right] . \quad (D.32)$$

Applying the boundary condition (D.14), we obtain:

(a) if ν is not an integer,

$$C_2 = \Gamma(-\nu)(\gamma_g \nu \Delta')^{(\nu+1)/2} ; \quad (D.33)$$

(b) if ν is an integer,

$$C_2 = -\frac{1}{\nu!}(\gamma_g \nu \Delta')^{(\nu+1)/2} . \quad (D.34)$$

Since $\bar{\kappa} \frac{d\bar{P}_c}{d\lambda}$ is finite and $\bar{\kappa} = \bar{\kappa}_o \lambda^{-\nu}$ ($\nu > 0$), $\frac{d\bar{P}_c}{d\lambda} \to 0$ as $\lambda \to 0$.

The other boundary condition (D.15) is then

$$\left.\frac{d\delta}{d\lambda}\right|_0 = \beta^{-(\gamma_g+1)/2} \bar{\rho}_\infty^{-(\gamma_g-1)} = \Delta' , \quad (D.35)$$

and this is automatically satisfied. This can be seen by differentiating equations (D.31) and (D.32) and letting $\lambda \to 0$. Finally, by expanding equations (D.31) and (D.32) for $\lambda \to 0$, we obtain the asymptotic solution of equation (D.3)

$$\bar{\rho} \sim \bar{\rho}_{\infty} (1 + \Delta' \lambda) \quad , \tag{D.36}$$

which is also just the Taylor series expansion of $\bar{\rho}$ around $\lambda = 0$.

APPENDIX E

ANALYTICAL SOLUTION AND BOUNDARY CONDITIONS AT THE ORIGIN

Analytical solutions (in test particle picture) to the steady state cosmic-ray energy equation (4.2) with some specfic velocity profiles are discussed in this appendix. As a consequence, some criteria can be set up for the boundary conditions at the origin.

§E.1 Analytical Solution

The steady state cosmic-ray energy equaion (4.2)

$$\frac{1}{\xi^2}\frac{d}{d\xi}\left(\xi^2\,\tilde{\kappa}\,\frac{d\tilde{P}_c}{d\xi}\right) - \tilde{u}\,\frac{d\tilde{P}_c}{d\xi} - \gamma_c\,\frac{1}{\xi^2}\frac{d}{d\xi}(\xi^2\,\tilde{u})\,\tilde{P}_c = 0 \quad , \tag{E.1}$$

where ξ, $\tilde{u}$, $\tilde{P}_c$ amd $\tilde{\kappa}$ defined by equation (4.1), can easily be solved if the divergence of the velocity is zero, i.e., in spherical case,

$$\tilde{u} = \tilde{u}_2\,\xi^{-2} \quad , \tag{E.2}$$

where $\tilde{u}_2$ is a constant. In this case equation (E.1) becomes

$$\frac{1}{\xi^2}\frac{d}{d\xi}\left(\xi^2\,\tilde{\kappa}\,\frac{d\tilde{P}_c}{d\xi}\right) - \tilde{u}\,\frac{d\tilde{P}_c}{d\xi} = 0 \quad , \tag{E.3}$$

with general solution:

$$\tilde{P}_c = B_1\,\exp\left(\int^{\xi}\frac{\tilde{u}_2}{\tilde{\kappa}}\,\xi'^{-2}\,d\xi'\right) + B_2 \quad , \tag{E.4}$$

where B_1 and B_2 are constants.

Analytical solutions of equation (E.1) exist if

$$\tilde{u} = \tilde{u}_1 \xi^{\mu} \quad \text{and} \quad \tilde{\kappa} = \tilde{\kappa}_1 \xi^{\nu} \ , \tag{E.5}$$

where $\tilde{u}_1$, $\tilde{K}_1$, μ and ν are constants. With a change of independent variable (provided that $\nu \neq 1$):

$$z = \frac{1}{(1+\mu-\nu)} \frac{\tilde{u}_1}{\tilde{\kappa}_1} \xi^{(1+\mu-\nu)} \ , \tag{E.6}$$

equation (E.1) becomes a version of Kummer's equation

$$z \frac{d^2\tilde{P}_c}{dz^2} + \left[\frac{(2+\mu)}{(1+\mu-\nu)} - z\right] \frac{d\tilde{P}_c}{dz} - \frac{(2+\mu)}{(1+\mu-\nu)} \gamma_c \tilde{P}_c = 0 \ . \tag{E.7}$$

The general solution of this equation is given in terms of confluent hypergeometric functions (e.g. see Erdélyi *et al.* 1953; Lebedev 1965). For $\gamma_c > 1$ and not an integer, there are three relevant cases (note for arbitrary γ_c, there may be five distinct cases).

(a) If $\frac{(2+\mu)}{(1+\mu-\nu)}$ is not an integer, then

$$\tilde{P}_c = A_1 \, {}_1F_1\left[\frac{(2+\mu)}{(1+\mu-\nu)}\gamma_c, \frac{(2+\mu)}{(1+\mu-\nu)}; z\right] + A_2 \, z^{-(1+\nu)/(1+\mu-\nu)} \, {}_1F_1\left[\frac{(2+\mu)}{(1+\mu-\nu)}\gamma_c - \frac{(1+\nu)}{(1+\mu-\nu)}, \frac{(\mu-2\nu)}{(1+\mu-\nu)}; z\right] \ , \tag{E.8}$$

where

$${}_1F_1(\alpha,\gamma;z) = \sum_{k=0}^{\infty} \frac{(\alpha)_k}{k!\,(\gamma)_k} z^k \ , \tag{E.9}$$

$$(\alpha)_k \equiv \frac{\Gamma(\alpha+k)}{\Gamma(\alpha)} \ , \qquad k \geq 0 \tag{E.10}$$

and $\Gamma(\alpha)$ is the Gamma function.

(b) If $\frac{(2+\mu)}{(1+\mu-\nu)}$ is a positive integer, then

$$\tilde{P}_c = A_1 \, {}_1F_1\left[\frac{(2+\mu)}{(1+\mu-\nu)}\gamma_c, \frac{(2+\mu)}{(1+\mu-\nu)}; z\right] + A_2 \, G\left[\frac{(2+\mu)}{(1+\mu-\nu)}\gamma_c, \frac{(2+\mu)}{(1+\mu-\nu)}; z\right] \ , \tag{E.11}$$

where

$$G(\alpha,\gamma;z) \equiv {}_1F_1(\alpha,\gamma;z) \log(z)$$

$$+ \sum_{k=0}^{\infty} \frac{(\alpha)_k}{k!\,(\gamma)_k} \{\Psi(\alpha+k) - \Psi(\gamma+k) - \Psi(1+k)\}\, z^k$$

$$+ \frac{(-1)^{\gamma}\Gamma(\gamma-1)\Gamma(\gamma)\Gamma(\alpha-\gamma+1)}{\Gamma(\alpha)} \sum_{k=0}^{\gamma-2} \frac{(\alpha-\gamma+1)_k}{k!\,(2-\gamma)_k}\, z^{(1-\gamma+k)} \qquad \text{(E.12)}$$

$$\Psi(\alpha) = \frac{\Gamma'(\alpha)}{\Gamma(\alpha)} \; . \qquad \text{(E.13)}$$

(c) If $\frac{(2+\mu)}{(1+\mu-\nu)}$ is a non-positive integer, then

$$\tilde{P}_c = A_1\, z^{-(1+\nu)/(1+\mu-\nu)}\; {}_1F_1\left[\frac{(2+\mu)}{(1+\mu-\nu)}\gamma_c - \frac{(1+\nu)}{(1+\mu-\nu)}, \frac{(\mu-2\nu)}{(1+\mu-\nu)}; z\right]$$
$$+ A_2\, z^{-(1+\nu)/(1+\mu-\nu)}\; G\left[\frac{(2+\mu)}{(1+\mu-\nu)}\gamma_c - \frac{(1+\nu)}{(1+\mu-\nu)}, \frac{(\mu-2\nu)}{(1+\mu-\nu)}; z\right] \; . \qquad \text{(E.14)}$$

Imposing suitable boundary conditions, the constants A_1, A_2, B_1 and B_2 can be determined. Although the solution can be written down in terms of special functions (confluent hypergeometric functions), its behaviour is not very transparent. The case where the solution is simple enough to analyze easily is the cases not included in the transformation (E.6), namely, $\mu = 0$ and $\nu = 1$. Let the velocity profile (4.18)

$$\tilde{u} = \tilde{u}_1\, [1 - H(\xi-\xi_{sh})] + \tilde{u}_2\, \xi^{-2}\, H(\xi-\xi_{sh}) \qquad \text{(E.15)}$$

($\tilde{u}_1$ and $\tilde{u}_2$ are constants), represents the stellar wind and consider a diffusion coefficient (4.19)

$$\tilde{\kappa} = \tilde{\kappa}_1\, [1 - H(\xi-\xi_{sh})] + \tilde{\kappa}_2\, \xi^{-2}\, H(\xi-\xi_{sh}) \qquad \text{(E.16)}$$

($\tilde{\kappa}_1$ and $\tilde{\kappa}_2$ are constants). The solution (Webb, Forman and Axford 1985) to equation (E.1) with boundary conditions, $\tilde{P}_c$ is finite at the origin, $\tilde{P}_c = \tilde{P}_{c\infty}$ at infinity and continuity of $\tilde{P}_c$ and $\tilde{F}_c$ at the shock, is

$$\tilde{P}_c = A_1\, \xi^{\alpha_+}\, [1 - H(\xi-\xi_{sh})]$$
$$+ \left[B_1 \exp(-\tfrac{1}{2}\,\eta_2\,\xi^{-2}) + B_2\right] H(\xi-\xi_{sh}) \; . \qquad \text{(E.17)}$$

where

$$A_1 = \frac{\tilde{P}_{c\infty}\ \tilde{u}_2\ \xi_{sh}^{-\alpha_+}}{\left[\tilde{u}_2 + \left[\exp(\frac{1}{2}\ \eta_2\ \xi_{sh}^{-2}) - 1\right]\left[\gamma_c\ (\tilde{u}_2\ \xi_{sh}^{-2} - \tilde{u}_1) + \tilde{\kappa}_1\ \alpha_+\right]\right]} \quad , \tag{E.18}$$

$$B_1 = \frac{\left[\tilde{P}_{c\infty} - A_1\ \xi_{sh}^{\alpha_+}\right]}{\left[1 - \exp(-\frac{1}{2}\ \eta_2\ \xi_{sh}^{-2})\right]} \quad , \tag{E.19}$$

$$B_2 = \tilde{P}_{c\infty} - B_1 \quad , \tag{E.20}$$

$$\alpha_+ = \frac{1}{2}\left((\eta_1 - 2) + [(\eta_1 - 2)^2 + 8\ \gamma_c\ \eta_1]^{1/2}\right) \quad , \tag{E.21}$$

$$\eta_1 = \frac{\tilde{u}_1}{\tilde{\kappa}_1} \quad , \tag{E.22}$$

$$\eta_2 = \frac{\tilde{u}_2}{\tilde{\kappa}_2} \quad . \tag{E.23}$$

This solution can easily be visualized. Starting from zero at the origin (r = 0), $\tilde{P}_c$ increases to some value $(A_1 \xi_{sh}^{\alpha_+})$ at the shock algebraically, and then approachs $\tilde{P}_{c\infty}$ exponentially outside the shock.

§E.2 Boundary Conditions at the Origin

We now study the behaviour of the solutions (E.8), (E.11) and (E.14) near the origin (as $\xi \to 0$):

(a) if $\frac{(2+\mu)}{(1+\mu-\nu)}$ is not an integer, then

$$\tilde{P}_c = A_1\left[1 + \frac{\gamma_c}{(1+\mu-\nu)}\frac{\tilde{u}_1}{\tilde{\kappa}_1}\xi^{(1+\mu-\nu)} + \cdots\right]$$

$$+ A_2\left[\frac{1}{(1+\mu-\nu)}\frac{\tilde{u}_1}{\tilde{\kappa}_1}\right]^{-(1+\nu)/(1+\mu-\nu)} \xi^{-(1+\nu)}$$

$$\cdot\left[1 + \frac{(2+\mu)\gamma_c - \nu - 1}{(\mu-2\nu)(1+\mu-\nu)}\frac{\tilde{u}_1}{\tilde{\kappa}_1}\xi^{(1+\mu-\nu)} + \cdots\right] \quad . \tag{E.24}$$

We notice that $\tilde{P}_c$ is finite if one of the following is true:

(1) $1+\mu-\nu > 0$, $1+\nu > 0$, A_1 is finite, and $A_2 = 0$;

(2) $1+\mu-\nu > 0$, $1+\nu < 0$, A_1 and A_2 are finite.

Also $\frac{d\tilde{P}_c}{d\xi} = 0$ if one of the following is true:

(1) $\mu > \nu$, $2+\nu > 0$, A_1 is finite, and $A_2 = 0$;

(2) $\mu > \nu$, $2+\nu < 0$, A_1 and A_2 are finite;

(3) $\mu < \nu$, $1+\mu-\nu > 0$, $2+\nu < 0$, $A_1 = 0$ and A_2 is finite.

(b) If $n \equiv \frac{(2+\mu)}{(1+\mu-\nu)}$ is a positive integer, then

$$\tilde{P}_c = A_1 \left[1 + \frac{\gamma_c}{(1+\mu-\nu)} \frac{\tilde{u}_1}{\tilde{\kappa}_1} \xi^{(1+\mu-\nu)} + \cdots\right]$$

$$+ A_2 \left[\log\left(\frac{1}{(1+\mu-\nu)} \frac{\tilde{u}_1}{\tilde{\kappa}_1}\right) + (1 + \mu - \nu) \log(\xi) + \cdots\right.$$

$$\left. + \{\Psi(n\gamma_c) - \Psi(n) - \Psi(1)\} + \cdots\right.$$

$$\left. + \frac{(-1)^n \Gamma(n-1)\Gamma(n)\Gamma(n\gamma_c - n+1)}{\Gamma(n\gamma_c)} \left(\frac{1}{(1+\mu-\nu)} \frac{\tilde{u}_1}{\tilde{\kappa}_1}\right)^{(1-n)} \xi^{-(1+\nu)} + \cdots\right] . \quad (E.25)$$

$\tilde{P}_c$ is finite if $1+\mu-\nu > 0$, A_1 is finite, and $A_2 = 0$, and $\frac{d\tilde{P}_c}{d\xi} = 0$ if $\mu > \nu$, A_1 is finite, and $A_2 = 0$.

(c) If $m \equiv \frac{(2+\mu)}{(1+\mu-\nu)}$ is a non-positive integer, then

$$\tilde{P}_c = A_1 \left(\frac{1}{(1+\mu-\nu)} \frac{\tilde{u}_1}{\tilde{\kappa}_1}\right)^{(1-m)} \xi^{-(1+\nu)}$$

$$\cdot \left[1 + \frac{m(\gamma_c - 1)+1}{(2-m)(1+\mu-\nu)} \frac{\tilde{u}_1}{\tilde{\kappa}_1} \xi^{(1+\mu-\nu)} + \cdots\right]$$

$$+ A_2 \left[\frac{1}{(1+\mu-\nu)} \frac{\tilde{u}_1}{\tilde{\kappa}_1}\right]^{(1-m)} \xi^{-(1+\nu)}$$

$$\cdot \left[\log\left[\frac{1}{(1+\mu-\nu)} \frac{\tilde{u}_1}{\tilde{\kappa}_1}\right] + (1 + \mu - \nu) \log(\xi) + \cdots\right.$$

$$+ \{\Psi(m\gamma_c - m+1) - \Psi(2-m) - \Psi(1)\} + \cdots$$

$$+ \frac{(-1)^{(2-m)}\Gamma(1-m)\Gamma(2-m)\Gamma(m\gamma_c)}{\Gamma(m\gamma_c - m+1)}$$

$$\left. \cdot \left[\frac{1}{(1+\mu-\nu)} \frac{\tilde{u}_1}{\tilde{\kappa}_1}\right]^{(m-1)} \xi^{-(1+\nu)} + \cdots\right] \quad . \tag{E.26}$$

$\tilde{P}_c$ is finite if $1+\mu-\nu > 0$, $1+\nu < 0$, A_1 and A_2 are finite, and $\frac{d\tilde{P}_c}{d\xi} = 0$ if $1+\mu-\nu > 0$, $2+\nu < 0$, $3+2\nu < 0$, A_1 and A_2 are finite.

As an example, if $\mu > 0$ .and $\nu > 0$, then case (c) is irrelevant, and $\tilde{P}_c$ is finite and $\frac{d\tilde{P}_c}{d\xi} = 0$ at the origin provided $\mu > \nu$.

From equation (E.17) we notice that for the case $\mu = 0$ and $\nu = 1$, $\tilde{P}_c = 0$ and $\frac{d\tilde{P}_c}{d\xi} = 0$ at the origin provided $\alpha_+ - 1 > 0$ (i.e., $\eta_1 > 3/(2\gamma_c+1)$).

LIST OF REFERENCES

Achterberg, A.: 1981, 'The Pondermotive Force Due to Cosmic Ray Generated Alfven Waves', *Astron. Astrophys.*, **98**, 195.

Achterberg, A., Blandford R. D. and Periwal, V.: 1984, 'Two-Fluid Models of Cosmic-Ray Shock Acceleration', *Astron. Astrophys.*, **132**, 97.

Axford, W. I.: 1970a, 'Energetic Solar Particles in the Interplanetary Medium', *Solar Terrestrial Physics/1970, Part II*, 110, ed. E. R. Dyer, J. G. Roederer and A. J. Hundhausen, D. Reidel Publ., Dordrecht.

Axford, W. I.: 1970b, 'A Review of Theoretical Work on the Effects of Solar Wind Transport on Energetic Solar Particles', Paper presented at *Seminar on Cosmic Ray Generation on the Sun, USSR Academy of Science, Leningrad, Dec. 1970.*

Axford, W. I.: 1972, 'The Interaction of the Solar Wind with the Interstellar Medium', *Solar Wind, NASA Space-308*, 609.

Axford, W. I.: 1981, 'Acceleration of Cosmic Rays by Shock Waves', *Proc. 17th Internat. Cosmic Ray Conf., Paris*, **12**, 155.

Axford, W. I.: 1985, 'The Solar Wind', *Solar Phys.*, **100**, 575.

Axford, W. I., Dessler, A. J. and Gottlieb, B.: 1963, 'Termination of Solar Wind and Solar Magnetic Field', *Astrophys. J.* **137**, 1268.

Axford, W. I., Leer, E. and McKenzie, J. F.: 1982, 'The Structure of Cosmic Ray Shocks', *Astron. Astrophys.*, **111**, 317.

Axford, W. I., Leer, E. and Skadron, G.: 1977, 'The Acceleration of Cosmic Rays by Shock Waves', *Proc. 15th Internat. Cosmic Ray Conf., Plovdiv*, **2**, 273.

Axford, W. I. and Newman, R. C.: 1965, 'The Effect of Cosmic Ray Friction on the Solar Wind', *Proc. 9th Internat. Conf. on Cosmic Rays, London*, **1**, 173.

Babayan, V. Kh. and Dorman, L. I.: 1984, 'Transition of the Solar Wind to a Subsonic Flow in a Nonlinear Model of the Modulation of Galactic Cosmic Rays', *Geomagn. Aeron.*, **24**, 308.

LIST OF REFERENCES—Continued

Badhwar, C. D., Deney, C. L., Dennis, B. R. and Kaplon, M. F.: 1967, 'Measurements of the Low-Energy Cosmic Radiation During the Summer of 1966', *Phys. Rev.*, **163**, 1327.

Bell, A. R.: 1878a, 'The Acceleration of Cosmic Rays in Shock Fronts—I', *Mon. Not. Roy. Astron. Soc.*, **182**, 147.

Bell, A. R.: 1878b, 'The Acceleration of Cosmic Rays in Shock Fronts—II', *Mon. Not. Roy. Astron. Soc.*, **182**, 443.

Bender, C. M. and Orszag, S. A.: 1978, *Advanced Mathematical Methods for Scientist and Engineers*, McGraw-Hill, New York.

Beuerman, K. P., Rice, C. J., Stone, E. C. and Vogt, R. E.: 1969, 'Cosmic-Ray Negatron and Positron Spectra Between 12 and 220 MeV', *Phys. Rev. Letters*, **22**, 412.

Biermann, L.: 1951, 'Kometenschweife und Solare Korpuskularstrahlung', *Z. Astrophys.*, **29**, 274.

Biermann, L.: 1953, 'Physical Processes in Comet Tails and Their Relation to Solar Activity', *Mem. Soc. Roy. Sci. Liege Quatr. Ser.*, **13**, 291.

Birkeland, K.: 1908, *The Norwegian Aurora Polaris Expedition 1902-1903, Vol. 1, On the Cause of Magnetic Storms and the Origin of Terrestrial Magnetism, First Section*, H. Aschehoug and Co., Christiania.

Birkeland, K.: 1913, *The Norwegian Aurora Polaris Expedition 1902-1903, Vol. 1, On the Cause of Magnetic Storms and the Origin of Terrestrial Magnetism, Second Section*, H. Aschehoug and Co., Christiania.

Birmingham, T. J. and Jones, F. C.: 1975, 'Cosmic-Ray-Diffusion Report of the Workshop on Cosmic-Ray Diffusion Theory', *NASA Tenhnical Note D-7873*.

Blandford, R. D.: 1980, 'On the Mediation of a Shock Front by Fermi-Accelerated Cosmic Rays', *Astrophys. J.*, **238**, 410.

Blandford, R. D. and Eichler, D.: 1986, 'Particle Acceleration at Astrophysical Shocks: A Theory of Cosmic Ray Origin', preprint - unpublished.

LIST OF REFERENCES—Continued

Blandford, R. D. and Ostriker, J. P.: 1978, 'Particle Acceleration by Astrophysical Shocks', *Astrophys. J.*, **221**, L29.

Bondi, H.: 1952, 'On Spherically Symmetrical Accretion', *Mon. Not. Roy. Astron. Soc.*, **112**, 195.

Burger, J. J. and Swanenburg, B. N.: 1971, 'Long-Term Solar Modulation of Cosmic-Ray Electrons with Energies above 0.5 GeV', *Proc. 12th Internat. Conf. on Cosmic Rays, Hobart*, **5**, 1858.

Caldwell, J., Evenson, P., Jordan, S. and Meyer, P.: 1975, 'The Cosmic Ray Electron Spectrum in 1973 and 1974', *Proc. 14th Internat. Cosmic Ray Conf., Munich*, **3**, 1000.

Chamberlain, J. W.: 1961, 'Interplanetary Gas. III. A Hydrodynamic Model of the Corona', *Astrophys. J.*, **133**, 675.

Chen, G. L. L.: 1975, 'Numerical Simulation of the Interaction of Charged Particles with Oblique Magnetohydrodynamic Shocks', *Ph.D. Thesis*, University of Kansas, Lawrence.

Clauser, F. H.: 1960, 'The Aerodynamics of Mass Loss and Mass Gain of Stars', *John Hopkins University Lab. Rept. AFOSR Technical Note 60-1386*.

Cocconi, G.: 1951, 'On the Origin of the Cosmic Radiation', *Phys. Rev.*, **83**, 1193.

Coddington, E. A. and Levinson, N.: 1955, *Theory of Differential Equations*, McGraw-Hill, New York.

Compton, A. H. and Getting, I. A.: 1935, 'An Apparent Effect of Galactic Rotation on the Intensity of Cosmic Rays', *Phys. Rev.*, **47**, 817.

Cowsik, R. and Lee, M. A.: 1982, 'Transport of Neutrinos, Radiation and Energetic Particles in Accretion Flows', *Proc. Roy. Soc. London*, **A 383**, 409.

Curtis Michel, F.: 1982, 'Theory of Pulsar Magnetospheres', *Rev. Mod. Phys.*, **54**, 1.

Decker, R. B.: 1979, 'A Numerical Simulation of Charged Particle Interactions with Interplanetary Shock Waves', *Ph.D. Thesis*, University of Kansas, Lawrence.

LIST OF REFERENCES—Continued

Dessler, A. J.: 1967, 'Solar Wind and Interplanetary Magnetic Field', *Rev. Geophys.*, **5**, 1.

Dolginov, A. Z. and Toptygin, I. N.: 1966, 'Multiple Scattering of Particles in Magnetic Field with Random Inhomogeneities', *J. Exptl. Theoret. Phys.*, **51**, 1771 (1967, *Sov. Phys. JEPT*, **24**, 1195).

Dolginov, A. Z. and Toptygin, I. N.: 1967, 'Diffusion of Cosmic Particles in the Interplanetary Medium', *Geomagn. Aeron.*, **7**, 785.

Dolginov, A. Z. and Toptygin, I. N.: 1968, 'Cosmic Rays in the Interplanetary Magnetic Fields', *ICARUS*, **8**, 54.

Dorfi, E. A. and Drury, L. O'C.: 1985, 'Acceleration of Cosmic Rays in Supernova-Remnants', *Proc. 19th Internat. Cosmic Ray Conf., La Jolla*, **3**, 136.

Dorman, L. I.: 1965, 'Galactic and Solar Cosmic Rays in Interplanetary Space', *Proc. 9th Internat. Conf. on Cosmic Rays, London*, **1**, 292.

Drury, L. O'C.: 1983, 'An Introduction to the Theory of Diffusive Shock Acceleration of Energetic Particles in Tenuous Plamsma', *Rept. Progr. Phys.*, **46**, 973.

Drury, L. O'C. and Völk, H. J.: 1981, 'Hydrodynamic Shock Structure in the Presence of Cosmic Rays', *Astrophys. J.*, **248**, 344.

Earl, J. A.: 1961, 'Cloud-Chamber Observations of Primary Cosmic-Ray Electrons', *Phys. Rev. Letters*, **6**, 125.

Eichler, D.: 1979, 'Particle Acceleration in Collisionless Shocks: Regulated Injection and High Efficiency', *Astrophys. J.*, 229, 419.

Eichler, D.: 1981, 'Energetic Particle Spectra in Finite Shocks: The Earth's Bow Shock', *Astrophys. J.*, **244**, 711.

Erdélyi, A., Magnus, W., Oberhettinger, F. and Tricomi, F. G.: 1953, *Higher Transcendental Functions, Vol. 1*, McGraw-Hill, New York.

Fan, C. Y., Gloeckler, G. and Simpson, J. A.: 1965, 'Solar Modulation of the Galactic Helium Spectrum above 30 MeV per Nucleon', *Proc. 9th Internat. Conf. on Cosmic Rays, London*, **1**, 380.

LIST OF REFERENCES—Continued

Fanselow, J. L., Hartman, R. C., Hildebrand, R. H. and Meyer, P.: 1969, 'Charge Composition and Energy Spectrum of Primary Cosmic-Ray Electrons', *Astrophys. J.*, **158**, 771.

Fermi. E.: 1949, 'On the Origin of the Cosmic Radiation', *Phys. Rev.*, **75**, 1169.

Fisk, L. A.: 1969, 'The Behaviour of Cosmic Rays in the Interplanetary Medium', *Ph.D. Thesis*, University of California, San Diego.

Fisk, L. A.: 1979, 'The Interactions of Energetic Particles with the Solar Wind', *Solar System Plasma Physics, Vol. 1*, 177, ed. E. N. Parker, C. F. Kennel and L. J. Lanzerotti, North-Holland, Amsterdam.

Forbush, S. E.: 1937, 'On the Effects of Cosmic-Ray Intensity Observed During the Recent Magnetic Storm', *Phys. Rev.*, **51**, 1108.

Forbush, S. E.: 1954, 'World-Wide Cosmic-Ray Variations', *J. Geophys. Res.*, **59**, 525.

Forman, M. A.: 1970, 'The Compton-Getting Effect for Cosmic-Ray Particles and Photons and the Lorentz-Invariance of Distribution Functions', *Planet. Space Sci.*, **18**, 25.

Forman, M. A., Jokipii, J.R. and Owens, A. J.: 1974, 'Cosmic-Ray Streaming Perpendicular to the Mean Magnetic Field', *Astrophys. J.*, **192**, 535.

Forman, M. A. and Webb, G. M.: 1985, 'Acceleration of Energetic Particles', *Collisionless Shocks in the Heliosphere: A Tutorial Review*, 91, ed. R. C. Stone and B. T. Tsurutani, American Geophysical Union, Washington D. C..

Freier, P. S., Long, C. F., Cleghorn, T. F. and Waddington, C. J.: 1971, 'The Charge and Energy Spectra of Heavy Cosmic Ray Nuclei', *Proc. 12th Internat. Conf. on Cosmic Rays, Hobart*, **1**, 252.

Fulks, G., Meyer, P. and L'Heureux, L. J.: 1973, 'The Cosmic Ray Electron Spectrum and Its Modulation from 1968 Through 1972', *Proc. 13th Internat. Cosmic Ray Conf., Denver*, **2**, 753.

Ginzburg, V. L. and Syrovatskii, S. I.: 1964, *The Origin of Cosmic Rays*, Pergamon Press, Oxford.

LIST OF REFERENCES—Continued

Gleeson, L. J.: 1972, ' Cosmic Ray Propagation and Modulation in the Interplanetary Medium', *Proc. Solar Terrestrial Relations Conf., Calgary*, 79.

Gleeson, L. J. and Axford, W. I.: 1967, 'Cosmic Rays in the Interplanetary Medium', *Astrophys. J.*, **149**, L115.

Gleeson, L. J. and Axford, W. I.: 1968, 'The Compton-Getting Effect', *Astrophys. Space Sci.*, **2**, 431.

Gleeson, L. J. and Webb, G. M.: 1980, 'The Propagation of Cosmic Rays in the Interplanetary Region (the Theory)', *Fund. of Cosmic Phys.*, **6**, 187.

Gloeckler, G. and Jokipii J. R.: 1966, 'Low-Energy Cosmic-Ray Modulation Related to Observed Interplanetary Magnetic Field Irregularities', *Phys. Rev. Letters*, **17**, 203.

Gloeckler, G. and Jokipii J. R.: 1967, 'Solar Modulation and the Energy Density of Galactic Cosmic Rays', *Astrophys. J.*, **148**. L41.

Hall, D. E. and Sturrock, P. A.: 1967, 'Diffusion, Scattering, and Acceleration of Particles by Stochastic Electromagnetic Fields', *Phys. Fluids*, **10**, 2620.

Heavens, A. F.: 1983, 'Particle Acceleration in Shocks: the Effect of Finite Cosmic-Ray Pressure on the Energy Distribution', *Mon. Not. Roy. Astron. Soc.*, **204**, 699.

Hess, V. F. and Graziadei, T. H.: 1936, 'On the Diurnal Variation of the Cosmic Radiation', *Terrestr. Magn. and Atmosph. Electr.* (*J. Geophys. Res.*), **41**, 9.

Hess, V. F. and Steinmaurer, R.: 1933, *Berlin, SitzBer. Ak. Wiss.*, (*Proc. of Berlin Academy of Sciences*) **15**, 521.

Hirsch, M. W. and Smale, S.: 1974, *Differential Equations, Dynamical Systems, and Linear Algebra*, Academic Press, New York.

Hollweg, J. V.: 1978, 'Some Physical Processes in the Solar Wind', *Rev. Geophys. Space Phys.*, **16**, 689.

Holzer, T. E. and Axford, W. I.: 1970, 'The Theory of Stellar Winds and Related Flows', *Ann. Rev. Astron. Astrophys.*, **8**, 31.

LIST OF REFERENCES—Continued

Hopper, V. D.:1964, *Cosmic Radiation and High Energy Interactions*, Prentice-Hall, Englewood Cliffs.

Hsieh, K. C.: 1970, 'Study of Solar Modulation of Low-Energy Cosmic Rays Using Differential Spectra of Protons, ^{3}He, and ^{4}He at $E \leq 100$ MeV per Nucleon During the Quiet Time in 1965 and 1967', *Astrophys. J.*, **159**, 61.

Hundhausen, A. J.: 1972, *Coronal Expansion and Solar Wind*, Springer-Verlag, New York.

Ipavich, F. M.: 1975, 'Galactic Winds Driven by Cosmic Rays', *Astrophys. J.*, **196**, 107.

Jokipii, J. R.: 1966, 'Cosmic-Ray Propagation. I. Charged Particles in a Random Magnetic Field', *Astrophys. J.*, **146**, 480.

Jokipii, J. R.: 1967, 'Cosmic-Ray Propagation. II. Diffusion in the Interplanetary Magnetic Field', *Astrophys. J.*, **149**, 405.

Jokipii, J. R.: 1971, 'Propagation of Cosmic Rays in the Solar Wind', *Rev. Geophys. Space Phys.*, **9**, 27.

Jokipii, J. R.: 1972, 'Fokker-Planck Equations for Charged-Particle Transport in Random Fields', *Astrophys. J.*, **172**, 319.

Jokipii, J. R.: 1982, 'Particle Drift, Diffusion, and Acceleration of Shocks', *Astrophys. J.*, **225**, 716.

Jokipii, J. R.: 1986, 'Particle Acceleration at a Termination Shock 1. Application to the Solar Wind and the Anomalous Component', *J. Geophys. Res.*, **91**, 2929.

Jokipii, J. R. and Kopriva, D. A.: 1979, 'Effects of Particle Drift on the Transport of Cosmic Rays. III. Numerical Models of Galactic Cosmic-Ray Modulation', *Astrophys. J.*, **234**, 384.

Jokipii, J. R. and Merényi, E.: 1986, 'Effect of the Solar Wind Termination Shock on Cosmic-Ray Modulation', submitted to *Astrophysical Journal*.

Jokipii, J. R. and Parker, E. N.: 1967, 'Energy Changes of Cosmic Rays in the Solar System', *Planet. Space Sci.*, **15**, 1375.

LIST OF REFERENCES—Continued

Jokipii, J. R. and Parker, E. N.: 1969, 'Stochastic Aspects of Magnetic Lines of Force with Application to Cosmic-Ray Propagation', *Astrophs. J.*, **155**, 777.

Jokipii, J. R. and Parker, E. N.: 1970, 'On the Convection, Diffusion, and Adiabatic Deceleration of Cosmic Rays in the Solar Wind', *Astorphys. J.*, **160**, 735.

Keller, H. B.: 1968, *Numerical Methods for Two Point Boundary-Value Problem*, Ginn-Blaisdell, Waltham.

Kennel, C. F.: 1981, 'Collisionless Shocks and Upstream Waves and Particles: Introductory Remarks', *J. Geophys. Res.*, **86**, 4325.

Kennel, C. F., Edmiston, J. P. and Hada, T.: 1985, 'A Quarter Century of Collisionless Shock Research', *Collisionless Shocks in the Heliosphere: A Tutorial Review*, 1, ed. R. C. Stone and B. T. Tsurutani, American Geophysical Union, Washington D. C..

Kevorkian, J. and Cole, J. D.: 1981, *Perturbation Methods in Applied Mathematics*, Springer-Verlag, New York.

Ko, C. M. and Jokipii, J. R.: 1985, 'A Numerical Study of Diffusive Shock Accerleration of Cosmic Rays in Supernova Shocks', *Proc. Internat. Cosmic Ray Conf., La Jolla*, **3**, 156.

Kóta, J. and Jokipii, J. R.: 1983, 'Effects of Drift on the Transport of Cosmic Rays. VI. A Three-Dimensional Model Including Diffusion', *Astrophys. J.*, **265**, 573.

Krymskii, G. F.: 1977, 'A Regular Mechanism of the Acceleration of Charged Paricles on the Front of a Shock Wave', *Dokl. Akad. Nauk. SSSR*, **234**, 1306 (1977, *Sov. Phys. Dokl.*, **22**, 327).

Landau, L. D. and Lifshitz, E. M.: 1959, *Fluid Mechanics*, *Course of Theoretical Physics*, *Vol. 6*, Pergamon Press, Oxford.

Laster, H., Lencheck, A. M. and Singer, S. F.: 1962, 'Forbush Decreases Produced by Diffusive Deceleration Mechanism in Interplanetary Space', *J. Geophys. Res.*, **67**, 2639.

Lebedev, N. N.: 1965, *Special Functions and Their Applications*, Prentice-Hall, Englewood Cliffs.

LIST OF REFERENCES—Continued

Lee, M. A.: 1982, 'Coupled Hydrodynamic Wave Excitation and Ion Acceleration Upstream of the Earth's Bow Shock', *J. Geophys. Res.*, **87**, 5063.

Lee, M. A.: 1983, 'Coupled Hydrodynamic Wave Excitation and Ion Acceleration at Interplanetary Traveling Shocks', *J. Geophys. Res.*, **88**, 6109.

Lee, M. A. and Axford, W. I.: 1986, personal communication via G. M. Webb.

Leer, E., Holzer, T. E. and Flå, T.: 1982, 'Acceleration of the Solar Wind', *Space Sci. Rev.*, **33**, 161.

Lockwood, J. A. and Webber, W. R.: 1967, 'The 11-Year Solar Modulation of Cosmic Rays as Deduced from Neutron Monitor Variation and Direct Measurements at Low Energies', *J. Geophys. Res.*, **72**, 5977.

Luhmann, J. G.: 1976, 'A Quasi-Linear Kinetic Equation for Cosmic Rays in the Interplanetary Medium', *J. Geophys. Res.*, **81**, 2089.

McKenzie, J. F. and Völk, H. J.: 1982, 'Non-Linear Theory of Cosmic-Ray Shocks Including Self-Generated Alfven Waves', *Astron. Astrophys.*, **116**, 191.

Mckracken, K. G. and Rao, U. R.: 1970, 'Solar Cosmic Ray Phenomena', *Space Sci. Rev.*, **11**, 155.

Melrose, D. B.: 1980, *Plasma Astrophysics: Nonthermal Processes in Diffuse Magnetized Plasmas, Vol. 2*, Gordon and Breach Science Publ., New York.

Mestel, L.: 1954, 'The Influence of Stellar Radiation on the Rate of Accretion', *Mon. Not. Roy. Astron. Soc.*, **114**, 437.

Meyer, P. and Vogt R. E.: 'Electrons in the Primary Cosmic Radiation', *Phys. Rev. Letters*, **6**, 193.

Meyer, P., Parker, E. N. and Simpson, J. A.: 1956, 'Solar Cosmic Rays of February, 1956 and Their Propagation Through Interplanetary Space', *Phys. Rev.*, **104**, 768.

LIST OF REFERENCES—Continued

Meyer, P., Schmidt, P. J. and L'Heureux, L. J.: 1971, 'Measurements of the Primary Cosmic Ray Electron Spectrum Between 20 MeV and 20 GeV and Its Changes with Time', *Proc. 12th Internat. Conf. on Cosmic Rays, Hobart*, **2**, 548.

Moraal, H.: 1976, 'Observations of the Eleven-Year Cosmic-Ray Modulation Cycle', *Space Sci. Rev.*, **19**, 845.

Murphy, G. M.: 1960, *Ordinary Differential Equations and Their Solutions*, D. Van Nostrand, Princeton.

Neugebauer, M. and Snyder, C. W.: 1962, 'Solar Plasma Experiment', *Science*, **138**, 1095.

O'Gallagher, J. J. and Simpson, J. A.: 1967, 'The Heliocentric Intensity Gradients of Cosmic-Ray Protons and Helium During Minimum Solar Modulation', *Astrophys. J.*, **147**, 819.

Ormes, J. F. and Webber, W. R.: 1968, 'Proton and Helium Nuclei Cosmic-Ray Spectra and Modulations Between 100 and 2000 MeV/Nucleon', *J. Geophys. Res.*, **73**, 4231.

Parker, E. N.: 1958a, 'Dynamics of the Interplanetary Gas and Magnetic Fields', *Astrophys. J.*, **128**, 664.

Parker, E. N.: 1958b, 'Cosmic-Ray Modulation by Solar Wind', *Phys. Rev.*, **110**, 1445.

Parker, E. N.: 1963, *Interplanetary Dynamical Processes*, Interscience Publ., New York.

Parker, E. N.: 1965a, 'The Passage of Energetic Charged Particles Through Interplanetary Space', *Planet. Space Sci.*, **13**, 9.

Parker, E. N.: 1965b, 'Dynamical Theory of the Solar Wind', *Space Sci. Rev.*, **4**, 666.

Parker, E. N.: 1966, 'The Effect of Adiabatic Deceleration on the Cosmic Ray Spectrum in the Solar System', *Planet. Space Sci.*, **14**, 371.

Pesses, M. E.: 1979, 'On the Acceleration of Energetic Protons by Interplanetary Shock Waves', *Ph.D. Thesis*, University of Iowa, Iowa City.

Pesses, M. E.: 1981, 'On the Conservation of the First Adiabatic Invariant in Perpendicular Shocks', *J. Geophys. Res.*, **86**, 150.

LIST OF REFERENCES—Continued

Pneuman, G. W.: 1985, 'Driving Mechanisms for the Solar Wind', *Space Sci Rev.*, **43**, 105.

Pomerantz, M. A.: 1971, *Cosmic Rays*, Van Nostrand Reinhold Co., New York.

Potgieter, M. S. and Moraal, H.: 1985, 'A Drift Model for the Modulation of Galactic Cosmic Rays', *Astrophys. J.*, **294**, 425.

Prishchep, V. L. and Ptuskin, V. S.: 1981, 'Fast-Particle Acceleration at a Spherical Shock Front', *Astron. Zh.*, **58**, 779 (1981, *Sov. Astron.*, **25**, 446).

Quenby, J. J.: 1965, 'Cosmic Rays and the Interplanetary Field', *Proc. 9th Internat. Conf. on Cosmic Rays, London*, **1**, 3.

Quenby, J. J.: 1984, 'The Theory of Cosmic-Ray Modulation', *Space Sci. Rev.*, **37**, 201.

Ramakrishnan, A.: 1962, *Elementary Particles and Cosmic Rays*, Pergamon Press, Oxford.

Ramaty, R. and Lingfelter, R. E.: 1969, 'Cosmic-Ray Deuterium and Helium-3 of Secondary Origin and the Residual Modulation of Cosmic Rays', *Astrophys. J.*, **155**, 587.

Rossi, B.: 1964, *Cosmic Rays*, McGraw-Hill, New York.

Silberberg, R.: 1966, 'Cosmic-Ray Modulations in the Solar System and in Interstellar Space', *Phys. Rev.*, **148**, 1247.

Simpson, J. A., Fonger, W. and Treiman, S. B.: 1953, 'Cosmic-Radiation Intensity-Time Variations and Their Origin. I. Neutron Intensity Variation Method and Meterological Factors', *Phys. Rev.*, **90**, 934.

Skilling, J.: 1971, 'Cosmic Rays in the Galaxy: Convection or Diffusion?', *Astrophys. J.*, **170**, 265.

Skilling, J.: 1975, 'Cosmic Ray Streaming—I Effect of Alfven Waves on Particles', *Mon. Not. Roy. Astron. Soc.*, **172**, 557.

Smith, G. D.: 1978, *Numerical Solution of Partial Differential Equations: Finite Difference Methods, 2nd ed.*, Oxford University Press, Oxford.

LIST OF REFERENCES—Continued

Snyder, C. W., Neugebauer, M. and Rao, U. R.: 1963, 'The Solar Wind Velocity and Its Correlation with Cosmic-Ray Variations and with Solar and Geomagnetic Activity', *J. Geophys. Res.*, **68**, 6361.

Sousk, S. F. and Lenchek, A. M.: 1969, 'The Effect of Galactic Cosmic Rays Upon the Dynamics of the Solar Wind', *Astrophys. J.*, **158**, 781.

Suess, S. T. and Dessler, A. J.: 1985, 'Probing the Local Insterstellar Medium', *Nature*, **317**, 702.

Summers, D.: 1982, 'On the Two-Fluid Polytropic Solar Wind Model', *Astrophys. J.*, **257**, 881.

Terasawa, T.: 1979, 'Energy Spectrum and Pitch Angle Distribution of Particles Reflected by MHD Shock Waves of Fast Mode', *Planet. Space Sci.*, **27**, 193.

Terletskii, Ia. P. and Logunov, A. A.: 1951, 'Energeticheskii Spektrpervichnoi Komponenti Kosmicheskikh Iuchei', *J. Exptl. Theoret. Phys.*, **21**, 567.

Toptygin, I. N.: 1980, 'Acceleration of Particles by Shocks in a Cosmic Plasma', *Space Sci. Rev.*, **26**, 157.

Toptygin, I. N.: 1985, *Cosmic Rays in Interplanetary Magnetic Fields*, D. Reidel Publ., Dordrecht.

Völk, H. J.: 1984, 'Nonlinear Theory of Cosmic-Ray Acceleration in Shock Waves', paper presented at *4th Moriond Conference Cosmic Rays and Elementary Particles, La Plagne*.

Völk, H. J., Breitschwerdt, D. and McKenzie, J. F.: 1986, personal communication via G. M. Webb.

Völk, H. J., Drury, L. O'C. and McKenzie, J. F.: 1984, 'Hydrodynamic Estimates of Cosmic Ray Acceleration Efficiencies in Shock Waves', *Astron. Astrophys.*, **130**, 19.

Wallis, M. K.: 1973, 'Interaction Between the Interstellar Medium and Solar Wind Plasma', *Astrophys. Space Sci.*, **20**, 3.

Wang, R. J.: 1970, 'Dynamics of the Eleven-Year Modulation of Galactic Cosmic-Rays', *Astrophys. J.*, **160**, 261.

LIST OF REFERENCES—Continued

Webb, G. M.: 1983, 'The Structure of Oblique MHD Cosmic-Ray Shocks', *Astron. Astrophys.*, **127**, 97.

Webb, G. M., Drury, L. O'C. and Völk, H. J.: 1986, 'Cosmic-Ray Shock Acceleration in Oblique MHD Shocks', *Astron. Astrophys.*, **160**, 335.

Webb, G. M., Forman, M. A. and Axford, W. I.: 1985, 'Cosmic-Ray Acceleration at Stellar Wind Terminal Shocks', *Astorphys. J.*, **298**, 684.

Webb, G. M. and Gleeson, L. J.: 1979, 'On the Equation of Transport for Cosmic-Ray Particles in the Interplanetary Region', *Astrophys. Space Sci.*, **60**, 335.

Webber, W. R. and Chotowski, C.: 1967, 'A Determination of the Energy Spectrum of Extraterrestrial Electrons in the Energy Range 70 - 2000 MeV', *J. Geophys. Res.*, **72**, 2783.

Webber, W. R. and Lezniak, J. A.: 1973, 'Interplanetary Radial Gradients of Galactic Cosmic Ray Protons and Helium Nuclei: Pioneer 8 and 9 Measurements from 0.75 to 1.10 AU', *J. Geophys. Res.*, **78**, 1979.

Webber, W. R. and Lezniak, J. A.: 1974, 'The Comparative Spectra of Cosmic-Ray Protons and Helium Nuclei', *Astrophys. and Space Sci.*, **30**, 361.

Whittaker, E. T. and Watson, G. N.: 1927, *A Course of Modern Analysis*, Cambridge University Press, London.

Wibberenz, G.: 1971, 'Solar Particle Propagation', *Proc 12th Internat. Conf. on Cosmic Rays, Hobart*, Invited and Rapporteur, 204.

Wilson, J. G.: 1976, *Cosmic Rays*, Wykeham Publ., London.